THE USE OF MANGANESE ION GRADIENTS IN THE PREPARATION OF ANTICANCER DRUG FORMULATIONS

by

Sheela Ann Abraham

B.Sc., University of Alberta, 1995

A THESIS SUBMITTED IN PARTIAL FUFILLMENT OF THE REQUIREMENT FOR THE DEGREE OF DOCTOR OF PHILOSOPHY

in

THE FACULTY OF GRADUATE STUDIES

DEPARTMENT OF PATHOLOGY AND LABORATORY MEDICINE

We accept this thesis as conforming to the required standard

.....

THE UNIVERSITY OF BRITISH COLUMBIA

January 2004

ABSTRACT

One goal of drug delivery systems is to increase the therapeutic index of an associated drug. Liposomes as lipid-based drug carriers have proven to be a versatile formulation technology for intravenous use, particularly when considering their use with anticancer drugs. Liposomes have the potential to increase the therapeutic index of a drug by altering the drug's pharmacokinetics and bio-distribution. It is understood for drug loaded liposomes that these attributes are often dictated by the materials used to prepared the liposomes, by the physical attributes of the resulting formulation and by the manner in which the drug is associated with carrier. This thesis characterises a novel method of encapsulating anticancer drugs within liposomes containing entrapped manganese. It is demonstrated that interactions between the transition metal manganese and doxorubicin, an anthracycline antibiotic and chemotherapeutic, are sufficient to promote drug loading in liposomes. These studies concluded that doxorubicin possesses co-ordination sites capable of complexing transition metals. This complexation reaction occurred at neutral pH and the loading reaction was not dependent on use of liposomes exhibiting or maintaining a transmembrane pH gradient. Unlike pH gradient based loading methods, which result in formation of a doxorubicin fibre bundles within the liposome core, doxorubicin-manganese complexation did not promote bundle formation as judged by cryo-electron microscopy. Studies assessing whether manganese complexation could promote encapsulation of another anticancer drug, topotecan, were completed. Although drug loading was not achieved through complexation, the studies confirmed that topotecan can be loaded into liposomes exhibiting a pH gradient. The stability of this formulation appeared to be dependent on the presence of sulfate as a counter ion and loading resulted in formation of precipitated structures within liposomes.

Given these initial data, it was suggested that manganese gradients could be used to encapsulate multiple drugs. This was demonstrated by pursuing development of a liposomal formulation containing two anticancer drugs, doxorubicin and vincristine. Doxorubicin loading was driven by complexation with manganese while vincristine was loaded using a pH gradient. The co-encapsulated doxorubicin/vincristine formulation exhibited pharmacokinetic attributes comparable to liposomal formulations containing only a single drug. Interestingly, the formulation containing both drugs proved to be less effective than liposomes containing only vincristine in the treatment of an established breast cancer model. These data were explained by in vitro studies suggesting that the co-formulated drugs exhibited antagonistic interactions when simultaneously added to tumour cells as free drugs.

Another advantage of achieving drug loading through manganese complexation was illustrated by characterizing drug loading in a novel thermosensitive liposomal formulation. Although efficacious when used in combination with mild heating, other investigators have shown that doxorubicin encapsulation achieved through use of transmembrane pH gradients (inside acid) was limited and the resulting doxorubicin loaded thermosensitive liposomes exhibited poor stability in vivo. It is demonstrated here that the limitation in drug loading capacity can be overcome through methods relying on metal-drug complexation. Drug loading limitations in these formulations may be dependent on the physical state in which doxorubicin exists within the liposomes. In total, the data presented provides new insights into the factors influencing drug encapsulation into liposomes containing manganese, an ion that can facilitate loading through a complexation reaction or via an ionophore mediated pH gradient formation.

TABLE OF CONTENTS

ABSTRACT ii

TABLE OF CONTENTS iv

LIST OF FIGURES viii

LIST OF TABLES xi

ABBREVIATIONS xii

ACKNOWLEDGEMENTS xiii

DEDICATION xiv

CHAPTER 1 INTRODUCTION 1

1.1. LIPOSOMES AS DRUG DELIVERY SYSTEMS 1
1.1.1. Anticancer Drug Carriers 4

1.2. LIPOSOMES 6
1.2.1. Phospholipids 7
1.2.2. Cholesterol 7
1.2.3. Phospholipid Bilayer 9
1.2.4. Gel–Liquid Crystalline Phase Behaviour 10
1.2.5. Phospholipid-Cholesterol Bilayer 12

1.3. MANUFACTURING LIPOSOMES 14
1.3.1. Multilamellar Vesicles 14
1.3.2. Lipid Hydration and Solute Distribution 14
1.3.3. Large Unilamellar Vesicles 15
1.3.4. Size of Large Unilamellar Vesicles 19
1.3.5. Characterisation using Cryo-Transmission Electron Microscopy 20

1.4. DRUG ENCAPSULATION 22
1.4.1. Encapsulated Agents 23
1.4.1.1. Doxorubicin 23
1.4.1.2. Vincristine 26
1.4.1.3. Topotecan 28
1.4.2. Methods of Encapsulation 31
1.4.2.1. Passive Encapsulation 31
1.4.2.2. Ion Gradient Mediated Encapsulation 32
1.4.2.3. Encapsulation Efficiency 38
1.4.2.4. Drug-to-Lipid Ratio 39

1.4.2.5. Drug Release 39
1.4.2.6. Biological Factors Affecting Drug Release of Systematically Administered Liposomes 41

1.5. WORKING HYPOTHESES AND RESEARCH OBJECTIVES 43

CHAPTER 2 MATERIALS AND METHODS 46

2.1. MATERIALS 46

2.2. PREPARATION OF LARGE UNILAMELLAR VESICLES 47

2.3. PREPARATION OF ION GRADIENTS FOR DRUG ENCAPSULATION 48

2.4. DRUG ENCAPSULATION 49
2.4.1. Doxorubicin Encapsulation 49
2.4.2. Topotecan Encapsulation 50
2.4.3. Vincristine Encapsulation 51
2.4.4. Co-Encapsulation of Doxorubicin and Vincristine 52

2.5. ABSORPTION AND CIRCULAR DICHROIC SPECTRA 53

2.6. DOXORUBICIN STABILITY 54

2.7. DOXORUBICIN-MANGANESE BINDING 55

2.8. pH GRADIENT DETERMINATION 55

2.9. CRYO-TRANSMISSION ELECTRON MICROSCOPY 56

2.10. IN VITRO DRUG RELEASE 56

2.11. IN VIVO DRUG RELEASE 57
2.11.1. Determination of Liposomal Lipid Concentrations in Plasma 57
2.11.2. Determination of Doxorubicin and Vincristine Concentrations in Plasma 57

2.12. HUMAN BREAST CANCER XENOGRAFT MODEL 59

2.13. MTT CYTOTOXICITY ASSAYS AND DRUG COMBINATION 60

2.14. STATISTICAL ANALYSIS 61

CHAPTER 3 FORMATION OF TRANSITION METAL-DOXORUBICIN CHELATES INSIDE LIPOSOMES 62

3.1. INTRODUCTION 62

3.2. RESULTS 64
3.2.1. The Encapsulation of Doxorubicin into DMPC/Chol Liposomes Using the Citrate Encapsulation Procedure or the Manganese Sulfate Encapsulation Procedure 64
3.2.2. Cryo-Transmission Electron Microscopic Analysis of the Drug Loaded Liposomes 72
3.2.3. The Encapsulation of Doxorubicin into Liposomes Prepared in Manganese Chloride 75
3.2.4. Assessment of the Transmembrane pH Gradient Prior to and Following Doxorubicin Encapsulation 81
3.2.5. Absorption and Circular Dichroic Spectra of Doxorubicin under Various Conditions 84
3.2.6. The Influence of Entrapped Doxorubicin Structure on Drug Release From Liposomes In vitro and In vivo 89

3.3. DISCUSSION 98

CHAPTER 4 THE USE OF TRANSMEMBRANE ION GRADIENTS IN THE ENCAPSULATION OF TOPOTECAN WITHIN LIPOSOMES 104

4.1. INTRODUCTION 104

4.2. RESULTS 108
4.2.1. The Encapsulation of Topotecan into DSPC/Chol Liposomes 108
4.2.2. Assessment of the Transmembrane pH Gradient Prior to and Following Topotecan Loading 112
4.2.3. Influence of Initial Drug-to-Lipid Ratio on Topotecan Encapsulation Efficiency 115
4.2.4. In vitro Topotecan Release From DSPC/Chol Liposomes 118
4.2.5. Cryo-Transmission Electron Microscopic Analysis of the Topotecan-Loaded Liposomes 121

4.3. DISCUSSION 125

CHAPTER 5 CO-ENCAPSULATION OF DOXORUBICIN AND VINCRISTINE WITHIN LIPOSOMES THROUGH USE OF METAL ION COMPLEXATION IN COMBINATION WITH IONOPHORE MEDIATED INDUCTION OF A PH GRADIENT 128

5.1. INTRODUCTION 128

5.2. RESULTS 131
5.2.1. Co-encapsulation of Doxorubicin and Vincristine into Manganese Sulfate containing DSPC/Chol Liposomes 131

5.2.2. In vivo Plasma Elimination of Liposomes with Co-Encapsulated Doxorubicin and Vincristine 140
5.2.3. Efficacy of the Co-Encapsulated Liposomal Doxorubicin/Vincristine Formulation Against a Human Breast Cancer Xenograft Model 146
5.2.4. In vitro Cytotoxicity Analysis of Doxorubicin and Vincristine Alone and in Combination 151

5.3. DISCUSSION 156

CHAPTER 6 DOXORUBICIN LOADED THERMOSENSITIVE LIPOSOMES: CHARACTERIZATION OF MANGANESE COMPLEXATION-BASED DRUG LOADING 160

6.1. INTRODUCTION 160

6.2. RESULTS 164
6.2.1. The Encapsulation of Doxorubicin Within Thermosensitive Liposomes 164
6.2.2. Confirmation that Doxorubicin Loaded DPPC/MSPC/DSPE-PEG Liposomes Remain Thermosensitive In Vitro 164
6.2.3. Cryo-Transmission Electron Microscopic Analysis of Drug Loaded LTSL 167
6.2.4. The Encapsulation of Doxorubicin Within Thermosensitive Liposomes Using the $MnSO_4$ Procedure in Conjunction With the A23187 Ionophore 170

6.3. DISCUSSION 178

CHAPTER 7 CONCLUSION 181

REFERENCES 189

LIST OF FIGURES

Figure 1.1. Stages of Liposome Development 3

Figure 1.2. Liposome Components 8

Figure 1.3. Physical States of Phospholipid Bilayers 11

Figure 1.4. Cholesterol-Phospholipid Bilayers 13

Figure 1.5. Multilamellar Vesicles, Large Unilamellar Vesicles and Small Unilamellar Vesicles 17

Figure 1.6. Schematic Representation of Two Dimensional Images of Spheres and Flat Disks Obtained Using Cryo-Transmission Electron Microscopy 21

Figure 1.7. Chemical Structure of Doxorubicin 24

Figure 1.8. Chemical Structure of Vincristine 27

Figure 1.9. Chemical Structure of Topotecan 30

Figure 1.10. Methods of Doxorubicin Encapsulation into Liposomes Exhibiting Ion Gradients 36

Figure 3.1. Methods of Doxorubicin Encapsulation into Liposomes 65

Figure 3.2. Doxorubicin Encapsulation in DMPC/Chol (55/45) Liposomes using Three Loading Methods 68

Figure 3.3. The Stability of Doxorubicin within DMPC/Chol (55/45) and DSPC/Chol Liposomes Containing either Citrate or Manganese Sulfate 70

Figure 3.4. Cryo-Transmission Electron Microscopy Images of DMPC/Chol (55/45) Liposomes Either Before or After Drug Loading 73

Figure 3.5. Doxorubicin Encapsulation using Liposomes Prepared in 300 mM Manganese Chloride 75

Figure 3.6. Cryo-Transmission Electron Microscopy Images of DMPC/Chol (55/45) Liposomes Either Before or After Drug Loading 79

Figure 3.7. Measured Transmembrane pH Gradients Prior to and Following Doxorubicin Loading 82

Figure 3.8. Absorption Spectra of Doxorubicin at Various pH and Concentrations of $MnSO_4$ as well as the Circular Dichroic Spectra of Doxorubicin Loaded Liposomes 85

Figure 3.9. The In Vitro Release of Doxorubicin From DMPC/Chol (55/45) Liposomes 91

Figure 3.10. The In Vivo Release of Doxorubicin From DMPC/Chol (55/45) Liposomes 93

Figure 4.1. Topotecan Encapsulation in DSPC/Chol (55/45) Liposomes using Four Loading Procedures 110

Figure 4.2. Transmembrane pH Gradients Measured Prior to and Following Topotecan Loading 113

Figure 4.3. Topotecan Encapsulation at Various Drug-to-Lipid Ratios within DSPC/Chol (55/45) Liposomes using Either the Ammonium Sulfate Loading Procedure or the Manganese Sulfate Loading Procedure with Added A23187 116

Figure 4.4. In Vitro Release of Topotecan From DSPC/Chol (55/45) Liposomes Loaded using Four Loading Procedures 119

Figure 4.5. Cryo-Transmission Electron Microscopy Images of DSPC/Chol (55/45) Liposomes Either Before or After Topotecan Loading 123

Figure 5.1. Doxorubicin or Vincristine Encapsulation in DSPC/Chol (55/45) Liposomes using the Manganese Sulfate Loading Procedure with or without the A23187 ionophore 133

Figure 5.2. Vincristine Encapsulation in DSPC/Chol (55/45) liposomes using the Manganese Sulfate Loading Procedure with the A23187 Ionophore 135

Figure 5.3. Changes in A_{550} (ΔA_{550}) of Doxorubicin Loaded DSPC/Chol Liposomes After the Addition of the Ionophore A23187 138

Figure 5.4. Doxorubicin and Vincristine Encapsulation within DSPC/Chol (55/45) Liposomes 141

Figure 5.5. The Lipid and Drug Plasma Elimination Profiles of Drug-Loaded DSPC/Chol (55/45) Liposomes Following i.v. Administration into Female Balb/c Mice 144

Figure 5.6. In Vivo Release of Doxorubicin and Vincristine From DSPC/Chol (55/45) Liposomes 147

Figure 5.7. IC_{90} Values Determined From In Vitro MTT Assays Assessing the Activity of Doxorubicin and Vincristine Combinations 153

Figure 6.1. Doxorubicin Encapsulation into DPPC/MSPC/DSPE-PEG (90/10/4 molar ratio) Liposomes 165

Figure 6.2. In vitro Release of Doxorubicin From DPPC/MSPC/DSPE-PEG (90/10/4 mol ratio) Liposomes Loaded Using Either the Citrate or the $MnSO_4$ Procedure 168

Figure 6.3. Cryo-Transmission Electron Microscopy Images of DPPC/MSPC/DSPE-PEG (90/10/4 mol ratio) Liposomes Prior to or After Doxorubicin Loading Using Either the Citrate or the $MnSO_4$ Loading Procedures 171

Figure 6.4. Doxorubicin Encapsulation into DPPC/MSPC/DSPE-PEG (90/10/4 molar ratio) Liposomes Using the $MnSO_4$ Plus A23187 Loading Procedure 174

Figure 6.5. In Vitro Release of Doxorubicin From DPPC/MSPC/DSPE-PEG (90/10/4 molar ratio) Liposomes Loaded Using the $MnSO_4$ Procedure With Addition of the A23187 After Drug Loading 176

Figure 7.1. Schematic Representation of Doxorubicin Equilibria Within DSPC/Chol Liposomes Using Either the Citrate or the Manganese Sulfate Encapsulation Procedure 183

LIST OF TABLES

Table 3.1. The Differential Molar Circular Dichroic Absorption Δε (M-1cm-1) of Doxorubicin-Encapsulation Liposomes 88

Table 3.2. Percent of Encapsulated Doxorubicin Obtained Following Intravenous Administration of DMPC/Chol and DSPC/Chol Liposomes 97

Table 5.1. Treatment of SCID RAG-2M Mice Bearing MDA 435/LCC6 Tumours 150

ABBREVIATIONS

Ab	Absorbance
aq	Aqueous
Chol	Cholesterol
^{3}H-CHE	[^{3}H]-cholesteryl hexadecyl ether
CD	Circular Dichroism
cTEM	Cryo-transmission electron microscopy
DMPC	1,2 Dimyristoyl-*sn*-glycero-3-phosphocholine
DOX	Doxorubicin
DPPC	1,2-dipalmitoyl-*sn*-glycerol-3-phosphocholine
DSPC	1,2-Distearoyl-*sn*-glycero-3-phosphocholine
DSPE-PEG	1,2-distearoyl-*sn*-glycero-3-phosphoethanolamine-N-[Methoxy(polyethylene-glycol)$_{2000}$]
$\Delta\Psi$	Electrochemical gradient
EDTA	Ethylenediamine-tetra acetic acid
FBS	Fetal bovine serum
HBS	HEPES-buffered saline
HEPES	N-[2-hydroxyethyl] piperazine-N'-[2-ethanesulfonic acid]
IC_{90}	Inhibition Concentration of 90% of cells
i.v.	Intravenous
LUV	Large unilamellar vesicle
MLVs	Multilamellar vesicles
MPS	Mononuclear Phagocyte System
MSPC	1-stearoyl-2-hydroxy-*sn*-glycero-3-phosphocholine
MTD	Maximum Tolerated Dose
MTT	3-(4,5-dimethylthiazol-2-yl)-2,5-diphenyltetrazolium bromide
PEG	Polyethylene glycol
Pgp	P-glycoprotein
QELS	Quasi-elastic light scattering
s.c.	Subcutaneous
SCID	Severely Compromised Immunodeficient
SDS	Sodium dodecyl sulfate
SHE	Sucrose-HEPES-EDTA
SUV	Small unilamellar vesicle
Tc	Phase Transition Temperature
TOPO	Topotecan
UV	Ultraviolet
VINC	Vincristine
VIS	Visible light
wt	Weight

ACKNOWLEDGEMENTS

I am extremely grateful for all the support and guidance I have received during the completion of this thesis. I would first like to thank Marcel Bally, my supervisor for giving me the opportunity to become one of his graduate students; I have learned so much and I will be forever indebted. I would also like to thank Murray Webb my industrial supervisor for his additional guidance and great talks. I also greatly appreciate all the help and advise from Göran Karlsson, Katarina Edwards, Benjamin Viglianti, and Mark Dewhirst our collaborators at both Uppsala University and Duke University.

I would also like to thank Dana, Rebecca, Hong and Sophia for all assistance with the animal work, Norma and Linda for all assistance with the HPLC work, Jean for all the osmolarity readings and Spencer for all the technical advice- you guys rock!

I would also like to mention that (a big) part of the reason I loved coming to work was to spend time/ chat/ have coffee/ go for ice cream/ have another break/ go to Cactus Club /laugh/ complain incessantly with a fantastic group of people at the BCCRC. I will especially miss the AT group including Daria, Margaret, Harry, Jean, Diana, Nataliya, Brian, Maria, Teddy, Corrina, Dawn, Euan, Nancy, Daniel, Lar, Maggie, Ghania, Mac, Yanping, Catherine and yes, even Aman. I will never forget my fellow Pit residents Jen, Ludgar, Gwyn, Jason and Gigi who always, created a great atmosphere with comfort, laughter and inspiring talks. I would also like to formally apologise for playing music too loud in the lab especially the Air Supply and Anne Murray CDs (sorry!). I would also like to thank my Pathology buddies Arek, Chris, and Matt and I would also like to express my deepest thank you to Michelle and Kevin who, with their unwavering support and friendship made my degree FUN. I love all you guys and you all kick ass.

DEDICATION

This thesis is dedicated to my parents

Joseph and Anna Abraham

And my husband

Edmond Chan

Whose love and support I felt every step of the way

CHAPTER 1

INTRODUCTION

1.1. LIPOSOMES AS DRUG DELIVERY SYSTEMS

Liposomes as model closed membrane systems have proven to be a valuable tool to characterise and define the functional roles of lipids in biological membranes. Liposomes have facilitated studies on lipid mobility, lipid phase behaviour and membrane permeability (Gruner, 1987). Membrane permeability studies were especially insightful in terms of resolving solute permeability (Cohen, 1975), ion gradient formation (Lasic et al., 1995; Perkins and Cafiso, 1987) and formation and stability of transmembrane electrochemical potentials (Redelmeier et al., 1989). An example of how these biochemical and biophysical assessments helped to define liposomes as drug carriers is illustrated by the observations of Nichols and Deamer (Nichols and Deamer, 1976), who demonstrated that liposomal systems possessing an acidic interior had the ability to sequester catecholamines. Their studies were focused on possible mechanisms of the storage of catecholamines in secretory organelles, but their results had far reaching effects. As first noted by Bally et al. (Bally et al., 1985), the accumulation of lipophilic weak bases provided an important method for loading therapeutic agents into preformed membrane bound vesicles.

Liposomes are spherical membrane vesicles spontaneously formed upon the hydration of dried lipids in aqueous solutions (Bangham et al., 1965). Early investigations into liposomes established that phospholipid vesicles were capable of retaining drugs. Several drug carrier characteristics were identified that contributed to altering the biological performance of the associated drug. When considering parenteral administration, these

characteristics included vesicle size (Abra and Hunt, 1981; Oku and Namba, 1994), the inclusion of cholesterol (Gregoriadis and Davis, 1979) and/or phospholipids with a high phase transition temperature and the manipulation of carrier surface charge with the incorporation of negatively charged lipids (Allen and Chonn, 1987). Later, researchers identified that the incorporation of phospholipids grafted with poly(ethylene glycol) (PEG) chains allowed liposomes to stay in the plasma compartment over extended time frames which facilitated and increased delivery of liposomes to sites of tumour growth (Allen et al., 1991). This discovery defined a 'second generation' of lipid-based carriers (Woodle and Lasic, 1992). More recently, multi-functional liposomes have begun to set the stage as the newest 'third generation' carriers that are able to incorporate targeting ligands (Ahmad and Allen, 1992; Leserman et al., 1980) or bioactive lipid components (Klapisz et al., 2000; Shabbits and Mayer, 2003) to improve disease site localisation and delivery (Figure 1.1.).

Carefully designed drug delivery carriers can offer solutions to delivering either newly emerging therapeutics such as peptides, proteins, oligonucleotides or genes as well as therapeutics that are well-established with the goal of improving the therapeutic activity of the associated drug. Preclinical work has clearly established liposomes as effective carriers for the delivery of anticancer drugs (Cowens et al., 1993; Mayer, 1998; Rahman et al., 1990), antimicrobial agents (Lopez-Berestein, 1987; Moribe and Maruyama, 2002), genes (Mukherjee et al., 1978) and antisense nucleotides (Leonetti et al., 1990; Pastorino et al., 2001). As a result, ten liposome formulations have been approved for human use while others are at various stages of clinical trials (Barenholz, 2003). By far the greatest effort directed towards the development of liposomal drugs has been the development of formulations for use in the treatment of cancer.

Figure 1.1. Stages of Liposome Development

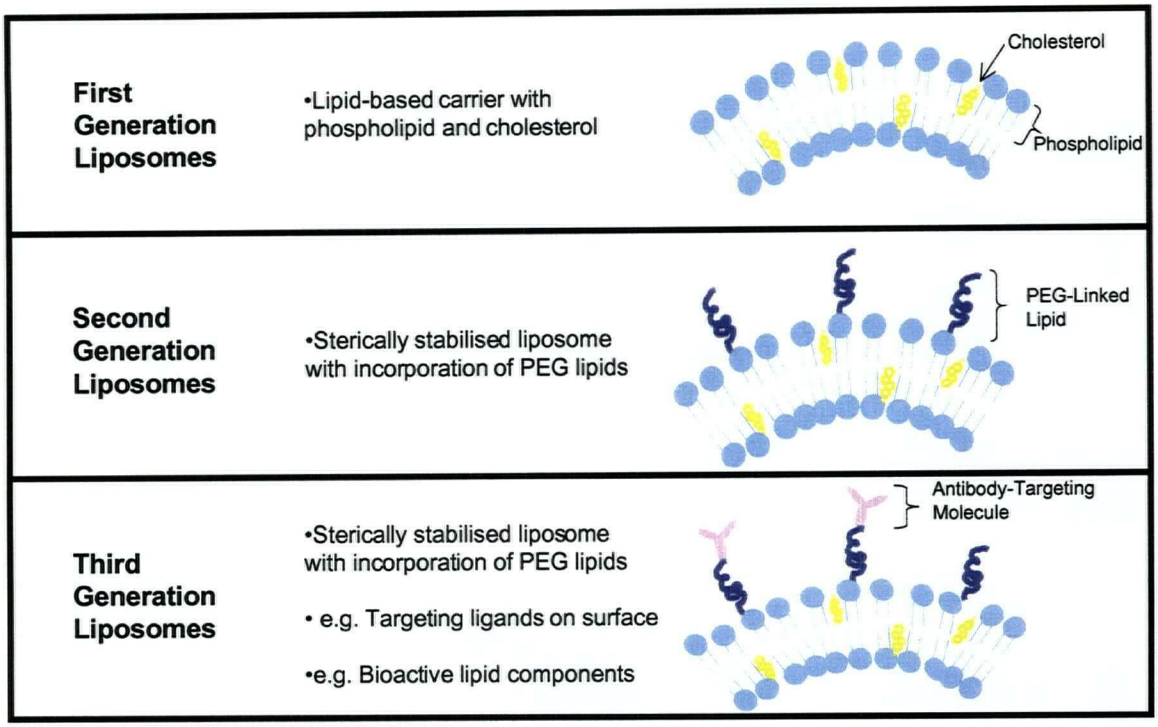

1.1.1. Anticancer Drug Carriers

Cancer arises as a result of the accumulation of genetic changes that confer a selective advantage to the cells in which they occur (Hill and Tannock, 1998). Surgery, radiation therapy and chemotherapy are the primary approaches used in treating cancer (Kaufman and Chabner, 1996). In addition to chemotherapy, hormones and immuno-modulating drugs are also employed. The type and extent of tumour involvement, the performance status, age and concomitant disease of the patient determine the appropriate type of therapy (Finley, 1991). Although surgery and radiation therapy may be very effective in treating localised tumours, they are of limited value in treating disseminated disease thereby necessitating a more systemic approach, such as chemotherapy. Chemotherapy is therefore often employed at some time during the course of illness of most cancer patients (Chabner, 1982).

Cytotoxic chemotherapy encompasses a group of drugs that inhibits DNA synthesis and/or function with potentially interfering with cell cycle progression. Cytotoxic chemotherapy is therefore toxic to all cells undergoing cell division, a factor that complicates the administration of drug to patients. The toxicity to normal tissues that contain rapidly proliferating cells such as bone marrow (stem cells), intestine (new cells produced by the crypts of Lieberkuhn), or proliferating cells in hair follicles limits the dose of drug that can be given (Hill and Tannock, 1998).

The use of drug carriers has been one solution to address problems associated with the systemic administration of chemotherapy. Drug carriers can modify the biodistribution of a carrier-associated drug. As a result they have the potential to improve the relationship between the desired and undesired effects of therapy (commonly referred to as the therapeutic index) of drugs by decreasing their toxicity. Although a veritable plethora of

carriers exist such as nanoparticles, nanocapsules, magnetic nanospheres and micelles, this thesis will focus on synthetic lipid-based carriers called liposomes.

Liposomes have specific characteristics that make them ideal chemotherapy delivery agents. Liposomes are useful anticancer drug formulations because they can increase the solubility of certain drugs. For example, liposomal formulations are being developed for the delivery of hydrophobic chemotherapeutics like TAXOL® (paclitaxel) to overcome solubility issues and thereby aid in their delivery to the diseased site (Schmitt-Sody et al., 2003). Liposomes are also able to increase the stability of drugs under physiological conditions. For example topotecan, a camptothecin, undergoes reversible hydrolysis to an inactive form of the drug within minutes of i.v. administration (Burke, 1996). Liposomal formulations of topotecan have been shown to increase the proportion of the active form (in comparison to the inactive form) of the drug within the plasma compartment following administration (Tardi et al., 2000) (see Chapter 1, section 1.4.1.3.). Liposomes can also decrease the elimination rate and effectively increase the concentration of an associated drug in the plasma compartment (when administered intravenously), a characteristic that has been shown to be effective at increasing the efficacy of certain drugs (Mayer et al., 1990a). Finally, many small molecule chemotherapeutics have a large volume of distribution; liposomal delivery of such agents decreases the volume of distribution or alters their biodistribution, which can potentially decrease the toxicity of the encapsulated agent (Drummond et al., 1999).

Liposomes have the added advantage of being able to deliver chemotherapy to the tumour site, based on their ability to accumulate within solid tumours. Solid tumour tissue possess two significant (with respect to drug delivery) types of blood vessels: the existing vessels in the normal tissue into which the tumour has invaded, and the tumour micro-vessels

arising from neovascularization resulting from increased expression of pro-angiogenic factors produced by the tumour cells (Brown and Giaccia, 1998; Jain, 1991). Both types of vessels develop structural and physiological abnormalities that typify tumour vasculature. Vascular casting techniques (Grunt et al., 1985) and window chamber preparations (Dewhirst et al., 1989) have identified that tumour blood vessels are highly irregular and tortuous with arterio-venous shunts, lacking smooth muscle and have discontinuous endothelial linings and basement membranes (Brown and Giaccia, 1998). Tumour microvasculature fenestrations range between 100-780 nm in diameter (Warren, 1979), resulting in an increased permeability to circulating large molecules (Dvorak et al., 1988; Jain, 1987), thus providing a route for liposomes to move from the blood compartment into the extravascular space surrounding the tumour cells. Liposomes, in the size range of 100–200 nm, are able to readily extravasate within the tumour and provide locally concentrated drug delivery. This thesis focuses on the development and characterisation of liposomal formulations designed for systemic administration, a route most commonly employed for chemotherapeutics. When administered intravenously, liposomes can serve as circulating reservoirs of drug (Barratt, 2003) whose extended circulation times allow for liposomes to accumulate at the disease site thereby improving the therapeutic index of the associated drug.

1.2. LIPOSOMES

Liposomes are comprised of lipids organised in a bilayer configuration, typically surrounding an aqueous core. The lipid composition dictates the properties of liposomes used as drug carriers, and key properties of any liposome drug delivery system include the partitioning and permeability of the drug into and across the lipid bilayer.

1.2.1. Phospholipids

Phospholipids, a common constituent of liposomes, possess hydrophobic acyl chains linked via an ester bond to a glycerol backbone and a phosphate-containing hydrophilic headgroup (Chapman, 1975; Seelig and Waespe-Sarcevic, 1978). The distinct properties of each phospholipid are determined by its acyl chains, which can differ in length and degree of saturation, and the chemistry of its head group (Figure 1.2. (A)). Choline-containing phospholipids (PC), the most abundant lipid in nature, are the most commonly used lipid for liposomal carriers due to the fact that they are zwitterionic and uncharged at physiological pH. Other less commonly employed phospholipids include phosphatidylethanolamine (PE), phosphatidylserine (PS), phosphatidylglycerol (PG), phosphatidic acid (PA) and phosphatidylinositol (PI). PC and PE are zwitterionic phospholipids, while PS, PG, PA and PI have a net negative charge at physiological pH (Vance, 2002).

1.2.2. Cholesterol

Cholesterol (Chol) is another common constituent of liposomes. When incorporated within bilayers, cholesterol has dramatic effects on the properties of liposomes. Cholesterol can be considered as a rigid lipid with 3 components: a polar hydroxyl group, a rigid planar steroid ring structure, and a short alkyl chain tail (Israelachvili et al., 1980) (Figure 1.2. (B)). Within lipid bilayers, cholesterol is thought to intercalate into the membrane perpendicular to the bilayer surface, with its polar hydroxyl group positioned in the vicinity of the glycerol backbone and its hydrophobic steroid ring near the acyl chains of the phospholipid (Subczynski et al., 1994). There is no evidence suggesting that the hydroxyl portion of cholesterol binds to any part of the phospholipid molecule acyl chain (Corvera et al., 1992).

Figure 1.2. Liposome Components:

(A): The general structure of a phosphatidylcholine lipid is indicated below. Image from (Wolfe, 1993). (B): The chemical structure of cholesterol. Image from (New, 1990). (C): The chemical structures of the phospholipids used in this thesis are: (i): 1,2-dimyristoyl-*sn*-glycero-3-phosphocholine (DMPC). (ii): 1,2-dipalmitoyl-*sn*-glycerol-3-phosphocholine (DPPC). (iii): 1,2-distearoyl-*sn*-glycero-3-phosphocholine (DSPC). (iv): 1-stearoyl-2-hydroxy-*sn*-glycero-3-phosphocholine (MSPC). (v):1,2-distearoyl-*sn*-glycero-3-phospho-ethanolamine-N-[Methoxy(polyethylene glycol)$_{2000}$] (DSPE-PEG).

(A)

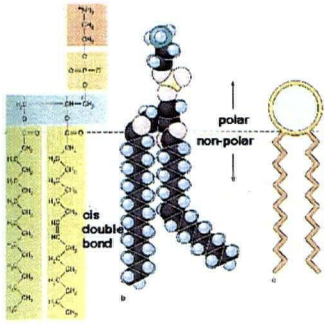

(B)

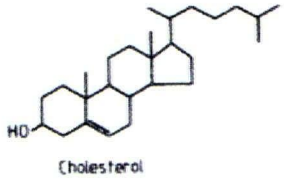

(C)

(i)

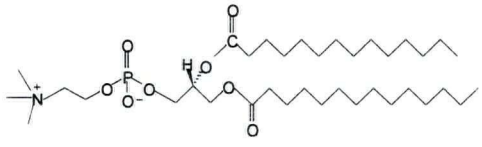

(ii)

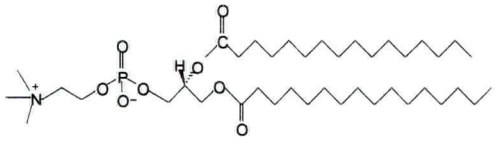

(iii)

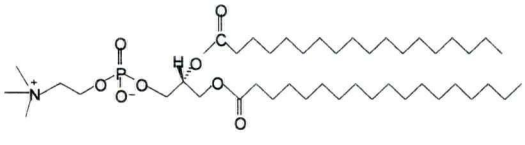

(iv)

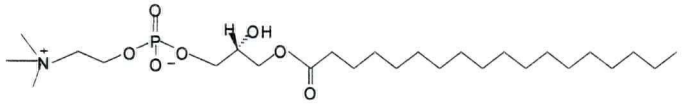

(v)

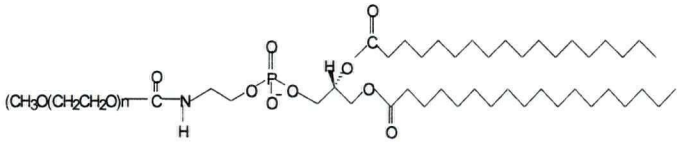

Cholesterol has remained a primary component of liposome formulations due to evidence indicating that cholesterol alters the permeability of the liposome bilayer (Betageri et al., 1993; New, 1990) and inhibits the binding of serum proteins *in vivo* (Moghimi and Patel, 1988; Patel et al., 1983; Szebeni et al., 1988).

In this thesis two cholesterol-phosphatidylcholine containing formulations, namely 1,2-dimyristoyl-*sn*-glycero-3-phosphocholine/cholesterol (DMPC/Chol) and 1,2,-distearoyl-*sn*-glycero-3-phosphocholine/cholesterol (DSPC/Chol) (Figure 1.2. (C)), have been used to characterise drug encapsulation in response to a transmembrane manganese ion gradient and will be further described in Chapters 3, 4 and 5. In light of third generation technologies, a cholesterol-free formulation containing 1,2-dipalmitoyl-*sn*-glycerol-3-phosphocholine/1-stearoyl-2-hydroxy-*sn*-glycero-3-phosphocholine/1,2-distearoyl-*sn*-glycero-3-phospho-ethanolamine-N-[Methoxy(polyethylene-glycol)$_{2000}$] (DPPC/MSPC/DSPE PEG$_{2000}$) was also used and will be further described in Chapter 6.

1.2.3. Phospholipid Bilayer

Individual lipids cannot be considered as isolated entities but as a co-operative bimolecular layer. The bilayer organisation of liposomes is driven by the amphipathic nature of phospholipids. Bilayer sheet formation is a self-assembly process; the resulting structure that forms is a compromise between the hydrophobic effect, entropy and intermolecular interactions such that the bilayer achieves the lowest free energy state possible. A key to developing an understanding of how phospholipid composition influences the properties of liposome drug carriers initiates from understanding the phase behaviour of the liposome bilayer.

1.2.4. Gel–Liquid Crystalline Phase Behaviour of Lipid Bilayers

Chemical composition and temperature dictate the physical state of a phospholipid bilayer. Upon heating, phospholipid bilayers exhibit an endothermic transition (Tc) at a specific temperature that is below its melting point (Tm). Below the Tc, the phospholipid bilayer exists in a gel state and above the Tc, the bilayer exists in a liquid-crystalline state (Figure 1.3. (A)) (Albon and Sturtevant, 1978; Gruner, 1987; Huang et al., 1993). Gel state lipid acyl chains are generally packed in highly ordered all-*trans* arrays, with a few *gauche* rotamers present (Figure 1.3. (B)).

In the gel state, a decreased molecular motion (due to decreased temperature with respect to the Tc) tends to increase fatty acyl chain contact, thereby allowing van der Waals interactions to stabilise the gel phase (Israelachvili et al., 1980). The liquid-crystalline phase acyl chains are markedly more disordered as a result *trans-gauche* isomerizations around the carbon-carbon bonds.

The Tc of a lipid bilayer is dictated by various factors. The length of the lipid fatty acyl chain has a significant effect; as the chain increases in length, each additional CH_2 group makes a favourable contribution to the free energy of interaction between adjacent hydrocarbon chains (Stryer, 1989). These interactions elevate the Tc. Lipids with *trans* double bonds in the middle of their acyl chains have a lower Tc in comparison to saturated acyl chains. Hydrogen bonding between lipid head groups has effects on the Tc, but these effects are dependent on the charge of the lipid head group itself, and on the pH of the environment (Boggs, 1987; Tanford, 1991).

Figure 1.3. Physical States of Phospholipid Bilayers:

(A): Phospholipid bilayers below the transition temperature (Tc) will exist in a gel or crystalline state, and above the Tc phospholipid bilayers exist in a liquid-crystalline state. Image from (Cullis and Hope, 1985).

(B): Position of phospholipid diacyl chains; configuration change caused by rotation about one C-C single bond from a *trans* to *gauche* conformation. Image from (New, 1990)

(A)

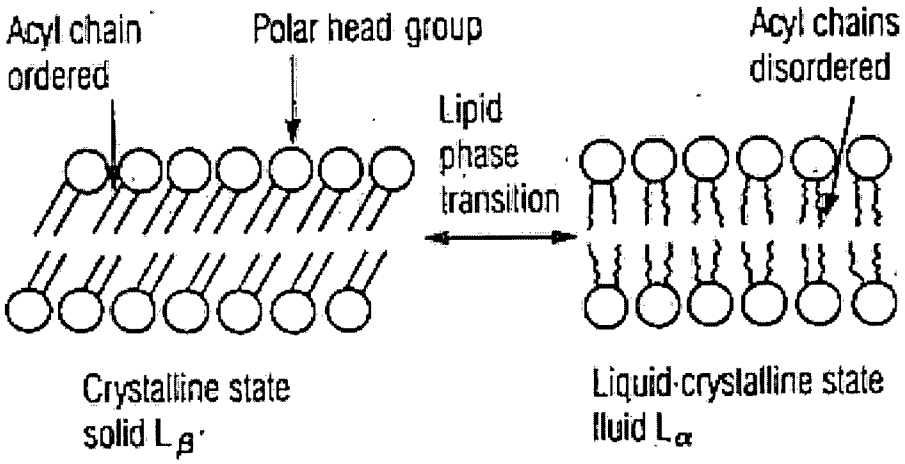

(B)

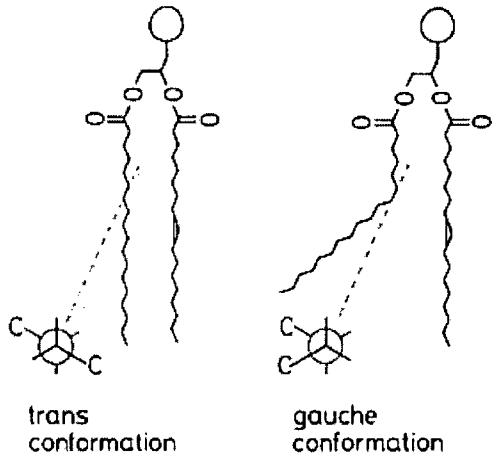

The distinctive Tc of a phospholipid bilayer has important implications in drug delivery. Drug encapsulation and release are dependent on several factors, one of which is the liposomes' physical state. At temperatures below the Tc, liposomes will be less permeable to drug. At temperatures above the Tc, where the liposome bilayer exists in the liquid-crystalline state, drug permeability generally increases.

1.2.5. Phospholipid-Cholesterol Bilayer

As indicated in section 1.2.2., cholesterol is a common constituent of liposome formulations. The effects of cholesterol in bilayers are dependent on the amount of cholesterol being incorporated and temperature. Increasing concentrations above 7 mole % cholesterol causes a decrease in the enthalpy of the phase transition, and concentrations of cholesterol above ~30 mole % eliminates detection of the gel-to-liquid crystalline phase transition (Figure 1.4.) (Chapman, 1975; Cullis and Hope, 1985).

Below the Tc of the lipid bilayer, the presence of cholesterol prevents the ordering and crystallisation of the lipid hydrocarbon chains (Needham et al., 1988). Cholesterol affects lipid packing by causing acyl chains to change from a tilted configuration to a vertical configuration and thus increases bilayer width (Needham and Nunn, 1990). A decrease of cohesive forces between acyl chains results from cholesterol intercalation. Cholesterol can thus increase the relative permeability of entrapped agents to bilayers below the Tc. If cholesterol containing lipid bilayers are at temperatures above the Tc, the most profound effect of cholesterol is the increase of order in the hydrocarbon matrix (Chapman, 1975). Cholesterol has a strong effect on the ordering of the upper portions of lipid acyl chains in relation to lower portions. The presence of cholesterol has a condensing effect on bilayers in

Figure 1.4. Cholesterol-Phospholipid Bilayers:

(A): Cholesterol-phospholipid mixtures can be thought of as an intermediary phase between the gel and liquid crystalline phases of pure lipid. Image from (Demel and De Kruyff, 1976).

(B): Cholesterol dramatically reduces the enthalpy of the phase transition (represented by the area under the endotherm). Image from (Houslay and Stanley, 1982).

(A)

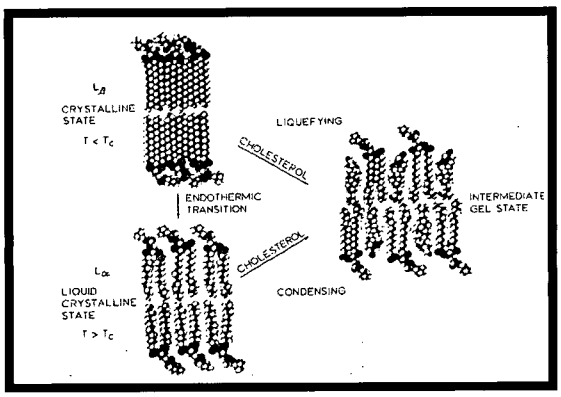

(B)

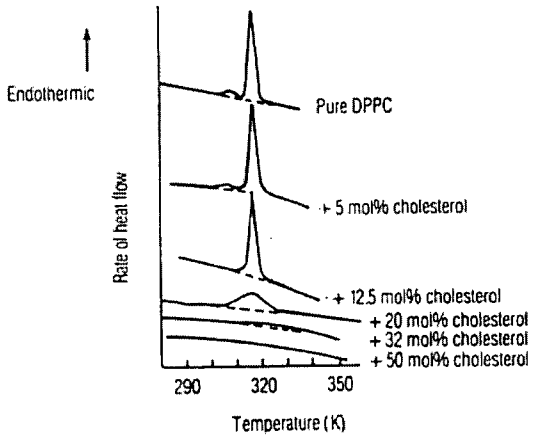

the liquid crystalline phase resulting in a general decrease in the permeability of drugs to the bilayer.

1.3. MANUFACTURING LIPOSOMES

Liposomes are characterised by their lipid composition, lamellarity and diameter, all of which govern their biological fate upon i.v. administration and therefore it is crucial to reproducibly prepare well-defined carriers.

1.3.1. Multilamellar Vesicles

Liposomes are classified by whether they have many concentric bilayers (multilamellar) or a single bilayer (unilamellar). Multilamellar vesicles (MLVs) can be prepared by simply adding an aqueous medium to a dried lipid film (Bangham et al., 1965). This method yields large structures (> 400 nm) with multiple membrane bilayers separated by aqueous channels (Figure 1.5.). The trapped volume (internal aqueous volume is typically measured as μl aqueous solution per μmole lipid) of MLVs is typically small due to membrane structures occupying the internal space (Mayer et al., 1985b). Because of their relatively small-trapped volume as well as large and heterogeneous sizes, MLVs do not typically serve as ideal lipid drug carriers for systemic administration.

1.3.2. Lipid Hydration and Solute Distribution

Variable solute distributions have been observed across the bilayers of liposomes produced by mechanically dispersing lipid, in an aqueous medium. Such distributions have been thought to arise from the hydration sequence when the dry lipid film contacts the

aqueous solution. Lipid on the surface of the dry film will first adopt a bilayer structure in response to the aqueous solution. Water can readily permeate through bilayers, but ions and other solutes permeate more slowly. Therefore the outermost bilayers act as a molecular sieve, allowing water to permeate through to achieve hydration of interior bulk lipid, but excluding solutes. This can lead to non-equilibrated solute distributions (Gruner, 1987; Gruner et al., 1985). Solute gradients contribute to interactions between bilayer properties and liposome morphology. When the inner and outer liposomal aqueous environments are of different concentrations, this leads to the formation of osmotic gradients. There is evidence that osmotic gradients of nonelectrolytes also change the bilayer properties by stretching the membrane and thereby altering the area per lipid (Gruner, 1987). Numerous approaches have been used to achieve better solute distribution across the membranes of MLVs including the stable pluri-lamellar vesicle method (Gruner et al., 1985), reverse phase evaporation method (Szoka et al., 1980) and freeze and thaw multilamellar method (Mayer et al., 1985b).

1.3.3. Large Unilamellar Vesicles

Unilamellar vesicles are structures containing a single bilayer membrane encapsulating an aqueous space and can be further classified as either small unilamellar vesicles (SUVs) (20-50 nm in diameter), large unilamellar vesicles (LUVs) (50-200 nm in diameter), or giant liposomes (> 500 nm). LUVs are the most commonly used delivery vesicles due to their improved structural stability with respect to smaller structures (< 50 nm), and larger entrapped aqueous volume (> 1μl/ μmole lipid) compared to other categories of vesicles (Hope et al., 1985; Mayer et al., 1985b). Large unilamellar vesicles in the size

range of 80-200 nm have also been shown to have an increased circulation lifetime in comparison to smaller (diameter < 70 nm) and larger (diameter > 300 nm) sizes following intravenous administration (Oku and Namba, 1994; Senior and Gregoriadis, 1982). Because of the significant advantages associated with LUVs as drug carriers, LUVs will be the focus of this section.

LUVs can be prepared using several procedures. Detergent dialysis methods involve the removal of detergent molecules from aqueous dispersions of phospholipid/detergent mixed micelles allowing the assembly of unilamellar vesicles (Enoch and Strittmatter, 1979). As the detergent is removed, the micelles become progressively richer in phospholipid and finally coalesce to form closed single-bilayer vesicles. Shortcomings of the approach include significant dilution during liposome formation, difficulty in removing the last traces of detergent after liposome formation, high cost and quality control (Hope et al., 1986).

Reverse phase evaporation is an alternative method involving dissolving lipids in immiscible organic solvents with the addition of an aqueous phase thereby allowing lipids to form an emulsion within the aqueous layer. Careful removal of the organic solvent under reduced pressure allows the phospholipid-coated droplets of water to coalesce. Removal of the final traces of solvent under high vacuum or mechanical disruption (such as vortexing) results in a suspension of LUVs or MLVs (depending on lipid composition). This method was pioneered by Szoka and Papahadjopoulos (Szoka and Papahadjopoulos, 1978), and is suitable for the encapsulation of water-soluble drugs demonstrating entrapment efficiencies up to 65% (Betageri et al., 1993). The size distribution obtained for most phospholipid mixtures is generally uniform, but preparations containing cholesterol have larger size distributions. This can be reduced (Szoka and Papahadjopoulos, 1980) by extrusion under low pressure

Figure 1.5. Multilamellar Vesicles, Large Unilamellar Vesicles and Small Unilamellar Vesicles. Schematic representations and freeze fracture electron microscopy images of:

(A) and (B): multilamellar vesicles (MLVs);

(C) and (D): large unilamellar vesicles (LUVs) and

(D) and (E): small unilamellar vesicles (SUVs). The bar in the freeze-fracture electron micrographs represents 200 nm with the arrow indicating the direction of shadowing. Image from (Madden, 1997).

Figure 1.5.

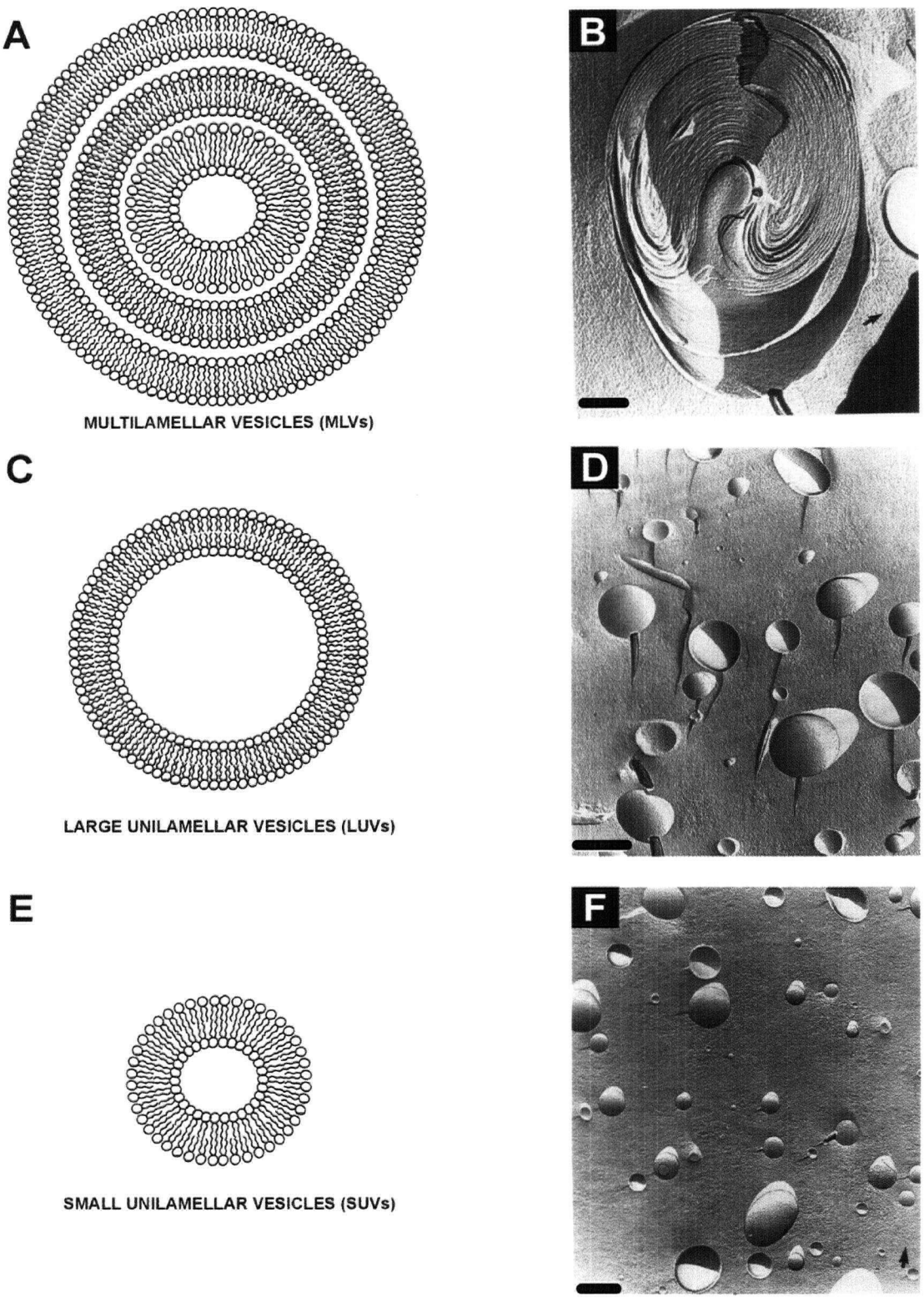
A
B
MULTILAMELLAR VESICLES (MLVs)
C
D
LARGE UNILAMELLAR VESICLES (LUVs)
E
F
SMALL UNILAMELLAR VESICLES (SUVs)

(~80 psi) though polycarbonate membranes (as described below).

The techniques described above for producing LUVs have major drawbacks, including the use of organic solvents and/or detergents during preparation, low entrapped aqueous volumes, time-consuming steps and the irreproducibility of liposome preparations. An alternative procedure to generate LUVs that avoids the use of both organic solvents and detergents, is the extrusion procedure. Extrusion methods are based on work (Hope et al., 1985; Olson et al., 1979) preparing LUVs by subjecting a lipid sample to pressure (approximately $\leq$800 lb/in^2 or 15 atm) through polycarbonate filters. Repetitious extrusion of a MLV lipid suspension through polycarbonate filters of a defined pore size, resulted in a homogenous population of unilamellar vesicles of uniform particle size. The extrusion procedure results in higher entrapped aqueous volumes, is rapid and leads to a well defined product in terms of size and reproducibility (Cullis et al., 1989; Hope et al., 1985), and is the procedure implemented to generate all liposome preparations used in this thesis.

1.3.4. Size of Large Unilamellar Vesicles

Particle size is an important indicator of batch-to-batch reproducibility and changes in liposome size can provide an indication of instability. The size distribution of liposomes is often difficult to estimate because no one technique can monitor all sizes present. The most accurate technique available to determine individual particle size is electron microscopy (Woodle and Papahadjopoulos, 1989). Because equipment associated with this technique may not be readily available to most laboratories, a less arduous and simpler way of determining the average particle size and the relative distribution for sample particles involves using a particle sizer (e.g. NICOMP 380 / DLS Submicron Particle Sizer). This

instrument employs a laser-based technique using quasi-elastic light scattering to determine the hydrodynamic equivalent diameter of particles. The advantage of this technique lies in the fact that information can be obtained relatively quickly from unimodal systems with mean diameters less than one micron, but caution must be taken for results obtained for heterogenous systems exhibiting bimodal or complex size distributions.

1.3.5. Characterisation using Cryo-Transmission Electron Microscopy

Cryo-Transmission Electron Microscopy (cTEM) is an important tool to derive information on the form and structure of liposomes as well as information on drug morphology within drug carriers. Using this technique, liposomes are rapidly frozen into a vitrified film without crystallisation thereby avoiding dehydration and re-organisation of the liposomes in the sample (Almgren et al., 2000). Images are obtained from the vitrified sample where contrast is due to differences in electron density between the atoms of the object being viewed in comparison to the surrounding solution. The three dimensional objects are imaged in two dimensions where objects such as spheres will appear as circles with high contrast around the edges due to the electron density being the greatest around the perimeter (see Figure 1.6.). A flat disk perpendicular to the microscope electron beam will appear as an evenly contrasted solid circle.

Cryo transmission electron microscopy is more often employed for liposomes due to the arduous drying, staining or fixation steps involved with conventional electron microscopy. With cTEM, liposomes can be directly applied to a microscope grid in order to obtain a thin film, followed by quickly vitrifying the sample to avoid crystallisation of water prior to observing the sample under the microscope.

Figure 1.6. Schematic Representation a Two Dimensional Image of Spheres and Flat Disks Obtained Using Cryo-Transmission Electron Microscopy. Image from (Almgren et al., 2000).

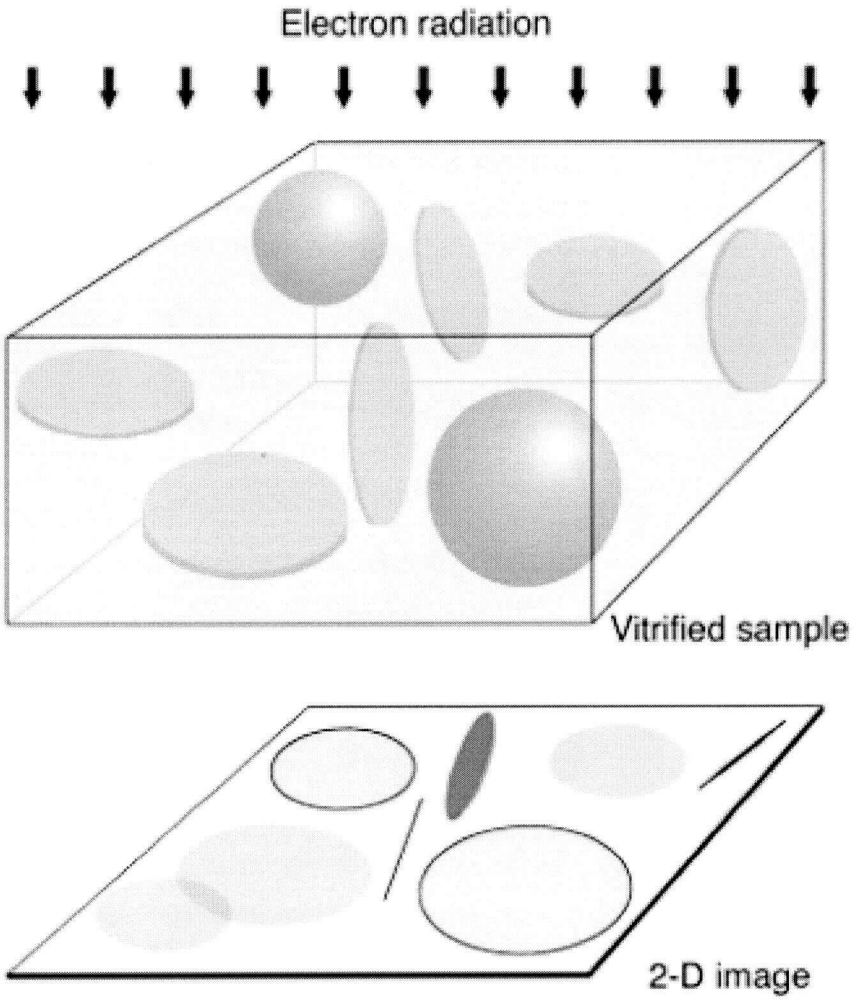

1.4. Drug Encapsulation

Liposomes as lipid-based drug carriers have the advantage of being able to sequester drugs within their aqueous interior. Because drugs vary considerably in their chemistry, the careful consideration of an appropriate encapsulation procedure for the specific drug of interest is crucial and often the liposome lipid composition must be selected for the drug based on empirical decisions. The selection of an appropriate encapsulation procedure is dependent on several factors. This thesis describes the encapsulation of three different anticancer agents within liposomes: doxorubicin, vincristine and topotecan. Liposomal formulations of these drugs are either presently FDA approved (doxorubicin (Myocet™ and Doxil®) (Tejada-Berges et al., 2002) or currently undergoing clinical (vincristine (ONCO-TCS)) (Gelmon et al., 1999) or pre-clinical trials (topotecan) (Tardi et al., 2000). Doxorubicin was initially used as a model drug to characterise the manganese sulfate encapsulation procedure (Chapter 3), a method that was also used to assess the feasibility of increasing doxorubicin-to-lipid ratios for thermosensitive formulations (Chapter 6). Doxorubicin was also used in conjunction with vincristine, where an encapsulation method was designed to trap multiple agents within a single liposome population (Chapter 5). Topotecan, a hydrophilic derivative of camptothecin, was also encapsulated using a manganese divalent cation-generated pH gradient (Chapter 4). The proceeding sections (1.4.1.1. - 1.4.1.3.) outline characteristics and drawbacks to each drug and the chemical attributes that aid in understanding encapsulation methodology as outlined in the subsequent chapters.

1.4.1. Encapsulated Agents

1.4.1.1. Doxorubicin

Doxorubicin Mode of Action

Doxorubicin (Figure 1.7.) is an anthracycline antibiotic originally isolated from *Streptomyces peucetius* var. *caesius* (Blum and Carter, 1974; Weiss et al., 1986). The precise mechanism of action of doxorubicin is not understood, however it is known to intercalate between DNA base pairs, resulting in DNA and DNA-dependent RNA synthesis inhibition due to template disordering and steric obstruction (Gewirtz, 1999; Simpkins et al., 1984). Intercalation leads to single and double strand breaks as well as exchange of sister chromatids. Scission of DNA is believed to be mediated through the action of topoisomerase II (Capranico et al., 1990) or by the iron-catalysed generation of free radicals, both hydrogen peroxide and hydroxyl, which are highly destructive to cells (Triton and Yee, 1982). Although it is active throughout the cell cycle, the maximal toxicity occurs during the DNA synthesis (S) phase (Kim and Kim, 1972). At low concentrations of drug, cells will continue through the S-phase, and die in G_2 (Hortobagyi, 1997).

Doxorubicin Toxicity

The therapy-limiting toxicity for this drug is cardiomyopathy, which may lead to congestive heart failure and death. Doxorubicin causes significant gastrointestinal toxicity with nausea, vomiting, diarrhoea, stomatitis and ulcerations of the mouth within 10 days after administration. Another dose-limiting toxicity for doxorubicin is that of a high incidence of myelosuppression, typically observed as leukopenia and thrombocytopenia. In severe cases, this may lead to neutropenic fever and sepsis, requiring hospitalisation (Krogh, 1994).

Figure 1.7. Chemical Structure of Doxorubicin

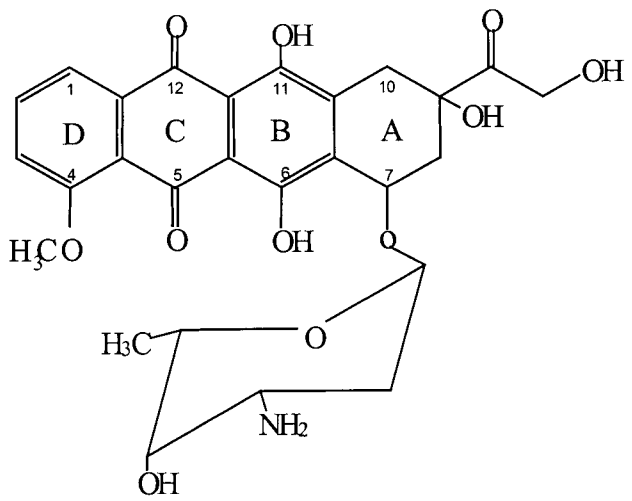

Doxorubicin Chemistry

Doxorubicin is typically available as a hydrochloride salt with a molecular formula of $C_{27}H_{29}NO_{11}$-HCl and a molecular weight of 579.99. Doxorubicin hydrochloride exists as a hygroscopic crystalline powder composed of orange-red thin needles. It is soluble in water ($\leq$35 mg/ml), methanol and aqueous alcohols. Doxorubicin has a melting point of 204-205°C and absorption maxima (in methanol) of 233, 252, 288, 479, 496 and 529 nm due to the dihydroxy-anthraquinone chromophore (Bouma et al., 1986). Doxorubicin has three significant prototropic functions with associated pK_a's: 1) the amino group in the sugar moiety (pK_1 = 8.15), 2) the phenolic group at C_{11} (pK_2 = 10.16) and 3) the phenolic group at C_6 (pK_3 = 13.2) (Bouma et al., 1986; Fiallo et al., 1998). Any variation of groups on the chromophore ultimately leads to changes in the absorption spectra, therefore the spectra depends on pH, binding ions and their concentration, drug concentration, solvent type and ionic strength (Bouma et al., 1986). Deprotonation of the chromophore results in a modification of the UV, visible and circular dichroic (CD) spectra causing a red shift due to

the deprotonation of the phenolic functions of the chromophore (Fiallo et al., 1998). Doxorubicin is documented to appear orange at pH = 7, violet at pH = 11 and blue at pH = 13 (Fiallo et al., 1999).

It has also been well documented that doxorubicin has a propensity to self-associate (Chaires et al., 1982; Menozzi et al., 1984). Self-association constants in the literature vary dramatically most likely due to differences in methods, experimental conditions, differences in pH and buffer compositions. Interactions between the π-electron systems have a measured thermodynamic value of ΔH = -33 kJ/mol (Bouma et al., 1986), making self-association a favourable interaction, with the mechanism of self-association being attributed to interactions between planar aromatic rings of individual molecules. The non-protonated neutral anthracycline is thought to be the dominant species involved in self-association (Menozzi et al., 1984).

Doxorubicin Indications

Doxorubicin is the most widely used member of the anthracycline antibiotic group of anticancer agents. It has been used successfully as a single agent and also in combination with other approved chemotherapeutics to treat acute lymphoblastic leukemia, Wilm's tumour, neuroblastoma, soft tissue sarcoma, bone sarcoma, breast carcinoma, gynecologic carcinoma, testicular carcinoma, bronchogenic carcinoma, lymphoma of both Hodgkin's and non-Hodgkin's types, thyroid carcinoma, squamous cell carcinoma of the head and neck, hepatic and gastric carcinoma (O'Niel, 2001b; Reynolds, 1989a; Weiss et al., 1986).

1.4.1.2. Vincristine

Mode of Action

Vincristine (Figure 1.8.), a vinca alkaloid, was discovered in 1959 and isolated from the plant *Vinca rosea* Linn. (*Catharanthus roseus*) of the family *Apocynaceae* (Madagascar periwinkle) (Sieber et al., 1976). The mode of action of vincristine has not been completely delineated. *In vitro* studies suggest that vincristine inhibits spindle formation and is associated with the initiation of the mitotic spindle in S-phase (Owellen et al., 1972). Vincristine specifically binds tubulin, the protein subunit of the microtubules that form the mitotic spindle (Sieber et al., 1976). The formation of vincristine-tubulin complexes prevents the polymerisation of the tubulin subunits into microtubules. This induces depolymerisation and results in inhibition of microtubule assembly and cellular metaphase arrest. At high concentrations, vincristine exerts complex effects on nucleic acid and protein synthesis (Owellen et al., 1976; Owellen et al., 1972). Vincristine also interferes with RNA synthesis, but it is not known if this effect is related to spindle formation inhibition. Vincristine is a cell cycle phase specific (S-phase) agent (Hill and Whelan, 1980).

Vincristine Toxicity

Vincristine's dose limiting toxicity includes neurological and neuromuscular effects. There is often a sequence in the development of neuromuscular side effects, with sensory impairment and paresthesias developing initially, and neuritic pain and motor difficulties developing with continued use. Walking may be impaired and the neurological effects may not be reversed for several months after the drug is discontinued (Reynolds, 1989b).

Figure 1.8. Chemical Structure of Vincristine. Figure from (O'Niel, 2001d).

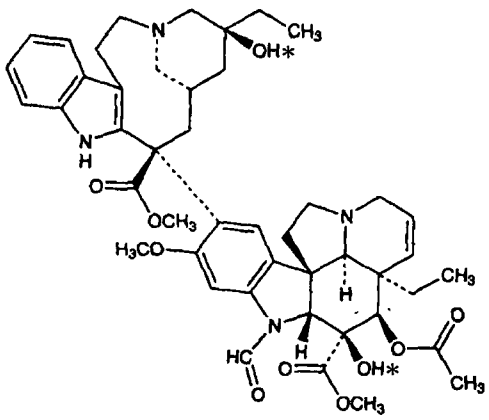

Vincristine Chemistry

Vincristine is distributed as a sulfate with a molecular formula of $C_{46}H_{56}N_4O_{10}$-H_2SO_4 and a molecular weight of 923.04 (Burns, 1972). Vincristine sulfate is a white to slightly yellow crystalline powder that is hygroscopic. Vincristine is freely soluble in water with solubility ≥10 mg/ml, and slightly soluble in 95% ethanol (< 1 mg/ml)(Burns, 1972). Vincristine sulfate has a melting point range of 273-281°C and has an ultraviolet spectrum with maxima of 221, 255 and 296 nm (Muhtadi and Afify, 1993). Vincristine has two titratable basic groups having pKa values of 5.0 and 7.4 (Burns, 1972; Svoboda, 1961).

Vincristine Indications

Vincristine is the second most widely used antineoplastic drug. It is used in the treatment of acute leukaemia and approved for use in Hodgkin's lymphomas, rhabdomyosarcoma, neuroblastoma and Wilm's tumour. It has also been used in combination with other antineoplastic drugs in Hodgkin's disease, soft-tissue sarcoma, bony-tissue sarcoma, sarcomas of specialised structures, breast cancer, small cell cancer of the

lung, cancer of the uterine cervix, malignant melanoma, colorectal cancer and non-Hodgkin's lymphoma. Vincristine is often a part of poly-chemotherapy because at the recommended doses it does not cause significant suppression of bone marrow (Gennaro, 1995; Reynolds, 1989b).

1.4.1.3. Topotecan

Topotecan Mode of Action

Topotecan (Figure 1.9.) is a semisynthetic water-soluble derivative of camptothecin, which is a cytotoxic alkaloid extracted from plants such as *Camptotheca acuminata* (Kingsbury et al., 1991; Wall et al., 1993). Topotecan specifically inhibits topoisomerase I, an enzyme that functions in DNA replication to relieve the torsional strain induced by the replication fork. Topotecan stabilises DNA-topoisomerase I covalent complexes, inducing breaks in DNA single strands that are converted to double strand breaks, eventually culminating in cell death (Hsiang et al., 1985; Hsiang and Liu, 1988; Hsiang et al., 1989). Topotecan is a cell cycle phase specific (S-phase) agent (Bahadori et al., 2001).

Topotecan Toxicity

The dose limiting toxicity of topotecan is leukopenia (primarily neutropenia) and is not cumulative over time (Takimoto et al., 1998). The clinical consequences of this myelosuppressive toxicity can be substantial with sepsis or febrile neutropenia. Non-hematologic toxicities associated with topotecan when given intravenously can include nausea and vomiting, alopecia, mucositis, elevated liver transaminases, skin rash and fever.

Topotecan Chemistry

The drug topotecan is distributed as a hydrochloride salt with a molecular formula of $C_{23}H_{23}N_3O_5$-HCl and a molecular weight of 457.9 (O'Niel, 2001c). Topotecan hydrochloride is a light yellow to greenish powder, with a melting point range of 213-218°C. The ultraviolet absorption maxima of topotecan include 207, 224, 269, 296, 318, 332, 371 and 384 nm in methanol (O'Niel, 2001c). Topotecan possesses an α-hydroxy-δ-lactone ring which hydrolyses under physiological conditions of pH ≥7. Hydrolysis of the lactone ring E (Figure 1.9. (B)) most probably involves the conversion of the lactone (A) to the corresponding acid (B) with post-equilibrium conversion of (B) to the carboxylate form (C) at pH values greater than the pKa for COOH (pKa^{COOH}~4) (Fassberg and Stella, 1992). The opening of this ring under alkaline conditions to form the acid salt or carboxylate species results in the loss of *in vitro* activity and apparent diminished *in vivo* anticancer activity (Jaxel et al., 1989). A closed lactone ring (ring E) is an important structural requisite for passive diffusion of drug into cancer cells as well as interaction with the topoisomerase I target (Hertzberg et al., 1989; Hsiang et al., 1985). Thus factors influencing the lactone-carboxylate equilibria of camptothecins are regarded as critical determinants of drug function.

Optical methods and quantum-chemical computations suggest that at concentrations of 1 x 10^{-5} M (or ~4.2 mg/ml), topotecan molecules start to form dimers. Topotecan dimerisation is accompanied by an increase in the pKa of a hydroxyl of ring (A) from 6.5 (topotecan concentration ~10^{-6} M) to 7.1 (topotecan concentration ~10^{-4} M), suggesting that this group is involved in dimer stabilisation probably through the formation of an inter-

Figure 1.9. Chemical Structure of Topotecan:

(A) Topotecan is reversibly hydrolysed to its hydroxy-carboxylate form at physiological pH.

(B) The hydrolysis of the lactone ring E, involves the conversion of the lactone to the corresponding acid, with post-equilibrium conversion to the carboxylate form (Fassberg and Stella, 1992).

(A)

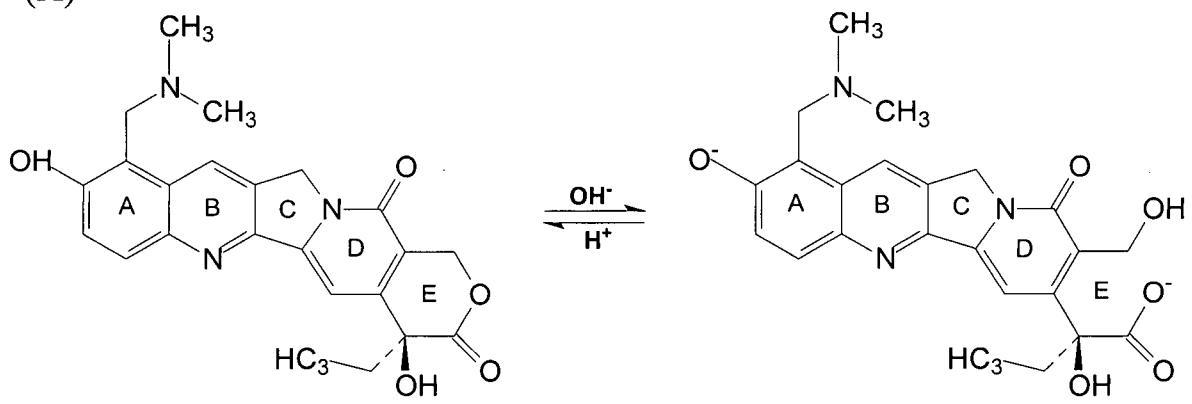

(B)

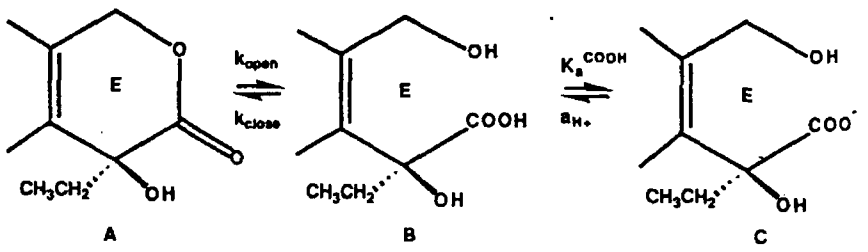

molecular hydrogen bond with N of the B ring of another topotecan molecule (Streltsov et al., 2001).

Topotecan Indications

Topotecan is approved for the treatment of metastatic carcinoma of the ovary after failure of initial or subsequent therapy. It is also approved for small cell lung cancer after failure of first-line chemotherapy (defined as recurrence at least 60 days after first-line chemotherapy). Topotecan has been shown to be active against gliomas, acute myelogenous leukaemia, chronic myelomonocytic leukaemia, non-small cell lung cancer, multiple myeloma, myelodysplastic syndrome, neuroblastoma, pancreatic cancer, retinoblastoma, rhabdomyosarcoma and Ewing's sarcoma (Broom, 1996; Dunton, 1997; O'Niel, 2001c).

1.4.2. Methods of Encapsulation

When generating a pharmaceutically viable liposomal drug formulation, one must consider several important factors. The methodology must be straightforward and conceptually easy. Drug-loaded liposomes must be uniformly generated with an optimal loading procedure that would approach 100% trapping efficiency at the desired drug-to-lipid ratio, therefore negating the need to remove unencapsulated drug from the sample. However, the chemical attributes of the drug often dictate which encapsulation procedure will be used.

1.4.2.1. Passive Encapsulation

Methods of drug encapsulation within liposomes are categorised as either passive or active. Passive encapsulation methods involve the addition of either hydrophilic or

hydrophobic drugs, to dried lipid film or as a part of an aqueous/solvent emulsion procedure. This method takes advantage of the fact that during the preparation of liposomes a certain aqueous volume is obtained within each liposome or relies on the ability of the drug to partition into the lipid bilayers. Drug and liposomes are co-dispersed with a certain fraction of the drug entrapped directly, resulting from the combination of the hydrophilic, hydrophobic and ionic interactions. With hydrophobic drugs, a portion of the drug will intercalate within the membrane and so entrapment efficiency is also dependent on the packing limitations of the drug within lipid bilayers. Typically, passive encapsulation methods are not efficient (Cullis et al., 1987) and a large portion of the drug added can be in a free form outside the liposome or as a non-liposomal structure. This depends on the solubility of the agent being trapped and the trapped volume of the liposomal formulation being made. Passive encapsulation methods require removal of unencapsulated drug. Although this can be accomplished easily in a laboratory setting, the methods for passive encapsulation are challenging for larger scaled productions of pharmaceutical batches for use in clinical trials.

1.4.2.2. Ion Gradient Mediated Encapsulation

Active encapsulation procedures typically involve the encapsulation of drug against the drug's concentration gradient where loading is dependent on temperature. Active encapsulation involves the addition of drugs with amine groups to pre-formed liposomes that possess a transmembrane pH gradient (Bally et al., 1985; Haran et al., 1993; Mayer et al., 1985a; Mayer et al., 1986b). Under appropriate conditions, when the drug is added to liposomes possessing such a gradient, a redistribution of the drug occurs such that the neutral

form of the drug crosses the liposomal bilayer and is subsequently trapped within the core of the liposome (Mayer et al., 1986a). Encapsulation occurs for reasons that involve the internal pH and perhaps drug precipitation, along with associated chemical reactions that affect the nature of the precipitate formed (Lasic et al., 1992; Madden et al., 1990). Active trapping procedures result in greater than predicted drug-to-lipid ratios based on theoretical models (Cullis et al., 1989; Lasic et al., 1995). Because virtually 100% of the drug is incorporated into liposomes, active encapsulation methods are cost efficient. These methods can also result in almost a 30-fold decrease of drug efflux, but this is dependent on a variety of factors such as internal solution composition, pH, lipid composition and the drug itself. Active encapsulation is performed after the preparation of liposomes and may be advantageous when working with labile drugs requiring immediate encapsulation prior to administration. Active encapsulation methods can be used with any lipid composition that is capable of forming a bilayer and maintaining a transmembrane ion gradient. These methods have been used to prepare liposomal doxorubicin formulations approved for clinical use, and because of the associated benefits of these procedures, active techniques have been pursued in all studies comprising this thesis.

For active procedures involving the use of transmembrane pH gradients, there are two general ways to impose the pH gradient across the liposome bilayer: directly or indirectly. To directly establish the trans-bilayer pH gradient, liposomes are prepared in the presence of an acidic buffer, and the exterior buffer of the liposomes is then adjusted to a desired pH using either added bases that increase the pH or alternatively exchanging the outside buffer using column chromatography or dialysis (Mayer et al., 1986b). It is critical that the pH gradient established across the bilayer is stable. Protons (H^+), relative to other cations, are

highly permeable (Deamer and Nichols, 1989). As H^+ diffuse outward they create an electrochemical gradient ($\Delta\Psi$ inside negative) (Harrigan et al., 1992) and this prevents/limits further H^+ efflux. Since this loading method relies on protonation of a drug that has permeated across the membrane, it is also critical to use a method that can ensure that the pH gradient is stable during drug loading. For direct methods, investigators typically rely on using an effective buffer present at high concentrations. A commonly used procedure to prepare liposomes with a transmembrane pH gradient relies on the entrapment of a 300 mM citrate buffer, pH 4.0 (Figure 1.10.(A)). Citrate is a triprotic buffer that possesses a large buffering capacity in the range of pH 3-6.5 (pKa_1 = 3.13, pKa_2 = 4.76, pKa_3 = 5.41 or 6.4) (O'Niel, 2001a).

Alternatively electrochemical gradients and ionophores can indirectly establish a pH gradient. For example, liposomes can be prepared in a potassium (K^+)-based solution and the external solution replaced with a sodium-containing solution by column chromatography or dialysis. In the presence of the created K^+ gradient, the addition of an ionophore such as valinomycin (a proton / K^+ exchanger) will shuttle K^+ to the liposomal exterior, thus creating an electrochemical gradient ($\Delta\Psi$), with the interior of the liposomes being negative. Stable electrical potentials in excess of 150 mV can be generated in LUVs using this technique (Redelmeier et al., 1989). Protons (H^+) cross the lipid bilayer into the interior in response to this $\Delta\Psi$ gradient, thus establishing a pH gradient (Cullis et al., 1991). It has been shown that this pH gradient is smaller than theoretically predicted for electrochemical equilibrium (Redelmeier et al., 1989).

By virtue of being able to exchange cations, other ionophores can also be used to form pH gradients from chemical gradients. Several researchers have documented both

nigericin (K^+ ionophore) and A23187 (divalent cation ionophore) exchange specific cations for either one or two protons, respectively (Fenske et al., 1998) (Figure 1.10.(D)). Liposomes possessing a transmembrane salt gradient (with the liposome interior containing either K_2SO_4 or $MnSO_4$) can be incubated with the specific ionophore and drug. The ionophores are able to transport the outward movement of cations for the inward movement of protons thus creating a pH gradient.

Another method capable of causing the formation of a pH gradient is one that relies on the encapsulation of ammonium sulfate (Bolotin et al., 1994; Haran et al., 1993) (Figure 1.10.(B)). Following the encapsulation of $(NH_4)_2SO_4$, the external solution is exchanged to a solution such as 145 mM NaCl to establish a $(NH_4)_2SO_4$ gradient. Due to the high permeability of NH_3 ($1.3x10^4$ cm/s), it readily crosses the liposome bilayer, leaving behind one proton for every molecule of NH_3 lost (Bolotin et al., 1994). This creates a pH gradient, the magnitude of which is determined by the $[NH_4^+]_{in}$ /$[NH_4^+]_{out}$ gradient. This approach differs from other chemical methods, in that the liposomes are not prepared in a very low pH buffer, or is there a need to alkalinize the exterior liposome solution.

Active loading methods have traditionally been dependent on an established and/or a created transmembrane pH gradient, with the intent to accumulate drug to levels within the liposome that exceed the solubility of the drug (Madden et al., 1990). Transmembrane pH gradients across the liposome can result in drug precipitation, through drug self-association or through interaction with salts present in the aqueous core of the liposome. Alternatively, the concentration inside the liposome may exceed the solubility of the agent being trapped. Others have suggested that drug partitioning into the inner leaflet of the liposomal membrane may account for drug loading in excess of that which may be predicted based on the gradient

Figure 1.10. Methods of Doxorubicin Encapsulation into Liposomes Exhibiting Ion Gradients:

(A) The citrate loading procedure. Liposomes are prepared in 300 mM citrate buffer, pH 3.5, and outside buffer is exchanged to HEPES buffered saline at pH 7.5.

(B) The ammonium sulfate loading procedure. Liposomes are prepared in 250 mM ammonium sulfate, pH 5.5, and outside solution is exchanged to 145 mM sodium chloride pH 5.5.

(C) The manganese sulfate loading procedure. Liposomes are prepared in 300 mM manganese sulfate, pH 3.5, and outside solution is exchanged to 300 mM sucrose / 20 mM HEPES / 15 mM EDTA at pH 7.5.

(D) The manganese sulfate loading procedure with the A23187 ionophore. Liposomes are prepared in 300 mM manganese sulfate, pH 3.5, and outside solution is exchanged to 300 mM sucrose / 20 mM HEPES / 15 mM EDTA at pH 7.5 with the A23187 added to the liposomes prior to doxorubicin addition. Figure from (Abraham, 2004).

Figure 1.10.

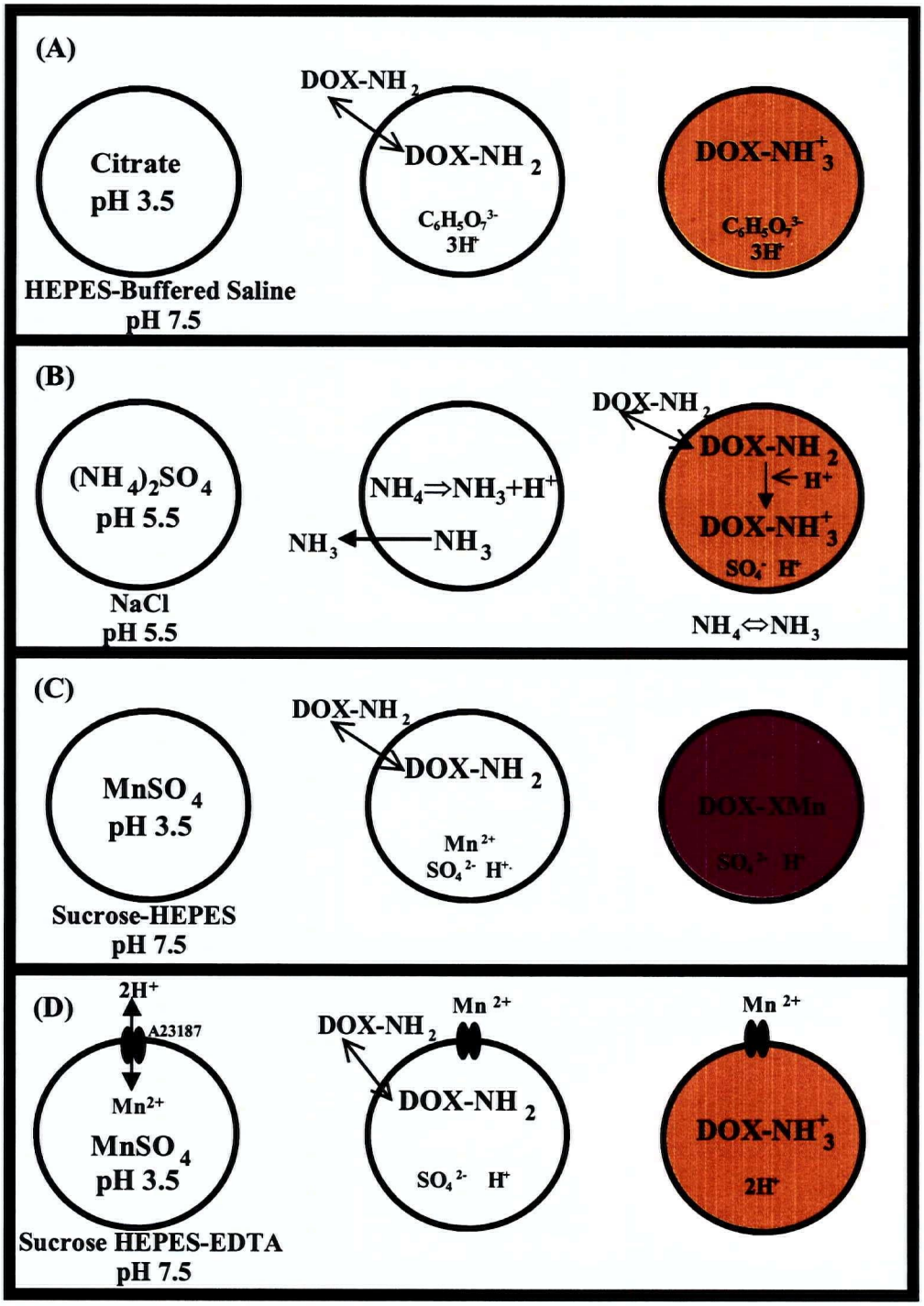
(A)
Citrate
pH 3.5
HEPES-Buffered Saline
pH 7.5
DOX-NH2
DOX-NH2
C6H5O7 3-
3H+
DOX-NH+3
C6H5O7 3-
3H+
(B)
(NH4)2SO4
pH 5.5
NaCl
pH 5.5
NH4⇒NH3+H+
NH3
NH3
DOX-NH2
DOX-NH2
H+
DOX-NH+3
SO4- H+
NH4⇔NH3
(C)
MnSO4
pH 3.5
Sucrose-HEPES
pH 7.5
DOX-NH2
DOX-NH2
Mn 2+
SO4 2- H+
DOX-XMn
SO4 2- H+
(D)
2H+
A23187
Mn2+
MnSO4
pH 3.5
Sucrose HEPES-EDTA
pH 7.5
DOX-NH2
Mn 2+
DOX-NH2
SO4 2- H+
Mn 2+
DOX-NH+3
2H+

used to facilitate drug uptake (Harrigan et al., 1993).

Recently there has been a study describing a novel active encapsulation procedure that potentially relied on metal complexation rather than a pH transmembrane gradient (Cheung et al., 1998). Work from this thesis (Abraham et al., 2002) suggests that manganese can theoretically bind doxorubicin at three sites: 1) the anthraquinone (hydroxyketone) moiety at the C_5-C_6, 2) the anthraquinone (hydroxyketone) moiety at the C_{11}-C_{12} position, and 3) the side chain at C_9 possibly in combination with the C_9 hydroxyl position and the amino-sugar group at the C_3-C_4 position (see Figure 1.7). Until this point, active encapsulation procedures have solely depended on a protonation mechanism to trap agents using pH gradients by creating a charged species that has a decreased permeability across liposome membranes. This thesis was initiated from investigations pursuing a novel active encapsulation procedure using metal complexation as a method of entrapment instead of protonation.

1.4.2.3. Encapsulation Efficiency

Once an appropriate encapsulation method has been chosen for a specific drug, there are several parameters that require experimental evaluation. Drug encapsulation efficiency must be determined. Encapsulation must occur within a time frame that does not compromise the established gradient (as will be described in Chapter 2 section 2.4.). Drug uptake requires incubation at specific temperatures. The time of incubation and the temperature are dependent on the drug, the lipid composition, the encapsulation methodology and the desired drug-to-lipid ratio. An optimal loading procedure exhibits encapsulation efficiencies of $\geq$90% or more. This limits the need for removal of non-entrapped material

and means costly drugs such as topotecan, can be efficiently loaded with minimal drug loss. Drug removal procedures such as dialysis and passage through an exclusion column can be used to remove unencapsulated drug, if necessary.

1.4.2.4. Drug-to-Lipid Ratio

Accumulation of drug, or alternatively, the release of drug from liposomes, can be quantified by measuring the drug-to-lipid ratio as a function of time. This is determined by initially separating unencapsulated drug from encapsulated, quantifying each component and subsequently calculating the ratio of drug associated with lipid. The optimum drug-to-lipid ratio of a particular liposomal formulation is generally dictated by the biological efficacy and toxicity of the preparation itself. From a pharmaceutical point of view, high drug-to-lipid ratios are more economical. From a biological perspective, high drug-to-lipid ratios are often considered to be therapeutically better. Often however, the drug-to-lipid ratio selected is based on parameters that may dictate drug release prior to or following administration.

1.4.2.5. Drug Release

Once encapsulated within liposomes, the drug must be retained until administration, upon which the drug should then be released at a controlled and defined rate to favourably alter the pharmacokinetics and biodistribution of the drug. The latter parameters are typically defined empirically in animal models while the former are defined in *in vitro* assays. The encapsulated drug should be trapped at high concentrations, existing in a well-buffered environment. The drug-loaded sample must exhibit drug release rates that are conducive to improvements in drug activity, through decreases in toxicity or increases in efficacy (Mayer

et al., 1994). In the extreme, rapid (instantaneous) doxorubicin release from liposomal formulations immediately following i.v. administration will result in a drug that is substantially no different from the free, unencapsulated drug. Such a formulation would typically not be classified as a drug carrier. In the opposite extreme, complete drug retention (no drug release) should, theoretically, result in a formulation that is neither toxic nor efficacious. Such a formulation may exhibit substantial improvements in drug delivery to sites of tumour growth and substantial reductions in drug delivery to cardiac tissue, but such a formulation would be of little therapeutic value or interest (Cullis et al., 1991). Thus *in vivo* drug release parameters between these extremes have become the goal to which liposomal formulations have been developed toward.

Drug Release in Vivo

In order to determine drug release from liposomes *in vivo*, a marker for liposomes is required. Liposome markers must remain stable on administration *in vivo* and remain associated with the intact liposome. They must also be rapidly cleared from the body once released from liposomes and should also be easily quantifiable (Allen et al., 1995). Liposome markers can be either associated with the lipid bilayer of the carrier or alternatively can be encapsulated within the liposomal interior aqueous compartment. In this thesis, both ^{3}H-cholesteryl hexadecyl ether (^{3}H-CHE) or ^{14}C-cholesteryl hexadecyl ether (^{14}C-CHE) have been used to estimate liposome levels in the plasma compartment (with doxorubicin quantified using its spectral properties and vincristine quantified using ^{3}H-vincristine sulfate). These lipid markers have been shown to incorporate within lipid bilayers

without significant alteration to the bilayer itself and demonstrate low rates of exchange out of liposomes (Pool et al., 1982).

1.4.2.6. Biological Factors Affecting Drug Release of Systemically Administered Liposomes

Studies indicate that liposomes can be rapidly removed from the circulation when administered *in vivo,* and their biological fate is governed by liposome interactions with the components of the blood compartment. Some have suggested that there appears to be a good correlation between total protein binding and liposome clearance (Semple et al., 1996), but the role of serum protein binding and liposome elimination remains an area of active interest (Allen et al., 2002; Johnstone et al., 2001). The individual protein binding profiles will differ depending on lipid composition, and specific proteins may play an important role in liposome elimination and stability *in vivo*. Many apolipoproteins, namely apo A-I, A-II, A-IV, B, C, and E have all been shown to interact with liposome membranes, and several can cause liposome disruption (Guo et al., 1980; Kamps and Scherphof, 1998; Williams et al., 1998). Class B scavenger receptors (SR-B) have also been shown to recognise liposomes containing phosphatidyl serine (Sambrano and Steinberg, 1995). Liposomes have been documented to interact with high density lipoproteins (HDL) or low density lipoproteins (LDL) (Hunter et al., 1982). High density lipoproteins have the ability to destabilise liposomes, most likely through the removal of phospholipids from the bilayer. Cholesterol has been shown to confer stability to phospholipid bilayers; net phospholipid transfer from liposomes to HDL was found to be suppressed by cholesterol (Damen et al., 1981). This destabilising role of

lipoproteins also can be minimised by the presence of surface associated polymers that can reduce the rate of lipoprotein interaction with liposomes (Woodle and Lasic, 1992).

Not all elimination mechanisms are protein-mediated. Alterations in liposome lipid composition over time may occur due to the net transfer of lipid components to cell membranes (Margolis et al., 1982) resulting in a net loss of liposomal membrane components that may be important in prolonging circulation times. Liposomes appear to be more stable in whole blood than in serum, which may be due to a HDL-erythrocyte interaction predominating over the HDL-liposome interaction (Guo et al., 1980). It is also possible that cholesterol transfers from erythrocytes to liposomes (Poznansky and Lange, 1978).

Liposomes are also recognised by the immune system and eliminated in two different ways. Phagocytic cells that comprise the mononuclear phagocyte system (MPS) can recognise particulate carrier systems as 'foreign'. Distribution to these phagocytic cells is dependent on the physical (size) and chemical (charge) attributes of the liposomes used (Scherphof et al., 1981). It should be noted that when liposomes contain a cytotoxic drug, the cells of the MPS can be adversely affected. For example, following uptake into phagocytic cells, the release of doxorubicin can cause these cells to die, thus reducing the capacity of the MPS to accumulate liposomes. This is reflected, in turn, by significantly increased liposome circulation lifetimes (Bally et al., 1990).

Earlier work elucidating mechanism of action of the complement system revealed that when liposomes are prepared from a lipid mixture extracted from sheep erythrocytes, they are susceptible to immune lysis when incubated with antiserum against sheep erythrocytes and a source of complement (Haxby et al., 1968; Kinsky, 1972). This work clearly shows that the full action of the complement system only requires a lipid membrane. This means

that liposomes, depending on lipid components can be lysed, through a complement-mediated pathway, provided surface antigens and the corresponding antibodies are present. The extent of damage will depend on the lipid composition of the liposomes (Cunningham et al., 1979).

The acute phase protein CRP (C-reactive protein) was also shown to initiate complement, analogous to antibody-antigen interactions (Kaplan and Volanakis, 1974). CRP binds specifically to phosphatidylcholine (PC) (Volanakis and Kaplan, 1971) and has been shown to activate the complement system following interaction with PC containing liposomes (Richards et al., 1977). It has been demonstrated that CRP binding to PC liposomes is drastically increased by the incorporation of lysophosphatidylcholine in the lipid bilayer. It has been suggested that CRP may act specifically on damaged cell membranes (Volanakis and Wirtz, 1979).

1.5. WORKING HYPOTHESIS AND OVERALL GOAL

Liposome anticancer drugs are having a therapeutic impact in the treatment of patients with cancer. To date encapsulation methods have relied on either passive or active encapsulation techniques. Passive encapsulation methods are dependent on using agents that are very soluble in water or conversely very lipid soluble. The latter property has proven to be of limited interest because such encapsulated agents tend to rapidly dissociate from the liposome *in vivo*. The pH gradient-based techniques are limited because they are dependent on using an agent that is membrane permeable in the neutral form, and membrane impermeable in the charged form. The presence of a protonizable function on certain drugs can facilitate such drug loading. Another potential loading mechanism has been described in

this thesis, one where loading is achieved through drug complexation to the transition metal manganese. We hypothesise that such metal complexation reaction provides an alternative loading method with the potential to achieve improved liposome drug carrier formulation properties.

The overall goal of this project is to further the understanding of ion gradient-based encapsulation methodology. Active encapsulation procedures for loading drugs into liposomes result in high drug-to-lipid ratios with correspondingly high encapsulation efficiencies. To date, active encapsulation procedures have relied on the use of pH gradient loading-based techniques, a procedure that is limited to encapsulating drugs containing protonizable chemical groups. Based on evidence from a study describing a new encapsulation procedure, we propose that a new active encapsulation procedure could be developed based on metal complexation. This would in turn contribute novel attributes to drug loading not achievable using pH gradient loading techniques. Specific objectives of this thesis were to:

(1) Demonstrate that anticancer drug loading can be achieved through the use of transition metal complexation reactions and that loading can be achieved in the absence of a pH gradient.

(2) Given the potential of manganese containing liposomes to encapsulate single anticancer drugs though transition metal complexation and ionophore mediated pH gradient formation, evaluate the potential of these liposomes to encapsulate two agents.

(3) Characterise the use of manganese complexation to promote increased anticancer drug loading in a novel thermosensitive liposome that exhibits limited encapsulation efficiencies when loading relies on pH gradient loading.

CHAPTER 2

MATERIALS AND METHODS

2.1. MATERIALS

Doxorubicin hydrochloride for injection (10 mg doxorubicin with 52.6 mg lactose) (Faulding, QU, Canada) or doxorubicin hydrochloride (pure) (Hande Tech Development, TX, USA), vincristine sulfate for injection (5 mg vincristine sulfate with 500 mg mannitol) (Faulding, QU, Canada) and topotecan hydrochloride for injection (4 mg topotecan hydrochloride with 48 mg mannitol and 20 mg tartaric acid) (SmithKline Beecham, ON, Canada) were purchased from the BC Cancer Agency. 1,2-distearoyl-*sn*-glycero-3-phosphocholine (DSPC), 1,2-dimyristoyl-*sn*-glycero-3-phosphocholine (DMPC), 1,2-dipalmitoyl-*sn*-glycero-3-phosphocholine (DPPC), 1-stearoyl-2-hydroxy-*sn*-glycero-3-phosphocholine (MSPC) and 1,2-distearoyl-*sn*-glycero-3-phosphoethanolamine-N-[Methoxy(polyethylene-glycol)$_{2000}$] (DSPE-PEG) were purchased from Avanti Polar Lipids (AL, USA). Cholesterol (Chol), A23187 ionophore, Sephadex G-50 and all other chemicals were obtained from the Sigma Chemical Company (MO, USA). (^{3}H)-cholesteryl hexadecyl ether (^{3}H-CHE) and (^{14}C)-cholesteryl hexadecyl ether (^{14}C-CHE) were obtained from NEN Life Science Products (MA, USA). ^{3}H-vincristine sulfate was obtained from Amersham Pharmacia Biotech (ON, Canada). Pico-Fluor15 and 40 scintillation fluid was purchased from Canberra-Packard (CT, USA). Balb/c mice and SCID RAG-2M mice (8-10 weeks of age) were obtained from the BC Cancer Agency Joint Animal Facility breeding colony and were housed in microisolator units according to established operating procedures. CD-1 mice (8-10 weeks of age) were obtained from Charles River Laboratories (QU, Canada).

Fetal bovine serum was obtained from Hyclone Laboratories (UT, USA). The MDA435/LCC6 human breast cancer cell line was a gift from Dr. Robert Clarke (Georgetown University, WA, USA). Cell culture medium was composed of Dulbecco's Modified Eagle's Medium (DMEM) (Stem Cell Technologies, BC, Canada) supplemented with 10% fetal bovine serum from Hyclone Laboratories (UT, USA), 1% L-glutamine, and 1% penicillin and streptomycin solution (Stem Cell Technologies, BC, Canada).

All animal studies were done according to procedures approved by the University of British Columbia Animal Care Committee. These studies met the requirements outlined in the guidelines for animal use established by the Canadian Council of Animal Care.

2.2. PREPARATION OF LARGE UNILAMELLAR VESICLES

Lipids (approximately 100 mg of DMPC/Chol 55/45 mol%, DSPC/Chol 55/45 mol% or DPPC/MSPC/DSPE-PEG 90/10/4 mol ratio) were dissolved in chloroform, and ^{3}H-CHE or ^{14}C-CHE was added to achieve approximately 5-10 μCi/100 mg lipid. Chloroform was removed under a gentle stream of nitrogen gas and subsequently the lipid samples were placed under a high vacuum for at least 3 h to remove residual solvent. Dried lipid films were hydrated with either 300 mM $MnSO_4$ (adjusted to pH 3.5 with 0.1 N HCl, 250 mM $(NH_4)_2SO_4$ (~pH 5.1), 150 mM or 300 mM citrate (adjusted to pH 3.5 with 0.1 N HCl) or 300 mM $MnCl_2$ (adjusted to pH 3.5 with 0.1 N HCl) to achieve a final lipid concentration of 100 mg/ml. Following hydration, the MLVs (excluding the thermosensitive formulations) were subjected to 5 freeze-and-thaw cycles (freezing in liquid nitrogen and thawing at either 40°C (DMPC/Chol liposomes) or 60°C (DSPC/Chol liposomes) (Mayer et al., 1985b)). Samples were extruded 10 times through stacked polycarbonate filters with 0.1 and 0.08 μm pore size

10°C above the Tc of the phospholipid, using a water-jacketed Extruder™ (Northern Lipids Inc., BC, Canada). The mean size distribution of the resulting liposome preparations ranged between 100 and 120 nm as determined by a NICOMP Submicron Particle Sizer Model 270 (Pacific Scientific, CA, USA) with an argon laser operating at 632.8 nm.

All liposomes, except those used for cryo-transmission electron microscopy (cTEM) analysis and circular dichroism (CD) studies were radiolabeled. In the cTEM and CD experiments, the phospholipid was quantitated using the Fiske and Subbarow phosphate assay (Fiske and Subbarow, 1925). Briefly 700 µl of 70% perchloric acid was added to lipid samples and heated to approximately 180-200°C for two hours until the samples were colourless. Samples were cooled and 700 µl of Fiske reagent (789 mM sodium bisulfite/40 mM sodium sulfite/10 mM 1-amino-2-napthol-4-sulfonic acid (ANSA)) and 7 ml of ammonium molybdate (1.8 mM ammonium molybdate/20% H_2SO_4) were added with subsequent re-heating again to 100°C for 20 min. Samples were cooled to room temperature and the absorbance was read at 820 nm.

2.3. PREPARATION OF ION GRADIENTS FOR DRUG ENCAPSULATION

Large unilamellar liposomes (prepared as described in section 2.2) in the indicated solutions were fractionated on Sephadex G-50 columns (1 ml samples were placed on columns with at least a 20 ml column bed volume) equilibrated with various buffers at pH 7.5. For liposomes prepared with 250 mM $(NH_4)_2SO_4$ or 150 or 300 mM citrate, the external environment buffer was exchanged to 25 mM HEPES/150 mM NaCl (HBS). For liposomes prepared with 300 mM $MnSO_4$ and 300 mM $MnCl_2$, the external environment solution was exchanged to 300 mM sucrose/20 mM HEPES (SH) buffer and for liposomes prepared with

300 mM $MnSO_4$ and 300 mM $MnCl_2$ and loaded with the A23187, the external environment buffer was 300 mM sucrose/20 mM HEPES/15 mM EDTA (SHE).

The manganese sulfate-based procedure for doxorubicin loading was a modification of the method described by Cheung et al. (Cheung et al., 1998). In particular it should be noted that the solubility of 300 mM $MnSO_4$ is highly variable under the pH conditions described in the original procedure, presumably due to the formation of $Mn(OH)_{2(S)}$. In the studies reported in this dissertation, liposomes were prepared in 300 mM $MnSO_4$ or 300 mM $MnCl_2$ solution at pH of 3.5. In our hands, solutions of 300 mM $MnSO_4$ or 300 mM $MnCl_2$ at pH 3.5 are stable for months at room temperature.

2.4. DRUG ENCAPSULATION

2.4.1. Doxorubicin Encapsulation

Doxorubicin in solution (doxorubicin-hydrochloride and lactose dissolved in dH_2O) was added to either DMPC/Chol or DSPC/Chol liposomes to achieve a final drug-to-lipid ratio (wt/wt) of 0.2 at 20°C, 40°C and 60°C. For the thermosensitive liposomes, doxorubicin in solution (dissolved in dH_2O) was added to either DPPC/MSPC/DSPE-PEG liposomes to achieve a final drug-to-lipid ratio (wt/wt) of 0.1, 0.2, and 0.3 at 37°C. For pH gradient loading using $MnSO_4$ or $MnCl_2$ containing liposomes, the divalent cation ionophore A23187 (dissolved in ethanol (stock concentration 1 mg/ml)) was added to the indicated liposome preparations (Abraham et al., 2002; Fenske et al., 1998). A23187 is an electro-neutral ionophore capable of translocating a divalent cation for the exchange of two hydrogen ions (Wang et al., 1998). A23187 shuttles protons to the vesicle interior in exchange for Mn^{2+} ions, which are subsequently chelated by the EDTA contained in the SHE buffer. For

particular experiments, A23187 was added prior to addition of drug to reach a final ratio of 0.2/1.0 (μg A23187 / μmol lipid) which results in approximately 0.15-0.3% ethanol (final concentration) per loading sample. Unless otherwise stated for loading samples, the final lipid concentration was 5-10 mg/ml and the final doxorubicin concentration was 1-2 mg/ml. Accumulation of doxorubicin into liposomes was quantified at the indicated time points by removing 100 μl aliquots and separating unencapsulated drug from encapsulated drug on 1 ml Sephadex G-50 (medium) spin columns equilibrated with either HBS, SH, or SHE (spin columns were centrifuged at 680 x *g* for 3 min). An aliquot of the excluded fraction (flow-through: representing liposome-encapsulated drug) was adjusted to 100 μl with HBS, SH or SHE buffer to which 900 μl of 1% Triton X-100 was added to disrupt liposomes. Samples for the standard were prepared using known concentrations of doxorubicin (doxorubicin-hydrochloride dissolved in dH_2O) adjusted to 100 μl with HBS, SH or SHE buffer to which 900 μl of 1% Triton X-100 was added. Prior to assessing absorbance, the samples were placed in a > 90°C waterbath until the cloud point of the detergent was observed. The concentration of doxorubicin was determined by measuring absorbance at 480 nm using a Hewlett Packard 8453 Spectrophotometer.

2.4.2. Topotecan Encapsulation

Topotecan in solution (topotecan-hydrochloride and mannitol dissolved in dH_2O) was added to DSPC/Chol liposomes to achieve a final drug-to-lipid ratio (wt/wt) of 0.1, 0.2, 0.3 or 0.4 at 20°C, 40°C and 60°C. For particular experiments, A23187 (dissolved in ethanol (stock concentration 1 mg/ml)) was added prior to addition of topotecan and was added at an ionophore to yield a final ratio of 0.2 μg A23187 / μmol lipid. Unless otherwise stated, the

final lipid concentration was 1-2 mg/ml and the final topotecan concentration was 0.1-0.4 mg/ml.

Accumulation of topotecan into liposomes was quantified at the indicated time points by removing 100 μl aliquots and separating unencapsulated drug from encapsulated drug on 1 ml Sephadex G-50 (medium) spin columns equilibrated with either HBS or SHE (spin columns were centrifuged at 680 x *g* for 3 min). An aliquot of the excluded fraction (flow-through: representing liposome-encapsulated drug) was solubilized with n-octyl B-D-glucopyranoside (OGP) at a concentration of ≥25 mM and a final pH of 6. Samples for the standard were prepared using known concentrations of topotecan (dissolved topotecan-hydrochloride in dH_2O) with n-octyl B-D-glucopyranoside (OGP) at a concentration of ≥25 mM and a final pH of 6. The concentration of topotecan was determined by measuring the fluorescence (excitation: 407 nm (slit width 2.5 nm), emission: 520 nm (slit width 2.5 nm)). Total liposome lipid was determined by assessing amounts of ^{3}H-CHE. Small aliquots of the excluded fraction were added to 5 ml of scintillation cocktail and the radioactivity in the samples were subsequently determined by scintillation counting using a Packard 1900TR Liquid Scintillation Analyzer.

2.4.3. Vincristine Encapsulation

Vincristine in solution (vincristine sulfate and mannitol dissolved in dH_2O) was added to DSPC/Chol liposomes to achieve a final drug-to-lipid ratio (wt/wt) of 0.05, at 20°C, 40°C, 50°C or 60°C. For particular experiments, A23187 (dissolved in ethanol (stock concentration 1 mg/ml)) was added prior to addition of vincristine to reach a final ratio of 0.2

μg A23187 / μmol lipid. Unless otherwise stated, the final lipid concentration was 5 mg/ml and the final vincristine concentration was 0.25 mg/ml.

Accumulation of vincristine into liposomes was quantified at the indicated time points by removing 100 μl aliquots and separating unencapsulated drug from encapsulated drug on 1 ml Sephadex G-50 (medium) spin columns equilibrated with SHE (spin columns were centrifuged at 680 x *g* for 3 min). Levels of ^{3}H-vincristine and the liposome lipid (^{14}C-CHE) were quantified by scintillation counting (Packard 1900TR Liquid Scintillation Analyzer).

2.4.4. Co-Encapsulation of Doxorubicin and Vincristine

For experiments requiring co-encapsulation of doxorubicin and vincristine, doxorubicin was first encapsulated without A23187 into DSPC/Chol liposomes containing 300 mM $MnSO_4$. Doxorubicin was added to liposomes at 60°C, to achieve a final doxorubicin-to-lipid ratio (wt/wt) of 0.2. The doxorubicin-loaded liposomes were cooled to room temperature and A23187 (dissolved in ethanol (stock concentration 1 mg/ml)) was added to achieve an ionophore to lipid ratio of 0.2 μg / μmol. This mixture was incubated at 50°C for 5 min prior to vincristine addition. Vincristine in solution at 50°C was added to achieve a final vincristine-to-lipid ratio (wt/wt) of 0.05 and incubated for 60 min. Unless otherwise indicated, the final doxorubicin concentration was 1 mg/ml, the final vincristine concentration was 0.25 mg/ml and the final lipid concentration was 5 mg/ml for the co-encapsulated liposomes.

Accumulation of the co-encapsulated drugs into liposomes was quantified at the indicated time points by removing 100 μl aliquots and separating unencapsulated drug from

encapsulated drug on 1 ml Sephadex G-50 (medium) spin columns equilibrated with SHE (spin columns were centrifuged at 680 x *g* for 3 min). An aliquot of the excluded fraction (flow-through: representing liposome-encapsulated drug) was adjusted to 100 µl with SHE buffer to which 900 µl of 1% Triton X-100 was added to disrupt liposomes. Samples for the standard were prepared using known concentrations of doxorubicin (dissolved doxorubicin-hydrochloride in dH_2O) adjusted to 100 µl with SHE buffer to which 900 µl of 1% Triton X-100 was added. Prior to assessing absorbance, the samples were placed in a > 90°C waterbath until the cloud point of the detergent was observed. The concentration of doxorubicin was determined by measuring absorbance at 480 nm using a Hewlett Packard 8453 Spectrophotometer. ^{3}H-vincristine and liposome lipid (as measured using ^{14}C-CHE) concentrations were determined by scintillation counting (Packard 1900TR Liquid Scintillation Analyzer).

2.5. ABSORPTION AND CIRCULAR DICHROIC SPECTRA

To verify that manganese was binding doxorubicin, changes in doxorubicin absorption spectra under various proton and metal concentrations was determined using a Hewlett Packard 8453 UV-visible Spectroscopy System (cell path length = 1.00 cm). Doxorubicin-hydrochloride (no additives) was added to buffers at pH 6 (100 mM MES), pH 8 (100 mM HEPES), pH 9 (100 mM CHES), pH 10 (100 mM CAPS), pH 11 (100 mM CAPS) and pH 13 (100 mM glycine + 100 mM NaCl) at a constant doxorubicin concentration of 86 µM. Solutions of 300 mM $MnSO_4$ have a very low solubility in basic solutions. In order to circumvent this problem, $MnSO_{4\ (S)}$ (as indicated) was added to buffered solutions (in order to obtain final concentrations of 100 mM HEPES at pH 8) and

vigorously vortexed. Due to the formation of $Mn(OH)_2$ precipitate (within 12 hours), absorbance readings were done prior to formation of any visible precipitate. To monitor electronic state changes within doxorubicin-loaded liposomes, the CD spectra of each doxorubicin-loaded liposome preparation were analysed. CD measurements were obtained using the Jasco J-720 spectropolarimeter, which was calibrated using 0.06% (w/v) ammonium-d-10-camphorsulfonate. All spectra were recorded using a 0.1 cm cell and the following parameters: λ = 220-750 nm, step resolution = 1 nm, speed = 20 nm/min, response = 0.25 s, bandwidth = 1.0 nm. Results are expressed as differential molar circular dichroic absorption $\Delta\varepsilon$ ($M^{-1}cm^{-1}$), as defined by:

$$\Delta\varepsilon = \theta/32980 \times C \times l$$

where θ = molar ellipticity, C = Molar concentration, and l = path length of cell in cm.

2.6. DOXORUBICIN STABILITY

To assess the stability of doxorubicin within the manganese containing liposomes and confirm that manganese is not inducing doxorubicin degradation, high performance liquid chromatography (HPLC) was used to resolve intact doxorubicin. Drug-loaded liposomes (0.2 drug-to-lipid ratio, wt/wt) were incubated and at various time-points, 100 µl aliquots were placed onto 1 ml spin columns. The liposome lipid concentration was quantitated via liquid scintillation techniques and encapsulated doxorubicin was assayed using HPLC (Embree et al., 1993). HPLC was performed using a Waters Alliance 2690 HPLC system with a Waters 474 Fluorescence Detector set at an excitation wavelength of 480 nm and emission wavelength of 580 nm, controlled by Waters Millennium 32 software. Fifty microlitres of sample was injected onto a Waters Symmetry C18 column (4.6 x 75 mm) using

a mobile phase of 78% 16 mM ammonium formate solution, pH 3.5, 15% acetone and 7% isopropanol at 1 ml/min. Column temperature was maintained at 40°C and samples at 5°C.

2.7. DOXORUBICIN-MANGANESE BINDING

To assess doxorubicin binding to and dissociation from manganese, a spectrophotometric assay was developed. Changes in the A_{480} (ΔA_{480})(free doxorubicin) and ΔA_{550} (doxorubicin complexed to Mn^{2+}) were determined following addition of A23187. Doxorubicin-loaded liposomes were prepared as described above (without A23187) at a final lipid concentration of 1 mg/ml. After doxorubicin loading, the sample was diluted to 0.6 mg lipid/ml, A23187 (in ethanol (stock 1 mg/ml)) was added (0.2μg/μmol lipid) and the A_{400}-A_{600} measured. The Mn^{2+} complexed doxorubicin appeared purple in colour on visual inspection. As the pH gradient formed, resulting in dissociation of the metal-drug complex, the colour changed to an orange-red and the absorbance wavelength (Aλ) maximum shifted from 550 to 480 nm.

2.8. pH GRADIENT DETERMINATION

Transmembrane pH gradients were monitored using [^{14}C]-methylamine. Briefly, [^{14}C]-methylamine (0.5 μCi/ml) was added to a liposome solution containing < 10 mg/ml of lipid. After 30 min, 150 μl aliquots were passed through 1 ml Sephadex G-50 spin columns equilibrated in HBS to remove unencapsulated methylamine (column run time of 3-5 min). Lipid and methylamine concentrations before and after column chromatography were determined by scintillation counting. The transmembrane pH gradient was then calculated according to the relationship:

$$\Delta pH = \log\{[H^+]_{inside}/[H^+]_{outside}\} = \log\{[methylamine]_{inside}/[methylamine]_{outside}\}$$

Under the conditions employed, the exterior pH did not change during the uptake process.

2.9. CRYO-TRANSMISSION ELECTRON MICROSCOPY

Liposomes were prepared as described in section 2.2., without the ^{3}H-CHE lipid marker. In a humidified 25°C chamber, 1-2 µl of liposome sample (~1-5 mg/ml lipid)(before or after the addition of drug) was blotted onto copper grids coated with a cellulose acetate butyrate polymer. The samples were quickly vitrified by plunging into liquid ethane and transferred to liquid nitrogen keeping the sample below -165°C, therefore minimising sample pertubation and formation of ice crystals. The grid was transferred to a Zeiss EM902 transmission electron microscope where observations were made in a zero-loss bright-field mode and an accelerating voltage = 80 kV. All images presented are representative of the sample viewed.

2.10. IN VITRO DRUG RELEASE

Liposomes with encapsulated drug were mixed with fetal bovine serum such that the final lipid concentration was 0.4-2 mg/ml and the final serum concentration was 80%. These samples were incubated at 37°C and at the indicated time-points 100 µl aliquots were collected and unencapsulated drug was separated from encapsulated drug on 1 ml Sephadex G-50 (medium) spin columns equilibrated with buffer (spin columns were centrifuged at 680 x *g* for 3 min). The liposome lipid concentration was quantitated via liquid scintillation techniques and encapsulated doxorubicin (section 2.4.1.) or topotecan (section 2.4.2.) were assayed as described above.

2.11. IN VIVO DRUG RELEASE

2.11.1. Determination of Liposomal Lipid Concentrations in Plasma

Drug-loaded liposomes were adjusted to a lipid concentration required to administer a 100 mg/kg liposomal lipid or 20 mg/kg doxorubicin dose in an injection volume of 200 µl. This dose translates to approximately 41-46 µmol Mn^{2+}/kg for manganese containing formulations, which is well below the acute LD_{50} value of 272 µmol Mn^{2+}/kg (95% confidence limits: 227-326 µmol Mn^{2+}/kg) determined for mice (Niesman et al., 1990). Various formulations were injected intravenously (via the lateral tail vein) into 20-22 g mice. At 1, 4 and 24 hours after injection the animals were terminated by CO_2 asphyxiation and blood was collected by cardiac puncture and placed into EDTA coated microtainers. Plasma was prepared by centrifuging the blood samples at ~500 x *g* for 10 min. Plasma was removed carefully such that the buffy coat was not disturbed and collected into Eppendorf tubes. The liposome concentrations in the plasma were determined on the basis of the incorporated ^{3}H-CHE or ^{14}C-CHE markers. CHE has been shown to be non-exchangeable and non-metabolizable (Pool et al., 1982). Samples of 50 to 100 µl were mixed with 5 ml of PicoFluor-40 scintillation cocktail prior to assessing the radioactivity.

2.11.2. Determination of Doxorubicin and Vincristine Concentrations in Plasma

For *in vivo* studies that assessed doxorubicin and vincristine release, liposomes were prepared such that doxorubicin was loaded at a 0.2 drug-to-lipid ratio (wt/wt) and/or vincristine was loaded at a 0.05 drug-to-lipid ratio (wt/wt). For the doxorubicin loaded samples with or without A23187, doxorubicin in solution was added to liposomes and incubated at 60°C for ~15 min. The final lipid concentration was typically 12 mg/ml and the

final doxorubicin concentration was 2.4 mg/ml. For vincristine loading, vincristine in solution was added to liposomes (with an A23187 ionophore-to-lipid ratio of 0.2 μg/μmol) to achieve a drug-to-lipid ratio (wt/wt) of 0.05 and incubated at 50°C. The final lipid concentration was 12 mg/ml and the final vincristine concentration was 0.6 mg/ml. For the *in vivo* studies requiring co-encapsulated doxorubicin and vincristine, liposomes were prepared as described for the *in vitro* studies except the final doxorubicin concentration was 2.4 mg/ml, the final vincristine concentration was 0.6 mg/ml and the final lipid concentration was 12 mg/ml.

All drug loaded samples were fractionated on a Sephadex G-50 column equilibrated with HBS at pH 7.5 in order to remove the SHE buffer and/or the A23187 (Fenske et al., 1998). The drug-loaded liposomes were diluted with HBS to a lipid concentration required to administer a 10 mg/kg doxorubicin dose or a 2.5 mg/kg vincristine dose in an injection volume of 200 μl. The liposomal lipid dose was approximately 50 mg/kg. Formulations were injected via the lateral tail vein into 20-22 g female Balb/c mice. At 1, 4 and 24 h after injection the animals (4 mice per group) were killed by CO_2 asphyxiation and blood was collected by cardiac puncture and placed into EDTA coated microtainers. Plasma was prepared by centrifuging the blood samples at ~500 x *g* for 10 min. The liposomal lipid concentrations in plasma were measured on the basis of incorporated ^{14}C-CHE. Plasma vincristine concentrations were measured via the ^{3}H-vincristine marker.

Doxorubicin was extracted by mixing the plasma with 10% SDS and 10 mM H_2SO_4 (1/1/1), then adjusting the volume of the sample to 1 ml with H_2O followed by organic extraction with an isopropanol-chloroform solution (1/1) in a 2/1 ratio with the sample. To facilitate the precipitation of plasma proteins, the samples were frozen at -80°C for 48 h and

then thawed at room temperature. The doxorubicin-containing organic phase was separated by centrifugation at 3000 x *g* for 10 min at room temperature. Fluorescence in the organic phase was determined using a Perkin Elmer LS50B luminescence spectrometer using an excitation wavelength of 470 nm (slit width = 2.5) and an emission wavelength of 550 nm (slit width = 10). The fluorescence readings were compared to a standard curve of doxorubicin that was extracted into the organic phase using the procedure described above.

2.12. HUMAN BREAST CANCER XENOGRAFT MODEL

Tumours were established in SCID RAG-2M mice (four mice per group) by a single s.c. injection of 2 x 10^6 MDA435/LCC6 cells. Control mice were treated with 0.9% saline. Tumour growth was noted 12 to 14 days after cell injection and within 18 days, measurable tumours (~0.1 g) were observed. Animal weights and tumour weights were measured daily until the tumour mass exceeded 10% of the animals original body weight or until the tumours showed signs of ulceration. Tumour weight was calculated as weight (g) = [(width (mm))^2 x (length (mm))]/2. When the tumours reached 0.1 g, mice were treated with doxorubicin and/or vincristine (free or liposomal form) via the lateral tail vein. Liposomal drugs were prepared as described above (section 2.4.1., 2.4.3., and 2.4.4.) and exchanged into HBS using column chromatography prior to administration at the specified doses. All treatments were given in 200 µl injections, therefore when two drugs were combined the mice received two 200 µl injections separated by approximately 4 to 6 h with doxorubicin (free or encapsulated) injected first. Co-formulated liposomal doxorubicin and vincristine was administered in one injection of 200 µl. The control group received 200 µl of sterile saline injection.

2.13. MTT CYTOTOXICITY ASSAYS AND DRUG COMBINATION STUDIES

Logarithmically growing MDA435/LCC6 human breast cancer cells were counted and plated onto 96-well microtiter Falcon plates at a density of 2.0 x 10^3 cells / well in 0.1 ml of Dulbecco's Modified Eagle's Medium supplemented with 10% fetal bovine serum (FBS), 1% L-glutamine, 1% penicillin and streptomycin solution (Stem Cell Technologies, Vancouver, BC, Canada). The perimeter wells of the 96-well plates were not used and contained 0.2 ml of sterile water. After incubation for 24 h at 37°C in humidified air with 5% CO_2, the media in the wells were replaced with 0.2 ml of fresh media containing a range of concentrations of doxorubicin or vincristine. For drug combination studies, doxorubicin and vincristine were added simultaneously at fixed ratios of 4/1, 7/1 or 20/1 doxorubicin to vincristine (mol/mol). Control cells received 0.2 ml of medium. After 72 h incubation with drug, cell viability was assessed using a conventional MTT dye reduction assay. Fifty microliters of 1.25 mg/ml MTT reagent in complete media was added to each well and the plates were incubated for 3.5 h at 37°C. The coloured formazan product was then dissolved using 200 µl of DMSO. Plates were read (A_{570}) using a microtiter plate reader (Dynex Technologies Inc., Chantilly, VA).

The percentage of cell survival following treatment was normalised to untreated controls. All assays were performed at least three times in triplicate. To determine the IC_{90}, CalcuSyn software (Biosoft, MO, USA) was used to analyse data from the MTT assays. The program provides a measure of whether the combined agents act in an additive, synergistic or antagonistic manner. The combination index (CI) equation in CalcuSyn is based on the multiple drug-effect equation of Chou and Talalay (Chou and Talalay, 1984) and defines synergism as a more-than-expected activity effect and antagonism as a less-than-expected

additive effect. Chou and Talalay defined the parameter, CI, which can be based to assess synergism ($CI < 1$), additivity ($CI = 1$) or antagonism ($CI > 1$).

2.14. STATISTICAL ANALYSIS

For data obtained from drug elimination profiles and tumour growth of treated mice, one-way ANOVA with Student-Newman-Keuls Multiple Comparisons Test was performed using GraphPad InStat version 3.00 for Windows 95 (GraphPad Software, San Diego, California, USA). Differences were considered significant at $p < 0.05$.

CHAPTER 3

FORMATION OF TRANSITION METAL-DOXORUBICIN CHELATES INSIDE LIPOSOMES *

3.1. INTRODUCTION

Liposome encapsulation procedures that have been developed for drugs with protonizable amine functions involve the addition of drug to preformed liposomes possessing a pH gradient or an ion gradient capable of generating a pH gradient (Bally et al., 1988; Mayer et al., 1990b). Encapsulation relies on the neutral form of the drug penetrating through the lipid bilayer, where the drug encounters an acidic environment. The drug becomes protonated, charged and thus is retained within the liposome interior (Madden et al., 1990; Mayer et al., 1985a). As more of the neutral form of the drug enters the liposome and is protonated, the amount of the neutral form on the exterior of liposomes will be depleted as the drug equilibrates across the membrane according to the Henderson-Hasselbalch equation. Protons (H^+) are (relative to other cations) highly permeable across the lipid bilayer and will diffuse outward creating an electrochemical gradient ($\Delta\Psi$ outside positive) (Harrigan et al., 1992), but this process will cease at a certain point due to the generation of an electrochemical gradient ($\Delta\Psi$ negative inside) (also refer to Chapter 1 section 1.4.2.2.).

It is known that gradient based trapping procedures can result in entrapped drug levels that greatly exceed those predicted on the basis of an equilibrium established in accordance to the measured proton gradient. This is exemplified by the anthracycline

*Published in Biochimica et Biophysica Acta 1565 (2002) 41-54

doxorubicin. It has been argued that the higher than predicted drug levels can be accounted for by calculations that consider drug membrane partitioning (Cullis et al., 1997). The more generally accepted explanation is based on the formation of an insoluble drug precipitate (Lasic, 1996; Lasic et al., 1992; Li et al., 2000; Li et al., 1998). Cryo-transmission electron microscopy (cTEM) reveals doxorubicin precipitates as fibrous-bundle aggregates in both citrate and sulfate containing liposomes (Lasic et al., 1992; Li et al., 1998). Recently, certain researchers have suggested that the physical state of doxorubicin may also play a role in drug release (Li et al., 2000). It is argued here that attempts to use ion gradient-based procedures to prepare drug loaded liposomes exhibiting optimised drug pay-out characteristics have been stymied, in part, by our lack of understanding of the physical and chemical characteristics of the encapsulated drug. For this reason studies evaluating the role of doxorubicin precipitation in controlling the rate of drug release *in vivo* have been conducted. Our investigation differentiates between a drug loading method which results in formation of a transition metal-doxorubicin complex as compared to either citrate- or sulfate-based fibrous aggregates, and suggests that drug release from liposomes is dependent on a combination of internal pH, membrane lipid composition as well as the nature of the drug precipitate.

3.2. RESULTS

3.2.1. The Encapsulation of Doxorubicin into DMPC/Chol Liposomes using the Citrate Loading Procedure or the Manganese Sulfate Loading Procedure

The first objective of this study was to compare the $MnSO_4$ loading procedure (Cheung et al., 1998; Maurer-Spurej et al., 1999) to the citrate-based loading method, using doxorubicin as a model drug. The citrate loading procedure relies on an established pH gradient across the liposome bilayer and the use of encapsulated 300 mM citrate as a buffer to minimise changes in interior pH as doxorubicin redistributes across the liposomal membrane according to the transmembrane gradient (interior acidic) (See Figure 3.1.(A)). It should be noted that when doxorubicin is encapsulated using this method, the resulting drug-loaded liposomes appear as a bright opaque orange colour. When doxorubicin is encapsulated using the $MnSO_4$-based loading procedure described by Cheung *et al.* (Cheung et al., 1998) (Figure 3.1.B and Figure 3.1.C), a pH and a metal ion gradient are present across the liposome. Similar to the citrate-based loading method for doxorubicin, it is anticipated that the neutral form of the drug crosses the lipid bilayer. Subsequently, the amine group becomes protonated, resulting in an increase in the liposomes' interior pH. In order to maintain the interior pH, other researchers (Cheung et al., 1998) have used the divalent cation ionophore A23187 (an electro-neutral ionophore capable of translocating a divalent cation for the exchange of two hydrogen ions). A23187 shuttles protons to the vesicle interior in exchange for Mn^{2+} ions (Wang et al., 1998), which are subsequently chelated by EDTA contained in the exterior buffer (Figure 1C). The opaque orange colour of the resulting drug loaded liposomes is visually comparable to solutions prepared using the

Figure 3.1. Methods of Doxorubicin Encapsulation into Liposomes Exhibiting the Indicated Gradients:

(A) liposomes prepared in 300 mM citrate buffer, pH 3.5, and outside buffer exchanged to HBS at pH 7.5,

(B) liposomes prepared in 300 mM $MnSO_4$, pH 3.5, and outside solution is exchanged to 300 mM sucrose / 20 mM HEPES / 15 mM EDTA at pH 7.5 and

(C) which is identical to (B) except the ionophore A23187 was added to the liposomes prior to doxorubicin addition.

Figure 3.1.

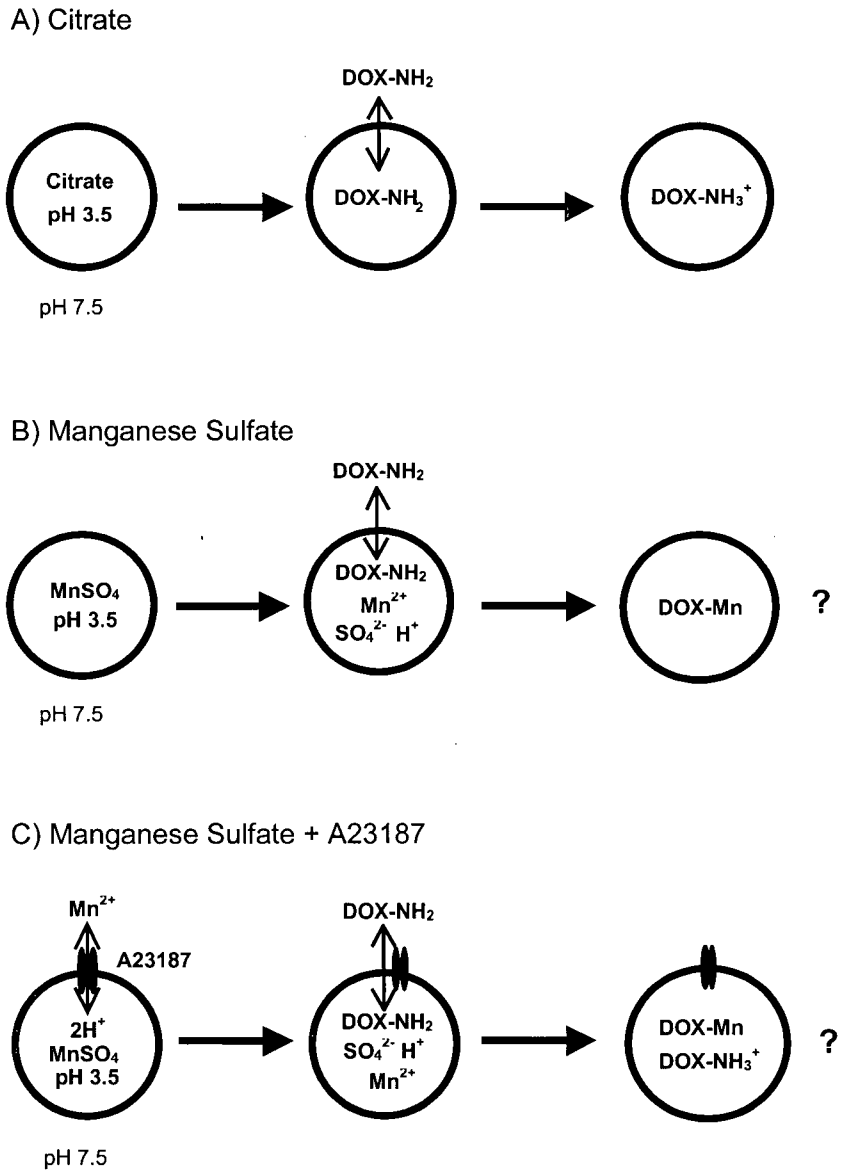
A) Citrate
DOX-NH2
Citrate
pH 3.5
DOX-NH2
DOX-NH3+
pH 7.5
B) Manganese Sulfate
DOX-NH2
MnSO4
pH 3.5
DOX-NH2
Mn2+
SO4 2- H+
DOX-Mn
?
pH 7.5
C) Manganese Sulfate + A23187
Mn2+
A23187
2H+
MnSO4
pH 3.5
DOX-NH2
DOX-NH2
SO4 2- H+
Mn2+
DOX-Mn
DOX-NH3+
?
pH 7.5

citrate-based loading method and free doxorubicin at pH 3 to pH 7. Perhaps most interestingly, in the absence of the ionophore (Figure 3.1.(B)), doxorubicin loading is accompanied by a change in the colour of the solution from orange to an opaque royal purple colour.

To compare the three different loading methods described in Figure 3.1., the accumulation of doxorubicin into DMPC/Chol liposomes was determined as a function of temperature and time. The drug loading parameters were determined under conditions where the drug and liposomes were mixed at a drug-to-lipid ratio of 0.2 (wt/wt), and the final liposome lipid concentration was adjusted to 10 mM for each method. The doxorubicin loading data, summarised in Figure 3.2., indicate that the loading attributes for all three methods are comparable at all temperatures. At 20°C the drug-to-lipid ratio does not change over the entire time course, a result consistent with drug membrane partitioning with no accumulation. Optimal loading occurs when the incubation temperature is adjusted to 60°C, where > 95% of the added doxorubicin is encapsulated within the liposomes within 5 min.

To assess the stability of doxorubicin within the manganese containing liposomes and confirm that manganese is not inducing doxorubicin degradation, high performance liquid chromatography (HPLC) was used to resolve intact doxorubicin (Figure 3.3.). Doxorubicin loaded DMPC/Chol and DSPC/Chol liposomes (0.2 drug-to-lipid ratio, wt/wt), were prepared using the citrate or the $MnSO_4$-based loading procedures. Changes in drug-to-lipid ratios were used to calculate the percent of remaining doxorubicin, measured at various time points over a 48 h time course. In both the DMPC/Chol (Figure 3.3.(A)) and DSPC/Chol (Figure 3.3.(B)) liposomes, total intact doxorubicin concentrations within citrate and manganese containing liposomes were comparable over the time course. Overall there was a

Figure 3.2. Doxorubicin Encapsulation in DMPC/Chol (55/45) Liposomes Using Three Loading Methods. Liposomes were prepared using:

(A) citrate loading procedure,

(B) the $MnSO_4$ loading procedure or,

(C) the $MnSO_4$ loading procedure with the A23187 ionophore. Liposomes were prepared as described in the Chapter 2 section 2.2., and the outer solutions were exchanged using column chromatography in order to create a pH or a Mn^{2+} gradient. For the $MnSO_4$ loading procedure, the A23187 was added and incubated 5 min prior to the addition of drug. Doxorubicin was added to the liposomes to achieve a 0.2 drug-to-lipid ratio (wt/wt) and incubated at either 20°C (■), 40°C (●) or 60°C (▲). At the indicated time points, aliquots were fractionated on 1 ml spin columns to separate encapsulated drug (collected in the void volume) from unencapsulated drug. Lipid concentrations were determined using ^{3}H-CHE and doxorubicin was quantitated by reading the A_{480} of a detergent solubilized sample as described in Chapter 2 section 4.2.1.. Data points represent the mean drug-to-lipid ratios of at least three replicate experiments and the error bars indicate the standard deviation.

Figure 3.2.

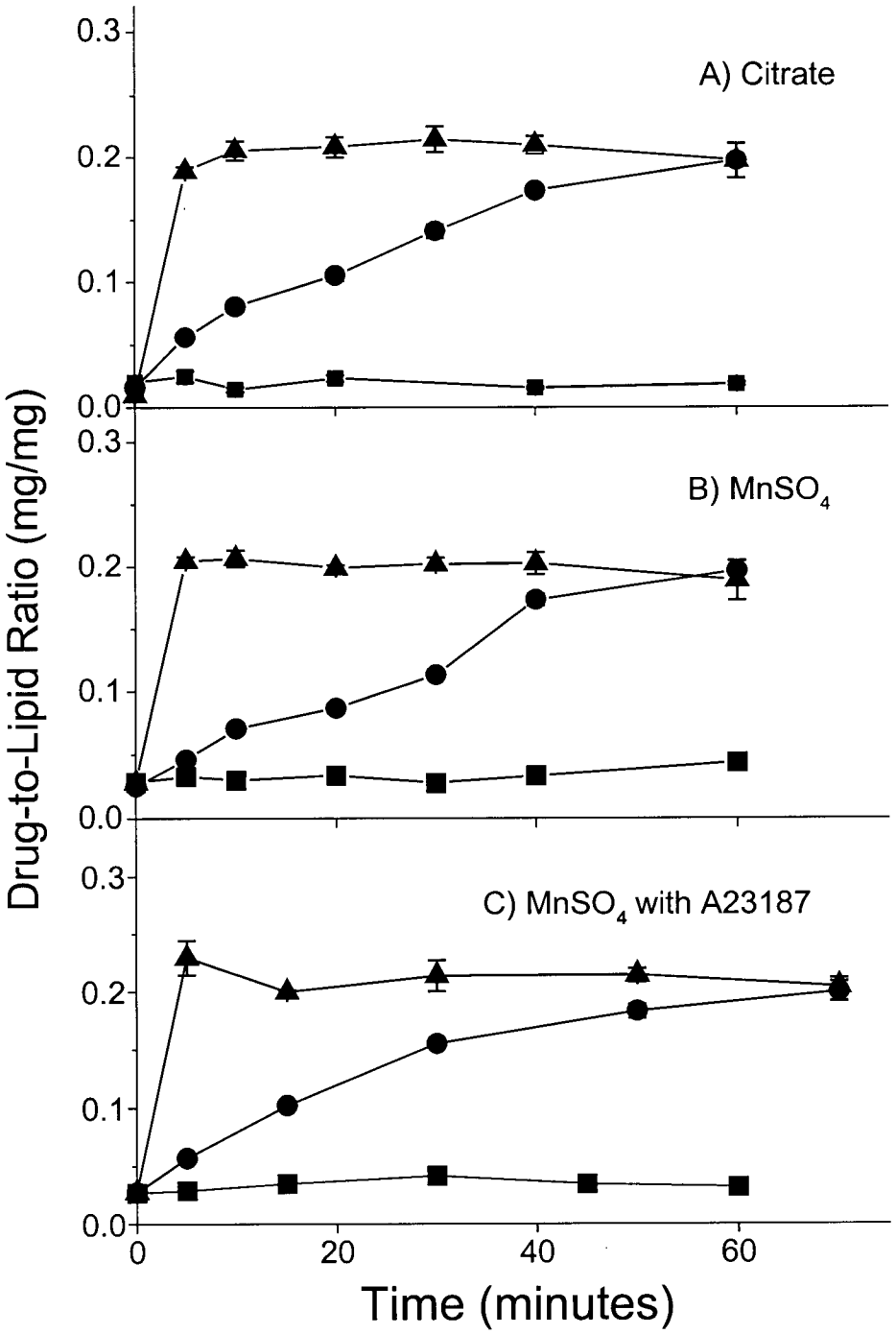
A) Citrate
B) MnSO4
C) MnSO4 with A23187
Drug-to-Lipid Ratio (mg/mg)
Time (minutes)
0.0
0.1
0.2
0.3
0
20
40
60

Figure 3.3. The Stability of Doxorubicin within DMPC/Chol (55/45) and DSPC/Chol (55/45) Liposomes Containing Either Citrate or $MnSO_4$:

(A) DMPC/Chol or

(B) DSPC/Chol liposomes were loaded with doxorubicin to achieve a final drug-to-lipid ratio of 0.2 (wt/wt) using the citrate (white bars) or the $MnSO_4$ (black bars) procedures. At the indicated time points, the drug and liposomal lipid concentrations were measured after fractionating samples on a 1 ml spin column as described in Chapter 2 section 2.6., with measuring doxorubicin using HPLC. These data were used to calculate the percentage of remaining doxorubicin at various time-points. Data points represent the mean of data obtained from six separate experiments and the error bars indicate the standard deviation for each data point.

Figure 3.3.

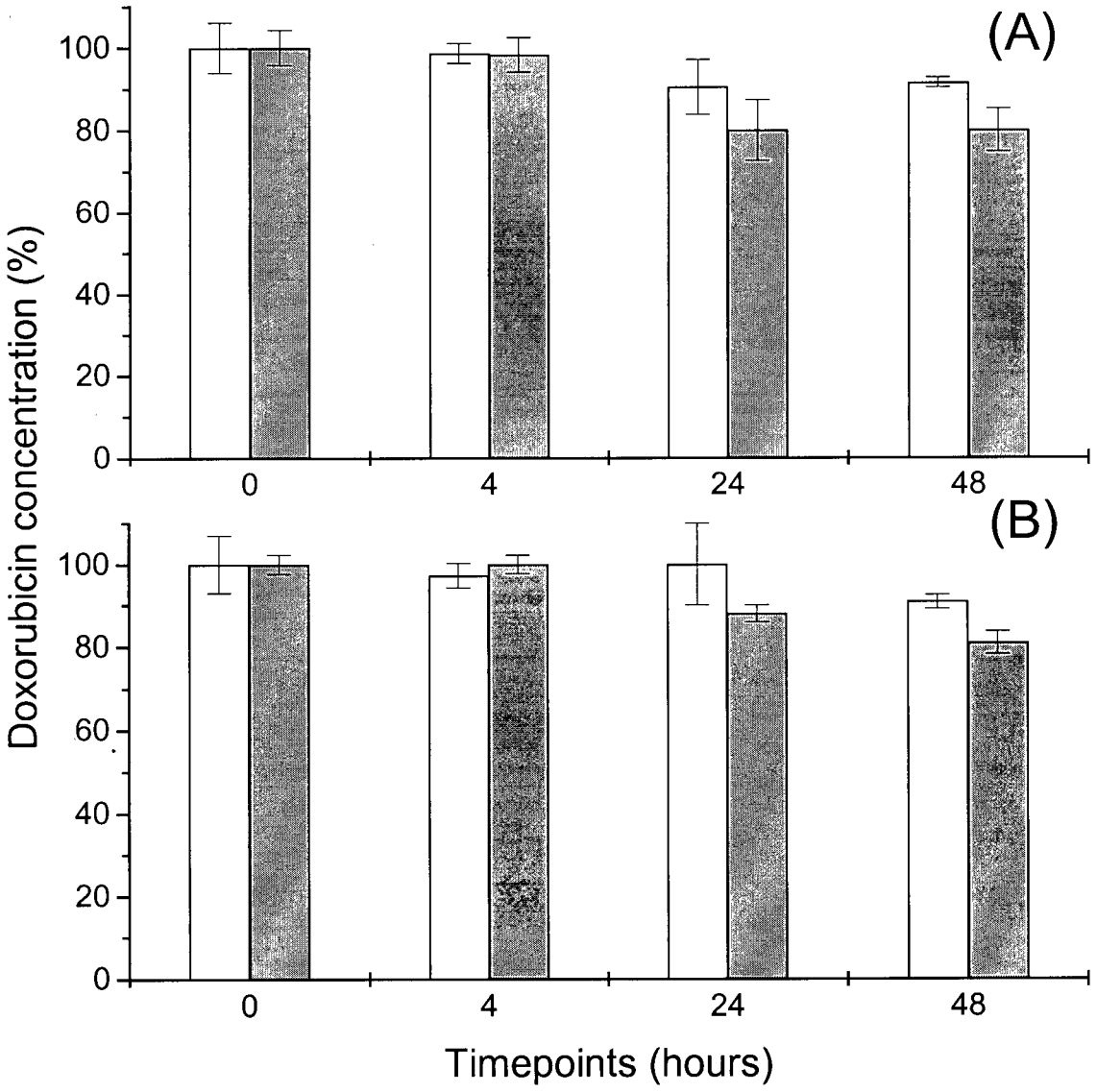
(A)
(B)
Doxorubicin concentration (%)
100
80
60
40
20
0
0
4
24
48
Timepoints (hours)

< 9% ± 0.52 change between the citrate and the manganese loaded DMPC/Chol liposomes and a < 10% ± 3 change between the citrate and the manganese loaded DSPC/Chol liposomes over the course of 48 h. These results clearly confirm that the decreased drug concentrations are a direct result of doxorubicin release rather than the result of doxorubicin degradation. It is also important to note that the methods described are consistent with a reconstitution procedure that involves encapsulation of the drug in preformed liposomes just prior to drug administration. This procedure has been validated in the clinic for formulations of doxorubicin and vincristine.

3.2.2. Cryo-Transmission Electron Microscopic Analysis of the Drug Loaded Liposomes

Doxorubicin, when loaded into sulfate or citrate containing liposomes with an acidic interior (pH < 5), will form a precipitate, particularly when the final drug-to-lipid ratio is in excess of 0.05 (wt/wt) (Lasic et al., 1995; Lasic et al., 1992; Li et al., 2000; Li et al., 1998). One of the best methods to evaluate formation of the drug precipitate within liposomes relies on the use of cTEM (Almgren et al., 2000; Lasic et al., 1995). For this reason cryo-electron micrographs of the DMPC/Chol liposomal formulations, before and after drug loading, were obtained and representative images are shown in Figure 3.4.. The image shown in Figure 3.4. (IA) is of liposomes prepared in a 300 mM citrate buffer (pH 3.5) after the exterior buffer was exchanged to HBS (pH 7.5). These liposomes appear to be mostly spherical and uniform in size ranging around 120 nm; a value that is consistent with the size determined by light scattering analysis (see Chapter 1, section 1.3.4.).

Figure 3.4. Cryo-Transmission Electron Microscopy Images of DMPC/Chol (55/45) Liposomes Either Before or After Drug Loading Achieving a Final Drug-to-Lipid Ratio of 0.2 (wt/wt). The liposomes were prepared and loaded with doxorubicin as summarised in Figure 3.2.. Briefly, the samples were incubated at 60°C for 30 min in order to facilitate >95% doxorubicin encapsulation. cTEM images were obtained from liposome samples prior to drug addition and from liposomes with encapsulated drug.

Panel (IA): DMPC/Chol liposomes prepared in 300 mM citrate, pH 3.5, and with the outside buffer changed to HEPES-buffered saline, pH 7.5, as the exterior buffer.

Panel (IIA): Same as those described for IA except after liposomes have been loaded with doxorubicin.

Panel (IB): DMPC/Chol liposomes prepared in 300 mM $MnSO_4$, pH 3.5, and with the outside solution changed to sucrose-HEPES-EDTA, pH 7.5.

Panel (IIB): Same as those described in (IB) except after liposomes have been loaded with doxorubicin.

Panel (IC): DMPC/Chol liposomes prepared in 300 mM $MnSO_4$, pH 3.5, with the outside solution changed to sucrose-HEPES-EDTA, pH 7.5, and following addition of the ionophore A23187.

Panel (IIC): Same as those described in (IC) except after liposomes have been loaded with doxorubicin. The bar in panel (IA) is equivalent to 100 nm and all micrographs are shown at the same magnification. Each individual panel is representative of at least 15 images obtained.

Figure 3.4.

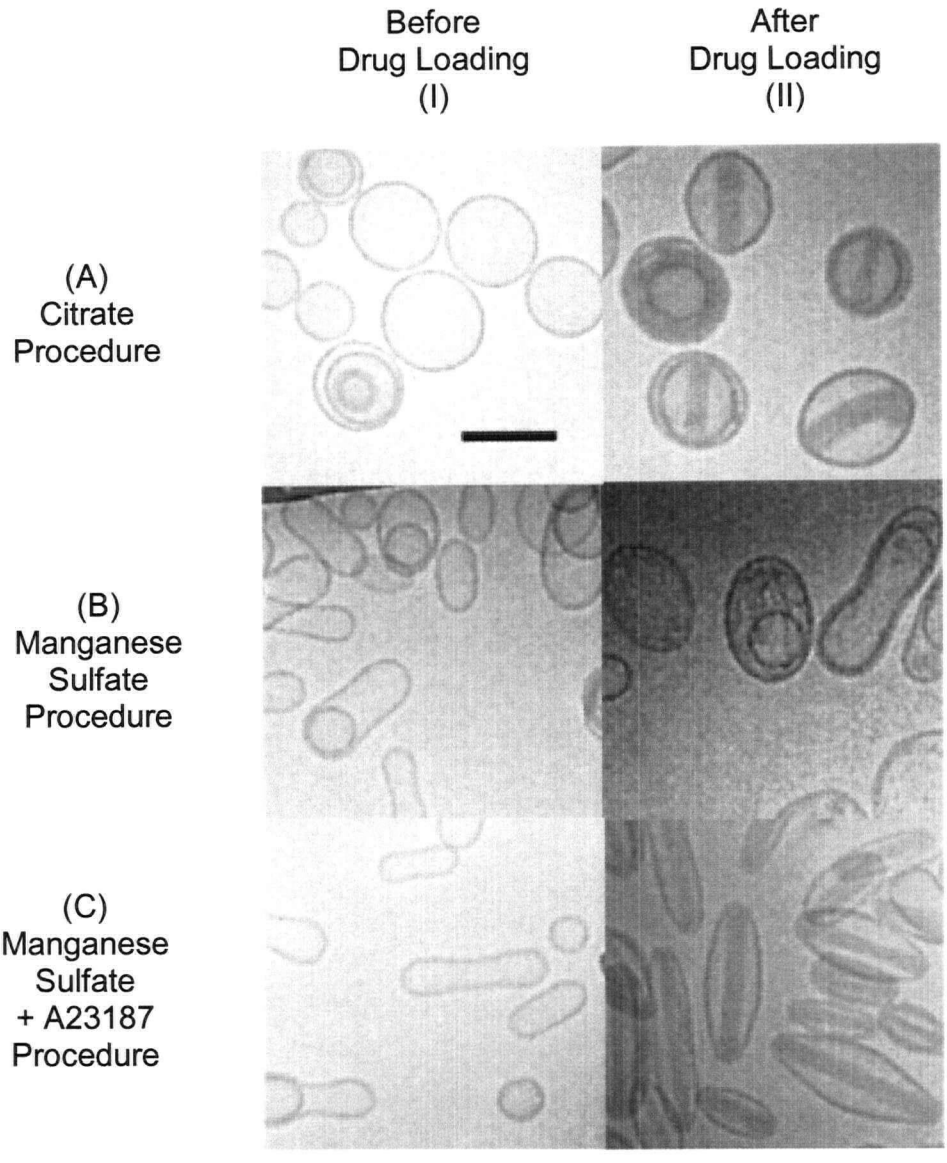
Before
Drug Loading
(I)
After
Drug Loading
(II)
(A)
Citrate
Procedure
(B)
Manganese
Sulfate
Procedure
(C)
Manganese
Sulfate
+ A23187
Procedure

Following accumulation of doxorubicin to a final drug-to-lipid ratio of 0.2 (wt/wt), a precipitate is readily visible within the vesicular structures (Figure 3.4. (IIA)). The doxorubicin bundles appear as linear or circular structures, and drug precipitation can induce a change in the shape of the liposomes, resulting in a "coffee bean" like appearance. Liposomes prepared in 300 mM $MnSO_4$ with the exterior solution exchanged to the EDTA-containing pH 7.5 buffer appear as elongated and tubular structures (Figure 3.4. (IB) and (IC)) in comparison to the citrate containing liposomes (Figure 3.4. (IA)). When these liposomes are loaded with doxorubicin using A23187, the resulting liposomes have a pronounced elongated structure and what appears to be a linear bundle of precipitated doxorubicin within the core. In contrast, there are no doxorubicin fibre bundles inside doxorubicin loaded liposomes prepared in the absence of A23187. The cryo-electron microscopic images of these liposomes reveal a stippled and diffuse morphology within the liposome core (Figure 3.4. (IIB)). These results clearly indicate significant differences in the doxorubicin containing liposomes prepared with and without A23187. The next series of experiments were designed to assess the role of entrapped sulfate and interior pH on the formation of the doxorubicin precipitate.

3.2.3. The Encapsulation of Doxorubicin into Liposomes Prepared in Manganese Chloride

In order to assess the role of the sulfate anion in mediating precipitation of doxorubicin, drug loading into liposomes with encapsulated $MnCl_2$ was characterised. A solution of 300 mM $MnCl_2$ (pH 3.5) was used to prepare DMPC/Chol liposomes and following gradient formation (see Chapter 2 section 2.4.1.) doxorubicin was added to achieve

a final drug-to-lipid ratio of 0.2 (wt/wt). Similar to results obtained when using entrapped $MnSO_4$ in the absence of A23187, doxorubicin loading occurred optimally at 60°C and no loading was observed at 20°C (Figure 3.5.(A)). The resulting drug loaded liposomes were opaque royal purple in colour. Under conditions where $MnCl_2$ loaded liposomes were incubated with doxorubicin in the presence of A23187 (Figure 3.5.(B)), drug loading was also achieved at 60°C, however the resulting liposome preparation had an orange appearance. Following drug loading to achieve the maximum 0.2 drug-to-lipid ratio (wt/wt), there was a time dependent decrease in the drug-to-lipid ratio from 0.2 (measured at 20 min) to less than 0.15 (measured at 60 min).

Representative cryo-electron micrographs obtained from the $MnCl_2$ liposome formulation are shown in Figure 3.6.. These images suggest that in the presence or absence of A23187, the core of the drug loaded liposomes have a stippled and diffuse precipitate (Figure 3.6. (IIA) and (IIB)). The results suggest that formation of the fibrous bundle, observed following A23187 mediated doxorubicin loading into liposomes prepared in 300 mM $MnSO_4$ was due, in part, to the presence of the sulfate anion. Osmotic gradients across liposomes influence liposome shape and it should be noted that when preparing the citrate and $MnCl_2$ (300 mM citrate (580 mOsm/l) 300 mM $MnCl_2$ (785 mOsm/l)) liposomes, there is a substantial osmotic gradient across the membrane (exterior solutions of HBS (326 mOsm/l) and SHE (517 mOsm/l) respectively), which results in the inward movement of water. This results in a "swelling" of the liposomes and thus they appear round (Figure 3.6. (IA) and (IB) and Figure 3.4.(IA)). In contrast, the $MnSO_4$ loaded liposomes are hypo-osmotic (300 mM $MnSO_4$ (319 mOsm/l) with respect to their environment SHE

Figure 3.5. Doxorubicin Encapsulation Using Liposomes Prepared in 300 mM $MnCl_2$, pH 3.5, and with the External Solution Exchanged to SHE, pH 7.5. Drug loading was determined using either:

(A) $MnCl_2$-containing liposomes or

(B) $MnCl_2$-containing liposomes + A23187. The methods used were identical to those described for the $MnSO_4$ loading procedure and are summarised in the legend to Figure 3.2. and Chapter 2 section 2.4.1.. Briefly doxorubicin was added to achieve a final drug-to-lipid ratio of 0.2 (wt/wt). Subsequently the samples were incubated at either 20°C (■), 40°C (●) or 60°C (▲) and at the indicated time points the sample was passed through a 1 ml spin column to separate free drug from encapsulated. The data points represent the mean drug-to lipid ratios obtained from three separate experiments and the error bars indicate the standard deviation.

Figure 3.5.

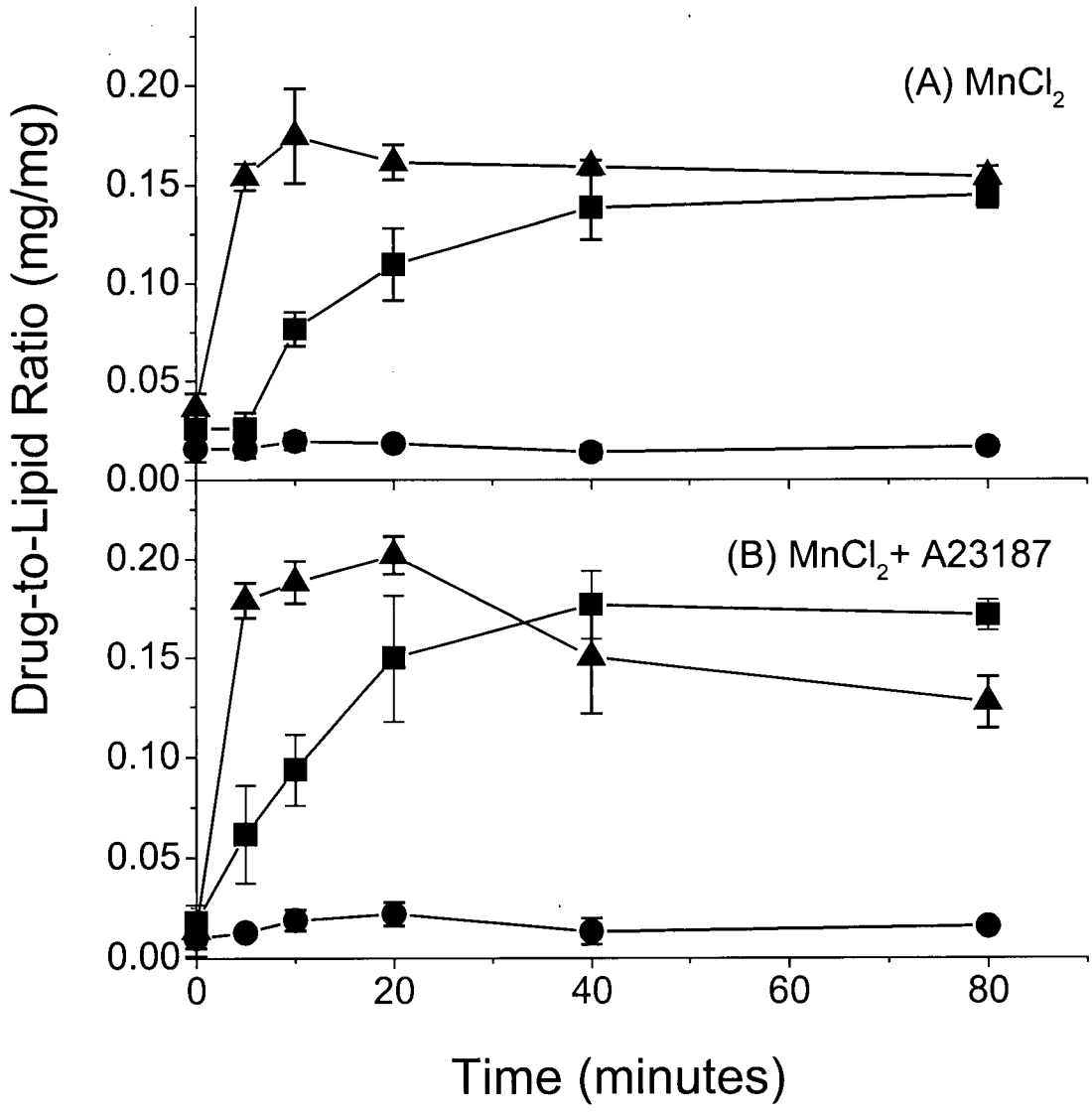
(A) MnCl2
(B) MnCl2+ A23187
Drug-to-Lipid Ratio (mg/mg)
0.20
0.15
0.10
0.05
0.00
0
20
40
60
80
Time (minutes)

Figure 3.6. Cryo-Transmission Electron Microscopy Images of DMPC/Chol (55/45) Liposomes Either Before or After Drug Loading, Achieving a Final Drug-to-Lipid Ratio of 0.2 (wt/wt). The liposomes were prepared and loaded with doxorubicin as summarised in Figure 3.5.. Briefly, the samples were incubated at 60°C for 30 min in order to facilitate >95% doxorubicin encapsulation. cTEM images were obtained from a liposome sample prior to drug addition and from liposomes with encapsulated drug.

Panel (IA): DMPC/Chol liposomes prepared in 300 mM $MnCl_2$, pH 3.5, and with the outside solution changed to SHE, pH 7.5, as the exterior buffer.

Panel (IIA): Same as those described for (IA) except after liposomes have been loaded with doxorubicin.

Panel (IB): DMPC/Chol liposomes prepared in 300 mM $MnCl_2$, pH 3.5; with the outside solution changed to SHE, pH 7.5, and after the addition of the ionophore A23187.

Panel (IIB): Same as those described in (IB) except after liposomes have been loaded with doxorubicin. The bar in panel (IA) is equivalent to 100 nm and all micrographs are shown at the same magnification. Each individual panel is representative of at least 15 images obtained.

Figure 3.6.

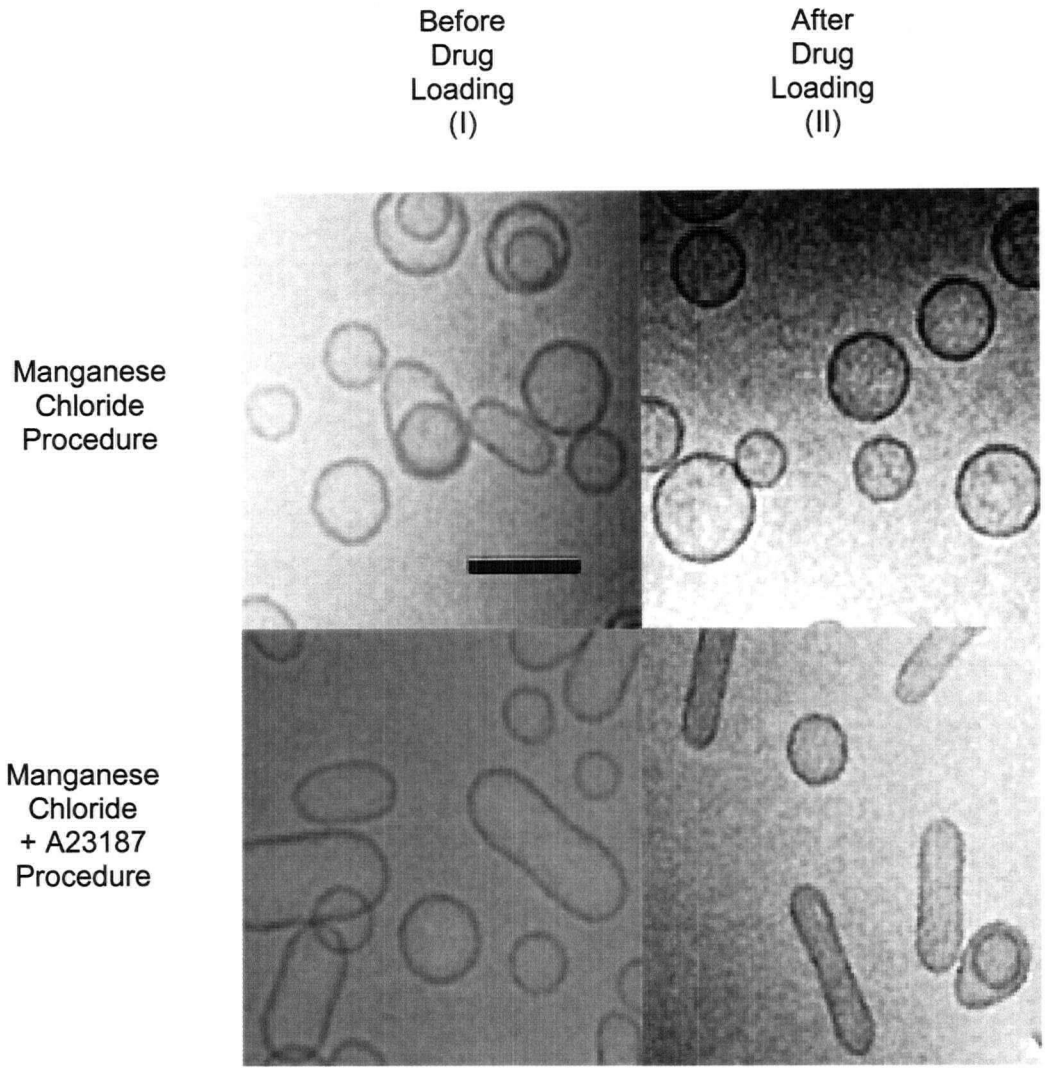
Before
Drug
Loading
(I)
After
Drug
Loading
(II)
Manganese
Chloride
Procedure
Manganese
Chloride
+ A23187
Procedure

(517 mOsm/l)) and results in the movement of water to the outside. Thus these liposomes appear as oblong structures (see Figure 3.4. (IB) and (IC) for comparison). Following addition of A23187 (with the shuttling of the divalent cations out of the liposomes) and doxorubicin loading, the liposomes become even more elongated.

3.2.4. Assessment of the Transmembrane pH Gradient Prior to and Following Doxorubicin Encapsulation

One of the distinguishing features of the loading procedure that relies on encapsulated $MnSO_4$ is the absence of an effective internal buffer. In fact, doxorubicin loading in the absence of A23187 should result in a rapid dissipation of the transmembrane pH gradient. Radiolabeled methylamine was used as a pH sensitive probe (Harrigan et al., 1992; Redelmeier et al., 1989) to measure the pH gradient across the liposomal formulations after exchanging the exterior buffers and following doxorubicin uptake. As noted in Chapter 2, section 2.3., all liposomal formulations were prepared in solutions with a pH of 3.5. Thus following the external buffer exchange it was anticipated that the transmembrane pH gradient would be approximately 4 units. Three formulations were evaluated in these studies and the results have been summarised in Figure 3.7.. Following the establishment of the pH gradient, but prior to doxorubicin loading, the formulations with encapsulated citrate (column 1), $MnSO_4$ (column 3), and $MnCl_2$ (column 7) exhibited measured transmembrane pH gradients of 3.4, 1.6, and less than 0.18 respectively. Therefore even in the absence of drug loading or ionophore addition, the Mn-based formulations had significantly smaller pH gradients. Following addition of doxorubicin, the pH gradient of the citrate based formulation

Figure 3.7. Measured transmembrane pH gradients prior to and following doxorubicin loading under the various conditions described in Figures 3.2. and 3.5.. The pH gradient was estimated through use of radiolabeled methylamine as described in Chapter 2 section 2.8.. Radiolabeled methylamine was added to liposomes after they were incubated at 60°C for 30 min either in the presence or absence of doxorubicin. Doxorubicin was added to achieve a final drug-to-lipid ratio of 0.2 (wt/wt). The samples include those based on the citrate loading method (column1), with doxorubicin (column 2) and the $MnSO_4$ loading method (column 3), with doxorubicin (column 4). The $MnSO_4$ loading method with A23187 (column 5), with doxorubicin (column 6), the $MnCl_2$ loading method (column 7), with doxorubicin (column 8) and the $MnCl_2$ loading method plus the ionophore A23187 (column 9) with doxorubicin (column 10). The results represent the mean pH gradient of three separate experiments and the error bars indicate the standard deviation.

Figure 3.7.

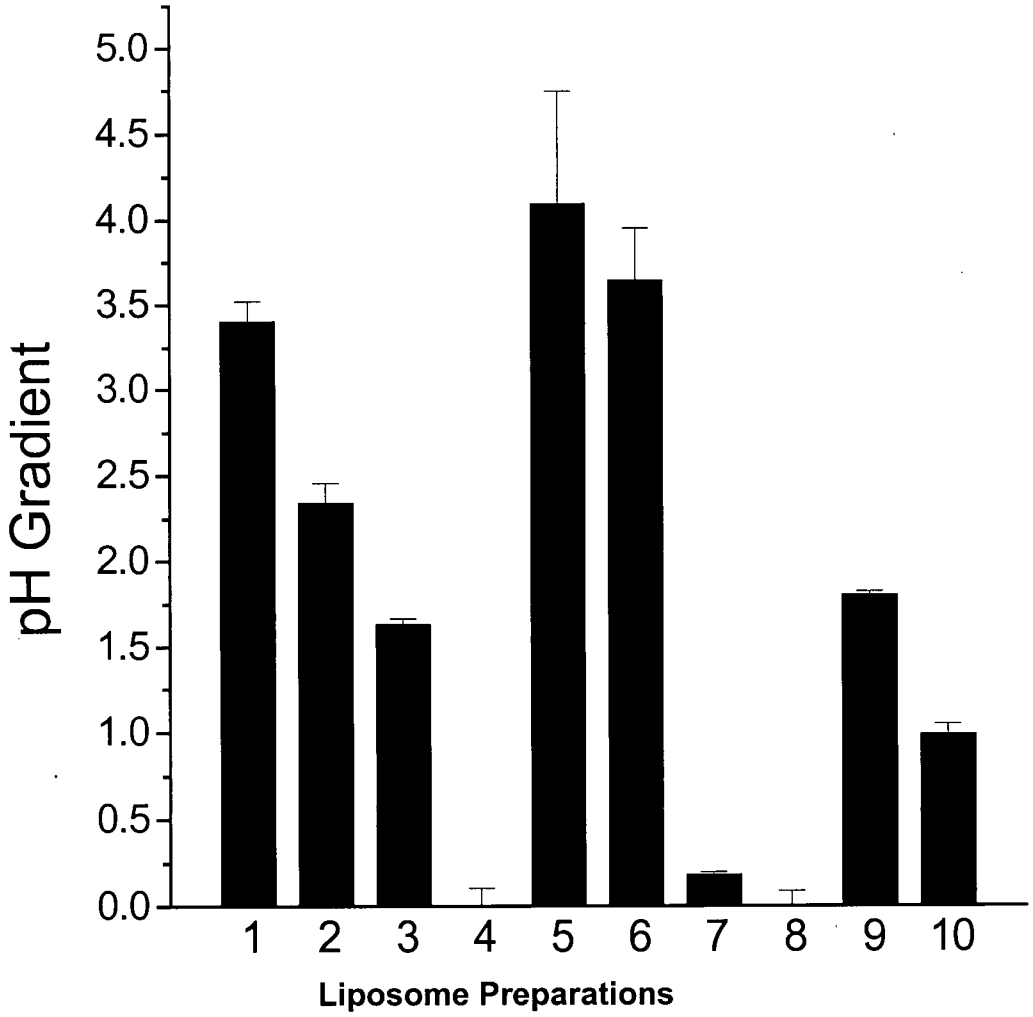
pH Gradient
5.0
4.5
4.0
3.5
3.0
2.5
2.0
1.5
1.0
0.5
0.0
1
2
3
4
5
6
7
8
9
10
Liposome Preparations

decreased from 3.4 (column 1) to 2.3 (column 2), a result that is consistent with previous reports demonstrating doxorubicin mediated collapse of the pH gradient in these formulations (Mayer et al., 1986a).

In the absence of the ionophore, but following doxorubicin loading, the Mn^{2+}-containing formulations exhibited no measurable transmembrane pH gradient (refer to Figure 3.7., columns 4 and 8). This result indicates, unequivocally, that these doxorubicin loaded preparations no longer maintain a pH gradient and this is consistent with the fact that these formulations have little or no ability to buffer against changes in pH induced by drug loading. In contrast, the addition of A23187 to either the $MnSO_4$ (column 5) or $MnCl_2$ (column 9) containing liposome formulations, resulted in generation of a substantial pH gradient. As estimated using methylamine, these pH gradients were approximately 4.0 and 1.8 respectively. Even following doxorubicin loading these two formulations (columns 6 and 10) maintained pH gradients of 3.6 and 1.0 respectively.

3.2.5. Absorption and Circular Dichroic Spectra of Doxorubicin Under Various Conditions

The results summarised in Figure 3.7. suggest that such differences could be due, in part, to the internal pH of the resulting drug loaded liposomes. In order to explore the role of Mn^{2+} ion complexation with doxorubicin, and the associated influence of pH, spectroscopic studies were completed. Doxorubicin (see inset to Figure 3.8.) possesses a chromophore with multiple $\pi \rightarrow \pi^*$ and $n \rightarrow \pi^*$ transitions rendering doxorubicin's electronic absorption and circular dichroic spectra sensitive to the deprotonation of the chromophore and the binding of metal ions (Bouma et al., 1986) (Fiallo et al., 1998). As shown in Figure 3.8.(A), when the

Figure 3.8. Absorption Spectra of Doxorubicin at Various pH and Concentrations of $MnSO_4$ as well as the Circular Dichroic Spectra of Doxorubicin Loaded Liposomes:

(A): absorbance spectra of an 86 μM doxorubicin solution at pH 6, 8, 9, 10, 11, and 13. The pH of each sample was maintained by either 100 mM MES (pH 6), 100 mM HEPES (pH 8), 100 mM CHES (pH 9), 100 mM CAPS (pH 10), 100 mM CAPS (pH 11) and 100 mM glycine + 100 mM NaCl (pH 13). The absorbance spectra were obtained immediately after drug solubilisation to minimise doxorubicin degradation.

(B): Absorption spectra of an 86 μM doxorubicin solution in the presence of various concentrations of $MnSO_4$ at pH 8. $MnSO_{4(S)}$ was added to 1 ml of 100 mM HEPES at pH 8 and vigorously vortexed, then doxorubicin was added to obtain a final concentration of approximately 86 μM. The solubility of $MnSO_4$ at pH 8 is low and the formation of $Mn(OH)_{2(S)}$ is a limiting factor, therefore absorption readings were taken immediately. There was no visible precipitation in the sample within the time frame required to obtain the spectra.

(C) Circular dichroism spectra of doxorubicin loaded DMPC/Chol liposomes, where drug loading was achieved using either the citrate or the $MnSO_4$ ± A23187 loading procedures.

Figure 3.8.

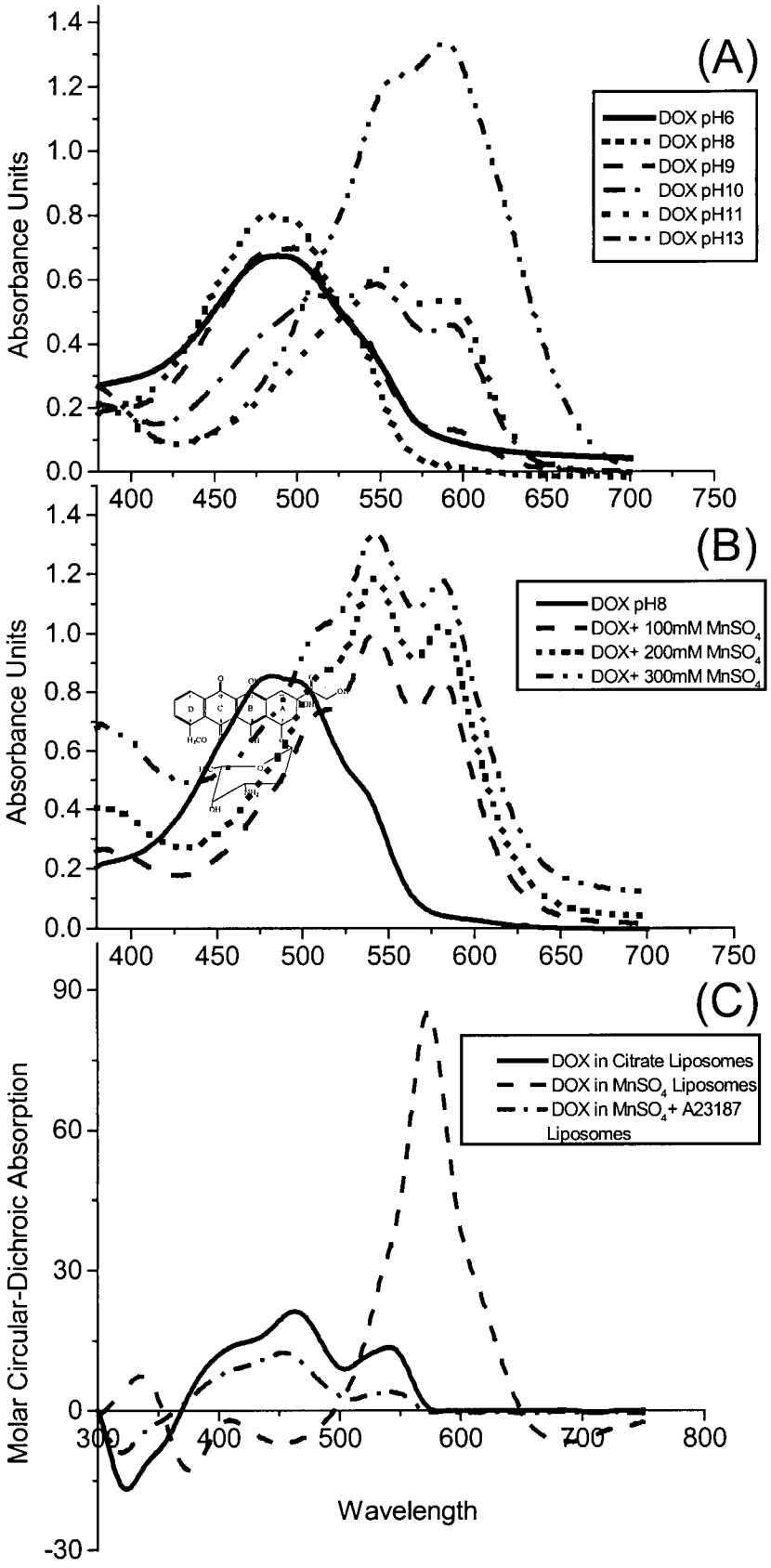
(A)
Absorbance Units
DOX pH6
DOX pH8
DOX pH9
DOX pH10
DOX pH11
DOX pH13
(B)
Absorbance Units
DOX pH8
DOX+ 100mM MnSO4
DOX+ 200mM MnSO4
DOX+ 300mM MnSO4
(C)
Molar Circular-Dichroic Absorption
DOX in Citrate Liposomes
DOX in MnSO4 Liposomes
DOX in MnSO4+ A23187 Liposomes
Wavelength

pH increases there is a visible bathochromic shift observed with two predominant absorption bands appearing at 550 and 590 nm. This spectral shift has been attributed to the deprotonation of the hydroxyls at the C(6) (pK_a = 13.2) and C(11) (pK_a = 10.16) positions (Fiallo et al., 1998). We observed a similar shift of the doxorubicin spectra at a fixed pH of 8.0 following the addition of increasing concentrations of $MnSO_4$ (Figure 3.8.(B)). The observed bathochromic shift resulted in two predominant absorption bands centred around 542 and 581 nm. The shift was observed even in the presence of 100 mM $MnSO_4$. These results suggest that in the presence of Mn^{2+}, the ion is potentially capable of deprotonating the chromophore at the C(11)-OH and C(6)-OH positions.

To further characterise the interactions of Mn^{2+} with doxorubicin, CD spectra of doxorubicin loaded liposomes were obtained. The formulations evaluated include ones where the drug was encapsulated using the citrate-based and the $MnSO_4$-based loading procedures. The latter was completed in the absence and presence of A23187. As shown in Figure 3.8.(C), the CD spectra obtained for encapsulated doxorubicin prepared using the citrate and the $MnSO_4$ plus A23187 loading methods were similar. This result is likely due to the similar conformations doxorubicin assumes at an internal pH of < 5.5 (see Figure 3.4. (IIA) and (IIC)) within liposomes containing citrate and sulfate respectively. Using CD analysis as a tool to evaluate doxorubicin, Fiallo *et al.* (Fiallo et al., 1998) have attempted to assign specific absorption bands to specific electronic transitions. These are summarised in Table 3.1., and suggest that absorption bands appearing at 330 and 346 nm wavelengths correspond to a $n \rightarrow \pi^*$ transition at the C(12) position and a $n \rightarrow \pi^*$ transition at the C(5) position. The results in Figure 3.8.(C) indicate an inverse of chirality at 330 nm for the citrate ($\Delta\varepsilon$ =-15.37) and the $MnSO_4$ plus A23187 ($\Delta\varepsilon$ =-6.94) loaded liposomes as compared

Table 3.1. The Differential Molar Circular Dichroic Absorption Δε ($M^{-1}cm^{-1}$) of Doxorubicin-Encapsulated Liposomes. Doxorubicin, was loaded into liposomes using the citrate, the $MnSO_4$ or the $MnSO_4$ with A23187 procedure as described in Chapter 2, section 2.4.1.. Specific wavelengths correspond to potential electronic transitions undergone by doxorubicin following encapsulation.

Loading procedures	π→ π* (z-axis) 300 nm[a]	n→ π*C(12)=O 330 nm[a]	n→ π*C(5)=O 346 nm[a]	π→ π* (y-axis) 448 nm[a]	513 nm[a]	542 nm[a]
$MnSO_4$ (Δε)	-1.08	6.79	5.02	-6.84	8.60	35.20
Citrate (Δε)	0.062	-15.37	-9.51	18.85	10.13	13.63
$MnSO_4$ (Δε) with A23187	-0.94	-6.94	-3.14	12.30	2.60	4.03

[a]Wavelengths adapted from CD bands of anthracyclines in 0.05 M HEPES and 0.1 M KCl (Fiallo et al., 1998)

to doxorubicin encapsulated into the $MnSO_4$ ($\Delta\varepsilon$ = 6.79) loaded liposomes in the absence of ionophore.

These results also indicate an inverse of chirality at 346 nm for the citrate ($\Delta\varepsilon$ =-9.51) and the $MnSO_4$ plus A23187 ($\Delta\varepsilon$ =-3.14) loaded liposomes as compared to the spectra obtained for doxorubicin loaded into $MnSO_4$ ($\Delta\varepsilon$ = 5.02) liposomes without ionophore. En bloc these observations strongly suggest that in the presence of Mn^{2+} and an internal pH of > 7.0, doxorubicin complexes with two metal ions, interacting with the oxygen groups associated with the C(11)-$O^-$and C(12)=O positions or the C(5)=O and C(6)-O^- positions.

3.2.6. The Influence of Entrapped Doxorubicin Structure on Drug Release From Liposomes In Vitro and In Vivo

The loading methods described provide effective means through which to prepare an encapsulated form of doxorubicin. The results also suggest that one can control the chemical and physical properties of the encapsulated drug by considering the use of an entrapped transition metal, such as Mn^{2+}, and a method whereby the drug loaded liposome no longer exhibits a transmembrane pH gradient (pH 7.5 inside and out). From a practical point of view, however, it is critical to determine whether the loading methods used change drug release attributes *in vitro* and *in vivo*. These studies have focused, thus far, on liposomes prepared of DMPC/Chol, a lipid composition selected specifically because it is known that doxorubicin readily permeates across this lipid bilayer, as opposed to formulations composed of DSPC/Chol, which retain drug for extended time periods both *in vitro* and *in vivo*. It is also important to recognise that others have indicated that formation of the doxorubicin-citrate or sulfate precipitate as well as maintenance of a transmembrane pH gradient (inside

acidic) are necessary if doxorubicin is to be well retained within a liposome following drug loading (Li et al., 2000; Mayer et al., 1990b). Therefore it was anticipated that those formulations prepared in a manner that did not facilitate formation of the fibrous bundles and which resulted in substantial dissipation of the pH gradient would not be able to retain the entrapped doxorubicin. As shown in Figure 3.9. (*in vitro* data) and Figure 3.10. (*in vivo* data) this was not observed when the liposomal lipid composition was DMPC/Chol (55/45).

For the *in vitro* assay doxorubicin loaded DMPC/Chol liposomes (0.2 drug-to-lipid ratio, wt/wt), were prepared using the citrate or the $MnSO_4$-based loading procedures (with and without A23187), and diluted with fetal bovine serum and incubated at 37°C (Figure 3.9.). Changes in drug-to-lipid ratios, measured at various time points over a 75 h time course, indicated that all three formulations exhibit comparable drug release profiles. It can be suggested on the basis of these *in vitro* data that more drug is released from the $MnSO_4$ loaded liposomes prepared in the absence of A23187. This difference in drug release, however, can be accounted for by an observed 20% loss in encapsulated drug measured at the first time point (4 h after dilution into the serum containing buffer).

Similar results were obtained *in vivo* following i.v. administration of the DMPC/Chol formulations (Figure 3.10.), where plasma elimination measurements for liposomal lipid (Figure 3.10. (A)) and drug (Figure 3.10.(B)) can be used to calculate changes in drug release (Figure 3.10.(C)). These *in vivo* studies attempted to differentiate between the release of doxorubicin from DMPC/Chol liposomes where the drug exists as doxorubicin bundles (citrate loading technique) or a manganese complex ($MnSO_4$ procedure without A21387). Following intravenous injection in CD-1 mice (lipid dose of 100 mg/kg and drug dose of

Figure 3.9. The Release of Doxorubicin From DMPC/Chol (55/45) Liposomes Loaded Using the Procedures Described in Figure 3.2.. Drug release was determined *in vitro* as described in Chapter 2, section 2.10., where liposomes were loaded with doxorubicin to achieve a final drug-to-lipid ratio of 0.2 (wt/wt) using the citrate (■), the $MnSO_4$ (●), or the $MnSO_4$ loading procedure with the A23187 ionophore (▲). After drug encapsulation, each sample was mixed with fetal bovine serum (final serum concentration of 80% and lipid concentration of 2 mg/ml) and incubated at 37°C. At the indicated time points, the drug and liposomal lipid concentrations were measured after fractionating samples on a 1 ml spin column as described in the Methods. These data were used to calculate drug-to-lipid ratios at various time-points. Data points represent the mean of data obtained from three separate experiments and the error bars indicate the standard deviation for each data point.

Figure 3.9.

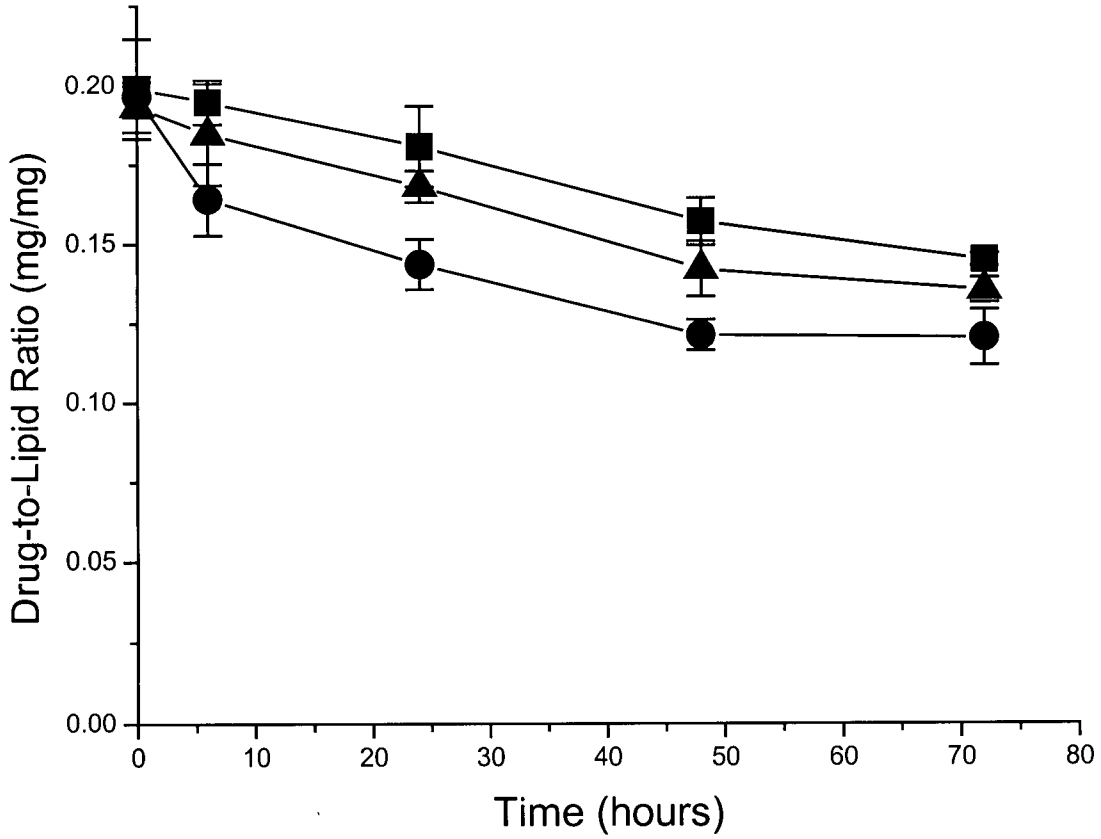
Drug-to-Lipid Ratio (mg/mg)
0.00
0.05
0.10
0.15
0.20
0
10
20
30
40
50
60
70
80
Time (hours)

Figure 3.10. The In Vivo Release of Doxorubicin From DMPC/Chol (55/45) Liposomes. Liposomes were loaded with doxorubicin using the procedures described in Figure 3.2., following with i.v. administration to female CD-1 mice. Liposomes were loaded with drug to achieve a final drug-to-lipid ratio of 0.2 (wt/wt) using the citrate (■) or the $MnSO_4$ (●) procedures. Doxorubicin loaded liposomes were adjusted to a concentration such that the lipid dose of 100 mg/kg could be administered in an injection volume of 200 μl. At the indicated time points following injection, blood samples were obtained and plasma was prepared as described Chapter 2, section 2.11.1..

(A): plasma lipid levels determined from measurements of ^{3}H-CHE as a liposomal lipid marker.

(B): doxorubicin fluorescent equivalents, measured in plasma using the drug extraction procedure.

(C): drug-to-lipid ratios calculated on the basis of the data shown in panels (A) and (B). Each data point represents the mean drug-to-lipid ratios obtained from at least 6 mice and the error bars indicate the standard deviation of each data point.

Figure 3.10.

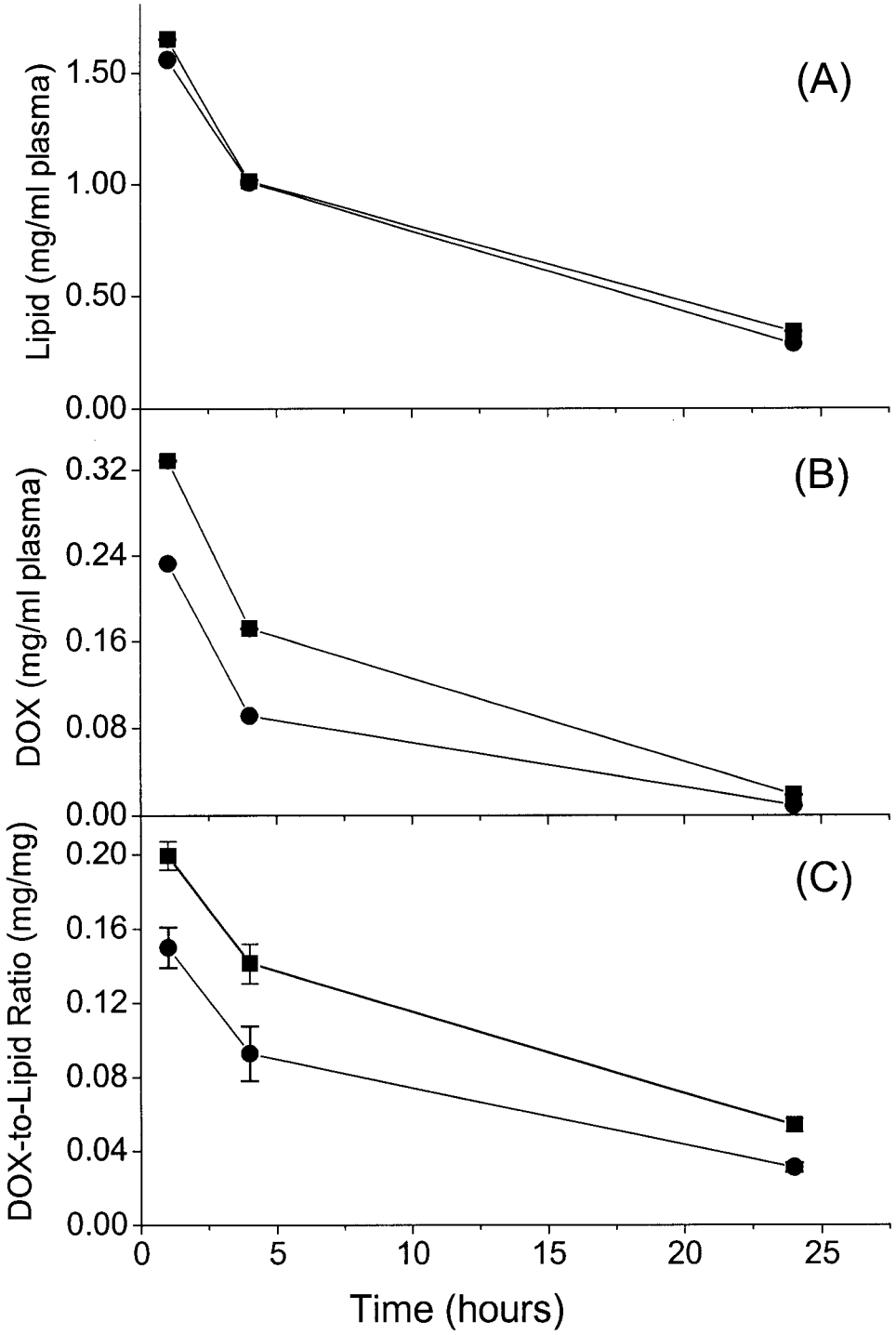
(A)
Lipid (mg/ml plasma)
1.50
1.00
0.50
0.00
(B)
DOX (mg/ml plasma)
0.32
0.24
0.16
0.08
0.00
(C)
DOX-to-Lipid Ratio (mg/mg)
0.20
0.16
0.12
0.08
0.04
0.00
0
5
10
15
20
25
Time (hours)

20 mg/kg), measurements of plasma liposomal lipid levels (Figure 3.10.(A)) over 24 h indicated that the two formulations were eliminated from the plasma compartment at identical rates.

Assessments of plasma doxorubicin levels (Figure 3.10.(B)) indicated that there were significantly lower levels of drug in the plasma at the 1 and 4 h time points when the drug was administered in the $MnSO_4$ liposomes loaded with drug in the absence of A23187 (two-tailed p values were < 0.0001 and 0.001 respectively, refer to Chapter 2, section 2.14). Consistent with the *in vitro* results, there was a rapid 20% loss of drug from these liposomal formulations within one hour after administration. Subsequently, the rate of drug release from the two liposomal formulations were comparable (Figure 3.10.(C)). This result was unexpected considering that the two liposomal formulations exhibited remarkably different interior pH, however this result may just be a reflection of the increased permeability of the DMPC/Chol formulations. Under the time frame assessed this formulation did not exhibit pH dependent differences in drug release rates.

In order to demonstrate that drug release rates are dependent on liposomal lipid composition, the studies summarised in Figure 3.10. were repeated for formulations prepared with DSPC/Chol liposomes. The results of this study are summarised in Table 3.2.. Drug release attributes of the DMPC/Chol and DSPC/Chol formulations were estimated by calculating the percent change in the measured drug-to-lipid ratio determined at 1 h. As indicated by the data in Figure 3.10.(C), the change in drug-to-lipid ratio determined for the DMPC/Chol formulations are comparable, regardless of whether the drug was encapsulated using the citrate-based methodology or the $MnSO_4$ without ionophore. In contrast, results obtained with DSPC/Chol liposomes clearly demonstrate that the rate of drug release is more

rapid when the drug is encapsulated using the $MnSO_4$ (without ionophore) method. At the 24 h time point liposomes prepared using this methodology exhibited a drug-to-lipid ratio of 0.09 (wt/wt) as compared to measured values of 0.18 (wt/wt) obtained for formulations prepared using the citrate method.

Table 3.2. Percent of Encapsulated Doxorubicin Obtained Following Intravenous Administration of DMPC/Chol and DSPC/Chol Liposomes. Liposomes were loaded with drug using encapsulated 300 mM citrate (pH 3.5) or the $MnSO_4$ method without the ionophore A23187. After drug loading the latter formulations exhibited a transmembrane pH gradient of less than 0.5 units while the former exhibited pH gradients in excess of 3 units.

Formulation	Time Following Administration[a]		
	1 h	4 h	24 h
DMPC/Chol - Citrate	100 ±3.9[b]	75 ±5.5	27 ±1.8
- $MnSO_4$	100 ±5.5	63 ±7.3	21±1.3
DSPC/Chol - Citrate	100 ±5.4	95 ±10.9	100 ±3.8
- $MnSO_4$	100 ±6.4	73 ±6.1	53 ±3.5

[a] As described in Figure 3.10., following i.v. administration in CD-1 mice, plasma concentrations of liposomal lipid and doxorubicin are measured at the indicated time points. These data are then used to calculate the drug-to-lipid ratio of the liposomes within the plasma compartment, a parameter that is used as a measure of *in vivo* drug release.

[b] The percent drug-to-lipid ratio was calculated using the measured drug-to-lipid ratio determined 1 h after administration as a value indicative of 100%.

3.3. DISCUSSION

Doxorubicin has a broad spectrum of anticancer activity and is used to treat a variety of solid tumours as well as lymphomas and acute leukemias. One of many problems attributable to the use of this drug in its free form, is its ability to engender cardiac toxicity, a toxicity that limits the amount of drug that can be given chronically (Ferrans, 1978; Von Hoff et al., 1982). Eliminating cardiotoxicity has been attempted with methods such as: 1) alternative dosing (de Valeriola, 1994), 2) pre/co-administration of free radical scavengers (Banks et al., 1983), 3) the development of semi-synthetic derivatives (Platel et al., 1999; Sikic et al., 1985) or 4) by liposomal encapsulation (Batist et al., 2001). The latter approach provides a means of altering the biodistribution of drug whereby there are significant reductions in drug accumulation in cardiac tissues. There are now two liposomal-doxorubicin formulations approved for human use (Doxil™ or Caelyx™ and Myocet™). Despite the clinical development of this technology, there are still important questions to be addressed about the physical state of the entrapped drug. We believe that this information will be essential when considering the development of other liposomal anthracyclines as well as other drug classes.

Consistent with previous studies, the results presented here support the concept that drugs encapsulated in liposomes through use of ion gradients can form precipitates within the liposome. Our studies, however, clearly suggest that the nature of the entrapped precipitate is dependent on the internal pH and chemical composition. Importantly, these data also indicate that for a drug like doxorubicin, the resulting formulation can retain entrapped drug even under conditions where there is little or no residual pH gradient. Investigations focused

on determining the factors controlling doxorubicin release from liposomes provide conflicting viewpoints. Certain studies indicate that high trapping efficiency, high drug-to-lipid ratios and stable drug retention are linked to the maintenance of a large pH gradient (Lee et al., 1998; Maurer-Spurej et al., 1999; Mayer et al., 1990b). A reasoned explanation for these results was that as doxorubicin was encapsulated, the pH (inside) increased due to the consumption of protons as the neutral drug became protonated. In turn, drug retention was thought to hinge on the equilibrium between the protonated and non-protonated forms of doxorubicin. It was concluded that if a low interior pH were maintained, more doxorubicin would be protonated (charged) and thus in a membrane impermeable state. In the case of liposomes prepared with DMPC/Chol, the *in vivo* release rates for preparations with and without a measurable pH gradient are essentially the same. For DSPC/Chol liposomes, there is a measurable change in the rate of drug release following i.v. administration, where drug release is greater for those formulations that lack a pH gradient. These observations would suggest that when liposomes are incubated at a temperature above the bulk phospholipid Tc, drug release occurs in a time frame that is not substantially influenced by the internal pH. Results obtained with DSPC/Chol liposomes, however, allow interior pH associated differences in *in vivo* drug release rates to be discerned. Perhaps most interestingly, the methods described here provide a means to develop liposomal drug formulations where drug is encapsulated through very distinct mechanisms and chemical reactions.

It has been well recognised by those using methods of drug loading that rely on ion gradients, that drug accumulation levels often exceed that which would be predicted on the basis of ion redistribution according to the Henderson-Hasselbalch equation (Madden et al., 1990; Maurer-Spurej et al., 1999; Mayer et al., 1986a; Mayer et al., 1990b). In the case of

the anthracycline doxorubicin these data have been explained by mechanisms involving membrane partitioning and/or drug precipitation (Lasic, 1996; Lasic et al., 1992; Li et al., 2000; Li et al., 1998). It is well established, for example, that doxorubicin at concentrations of > 30 mg/ml, in the presence of ammonium sulfate (Lasic et al., 1992) or citrate (Li et al., 1998), flocculates as a consequence of the formation of fibrous structures. Cryo-transmission electron microscopy studies indicated that the doxorubicin precipitate consisted of fibrous-bundle aggregates in both citrate and sulfate containing liposomes, with electron micrographs comparable to those shown here (Figures 3.4. and 3.6.). In terms of the physical state of doxorubicin, it has been proposed that the planar aromatic anthracycline rings stack longitudinally to form linear fibres within both citrate and sulfate containing liposomes (Lasic, 1996). These fibres are aligned in a hexagonal arrangement to form bundles, with approximately 12-60 fibres per bundle. It was noted by these investigators that doxorubicin-citrate aggregates appear mostly as linear or curved structures (inter-fibre spacing was approximately 30-35 Å). Similarly, doxorubicin-sulfate aggregates are proposed to consist of rigid linear fibre bundles (inter-fibre spacing estimated to be approximately 27 Å). It was proposed that the sulfate anion, which is smaller than the citrate anion, might form a tighter packing arrangement resulting in decreased flexibility. As noted here under conditions where doxorubicin precipitates formed, the formulation containing citrate exhibited both curved and circular electron dense structures that caused a slight distortion of the liposome shape (Figure 3.4. (IIA)). In contrast, the sulfate containing formulations exhibited primarily linear precipitates and a significant elongation of the liposome (Figure 3.4. (IIC)). These differences in liposome shape appear to have little or no impact on the plasma liposomal lipid elimination profiles obtained following i.v. administration (See Figure 3.10. (A)).

Our studies indicate that doxorubicin loaded liposomes prepared using the $MnSO_4$ and $MnCl_2$ based procedures in the absence of A23187, are strikingly different than doxorubicin loaded liposomes using the citrate procedure. Following drug loading, both of these formulations were a royal purple colour, as compared to the citrate-loaded preparations that are orange in appearance. Cryo-electron micrographs of the purple liposomal formulations indicated the appearance of an electron dense precipitate without any distinguishable crystalline structure. The resulting drug loaded liposomes (prepared in the absence of A23187) also exhibited little or no transmembrane pH gradient. As shown in Figures 3.9. and 3.10., these differences had little impact on drug retention attributes within the DMPC/Chol formulation but significant differences in drug release were observed for the DSPC/Chol formulation (Table 3.2.). It was noted that on addition of the ionophore A23187 to these formulations, the encapsulated drug was in a form where it could readily assemble into fibre-bundles, particularly in the $MnSO_4$ containing liposomes where addition of the ionophore generates a > 2.5 unit pH gradient (inside acidic). Thus the encapsulated drug is free to assume different chemical structures depending on the pH and the chemical composition within the liposomes.

Several studies have examined the role of transition metal-anthracycline interactions (Bouma et al., 1986; Fiallo et al., 1999; Greenaway and Dadrowiak, 1982). These studies, which relied on a variety of spectroscopic methods, concluded that primary metal binding involved the deprotonation of the hydroxy-anthraquinone moieties. The absorbance spectra of doxorubicin in various concentrations of $MnSO_4$ clearly showed a shift to higher wavelengths (lower energy). These absorption bands closely mimic those bands obtained following the deprotonation of doxorubicin at pH values above 10. Based on the

spectroscopic information gathered from studies of multiple anthracycline derivatives (Fiallo et al., 1999; Fiallo et al., 1998), our data support the proposal that Mn^{2+} is interacting at both the C(11)-O^- and C(12)=O positions and the C(5)=O and C(6)-O^- positions. Other investigators looking at the binding of Fe^{2+} to anthracyclines, have observed the deprotonation at the C (11)-OH and the C (6)-OH positions and the bathochromic shift from 480 to either 550-590 or 580-615 nm, respectively, for a variety of anthracycline derivatives including doxorubicin, pirarubicin, daunorubicin and idarubicin (Fiallo et al., 1999). The strong CD band centred around 573 nm in the manganese doxorubicin loaded liposome spectra confirms our belief that Mn^{2+} is complexed within these proposed co-ordination sites. Similar to the studies reported here, these investigators also reported that metal-anthracycline complexation resulted in a colour change from orange to blue-violet.

Complexation involving anthracyclines generally accompanies a theoretical increase in protons or a decrease in observed pH. This is not consistent with the results presented in Figure 3.7., which clearly demonstrate that metal ion complexation does not result in formation of a pH gradient. It is suggested here that manganese complexes with doxorubicin in the following manner:

$$MnSO_{4\,(aq)} \leftrightarrows Mn^{2+}{}_{(aq)} + SO_4{}^{2-}{}_{(aq)} \quad (1)$$

In water, the transition metal cations are always present as complex-hydrated ions;

$$Mn^{2+}{}_{(aq)} + 6H_2O \leftrightarrows Mn(H_2O)_6{}^{2+}{}_{(aq)} \quad (2)$$

The hydrated transition metal cations behave as weak acids in water:

$$Mn(H_2O)_6{}^{2+}{}_{(aq)} \leftrightarrows H^+ + Mn(H_2O)_5(OH)^{1+}{}_{(aq)} \quad (3)$$

$$K_a \text{ of } Mn(H_2O)_6{}^{2+}{}_{(aq)} = 3x10^{-11}$$

Because the hydrated manganese cation behaves as a weak acid and can dissociate to $Mn(H_2O)_5(OH)^{1+}_{(aq)}$, it most likely co-ordinates with the bidentate site offered by the C(11)-OH and C(12)=O positions or the C(5)=O and C(6)-OH positions neutralising the displaced hydrogen ion.

In summary, our studies have characterised the interactions between the transition metal manganese and doxorubicin, an interaction that promotes the accumulation of drug inside liposomes that contain this metal. The resulting drug loaded liposome is unique in that the complexed drug is maintained in a form that is distinct from that identified for loading methods relying on maintenance of a pH gradient and formation of citrate- or sulfate-based precipitates. The resulting liposomal drug formulation lacks a pH gradient, but still allows for effective drug retention attributes following i.v. administration. We are most excited, however, because the mechanism of drug loading occurs in a manner that is clearly distinct from methods involving use of pH gradients and it may be applicable to other drugs that possess co-ordination sites capable of complexing transition metals. The development of liposomal drug formulations for therapeutic use specifically containing manganese may be hampered by the fact that exposure to the metal at various concentrations may be neurotoxic (Malecki, 2001; Roth et al., 2002). Future studies will need to both confirm this and look at the possibility of developing other drug complexes using various transition metals.

CHAPTER 4

AN EVALUATION OF TRANSMEMBRANE ION GRADIENT-MEDIATED ENCAPSULATION OF TOPOTECAN WITHIN LIPOSOMES*

4.1. INTRODUCTION

Topotecan, a water-soluble analogue of camptothecin, is a topoisomerase I inhibitor (Ulukan and Swaan, 2002; Wall, 1998) and is one of two camptothecin analogues currently approved for clinical use by the US Food and Drug Administration (FDA) (Pizzolato and Saltz, 2003). Topotecan is used for the treatment of ovarian cancer after failure of initial or subsequent chemotherapy and small-cell lung cancer after failure of first-line chemotherapy (Broom, 1996; Herzog, 2002), and is increasingly being combined with other standard chemotherapeutic agents for improved therapy (Dunton, 1997; Emerson, 2000). The primary dose-limiting toxicity for topotecan is myelosuppression regardless of schedule (Takimoto et al., 1998) and this toxicity has been shown to be non-cumulative (Grochow et al., 1992).

Camptothecins possess an α-hydroxy-δ-lactone ring (ring E Chapter 1, Figure 1.9. (A)) which undergoes reversible hydrolysis at physiological pH (pH ~ 7) to an open ring-carboxylate form (Fassberg and Stella, 1992; Wall et al., 1993). The closed α-lactone ring appears to be structurally important for both passive diffusion of topotecan into cancer cells (Hertzberg et al., 1989; Hsiang et al., 1985), as well as successful interaction with the topoisomerase target (Burke, 1996).

*Submitted to the Journal of Controlled Release

Methods employed to minimise lactone ring opening include: (1) the structural modification of the drug itself to prevent high affinity binding of the carboxylate form to serum albumin binding pockets (Burke and Mi, 1994; Emerson et al., 1995), (2) derivitization of the lactone ring (Larsen et al., 2001) or (3) encapsulation into drug carriers such as liposomes and polymeric particles (Emerson, 2000; Hatefi and Amsden, 2002; Kehrer et al., 2002b).

Pre-clinical studies have shown that camptothecin and its water-soluble analogues benefit from liposomal encapsulation (Burke and Bom, 2000). For example, liposomal irinotecan (CPT-11) has been shown to increase drug serum half-life with a concurrent reduction in liver drug levels as compared to free drug (Sadzuka et al., 1998). A significant reduction in toxic side effects has also been observed. The antitumour effects of liposomal irinotecan were also superior to free drug and this was correlated to increased drug delivery to tumours (Emerson, 2000). Although lurtotecan, another camptothecin analogue, was not approved for clinical use (as a free drug), it is currently undergoing Phase II clinical trials as a liposomal formulation (NX211/OSI211) (Kehrer et al., 2002a). The active lactone form of lurtotecan is trapped in the aqueous core of liposomes and maintains activity under low pH conditions. Liposomal lurtotecan appears to exhibit an improved therapeutic index (Lynam et al., 1999) with greater plasma residence time and increased delivery of active drug to tumours (Desjardins et al., 2001).

Liposomal encapsulation of topotecan has also been shown to enhance this drug's therapeutic index (Tardi et al., 2000). Several studies have clearly demonstrated increased drug stability (Burke and Gao, 1994) and decreased toxicity combined with reduced blood elimination rates (Tardi et al., 2000). Topotecan displays markedly reduced affinity to lipid

compared to other camptothecins (Burke et al., 1993) and as a result, alternative approaches to stabilising the pH-sensitive lactone from hydrolysis have been pursued including the use of large multilamellar liposomes with an interior pH of 5. Previous studies have demonstrated that in the low pH environment, the lactone ring is maintained when packaged into DSPC multilamellar vesicles prepared at a drug-to-lipid ratio of 0.06 (wt/wt) using passive encapsulation techniques (Burke and Gao, 1994). Subramanian and Muller (Subramanian and Muller, 1995) showed that the same formulation with a drug-to-lipid ratio of 0.086 (wt/wt) (with an encapsulation efficiency of 40%) was 3-4 fold more effective relative to free topotecan in stabilising covalent topoisomerase I-DNA complexes using cell culturing techniques. These authors suggest that the increased activity of liposomal topotecan was due to both increased stability of pharamacologically active drug and greater intracellular delivery of drug.

It has been demonstrated that pH gradient loading methods can result in high drug-to-lipid ratio formulations (0.2 (wt/wt)) that exhibit improved topotecan lactone stability and increased drug levels in the plasma compartment, with an associated increase in efficacy in murine cancer models (Tardi et al., 2000). Others (Liu et al., 2002a) have also demonstrated that topotecan can be encapsulated in liposomes using an active loading technique that relies on formation of an $(NH_4)_2SO_4$ gradient to help generate and maintain a transmembrane pH gradient prior to and following loading. This formulation exhibited a high drug-to-lipid ratio, increased drug stability and enhanced anti-tumour activity. Given the recent interest in the development of liposomal formulations of topotecan, it is reasonable to ask why other pH gradient-based loading methods, such as those where a low pH buffer (e.g. 300 mM citrate pH 4.0) is employed, have not been explored. Further, there is surprisingly little information

on the nature of encapsulated topotecan and the role that encapsulated salts play in determining drug loading and drug release attributes. In order to investigate this, we have assessed several approaches to encapsulate topotecan by pH gradient dependent methods. It is demonstrated that all of the approaches tested result in drug loaded liposomes that exhibit a pH gradient (inside acidic) and an entrapped precipitate, as judged by cryo-TEM imaging. However, the stability of the resulting formulations, as judged by *in vitro* release assays, appears to be dependent on the presence of encapsulated sulfate and interestingly, formulations with higher drug-to-lipid ratios exhibit improved drug retention.

4.2. RESULTS

4.2.1. The Encapsulation of Topotecan into DSPC/Chol Liposomes

The first objective of this study was to compare topotecan encapsulation procedures that relied on the presence of a pH gradient across the liposome bilayer. pH gradients were established directly or indirectly. To directly establish the pH gradient, liposomes were prepared in the presence of an acidic buffer with substantial buffering capacity, such as 300 mM citrate, pH 3.5. The exterior buffer of the liposomes was then adjusted to the desired pH by exchanging the buffer by column chromatography. The $(NH_4)_2SO_4$ loading procedure was first described by the Barenholz group (Bolotin et al., 1994; Haran et al., 1993; Lasic et al., 1992) to encapsulate doxorubicin. Following encapsulation of $(NH_4)_2SO_4$, the external solution is exchanged for an iso-osmotic solution to establish a $(NH_4)_2SO_4$ gradient. Due to the high permeability of NH_3 ($1.3x10^4$ cm/s), it readily crosses the liposome bilayer, leaving behind one proton for every molecule of NH_3 lost (Bolotin et al., 1994). This creates a pH gradient, the magnitude of which is determined by the $[NH_4^+]_{in}/[NH_4^+]_{out}$ gradient. A pH gradient can also be established using ionophores. Researchers (Cheung et al., 1998; Deamer and Nichols, 1989; Fenske et al., 1998) have demonstrated that the addition of nigericin (a K^+ ionophore) or A23187 (a divalent cation ionophore) can establish a pH gradient across liposomes exhibiting the appropriate ion gradient (K^+ inside/Na^+ outside or Mn^{2+} inside/H^+ outside). For example, liposomes possessing a transmembrane $MnSO_4$ gradient can be incubated with A23187 facilitating the outward movement of one Mn^{2+} for the inward movement of two protons thus creating or maintaining a pH gradient. The presence of a chelator, such as EDTA, in the exterior buffer facilitates the activity of the ionophore. It is

important to note that the Mn^{2+} containing solutions used are typically prepared at a low pH (i.e. pH 3.5) to help maintain the Mn^{2+} in solution; however these solutions do not contain solutes that buffer changes in proton concentrations. The existing pH gradient (interior acidic) across these liposomes therefore can drive the uptake of a proportion of the added drug, however once drug uptake occurs, the pH gradient collapses (Abraham et al., 2002). Thus the presence of A23187 in these formulations is required to maintain the pH gradient during drug encapsulation.

To compare the four different pH gradient loading methods, accumulation of topotecan into DSPC/Chol liposomes was determined as a function of temperature and time. Drug loading was determined under conditions where topotecan and liposomal lipid were mixed at a drug-to-lipid ratio of 0.2 (wt/wt), and the final liposome lipid concentration was adjusted to 1 mg/ml. The topotecan loading data, summarised in Figure 4.1., indicate that at 20°C there is no appreciable drug uptake over the entire time course regardless of the ion gradient used. Topotecan encapsulation was found to be temperature dependent with the fastest rate of loading being observed at 60°C. The citrate and the $MnCl_2$ + A23187 procedures resulted in less than optimal encapsulation at 60°C. Both systems achieved maximal loading efficiencies of topotecan (65 and 100% respectively) within 10 min, however the drug-to-lipid ratios were not stable and the loading efficiencies measured at 80 min were less than 50% for both formulations. Both the $(NH_4)_2SO_4$ and $MnSO_4$ + A23187 procedures showed excellent encapsulation efficiencies approaching 100% within 5 min at 60°C. These formulations remained stable over the 80 min time course. At 40°C, > 98% encapsulation of topotecan was achieved using the $(NH_4)_2SO_4$ procedure within the 80 min time course in comparison to less than 25% encapsulation efficiency observed using the

Figure 4.1. Topotecan Encapsulation in DSPC/Chol (55/45) Liposomes Using Four Loading Procedures. Liposomes were prepared using:

(A) an $(NH_4)_2SO_4$ gradient,

(B) a $MnSO_4$ gradient with added A23187

(C) a citrate gradient or

(D) a $MnCl_2$ gradient with added A23187. Liposomes were prepared as described in Chapter 2, (section 2.3. and 2.4.2.), with the outer solutions exchanged using column chromatography in order to create the ion gradients. For the Mn^{2+} containing liposomes, A23187 was added and incubated 5 min prior to the addition of drug. Topotecan was added to the liposomes to achieve a 0.2 drug-to-lipid ratio (wt/wt) and incubated at either 20°C (■), 40°C (●) or 60°C (▲). At the indicated time points, aliquots were fractionated on 1 ml spin columns to separate encapsulated drug (collected in the void volume) from unencapsulated drug. Lipid and topotecan concentrations in the excluded fraction were quantitated. Data points represent the mean drug-to-lipid ratios of at least three replicate experiments and the error bars indicate the standard deviation.

Figure 4.1.

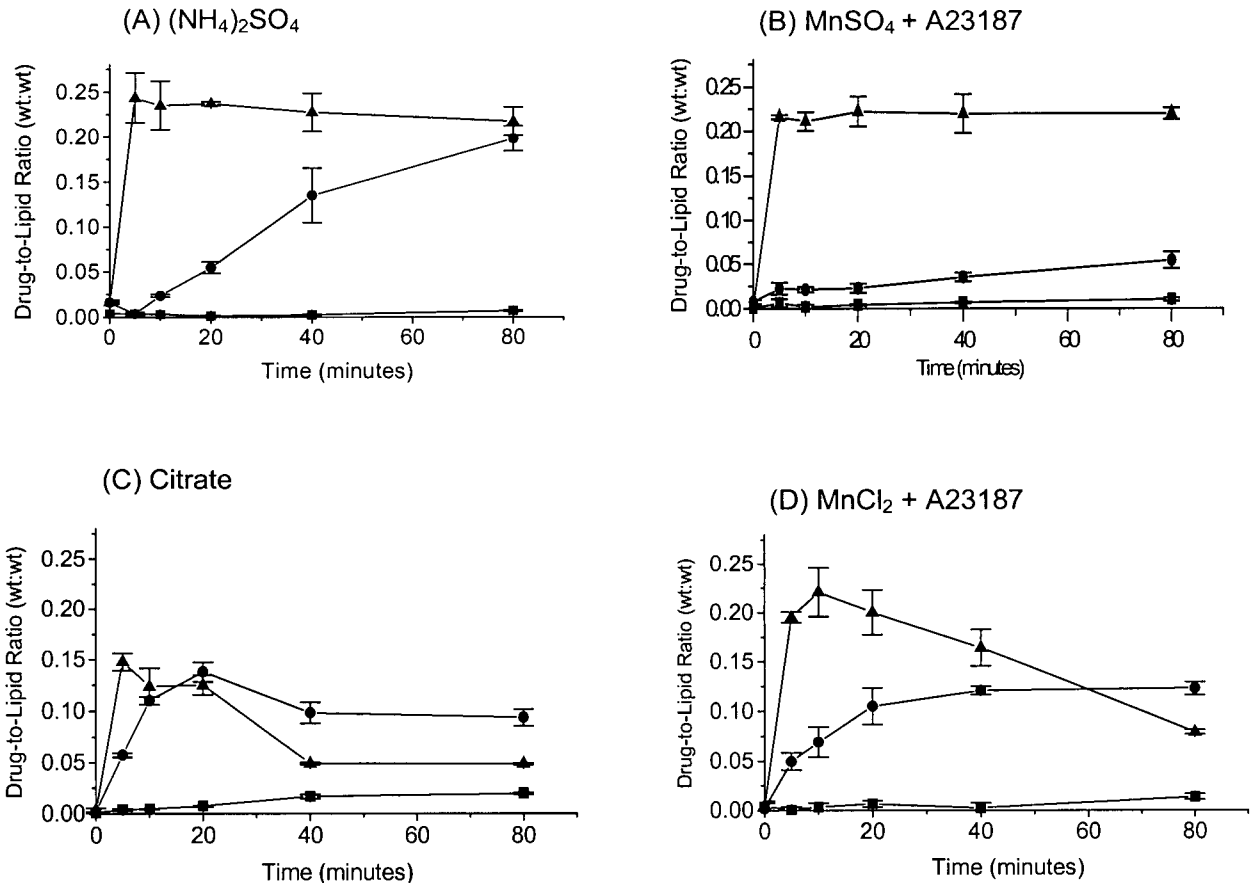
(A) $(NH_4)_2SO_4$
(B) $MnSO_4$ + A23187
(C) Citrate
(D) $MnCl_2$ + A23187
Drug-to-Lipid Ratio (wt:wt)
Time (minutes)
0.00
0.05
0.10
0.15
0.20
0.25
0
20
40
60
80

$MnSO_4$ + A23187 loading procedure. This difference is most likely a consequence of reduced A23187 incorporation into the DSPC/Chol liposome or reduced activity of the ionophore at this temperature.

4.2.2. Assessment of the Transmembrane pH Gradient Prior to and Following Topotecan Loading

In order to determine if differences in loading efficiencies were due to the magnitude of the transmembrane pH gradient before and after drug loading, radiolabeled methylamine was used as a pH sensitive probe (Harrigan et al., 1992; Redelmeier et al., 1989) to assess the transmembrane pH gradient. Each of the four formulations was evaluated prior to and following drug uptake, and the results are summarised in Figure 4.2. Following the establishment of the pH gradient but prior to topotecan loading, the formulations with encapsulated $(NH_4)_2SO_4$ (column 1), $MnSO_4$ + A23187 (column 3), citrate (column 5) and $MnCl_2$ (column 7) exhibited measured pH gradients of 3.6, 3.6, 3.8 and 2.6 units respectively. This demonstrated that a sufficient transmembrane pH gradient (inside acidic) was present for all formulations prior to drug encapsulation. Following the uptake of topotecan, to achieve a 0.1 drug-to-lipid ratio (wt/wt), the size of the pH gradients did not change significantly for the $MnSO_4$ + A23187 (column 4), citrate (column 6) and $MnCl_2$ (column 8) containing liposomes. Following drug loading, there was a significant ($p < 0.05$) 0.9 unit decrease in the measured pH gradient for topotecan containing liposomes loaded using the $(NH_4)_2SO_4$ gradient method. Importantly, all formulations maintained substantial (> 2 unit) pH gradients, thus differences in the stability of the different formulations could

Figure 4.2. Transmembrane pH Gradients Measured Prior to and Following Topotecan Loading. pH gradients were estimated through use of radiolabeled methylamine as described in Chapter 2, section 2.8.. Liposomes were incubated at 60°C for 15 min either in the presence or absence of topotecan and allowed to equilibrate to room temperature prior to the addition of methylamine. Topotecan was added to achieve a final drug-to-lipid ratio of 0.1 (wt/wt). The samples include those where the drug was encapsulated using the $(NH_4)_2SO_4$ loading method, the $MnSO_4$ + A23187 loading method, the citrate loading method, and the $MnCl_2$ + A23187 loading method without added topotecan (hollow bars) or following topotecan accumulation (filled bars). The results represent the mean pH gradient (inside acidic) determined from three separate experiments and the error bars indicate the standard deviation.

Figure 4.2.

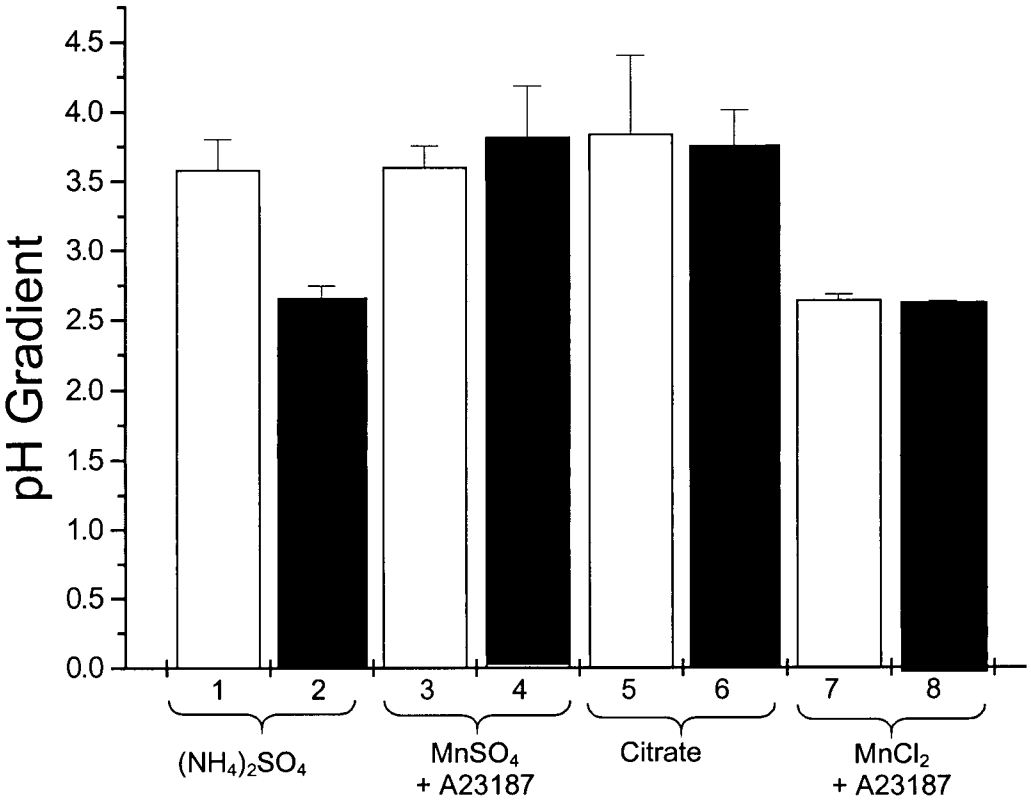
pH Gradient
4.5
4.0
3.5
3.0
2.5
2.0
1.5
1.0
0.5
0.0
1
2
3
4
5
6
7
8
(NH4)2SO4
MnSO4
+ A23187
Citrate
MnCl2
+ A23187

not be attributable to the depletion of the transmembrane pH gradient after loading. This is best exemplified by comparing $MnSO_4$ + A23187 loaded formulations to those prepared with 300 mM citrate (Figure 4.1.).

4.2.3. Influence of Initial Drug-to-Lipid Ratio on Topotecan Encapsulation Efficiency

The results in Figure 4.1. established that the topotecan loading capacity of liposomes, with encapsulated $MnCl_2$ and 300 mM citrate was 0.1 drug-to-lipid ratio (wt/wt). These results however, did not address questions of loading capacity for the other methods. In order to determine if increasing drug concentrations would affect loading efficiencies and/or formulation stability, topotecan was added to achieve initial drug-to-lipid ratios of 0.1, 0.2, 0.3 or 0.4 (wt/wt) to liposomes exhibiting $(NH_4)_2SO_4$ or $MnSO_4$ + A23187 gradients. Topotecan uptake into the liposomes, shown in Figure 4.3., was measured at 80 min. Encapsulation efficiencies of ≥95% were observed for initial drug-to-lipid ratios of 0.1, 0.2 and 0.3 (wt/wt) for both formulations. When the starting drug-to-lipid ratio was 0.4 (wt/wt), 77% and 70% of the added topotecan was encapsulated using the $(NH_4)_2SO_4$ and the $MnSO_4$ + A23187 loading procedures respectively. These results suggest that the loading capacity for these preparations is 0.3 mg topotecan per 1 mg liposomal lipid, a value that is 3 fold greater than that which can be achieved using the citrate and the $MnCl_2$ + A23187 formulations. This ratio is equivalent to a 0.22 mol drug to 1.0 mol lipid, and is almost 2-fold higher than previously described formulations (Liu et al., 2002a; Subramanian and Muller, 1995; Tardi et al., 2000).

Figure 4.3. Topotecan Encapsulation at Various Drug-to-Lipid Ratios Within DSPC/Chol (55/45) Liposomes. Liposomes were loaded with topotecan using either the $(NH_4)_2SO_4$ loading procedure (hollow bars) or the $MnSO_4$ loading procedure with added A23187 (filled bars). Liposomes were prepared as described in Chapter 2, (section 2.3. and 2.4.2.), and drug was loaded as described in Figure 4.1., where topotecan was added to the liposomes and incubated at 60°C for 80 min. The samples included those with topotecan added at a drug-to-lipid ratio (wt/wt) of either 0.1, 0.2, 0.3 or 0.4. At the 80 min time point, aliquots were fractionated on 1 ml spin columns to separate encapsulated drug (collected in the void volume) from unencapsulated drug. Lipid and drug concentrations were determined as described in Figure 4.1.. Data points represent the mean drug-to-lipid ratio of at least three replicate experiments and the error bars indicate the standard deviation.

Figure 4.3.

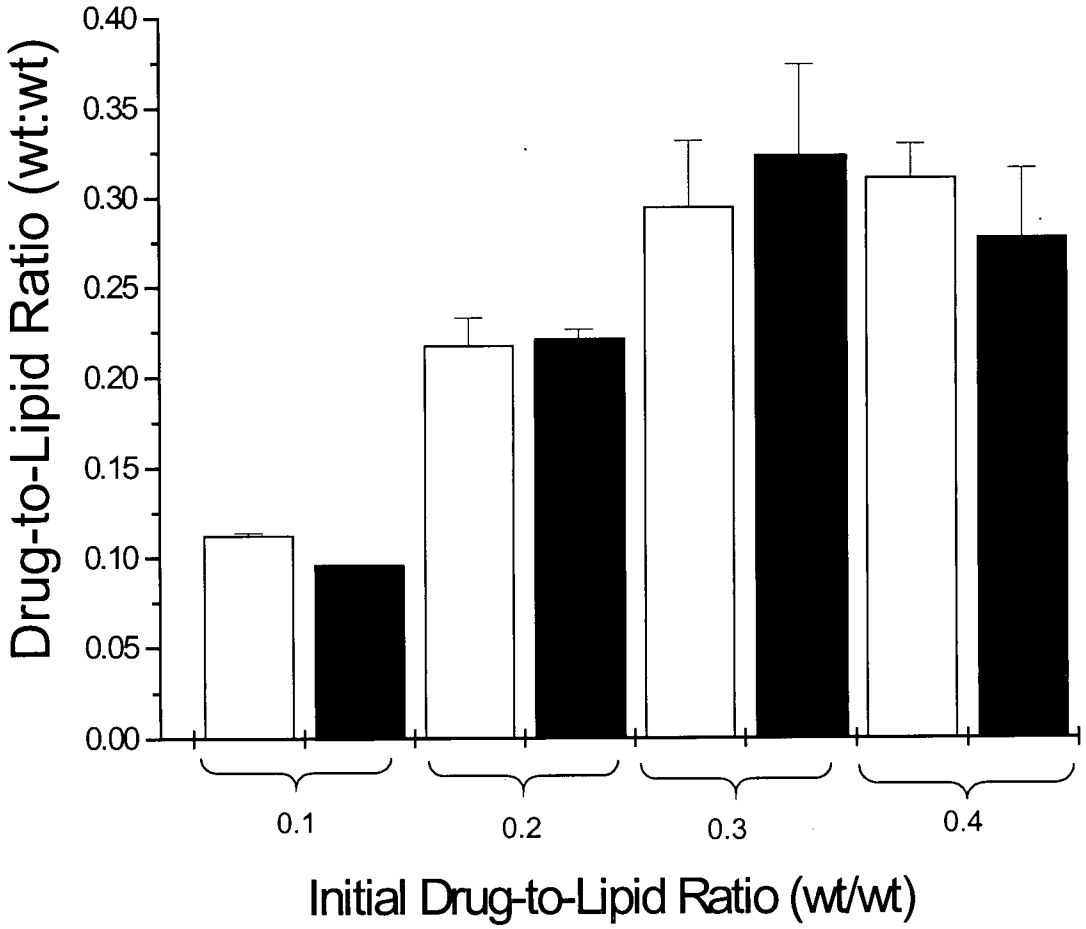
Drug-to-Lipid Ratio (wt:wt)
0.40
0.35
0.30
0.25
0.20
0.15
0.10
0.05
0.00
0.1
0.2
0.3
0.4
Initial Drug-to-Lipid Ratio (wt/wt)

4.2.4. In Vitro Topotecan Release From DSPC/Chol Liposomes

In order to determine if the loading methods affect drug release attributes, *in vitro* release studies were completed (Figure 4.4.). These studies evaluated topotecan loss from liposomes incubated at 37°C in the presence of fetal bovine serum (80% (v/v)). Liposomes were loaded with topotecan using all four methods such that the final drug-to-lipid ratio of each formulation was 0.1 (wt/wt). Changes in the percent topotecan remaining associated with liposomes, measured at various time points, indicated that all liposome formulations released drug rapidly. Greater than 90% loss was observed over the 24 h incubation period. It is worth noting that there was a measurable, albeit small, decrease in the rate of drug release for the formulations prepared with $(NH_4)_2SO_4$. This is most notable at the 6 h and 12 h time points where two to three times more drug was retained when compared to the citrate preparations. When drug release was assessed for those formulations that could be prepared at a 0.2 drug-to-lipid ratio (wt/wt) (i.e. the $(NH_4)_2SO_4$ and the $MnSO_4$ + A23187 formulations) (see Figure 4.4. insert), the drug release rate was significantly reduced when compared to formulations exhibiting the lower (0.1) drug-to-lipid ratio, but prepared using identical trapping methods, over 72 h. Ammonium sulfate preparations at a 0.2 drug-to-lipid ratio (wt/wt) had on average almost 3 times more drug retained over 36 h in comparison to similar formulations loaded at a 0.1 drug-to-lipid ratio (wt/wt). Manganese sulfate + A23187 preparations at a 0.2 drug-to-lipid ratio (wt/wt) had on average almost 5 times more drug retained over 36 h in comparison to similar formulations loaded at a 0.1 drug-to-lipid ratio (wt/wt). Both $(NH_4)_2SO_4$ and $MnSO_4$ + A23187 formulations loaded at a 0.2 drug-to-lipid ratio (wt/wt) retained ~10 fold more drug than the citrate samples over the course of 24 h.

Figure 4.4. In Vitro Release of Topotecan From DSPC/Chol (55/45) Liposomes Loaded Using Four Loading Procedures. Drug release was determined *in vitro* as described in Chapter 2, section 2.10., where liposomes were loaded with topotecan at a 0.1 drug-to-lipid ratio (wt/wt) using the $(NH_4)_2SO_4$ loading procedure (■), the $MnSO_4$ procedure with A23187 (●), the citrate loading procedure (▲) or the $MnCl_2$ loading procedure with A23187 (▼). Inset: liposomes were also loaded with topotecan at a 0.2 drug-to-lipid ratio (wt/wt) using the $(NH_4)_2SO_4$ loading procedure (♦) or the $MnSO_4$ procedure with A23187 (*). After drug encapsulation, the formulations were mixed with fetal bovine serum (final serum concentration of 80% and lipid concentration of 0.4 mg/ml) and incubated at 37°C. At the indicated time points, the drug and liposomal lipid concentrations were measured after fractionating samples on a 1 ml spin column. Data points represent the mean drug-to-lipid ratios obtained from three separate experiments and the error bars indicate the standard deviation for each data point

Figure 4.4.

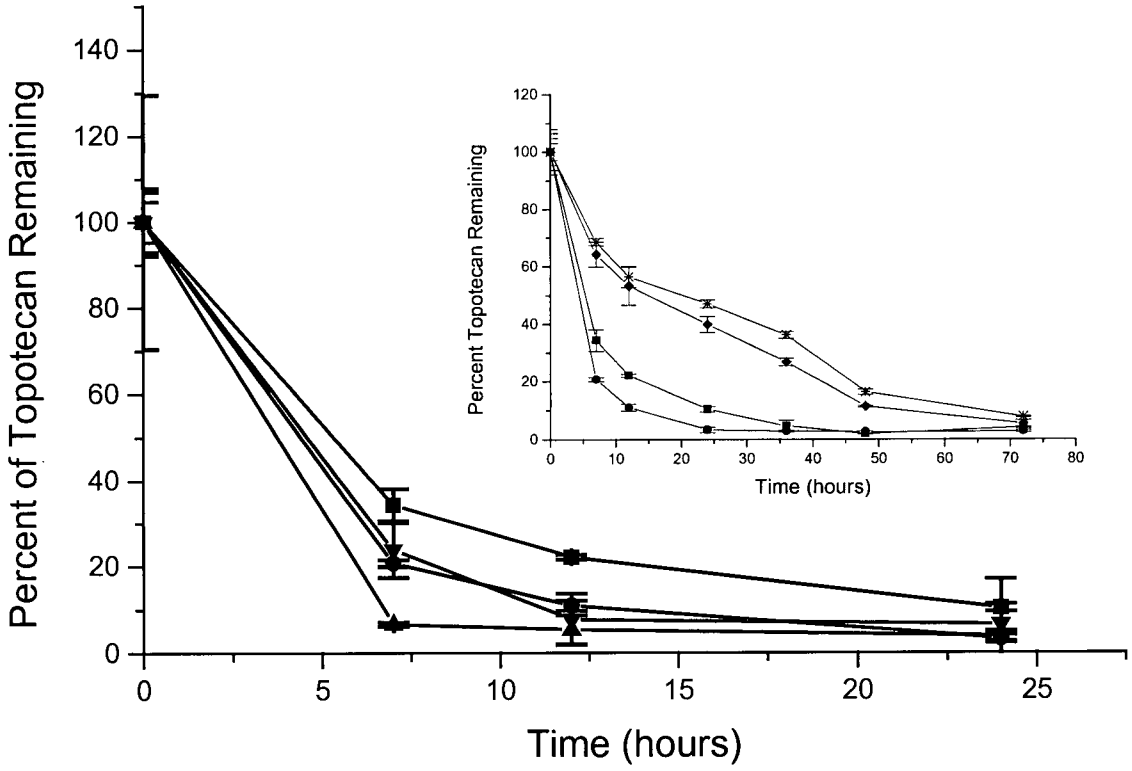
Percent of Topotecan Remaining
Time (hours)
0
20
40
60
80
100
120
140
0
5
10
15
20
25
Percent Topotecan Remaining
Time (hours)
0
20
40
60
80
100
120
0
10
20
30
40
50
60
70
80

4.2.5. Cryo-Transmission Electron Microscopic Analysis of the Topotecan-Loaded Liposomes

Changes in drug release rates have been attributed to changes in lipid composition (longer saturated acyl chain phospholipids exhibit improved retention when compared to short chain phospholipids) (Blok et al., 1975), presence of a pH gradient (in the absence of a pH gradient drug can be released at a faster rate) (Mayer et al., 1990b) and formation of an insoluble precipitate (formation of a precipitate at high loading efficiencies result in decreased drug release for doxorubicin formulations) (Lasic et al., 1995). Of these parameters, the one that could impact the formulations assessed here was drug precipitation. We therefore assessed whether differences in drug release could be due to drug precipitation following loading. Differences in liposome appearance were determined by cryo-electron micrograph analysis of the liposomal formulations before and after topotecan loading. Representative images are shown in Figure 4.5.. In the absence of drug, all liposomes (regardless of internal solute) appear to be mostly spherical and uniform in size (approximately 120 nm, a value that was consistent with the liposome size as determined by QELS analysis). Liposomes prepared with $MnSO_4$ appeared more oblong, potentially due to differences in trapped solute osmolarity. The osmolarity of $MnSO_4$ (~319 mOsm/l) was significantly less than that of the other solutions ($\geq$500 mOsm/l). Following accumulation of topotecan to a final drug-to-lipid ratio of 0.1 (wt/wt) (Figure 4.5. (IB)), all liposomes exhibited thin linear structures within the liposomes. The presence of these structures appeared to induce a change in the shape of the liposomes, which is most notable for liposomes prepared with $(NH_4)_2SO_4$ and $MnSO_4$ + A23187. When the $(NH_4)_2SO_4$ and $MnSO_4$ + A23187 containing liposomes were loaded with topotecan to a 0.2 drug-to-lipid

ratio (wt/wt) (Figure 4.5. (IIC)) there was no significant change in the entrapped structure. These results do not support the notion that improved drug retention observed at the higher drug-to-lipid ratios was due to formation of a precipitated structure not observable at lower drug-to-lipid ratios.

Figure 4.5. Cryo-Transmission Electron Microscopy Images of DSPC/Chol (55/45) Liposomes. Images of liposomes before (column A) or after topotecan loading to achieve a final drug-to-lipid ratio of either 0.1 (wt/wt)(column B) or 0.2 (wt/wt)(column C). The liposomes were prepared as described in Chapter 2 (section 2.3. and 2.4.2.) and loaded with topotecan as summarised in Figure 4.1..

Panel (IA): DSPC/Chol liposomes prepared in 250 mM $(NH_4)_2SO_4$, pH 5.5.

Panel (IB and IC): same as those described in IA except after liposomes are loaded with topotecan at a 0.1 and 0.2 drug-to-lipid ratio (wt/wt) respectively.

Panel (IIA): DSPC/Chol liposomes prepared in 300 mM $MnSO_4$, pH 3.5.

Panel (IIB and IIC): same as those described in IIA except after liposomes have been loaded with topotecan at a 0.1 drug-to-lipid ratio (wt/wt) and 0.2 drug-to-lipid ratio (wt/wt) respectively.

Panel (IIIA): DSPC/Chol liposomes prepared in 300 mM citrate, pH 3.5.

Panel (IIIB): same as those described for IIIA except after liposomes have been loaded with topotecan at a 0.1.

Panel (IVA): DSPC/Chol liposomes prepared in 300 mM $MnCl_2$, pH 3.5.

Panel (IVB): same as those described in (IVA) except after liposomes have been loaded with topotecan at a 0.1 drug-to-lipid ratio (wt/wt). The bar in panel (IA) is equivalent to 100 nm and all micrographs are shown at the same magnification. Each individual panel is representative of at least 15 images obtained.

Figure 4.5.

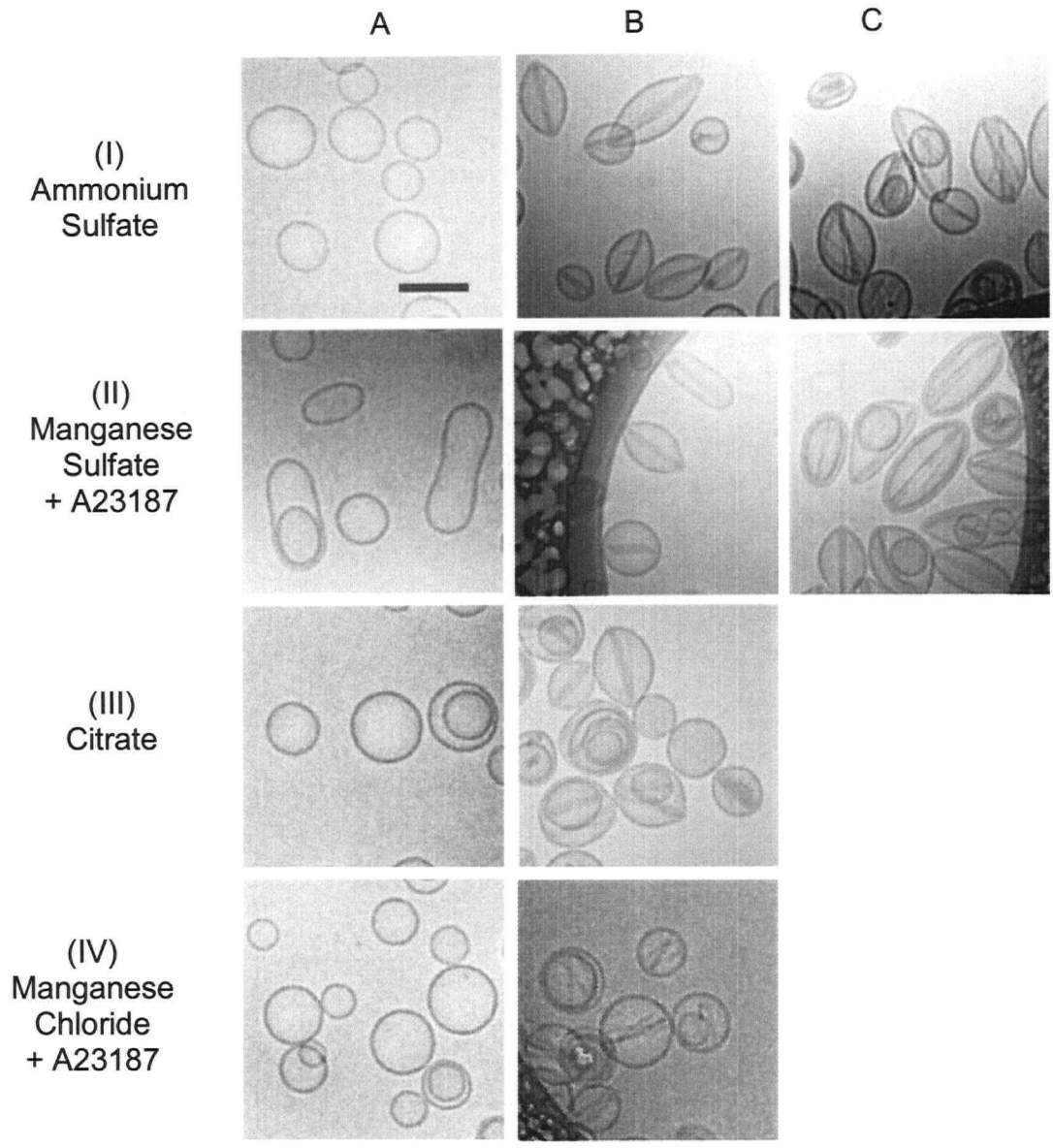
A
B
C
(I)
Ammonium
Sulfate
(II)
Manganese
Sulfate
+ A23187
(III)
Citrate
(IV)
Manganese
Chloride
+ A23187

4.3. DISCUSSION

Multiple pre-clinical and clinical studies provide evidence that liposomal encapsulation has the potential to improve the activity of encapsulated camptothecins (Burke and Bom, 2000; Emerson, 2000; Kehrer et al., 2002a; Liu et al., 2002b). Results suggest pH gradient loading techniques provide a versatile method to prepare liposomes with encapsulated topotecan, but relatively little is known about factors influencing drug loading and release properties. The studies presented here suggest that the counter ion may play an important role in the stability of the resulting drug loaded liposomes. The encapsulation methods used resulted in liposomes with an entrapped precipitated structure and all formulations exhibited similar pH gradients after drug loading. Importantly, unlike previous results obtained with other pH gradient-loaded drugs (e.g. doxorubicin, vincristine and daunorubicin), increased drug loading at high drug-to-lipid ratios resulted in formulations that exhibited reduced rates of drug release. These findings are discussed in terms of how the counter-ion could influence drug release and the nature of the precipitated structure as well as the potential mechanisms explaining decreased drug release with increasing drug-to-lipid ratio.

In this study, both the $(NH_4)_2SO_4$ and the $MnSO_4$ + A23187 based loading procedure proved superior. These methodologies resulted in stable formulations that could be prepared at drug-to-lipid ratios of 0.3 (wt/wt) with > 95% encapsulation efficiency. Contrary to previous studies (Cullis et al., 1997; Maurer-Spurej et al., 1999; Mayer et al., 1984), the stability of drug-loaded liposomes did not appear to be dependent on the magnitude or stability of the transmembrane pH gradient (see Figure 4.2.). It is worth noting that the rate

of drug release from DSPC/Chol liposomal doxorubicin and DSPC/Chol liposomal mitoxantrone (Gabizon et al., 1998; Maurer-Spurej et al., 1999) is relatively slow when compared to topotecan released from DSPC/Chol liposomes, as shown in this chapter. Other investigators made similar observations, suggesting that the more rapid release of topotecan was due to the fact that it did not precipitate within liposomes (Liu et al., 2002a). We clearly show that for the loading methods used, the resulting liposomes did exhibit a precipitated structure within the aqueous core (Figure 4.5.). Visually similar thin linear particles were observed in all topotecan-encapsulated formulations described. Drug precipitate morphologies within liposomes have been documented for doxorubicin, but it is understood that the nature of the topotecan precipitate observed here will be different than that observed for doxorubicin (Abraham et al., 2002; Li et al., 1998). Since all preparations had an acidic interior after drug encapsulation, the structure formed may simply be due to the high internal concentration of topotecan trapped in an acidic environment. Assuming a trapped volume of 1.2 μl/μmol lipid it can be estimated that the internal concentration of topotecan for those formulations prepared at a 0.1 drug-to-lipid ratio (wt/wt) would be approximately 114 mM which is well above the concentration at which topotecan exists as dimers (0.1 mM) (Streltsov et al., 2001). Others have suggested that citrate or sulfate is absolutely required for doxorubicin bundle formation (Li et al., 1998), but this does not appear to be the case for topotecan. However, the presence of sulfate appears to improve loading capacity as well as decreasing the rate of drug release when compared to formulations that do not contain sulfate ions (Figure 4.4.). The formation of a sulfate precipitate with a water soluble camptothecin has been observed previously (Tong et al., 1996). These authors suggested a stoichiometry of 2:1 (base to sulfate salt) at pH 3.5.

It is interesting to note that on increasing loading of topotecan from 0.1 to 0.2 drug-to-lipid ratio (wt/wt), there was an associated decrease in drug release yet the preparations exhibited no obvious differences in precipitated structure other than perhaps an increase in the number of structures observed. It is well established that the physical state of a drug dictates its pharmaceutical behaviour (Haleblian, 1975) and we can suggest that pH and sulfate ions may participate in stabilising the encapsulated topotecan precipitate. Decreased drug release from liposomes with higher topotecan concentrations could be due to formation of a more stabilised structure (different polymorphs) not detectable with cTEM, or perhaps the presence of more than one precipitated structure may affect the stability of the precipitate as they do with crystals (Byrn et al., 1999). Specifically, the degree to which topotecan is forming an amorphous precipitate versus a more ordered crystal structure could affect the rate of dissolution within the liposome and this may, in turn dictate drug release rates from the liposomes. It will be important to gain a better understanding of the physical state of topotecan in these liposomal formulations.

CHAPTER 5

IN VITRO AND IN VIVO CHARACTERISATION OF DOXORUBICIN AND VINCRISTINE CO-ENCAPSULATED WITHIN LIPOSOMES THROUGH USE OF TRANSITION METAL ION COMPLEXATION AND pH GRADIENT LOADING*

5.1. INTRODUCTION

Combination treatment regimes must take into consideration drug resistance mechanisms (Goldie, 2001) and tumour heterogeneity (Hobbs et al., 1998). In practice however, drug combinations usually take advantage of non-overlapping toxicities and unique mechanisms of action. There is an opportunity to capture the therapeutic potential of drug combinations through use of drug delivery technology. This hypothesis is supported by three lines of evidence: (1) appropriately designed drug delivery systems can improve drug delivery and efficacy for single agents (Burke and Gao, 1994; Mayer et al., 1990a; Rahman et al., 1980) (2) polymer, protein and lipid-based drug carriers have the capacity to co-formulate two or more therapeutic agents (Alakhov et al., 2001; Gariepy and Kawamura, 2001; Rihova, 2002) and (3) the pharmacokinetic behaviour of the co-formulated drugs will be dictated by the pharmacokinetic behaviour of the drug carrier system used, thus offering the potential to co-ordinate the plasma elimination and tissue distribution of the combined agents.

There are a multitude of approved chemotherapy combinations that could be used to test this principle and this chapter summarises data obtained using a novel liposomal formulation with co-encapsulated doxorubicin and vincristine. The rationale for selecting

*Published in Clinical Cancer Research *(in press)*

these drugs is due in part to the fact that liposomal formulations of the individual agents have already proven to be of clinical value in the treatment of patients with HIV-associated Kaposi sarcoma (Newell et al., 1998), ovarian cancer (Tejada-Berges et al., 2002), breast cancer (Batist et al., 2002), and various haematological malignancies (Christou et al., 2001; Sharpe et al., 2002), including relapsed non-Hodgkin's lymphoma. Furthermore, these liposomal formulations of doxorubicin and vincristine are now being evaluated as components of drug combinations used routinely in the management of patients with cancer. Liposomal formulations of doxorubicin, for example, have been evaluated as part of the VAD (vincristine, doxorubicin and dexamethasone) regimens used to treat patients with multiple myeloma (Hussein et al., 2002), and in the CHOP regimen (cyclophosphamide, doxorubicin, vincristine and prednisone) for treatment of aggressive non-Hodgkin's lymphoma (Tsavaris et al., 2002). Alternatively, this regimen has been modified by incorporation of a liposomal vincristine formulation for use in the treatment of a similar patient population (Sarris et al., 2000). A liposomal formulation of doxorubicin has been used in combination with cyclophosphamide for treatment of patients with metastatic breast cancer (Swenson et al., 2003) and with cyclophosphamide and fluorouracil for first-line treatment of patients with metastatic breast cancer (Valero et al., 1999). More recently, liposomal formulations of doxorubicin have been tested in combination with novel agents targeting the multidrug resistance protein Pgp as well as with trastuzumab (Herceptin®) for treatment of breast cancer patients with tumours over-expressing Her-2/neu (Gianni, 2002; Winer and Burstein, 2001).

These examples highlight two points. First, liposomal formulations of anticancer drugs are gaining wider acceptance by the clinical oncology community that is evaluating

how these formulations function when used as part of combination regimens. Second, vincristine and doxorubicin (or other anthracyclines) are still in use together as part of many combination regimens. This is likely a consequence of many decades of research providing data highlighting the different modes of action and non-overlapping toxicities of these agents.

Previous studies have attempted to co-formulate two drugs into a single liposomal formulation by means of an established transmembrane pH gradient, however this effort proved unsuccessful because of the instability of the resulting formulation (Saxon et al., 1999). Based on studies in Chapter 3 establishing the encapsulation of drug using metal complexation techniques, it is proposed here that a manganese metal gradient across liposomes could be used to encapsulate doxorubicin and, in a second step, to form a pH gradient across the doxorubicin loaded liposomes by addition of the electro-neutral ionophore, A23187 (divalent cation/proton exchanger). Studies in this chapter demonstrate that the resulting pH gradient can facilitate the rapid accumulation of vincristine without loss of encapsulated doxorubicin. The co-encapsulated formulation exhibited plasma elimination and drug release rates comparable to those observed with liposomes containing the individual active agents. Surprisingly however, the co-formulated combination of doxorubicin and vincristine exhibited anti-tumour activity that was no better than that observed using liposomal vincristine alone.

5.2. RESULTS

5.2.1. Co-Encapsulation of Doxorubicin and Vincristine into Manganese Sulfate Containing DSPC/Chol Liposomes

The primary objective of the studies in this chapter was to co-encapsulate doxorubicin and vincristine within one liposome population by taking advantage of two distinct loading methods. The first step relies on complexation of doxorubicin to the transition metal manganese , as outlined in Chapter 3 (Abraham et al., 2002; Cheung et al., 1998). The second step utilises an ionophore-generated transmembrane pH gradient (Fenske et al., 1998) driving the encapsulation of vincristine into the manganese-doxorubicin liposomes. Liposomes were prepared in 300 mM $MnSO_4$ (pH 3.5) followed by the exchange of outside solution to 300 mM sucrose / 20 mM HEPES / 15 mM EDTA (SHE) at pH 7.5, thereby establishing both a pH and a metal ion gradient. In this system the neutral species of doxorubicin crosses the lipid bilayer and subsequently the doxorubicin is protonated within the interior of liposomes. This causes the interior pH of the liposomes to increase because there is no entrapped solute that can buffer the change in proton concentration. When the internal pH is > 6.5, the encapsulated doxorubicin can form a complex with the entrapped transition metal. The complexation reaction is readily observed as the solution turns purple when doxorubicin complexes with manganese.

The entrapment properties of this loading reaction are presented in Figure 5.1.(A), where doxorubicin has been added to the liposomes at a drug-to-lipid ratio of 0.2 (wt/wt). Upon incubation at 60°C, > 98% of the added drug is sequestered within the interior of the liposomes within 10 min. Doxorubicin will also load into liposomes exhibiting a

transmembrane pH gradient. Thus if A23187 is added to the $MnSO_4$ loaded liposomes to generate a pH gradient, the resulting pH gradient is sufficient to load doxorubicin (Figure 5.1.(B)). The time course indicated that for both metal complexation and pH gradient loading, > 98% loading efficiencies are obtained within 10 min at 60°C for doxorubicin.

In contrast to doxorubicin, vincristine does not interact with Mn^{2+} in a manner that promotes drug accumulation; less than 5% loading was observed in the absence of the ionophore (Figure 5.1.(C)). However, following addition of A23187, the pH gradient generated promotes vincristine loading (Figure 5.1.(D)). Upon incubation with the ionophore at 60°C, > 98% of the added drug was encapsulated into liposomes within 10 min.

It is known that the drug accumulation process is temperature- and time- dependent for both doxorubicin and vincristine. Efficient loading of doxorubicin into DSPC/Chol (55/45) liposomes requires an incubation temperature of 60°C (Mayer et al., 1989). The influence of temperature on vincristine loading into liposomes using A23187 to generate a pH gradient is shown in Figure 5.2.. The results indicate that efficient vincristine loading occurs only when the incubation temperature is held between 50°C and 60°C. When the incubation temperature was 40°C, less then 20% of the added drug was loaded into the liposomes at the end of the 1 h time course. It is possible that reductions in vincristine loading efficiencies may be a consequence of reduced vincristine permeation across the lipid bilayer at these temperatures (Boman et al., 1993; Mayer et al., 1993) however, the temperature effects could also be attributed to reduced activity of the ionophore (Deleers and Malaisse, 1980).

Figure 5.1. Doxorubicin or Vincristine Encapsulation in DSPC/Chol (55/45) Liposomes. (A and C): the $MnSO_4$ Loading Procedure alone or (B and D): with A23187. Liposomes were prepared as described in Chapter 2 (section 2.3., 2.4.1.and 2.4.3.) and the outer solutions were exchanged using column chromatography in order to create a metal gradient. For (B and D) A23187 was added and incubated 5 min prior to the addition of drug. Doxorubicin was added to the liposomes to achieve a drug-to-lipid ratio of 0.2 (wt/wt) and vincristine was added to the liposomes to achieve a drug-to-lipid ratio of 0.05 (wt/wt) and all preparations were incubated at 60°C. Doxorubicin was quantitated by the A_{480} of a detergent-solubilized sample and vincristine was quantitated using a ^{3}H-vincristine radiolabeled marker. Data points represent mean drug-to-lipid ratios of at least three replicate experiments and the error bars indicate the standard deviation.

Figure 5.1.

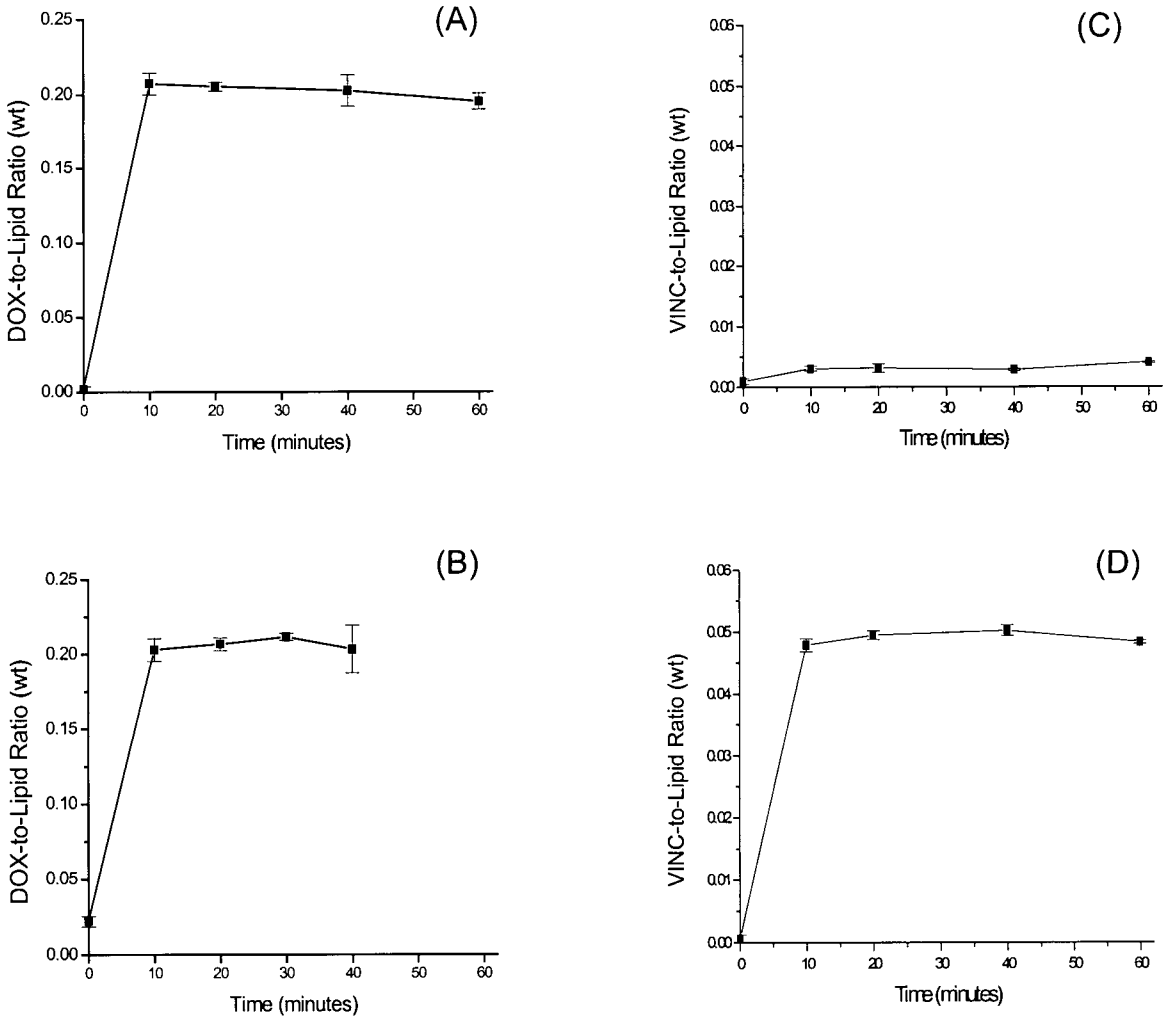
(A)
DOX-to-Lipid Ratio (wt)
0.25
0.20
0.15
0.10
0.05
0.00
0
10
20
30
40
50
60
Time (minutes)
(C)
VINC-to-Lipid Ratio (wt)
0.06
0.05
0.04
0.03
0.02
0.01
0.00
Time (minutes)
(B)
DOX-to-Lipid Ratio (wt)
Time (minutes)
(D)
VINC-to-Lipid Ratio (wt)
Time (minutes)

Figure 5.2. Vincristine Encapsulation in DSPC/Chol (55/45) Liposomes. Liposomes were prepared as described in Chapter 2 (section 2.3. and 2.4.3.) and the outer solutions were exchanged using column chromatography in order to create a metal gradient. Vincristine was added and incubated at 20°C (■), 40°C (●), 50°C (▲) and 60°C (▼) (with adding the A23187 5 min prior the addition of drug). Vincristine was added to the liposomes to achieve a 0.05 (wt/wt) drug-to-lipid ratio. Data points represent mean drug-to-lipid ratios of at least three replicate experiments and the error bars indicate the standard deviation.

Figure 5.2.

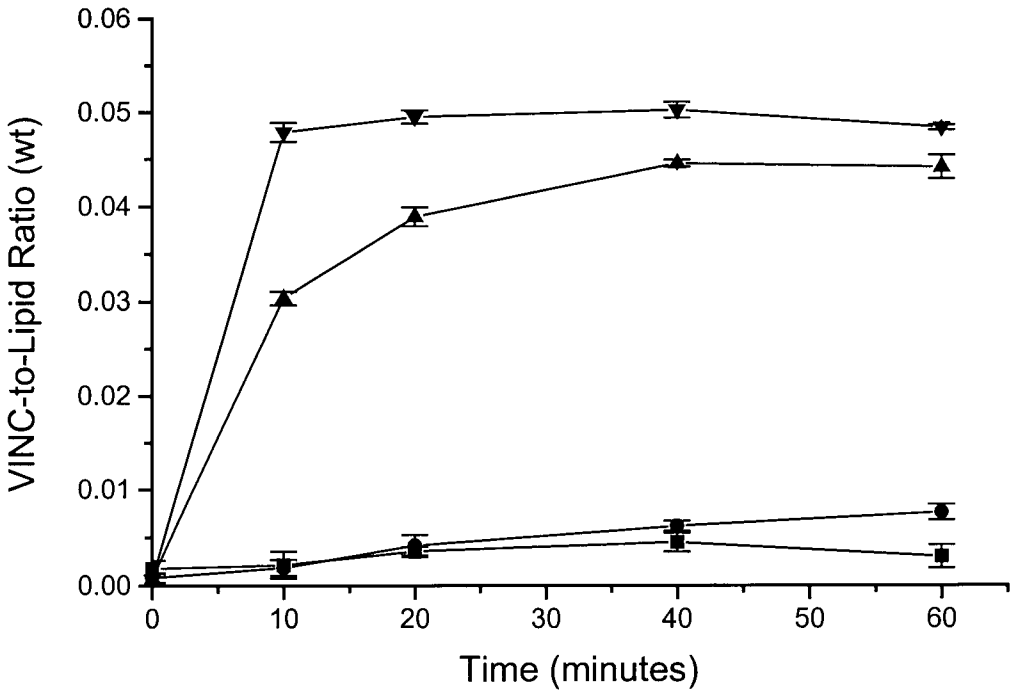
VINC-to-Lipid Ratio (wt)
0.06
0.05
0.04
0.03
0.02
0.01
0.00
0
10
20
30
40
50
60
Time (minutes)

Considering the objective of loading both doxorubicin and vincristine into the same liposome population using two loading methods (transition metal complexation and pH gradient) and knowing that the complexation reaction between doxorubicin and manganese is dependent on pH (greatest at pH > 6.5 (Bouma et al., 1986), it was important to define conditions where vincristine loading occurred prior to dissociation of the doxorubicin-manganese complex. In order to determine the rate of this dissociation reaction at different temperatures, $MnSO_4$-loaded DSPC/Chol (55/45) liposomes were prepared and incubated with doxorubicin at a drug-to-lipid ratio of 0.2 (wt/wt). On encapsulation of doxorubicin, the pH gradient was measured across liposome bilayers using methylamine as a pH sensitive probe (Harrigan et al., 1992) and have estimated the interior liposomal pH to be approximately 7.3. Following drug loading, A23187 was added and the conversion of the manganese-doxorubicin complex to uncomplexed doxorubicin was followed spectrophotometrically. The existing pH gradients were also measured across the doxorubicin-loaded liposomes with added A23187, and have estimated that the interior liposomal pH is approximately 3.9.

The results shown in Figure 5.3. were obtained by measuring the decrease in A_{550} as a function of time following addition of A23187 to the doxorubicin loaded liposomes. A23187 exchanges protons in and Mn^{2+} out of the liposomes reducing the interior liposomal pH. A decrease in absorbance at 550 nm indicates the dissociation of the doxorubicin-metal chelate and re-protonation of the chromophore at the reduced pH. At 40°C, no decrease in A_{550} was observed over the 40 min time course, indicating that the manganese-doxorubicin complex was stable under these conditions. As noted in Figure 5.2., vincristine does not load into these liposomes at 40°C, and it is likely that the ionophore is not functioning optimally at this

Figure 5.3. Changes in A_{550} (ΔA_{550}) of Doxorubicin Loaded DSPC/Chol Liposomes. Liposomes were prepared as described in Chapter 2, section 2.3., 2.4.1.and 2.7., with the outer solution exchanged using column chromatography in order to create a metal gradient. Doxorubicin was added to the liposomes to achieve a drug-to-lipid ratio of 0.2 (wt/wt). A23187 was added in each experiment at t = 0 and incubated at 40°C (■), 50°C (●), and 60°C (▲). A decrease in absorbance at 550 nm is indicative of the conversion of the manganese complex to un-complexed doxorubicin in a low pH environment. Data points are representative of at least six replicate experiments.

Figure 5.3.

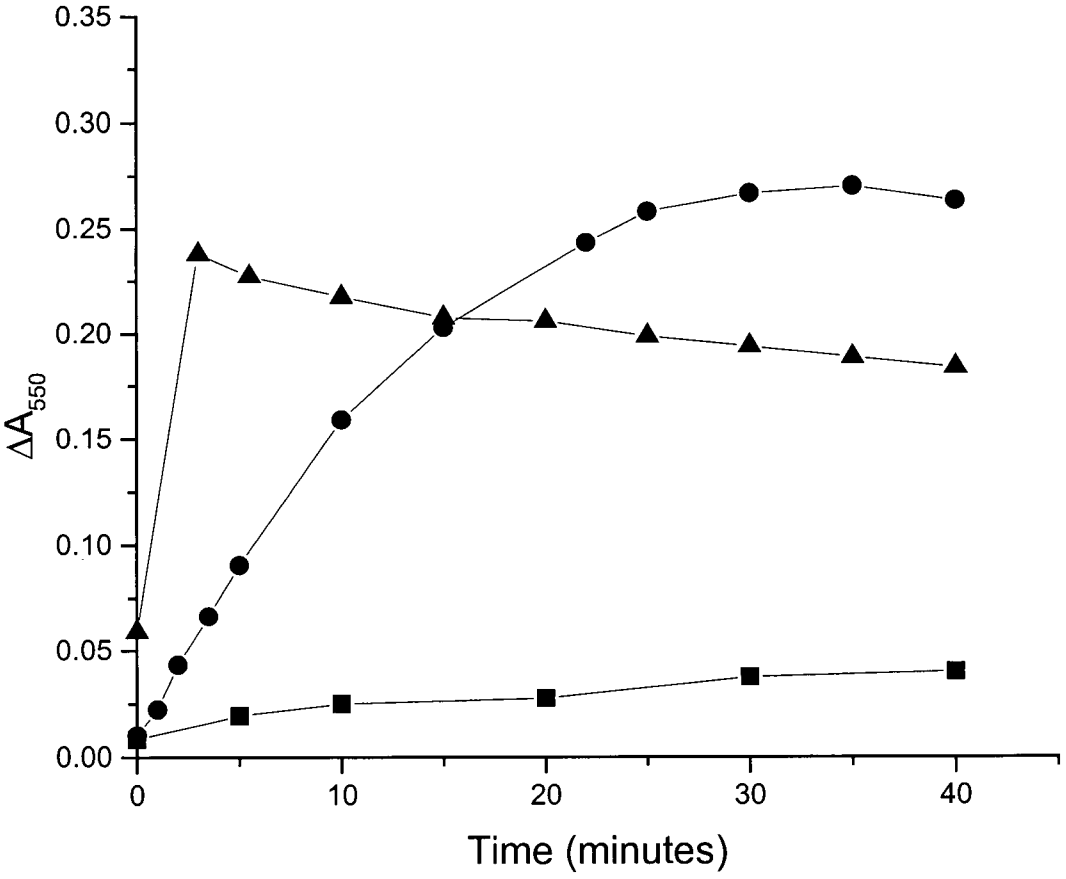
0.35
0.30
0.25
0.20
0.15
0.10
0.05
0.00
ΔA_{550}
0
10
20
30
40
Time (minutes)

temperature. When the incubation temperature was increased to 50°C and 60°C, a decrease in A_{550} occurred, indicating a dissociation of the manganese-doxorubicin complex. Destabilisation of this complex was much slower at 50°C, with the maximal changes in A_{550} observed in 30 min after A23187 addition. The visible colour change from purple to orange was not seen in the sample incubated at 40°C.

When considered together, the results in Figure 5.2. and 5.3. suggests that, at an incubation temperature of 50°C: (1) vincristine loading would occur within 40 min after A23187 addition to the $MnSO_4$ containing DSPC/Chol (55/45) liposomes and (2) over the same time period and under the same conditions the manganese-doxorubicin complex dissociates. It can be suggested that vincristine encapsulation could be achieved in doxorubicin loaded liposomes prior to or during dissociation of the manganese-doxorubicin complex. This loading reaction is shown in Figure 5.4.. Doxorubicin loaded DSPC/Chol liposomes (0.2 drug-to-lipid ratio (wt/wt)) were mixed with A23187 at 50°C just prior to the addition of vincristine (added at a 0.05 drug-to-lipid ratio (wt/wt)). Vincristine loading was complete within 40 min with no loss of doxorubicin from the liposomes during this time frame, indicating that the encapsulation efficiency approached 100% for both drugs using the co-encapsulation procedure.

5.2.2. In Vivo Plasma Elimination of Liposomes With Co-Encapsulated Doxorubicin and Vincristine

The procedure described above results in efficient encapsulation of both doxorubicin and vincristine into DSPC/Chol (55/45) liposomes. As noted elsewhere, it is possible that the

Figure 5.4. Doxorubicin and Vincristine Encapsulation Within DSPC/Chol (55/45) Liposomes. Liposomes were prepared as described in the Chapter 2, section 2.3. and 2.4.4., with the outer solution exchanged using column chromatography in order to create a metal gradient. Doxorubicin (●) was added to the liposomes to achieve a drug-to-lipid ratio of 0.2 (wt/wt) and incubated at 60°C. A23187 was added to the doxorubicin loaded liposomes and incubated 5 min prior to the addition of vincristine (■), which was added to achieve a final drug-to-lipid ratio of 0.05 (wt/wt). Vincristine loading was completed using an incubation temperature of 50°C. Doxorubicin was quantitated by the A_{480} of a detergent-solubilized sample. Data points represent mean drug-to-lipid ratios of at least three replicate experiments and the error bars indicate the standard deviation.

Figure 5.4.

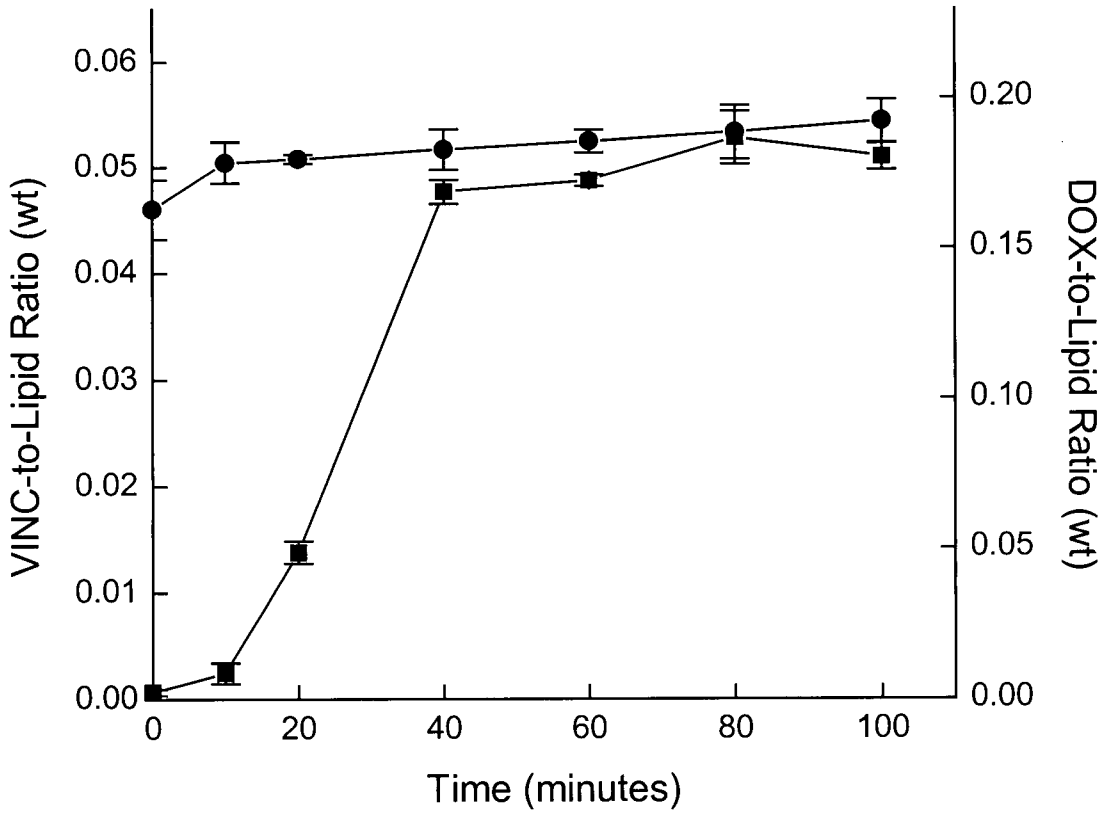
VINC-to-Lipid Ratio (wt)
DOX-to-Lipid Ratio (wt)
Time (minutes)
0.00
0.01
0.02
0.03
0.04
0.05
0.06
0.00
0.05
0.10
0.15
0.20
0
20
40
60
80
100

presence of two encapsulated drugs may alter drug release from liposomes in the plasma compartment (Saxon et al., 1999) and perhaps even the plasma elimination rate of the liposomes themselves. The plasma elimination of liposomal lipid and associated drugs was evaluated following i.v. administration in mice. These data have been summarised in Figure 5.5., where liposomal lipid and drug levels at 1, 4, and 24 h after i.v. injection are shown. Four DSPC/Chol liposomal formulations were evaluated in these studies: (1) doxorubicin encapsulated without the ionophore, (2) doxorubicin encapsulated with the ionophore, (3) vincristine encapsulated with the ionophore, and (4) doxorubicin and vincristine co-encapsulated as described above. Balb/c mice were injected with lipid doses of approximately 50 mg/kg and doxorubicin doses of 10 mg/kg and/or vincristine doses of 2.5 mg/kg. As judged by the plasma levels of liposomal lipid (Figure 5.5.(A)) all liposomes were eliminated from the plasma compartment at comparable rates, although there are significantly higher levels ($p < 0.016$) of liposomal lipid at the 24 h time point when liposomes contained both vincristine and doxorubicin compared to either alone. It is known that doxorubicin or vincristine, when loaded into a liposomal carrier, can alter the plasma elimination of the carrier (Bally et al., 1990; Mayer et al., 1993), therefore this result could suggest that the combination of drugs actually enhances this effect. Plasma doxorubicin levels (Figure 5.5.(B)) are consistent with previous studies where doxorubicin was eliminated more rapidly when the drug-loaded liposomes were prepared in the absence of the ionophore. This is most evident at the 24 h time point, where the plasma doxorubicin levels are almost 10-fold lower when compared to those achieved following administration of the doxorubicin loaded liposomes prepared with A23187. Plasma vincristine levels (Figure 5.5.(C)) were comparable to those observed for DSPC/Chol liposomal vincristine prepared using citrate-

Figure 5.5. The lipid and drug plasma elimination profiles of drug-loaded DSPC/Chol (55/45) liposomes following i.v. administration into female Balb/c mice. Liposomes were loaded with doxorubicin, vincristine or both. Loaded liposomes were adjusted to a concentration such that 10 mg/kg doxorubicin or 2.5 mg/kg vincristine could be administered in an injection volume of 200 μl.

(A): Plasma lipid levels in mice administrated either doxorubicin-loaded liposomes using the $MnSO_4$ loading procedure (●), doxorubicin loaded liposomes using the $MnSO_4$ loading procedure with A23187 ionophore (■), vincristine loaded liposomes using the $MnSO_4$ loading procedure with A23187 ionophore (▲) or simultaneously loaded doxorubicin and vincristine liposomes (▼). Lipid levels were determined using ^{3}H-CHE or ^{14}C-CHE as a liposomal lipid marker.

(B): The level of doxorubicin fluorescent equivalents in plasma from mice administered doxorubicin-loaded liposomes using the $MnSO_4$ loading procedure with (■) or without (●) the A23187 ionophore.

(C): Vincristine levels in plasma were determined from mice that received vincristine loaded liposomes prepared using the $MnSO_4$ loading procedure with A23187 (♦).

(D): Doxorubicin (▲) and vincristine (▼) levels were also measured in plasma of mice receiving co-encapsulated liposomes. Data points represent mean drug-to-lipid ratios ± SD (n = 6).

Figure 5.5.

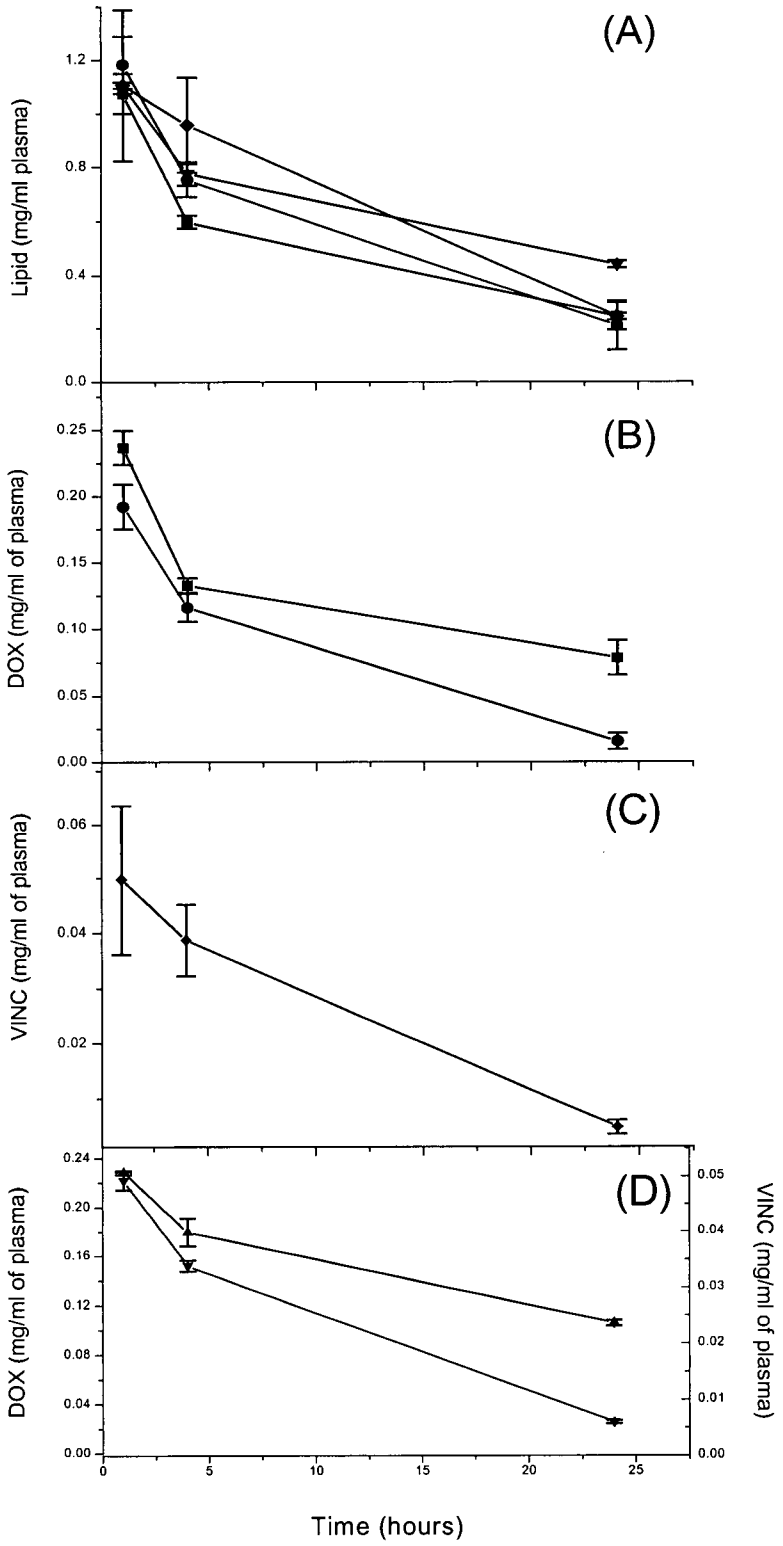
(A)
Lipid (mg/ml plasma)
1.2
0.8
0.4
0.0
(B)
DOX (mg/ml of plasma)
0.25
0.20
0.15
0.10
0.05
0.00
(C)
VINC (mg/ml of plasma)
0.06
0.04
0.02
(D)
DOX (mg/ml of plasma)
VINC (mg/ml of plasma)
0.24
0.20
0.16
0.12
0.08
0.04
0.00
0.05
0.04
0.03
0.02
0.01
0.00
0
5
10
15
20
25
Time (hours)

based loading methods (Mayer et al., 1990a). When both drugs were co-encapsulated within liposomes (Figure 5.5(D)) the plasma levels of doxorubicin and vincristine were comparable ($p > 0.1181$) to that observed for liposomal formulations containing only one of the agents.

Drug release from liposomes in the plasma compartment can be estimated from the data shown in Figure 5.5., by calculating the drug-to-lipid ratios at the indicated time points. Results for the doxorubicin loaded liposomes (single agent), shown in Figure 5.6.(A), clearly indicate that doxorubicin release from the DSPC/Chol liposomes is faster when loading is achieved through Mn^{2+}-doxorubicin complexation. The formulation prepared using A23187 in the procedure exhibited no measurable change in drug-to-lipid ratio over the 24 h time course, consistent with previous data for doxorubicin loaded into DSPC/Chol liposomes using the pH gradient procedure (encapsulated 300 mM citrate, pH 4.0 (Mayer et al., 1990b)). In contrast, vincristine is readily released from DSPC/Chol liposomes over the 24 h time course (Figure 5.6.(B)), where the vincristine-to-lipid ratio at 24 h is 3.3-fold lower than that of the injected formulation. When the injected liposomes contain doxorubicin and vincristine (Figure 5.6.(C)), the drug release profiles are comparable to those measured for liposomes containing the single agents encapsulated using A23187.

5.2.3. Efficacy of the Co-Encapsulated Liposomal Doxorubicin/Vincristine Formulation Against a Human Breast Cancer Xenograft Model

Vaage *et al.* (Vaage et al., 1993) have previously evaluated the therapeutic activity of vincristine and doxorubicin encapsulated in sterically stabilised liposomes. In these studies the drugs were not co-encapsulated and the drugs were used alone and in combination to treat murine MC2 tumours. The liposomal drugs were more active than free agents, however,

Figure 5.6. In Vivo Release of Doxorubicin and Vincristine From DSPC/Chol (55/45) Liposomes. Panels represent drug-to-lipid ratios calculated from Figure 5.5.. Liposomes containing:

(A): doxorubicin encapsulated using the $MnSO_4$ procedure either without A23187 (●); or with A23187 (■);

(B): vincristine encapsulated using the $MnSO_4$ procedure with A23187 (♦);

(C): doxorubicin (▲) and vincristine (▼) co-encapsulated using the $MnSO_4$ procedure as described in Figure 5.4. following i.v. administration to female Balb/c mice. Drug-loaded liposomes were adjusted to a concentration such that a dose of 10 mg/kg doxorubicin and/or 2.5 mg/kg vincristine could be administered in an injection volume of 200 μl. Drug levels in the plasma were assessed via measurements of doxorubicin fluorescent equivalents or the ^3H-vincristine sulfate marker. Data points represent mean drug-to-lipid ratios of at least six replicate experiments and the error bars indicate the standard deviation.

Figure 5.6.

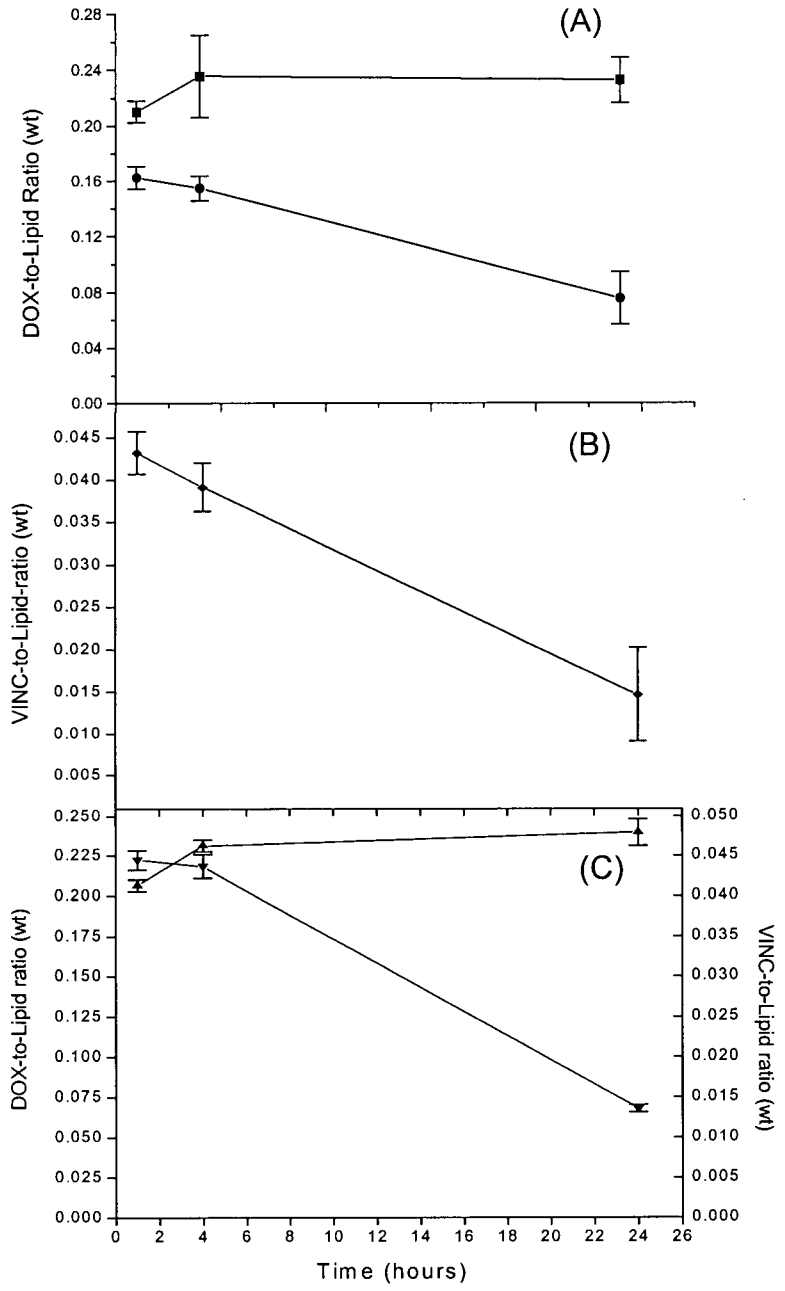
(A)
DOX-to-Lipid Ratio (wt)
0.28
0.24
0.20
0.16
0.12
0.08
0.04
0.00
(B)
VINC-to-Lipid-ratio (wt)
0.045
0.040
0.035
0.030
0.025
0.020
0.015
0.010
0.005
(C)
DOX-to-Lipid ratio (wt)
VINC-to-Lipid ratio (wt)
0.250
0.225
0.200
0.175
0.150
0.125
0.100
0.075
0.050
0.025
0.000
0.050
0.045
0.040
0.035
0.030
0.025
0.020
0.015
0.010
0.005
0.000
0 2 4 6 8 10 12 14 16 18 20 22 24 26
Time (hours)

when they were used in combination the liposomal vincristine and liposomal doxorubicin did not provide improved therapy when simultaneously injected (Vaage et al., 1993). Their results suggested that liposomal vincristine inhibited the activity of liposomal doxorubicin. These authors proposed that reduced activity could have been a consequence of vincristine's effects on the cell cycle which prevented/delayed progression into S-phase in which the impact of doxorubicin could be greatest (Vaage et al., 1993). Alternatively, they argued that inhibition of activity could have been a consequence of dosing schedules and liposome-mediated drug delivery, where liposomal vincristine administration may have interfered with the delivery of liposomal doxorubicin to the tumour. This latter concern would not arise if the drugs were co-encapsulated therefore a therapeutic assessment of this liposomal formulation is described here.

Efficacy was determined in SCID RAG-2M mice bearing solid tumours derived from the s.c. injection of MDA 435/LCC6 human breast cancer cells. This is an aggressive breast tumour model that has been described elsewhere (Leonessa et al., 1996). The results of these studies are summarised in Table 5.1.. Complete dose titrations were completed, however the activity observed at the maximum tolerated dose of drug (2.5 mg/kg vincristine + 10 mg/kg doxorubicin) resulted in only a 32% delay in tumour growth, thus only the results obtained at the MTD are presented here. Tumour growth delay values calculated as the time in days for the tumours to reach 200 mg in treated animals minus the time to reach the same size in saline treated control animals, are shown in Table 5.1. for animals treated with: (1) free vincristine and DSPC/Chol (55/45) liposomal vincristine (2.5 mg/kg); (2) free doxorubicin and DSPC/Chol (55/45) liposomal doxorubicin (10 mg/kg); (3) a combination of free

Table 5.1. Treatment of SCID RAG-2M Mice Bearing MDA 435 /LCC6 Tumours

Treatment Group	Time Taken For Tumour to Reach 0.2 Grams[ab] (Days ± SEM)	Growth Delay[c] (Days ± SEM)	Percent Growth Delay[d]
Saline	39 ± 4		0
Free vincristine (2.5 mg/kg) (MTD)	48 ± 3	8.5 ± 2.9	22
[e]Liposomal vincristine (2.5 mg/kg) (MTD)	55 ± 3	16 ± 2.6	41
Free doxorubicin (10 mg/kg)	42 ± 3	3.3 ± 2.9	8
Liposomal doxorubicin (10 mg/kg)	46 ± 3	7.5 ± 2.3	19
Free vincristine/doxorubicin (2.5/10 mg/kg) (MTD)	47 ± 2	8.5 ± 1.8	22
Co-encapsulated vincristine and doxorubicin (2.5/10 mg/kg) (MTD)	52 ± 2	12.5 ± 2.1	32
Liposomal vincristine and Liposomal doxorubicin (2.5 / 10 mg/kg) (MTD)	50 ± 3	11 ± 2.4	28

[a]Tumours were established in SCID RAG-2M mice by a single s.c. injection of 2 x 10^6 MDA435/LCC6 cells with 4 mice total per group. Tumour growth was noted within 12-14 days after cell injection and within 18 days, measurable tumours (~0.1g) were noted.

[b]Data represents days required for the tumour mass to reach 0.2 g. Results were averaged from at least 4 mice and an ANOVA analysis was performed to assess differences among the treatment groups. A p-value of < 0.05 was considered significant.

[c]Growth Delay is determined by subtracting the mean time taken for the control tumours to reach 0.2 g from the mean time taken for the treated tumours to reach 0.2 g.

[d]Percent Growth Delay is growth delay expressed as a percentage of mean time taken for the control tumours to reach 0.2 g.

[e]Growth delay for liposomal vincristine treated mice were statistically significant ($p < 0.05$) in comparison to all other treatment groups.

vincristine and free doxorubicin (2.5 and 10 mg/kg respectively); (4) the co-encapsulated liposomal vincristine and doxorubicin formulation (2.5 mg/kg vincristine / 10 mg/kg doxorubicin) and a combination of liposomal vincristine and liposomal doxorubicin (2.5 and 10 mg/kg respectively). The results demonstrate that optimal tumour growth inhibition is achieved when the tumour-bearing animals are treated with liposomal vincristine. This improvement in therapy was statistically significant ($p < 0.05$) in comparison to all other treatment groups. At the 2.5 mg/kg dose, liposomal vincristine caused a 16 day delay in tumour growth, which was almost two-fold greater than that achieved with free vincristine at the same dose. Liposomal doxorubicin used as a single agent resulted in a 7 day delay in tumour growth, and improved the activity of free doxorubicin > 2-fold. When combined with liposomal vincristine or administered co-encapsulated with vincristine, delays in tumour growth of 11 and 12 days were observed respectively.

5.2.4. In Vitro Cytotoxicity Analysis of Doxorubicin and Vincristine Alone and in Combination

Results presented here as well as those of Vaage *et al.* (Vaage et al., 1993) suggest that co-administration of liposomal doxorubicin and liposomal vincristine results in less than additive activity or antagonism. In an effort to gain a better understanding about the cytotoxic effects of vincristine and doxorubicin when used in combination, *in vitro* cytotoxicity studies were completed using MDA435/LCC6 cells as the target cell population. Cytotoxicity effects were determined using the MTT assay as described in Chapter 2, section 2.13.. The effects of the combined free drugs were analysed using the multiple drug equation developed by Chou and Talalay (Chou and Talalay, 1984). This method is most readily

applied to dose titration data collected for individual agents alone and the combination of drugs added at fixed ratios and over a broad range of effective doses.

In this study the vincristine-to-doxorubicin ratios were selected to reflect the drug ratios measured in the plasma following i.v. administration. Three fixed vincristine-to-doxorubicin ratios of 1/4, 1/7 and 1/20 (mol/mol) were evaluated against the MDA435/LCC6 cell line. The effects of the drugs alone and in combination were evaluated following a 72 h drug exposure. The MTT results (Figure 5.7.) were completed in triplicate, three separate times. The resulting nine data points at each concentration were then analysed using the CaluSyn Software program. This software package takes the non-linear dose response curves and applies an un-weighted linear regression analysis. This analysis, which assumed mutually exclusive interactions, provided a correlation coefficient of > 0.9 for all data sets. The regression analysis provided estimations of the drug concentrations required to inhibit cell growth/proliferation at a variety of effect levels. The IC_{90} of vincristine alone was approximately 3.7 nM while doxorubicin was 10 μM (Figure 5.7.). These data demonstrate that the therapeutic activity of the combination would be dominated by the activity of vincristine. The estimated drug combination concentrations required to achieve 90% inhibition of cell growth/proliferation at the 1/4 vincristine/doxorubicin ratio (mol/mol), indicate that the amount of vincristine required was comparable to that needed when vincristine was used alone (~3 nM). As the ratio changed to 1/20 vincristine-to-doxorubicin (mol/mol), the estimated amount of the drugs required to achieve 90% cell kill increased substantially for both vincristine and doxorubicin. Specifically, the IC_{90} observed was 4.3 μM for vincristine and 86 μM for doxorubicin.

Figure 5.7. IC_{90} Values Determined From In Vitro MTT Assays Assessing the Activity of Doxorubicin and Vincristine Combinations. MDA435/LCC6 human breast cancer cells were plated and allowed to adhere for 24 h. Drug was diluted and added at the indicated ratios. Control wells received 0.2 ml media without drug. After 72 h, the cell viability was assessed using a conventional MTT dye reduction assay (see Chapter 2, section 2.13.). Data were analysed using the Calcusyn program, which incorporates the median dose effect method developed by Chou and Talalay. This analysis was used to estimate drug concentrations required to inhibit cell growth/proliferation by 90% (IC_{90}). These cells were exposed to doxorubicin (solid black bars) and vincristine (light grey bars) separately (1) and combined in three different ratios (2) 4/1 DOX/VINC ratio (mol/mol), (3) 7/1 DOX/VINC ratio (mol/mol), and (4) 20/1 DOX/VINC ratio (mol/mol). The MTT results were completed in triplicate, three separate times.

Figure 5.7.

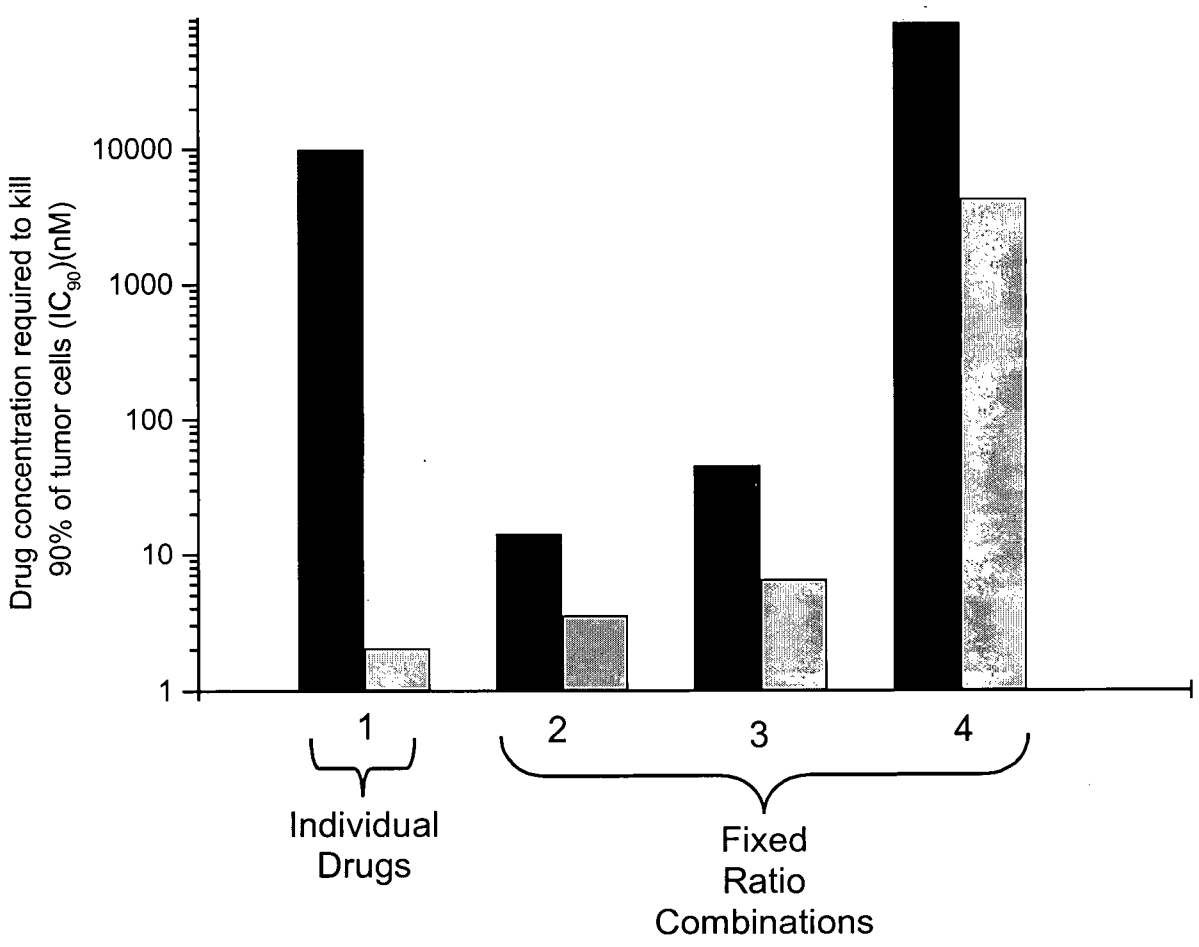
Drug concentration required to kill
90% of tumor cells (IC_{90})(nM)
10000
1000
100
10
1
1
2
3
4
Individual
Drugs
Fixed
Ratio
Combinations

These data reveal the presence of strong antagonism for this drug combination and this was reflected in the combination index (CI) values defined by the CalcuSyn Software (Chou and Hayball, 1996). It should be noted that a CI value of 0.9 to 1.1 is indicative of additive activity, while CI values below 0.9 indicate drug synergy and values above 1.1 indicate antagonism. When analysed in this manner, the combination of vincristine and doxorubicin, at all ratios studied, exhibited CI values > 1.1 over the entire range of effective concentrations. At the 1/20 vincristine-to-doxorubicin ratio (mol/mol) the CI value was > 20, indicative of strong antagonism.

5.3. DISCUSSION

The results summarised in this report can sustain two avenues of discussion. Of practical significance, a procedure to co-encapsulate two anticancer drugs into a single liposomal formulation has been delineated. However data is provided which clearly demonstrate that the co-encapsulated vincristine and doxorubicin formulation exhibits antagonistic effects. This discussion will consider the potential for encapsulating multiple drugs into liposomes using distinct loading methods as well as providing a rationale as to why the co-encapsulated vincristine-doxorubicin formulation exhibited antagonistic effects.

Our initial efforts to encapsulate two drugs into a single liposome population using pH gradient-mediated approaches was hindered in part because the stability of these formulations was poor both *in vitro* and *in vivo* (Saxon et al., 1999). Studies in Chapter 3 defined a unique drug loading method that relies on formation of a manganese-doxorubicin drug complex, rather than a transmembrane pH gradient. Applying this new method to the problem of co-encapsulating two anticancer drugs, it is demonstrated here that a stable formulation at drug-to-lipid ratios shown to be therapeutically relevant (Mayer et al., 1990a; Mayer et al., 1989), can be easily prepared. An established manganese metal gradient across liposomes permitted the efficient loading of doxorubicin (Figure 5.1.(A)) due to formation of a drug-metal complex. Sufficient levels of un-complexed Mn^{2+} remained to support the establishment of a transmembrane pH gradient following addition of A23187, an electroneutral divalent metal/proton pump. The pH gradient formed supported the efficient loading of vincristine. The methods described here are generally applicable to a wide range of drugs that have chemical groups capable of complexing transition metals like Mn^{2+} (for

example anthracyclines (Beraldo et al., 1985; Fiallo et al., 1999), camptothecins (Kuwahara et al., 1986; Kuwahara et al., 1985) and anticancer antibiotics such as bleomycin (Dabrowiak et al., 1978; Suzuki et al., 1984)) and second agents that can be encapsulated using pH gradients (for example mitoxantrone, camptothecins and vinca alkaloids (Burke and Gao, 1994; Fenske et al., 1998; Lim et al., 1997; Madden et al., 1990)).

Plasma elimination data suggest that the release rates of co-encapsulated drugs observed are consistent with what would be expected for the drugs encapsulated into DSPC/Chol liposomes using pH gradient loading methods (see Figures 5.5. and 5.6.). The doxorubicin and vincristine drug release profiles from individually loaded DSPC/Chol liposomes (Figure 5.6.(A) and 5.6.(B)) are not significantly different from the drug release rates observed in the co-encapsulated formulation (Figure 6.6.(C)). This suggests that the drugs are not interacting in a manner that affects their release from the liposomes. Our data illustrates that doxorubicin retention in these liposomes is influenced by the presence of a pH gradient. Greater than 50% of the encapsulated doxorubicin was released from liposomes within the plasma compartment when the injected formulation was prepared using encapsulated manganese sulfate, a situation where the internal pH of the liposomes is equal to the exterior pH (Abraham et al., 2002). In contrast, there is negligible release of doxorubicin from doxorubicin-loaded liposomes prepared using A23187 to generate a transmembrane pH gradient.

The rationale for selecting vincristine and doxorubicin for co-encapsulation was based on the fact that these two drugs are commonly used in combination chemotherapy. The drugs exhibit different dose limiting toxicities and different mechanisms of activity. Since liposomal forms of vincristine and doxorubicin are more active than the respective free

drugs, it was anticipated that combining the two liposomal drugs would be beneficial. One significant disadvantage of administrating individually encapsulated doxorubicin and vincristine is the potential interference each liposome population may exert on the other's pharmacokinetic profile, thereby altering drug delivery to tumour cells. This problem was addressed with co-encapsulation, which would make this an unlikely issue. However it should be noted that a previous study demonstrated that simultaneous administration of separately encapsulated liposomal doxorubicin and liposomal vincristine exhibited activity no better than that achieved for liposomal doxorubicin alone (Vaage et al., 1993). An explanation as to why co-delivery of vincristine and doxorubicin may result in less than additive activity can be developed when considering the mechanisms of action of the free drugs. It is established that free doxorubicin has some activity against cells in various phases of the cell cycle, but its maximal effects occur in early S-phase. This action causes a delay in the progression through all phases of the cell cycle except $M \rightarrow G_1$ (Barranco et al., 1973; Kim and Kim, 1972). Vincristine causes cells to accumulate in mitosis (Friedland, 1992; Hill and Whelan, 1980; Hill and Whelan, 1981). Based on this information, it is reasonable to suggest that these two drugs could interfere with each other's action. The Chou and Talalay analysis of vincristine and doxorubicin combinations at fixed ratios (where the drugs are added simultaneously) clearly indicated that this drug combination is antagonistic (Figure 5.7.). These findings (Figure 5.7. and Table 5.1.) indicate that drug combinations selected on the basis of non-overlapping toxicity and unique mechanisms of action can provide less than optimal therapeutic effects, even when the pharmacokinetics and therapeutic properties of the individual drugs are improved through use of carefully designed drug carriers.

Accepting the concerns identified above for co-encapsulated vincristine and doxorubicin, there is also a tremendous opportunity to define strategies where the drugs encapsulated within the liposomal formulation are selected using arguments that consider the potential for drug combinations to exhibit supra-additive activity or synergy. Based on evidence supporting the mechanism of selected agents on tumour cells, it should be possible to better rationalise the design of a formulation with an effective drug combination. The use of multiple agents has to date been developed based on pragmatic principles, addressing issues of overlapping toxicities, drug resistance and tumour cell heterogeneity. Yet there are now a variety of *in vitro* assays, like the Chou and Talalay analysis used here, that can establish whether two drugs act synergistically or antagonistically when used in combination (Greco and Hainsworth, 1995). Although these *in vitro* assays can provide information on drug sequencing effects, typically the drugs are added simultaneously to the cells in culture. Given the fact that it is established here that a method whereby two agents can be efficiently loaded into a liposomal formulation, which when given intravenously will dictate the plasma elimination and biodistribution of both agents, it is now reasonable to consider combining data obtained from *in vitro* synergy assays with liposomal drug formulation methods to define carrier systems capable of delivering co-encapsulated drugs in a synergistic manner. Importantly, it is also reasonable to consider the potential of formulated drug combinations, where the drugs selected are encapsulated in different liposomes, each optimised for the individual agents. These could then be combined and administered as a single drug product. If this strategy were to be pursued, it would be important to demonstrate that the pharmacokinetic and biodistribution attributes of the different liposomal carriers are comparable.

CHAPTER 6

DOXORUBICIN LOADED THERMOSENSITIVE LIPOSOMES: CHARACTERIZATION OF MANGANESE COMPLEXATION-BASED DRUG LOADING

6.1. INTRODUCTION

A major obstacle in the administration of cancer chemotherapy is the specific delivery of the agent to the target tumour cell population. Liposomes, as drug carriers for chemotherapy, effectively target the tumour by their propensity to accumulate preferentially within tumours when compared to other tissues. To improve the activity of liposomal drugs, investigators have pursued the development of lipid formulations that can be induced to release their contents following tumour localisation. Examples of externally applied 'triggers' to promote drug release from liposomes include light (Anderson and Thompson, 1992; Shum et al., 2001), pH sensitivity (Connor et al., 1984; Guo et al., 2003), mechanical disruption (Unger et al., 1998) or heat (hyperthermia) (Gaber et al., 1996; Yatvin et al., 1978).

Hyperthermia, the application of heat to increase the temperature of a site of tumour growth above physiological temperature, has been actively investigated as a direct treatment modality (Field and Bleehen, 1979), as well as to enhance radiation (Goldfeder et al., 1979) and chemotherapy effects (Wust et al., 2002). The use of heat to promote drug release from liposomes has been explored for over 25 years (Chelvi and Ralhan, 1997; Kong et al., 2000; Yatvin et al., 1978). The design of thermosensitive liposomes has been based on selecting lipid compositions that undergo a gel-to-liquid crystalline transition (see Chapter 1, section

1.2.4.) at temperatures above 37°C, but below temperatures where healthy tissue can be damaged (45°C). Permeability of lipid bilayers increases significantly in the transition region (temperatures close to the Tc) (Papahadjopoulos et al., 1973). Ideally a thermosensitive liposome formulation for systemic administration would comprise a lipid composition that retains drug well at body temperature (while in the circulation), yet releases its contents when encountering higher temperatures (Weinstein et al., 1979).

Initial studies developing thermosensitive liposomes focused on the use of dipalmitoyl phosphatidylcholine (DPPC) as the bulk membrane component due to its phase transition temperature (Tc = 41.5-41.9°C) (Iga et al., 1991; Merlin, 1991a; Yatvin et al., 1978). Importantly, in order to obtain a co-operative transition at a defined temperature, cholesterol could not be present in amounts > 30 mol%. This created problems for those developing this technology for *in vivo* use since cholesterol has often been required to enhance liposome stability (Gregoriadis and Davis, 1979). In order to achieve a balance between stability and temperature sensitivity, investigators added small amounts of cholesterol to these formulations designed for use in combination with hyperthermia. For example, liposomes composed of DPPC/DSPC/Chol (5/4/2 molar ratio), containing passively encapsulated doxorubicin were prepared (Merlin, 1991b). These formulations exhibited drug-to-lipid ratios of 0.0012/1 (wt/wt) and when compared to a number of other compositions, displayed optimal differences in drug release between 37°C and 43°C (Merlin, 1991a). These formulations also exhibited improved activity as judged by cytotoxicity against sensitive and multidrug-resistant MCF-7 cells in clonogenic assays when used in combination with heating to 43°C (Merlin et al., 1993).

With the goal of increasing the amount of thermosensitive liposomes accumulated within tumours, 'sterically stabilised' formulations have also been considered. Stabilisation of liposomes can be achieved by the incorporation of either monosialoganglioside (G_{M1}) (Maruyama et al., 1993) or polyethylene glycol (PEG) modified lipids (Gaber et al., 1995); which can prevent liposome-liposome aggregation (Allen et al., 2002) and facilitate increased circulation life times (Allen et al., 1989; Gabizon and Papahadjopoulos, 1988). Maruyama *et al.* developed thermosensitive liposomes composed of DPPC/DSPC/G_{M1} (9/1/0.13 molar ratio) that were able to entrap doxorubicin at a 0.2 drug-to-lipid ratio (wt/wt) using a pH gradient-based loading method. This formulation displayed an increased circulation half-life in blood following i.v. administration in Balb/c mice bearing colon carcinoma-26 tumours (Maruyama et al., 1993). Increased circulation lifetime was also associated with increased delivery to the tumour site. Although therapeutically active, these formulations released less than 45% of encapsulated drug upon heating over the course of 5 min.

In order to increase the release of drug from 'sterically stabilised' thermosensitive liposomes, the addition of lysolipids was attempted based on the hypothesis that the inclusion of a lysolipid would enhance the permeability at the gel-liquid crystalline phase transition (Anyarambhatla and Needham, 1999). This hypothesis led to the development of a new thermosensitive liposome formulation with an optimised composition of DPPC/MSPC/DSPE-PEG (90/10/4 molar ratio) (Ickenstein et al., 2003; Needham and Dewhirst, 2001). These liposomes have been termed low thermosensitive liposomes or lysolecithin-containing thermosensitive liposomes (LTSL) and were originally developed by Needham *et al.* (Kong et al., 2000; Needham et al., 2000). This formulation was found to be

more efficacious when compared to free drug or control liposomes as judged by reduced growth rates of human squamous cell (FaDu) carcinoma xenograft tumours. The LTSL, when used in combination with mild heating, produced complete regressions lasting up to 60 days post treatment for 11 out of 11 treated mice (Needham et al., 2000).

The LTSL formulation is of therapeutic interest, but the liposomes can be further optimised. One issue of concern is the fact that these liposomes appear to have a limited capacity to encapsulate doxorubicin when using pH gradient loading methods. The maximal doxorubicin-to-lipid ratio that can be achieved is 0.05 (wt/wt) (Needham et al., 2000) and, perhaps more importantly, data from plasma elimination studies suggest that these formulations release drug rapidly following i.v. injection (Ickenstein, 2003). This may be a consequence of the drug's permeability across the liposomal membrane, a problem that could potentially be overcome by selecting a different drug. Alternatively, it could be a consequence of increased drug release associated with lower drug-to-lipid ratio formulations. In order to address some of these issues, the studies summarised in this chapter evaluated if the $MnSO_4$ loading procedure could provide an alternative to pH gradient loading techniques that would result in increased doxorubicin loading in LTSL. The results demonstrate that metal complexation can be used to prepare liposomes with a higher drug-to-lipid ratio, and this may be due, in part, to the lack of formation of an organised drug precipitate within the liposomes when drug encapsulation relies on metal complexation.

6.2. RESULTS

6.2.1. The Encapsulation of Doxorubicin Within Thermosensitive Liposomes

The first objective of this study was to determine if the $MnSO_4$ encapsulation technique could provide an alternative procedure to load doxorubicin within LTSL. pH gradient based loading techniques can be used to encapsulate doxorubicin, but the extent of loading is less than that which can be achieved in cholesterol-containing formulations (Gaber et al., 1995; Kong et al., 2000; Needham et al., 2000). The accumulation of doxorubicin within LTSL using either the citrate or the $MnSO_4$ encapsulation procedure was determined as a function of time (Figure 6.1.). Drug loading was determined at 37°C where the drug and liposomes were mixed at drug-to-lipid ratios of 0.1, 0.2, and 0.3 (wt/wt), with the final lipid concentration adjusted to 5 mg/ml. As summarised in Figure 6.1.(A), doxorubicin loading for the citrate loading procedure resulted in a maximum level of drug uptake equivalent to 0.05 mg doxorubicin per mg total lipid, regardless of the initial drug-to-lipid ratio. In contrast, doxorubicin encapsulation using the $MnSO_4$ procedure (Figure 6.1.(B)) resulted in drug-to-lipid ratios (wt/wt) of 0.2 within 80 min. Thus, when the starting drug-to-lipid ratio was 0.2 (wt/wt), citrate based loading methods achieved a loading efficiency of 25% at 20 min and less than 15% at 80 min. In contrast the $MnSO_4$ based loading method resulted in > 95% loading at 80 min.

6.2.2. Confirmation that Doxorubicin Loaded DPPC/MSPC/DSPE-PEG Liposomes Remain Thermosensitive In Vitro

In order to assess if the encapsulation methodologies affected the thermosensitivity of the LTSL, drug release attributes were determined at 37°C and 42°C. Doxorubicin was added

Figure 6.1. Doxorubicin Encapsulation into DPPC/MSPC/DSPE-PEG (90/10/4 molar ratio) Liposomes. Doxorubicin was encapsulated using either the:

(A) citrate or

(B) $MnSO_4$ loading procedures at various drug-to-lipid ratios. Liposomes were prepared as described in Chapter 2, section 2.3. and 2.4.1., using either the citrate or the manganese-sulfate solutions, and doxorubicin was added to achieve a drug-to-lipid ratio of 0.1(■), 0.2 (•) or 0.3 (▲) (wt/wt). The encapsulated drug was separated from unencapsulated drug on a G-50 spin column. Doxorubicin was quantitated by measuring A_{480} of a detergent-solubilized sample, and lipid concentrations were quantitated using ^{3}H-CHE. Data points represent mean drug-to-lipid ratios of at least three replicate experiments and the error bars indicate the standard deviation.

Figure 6.1.

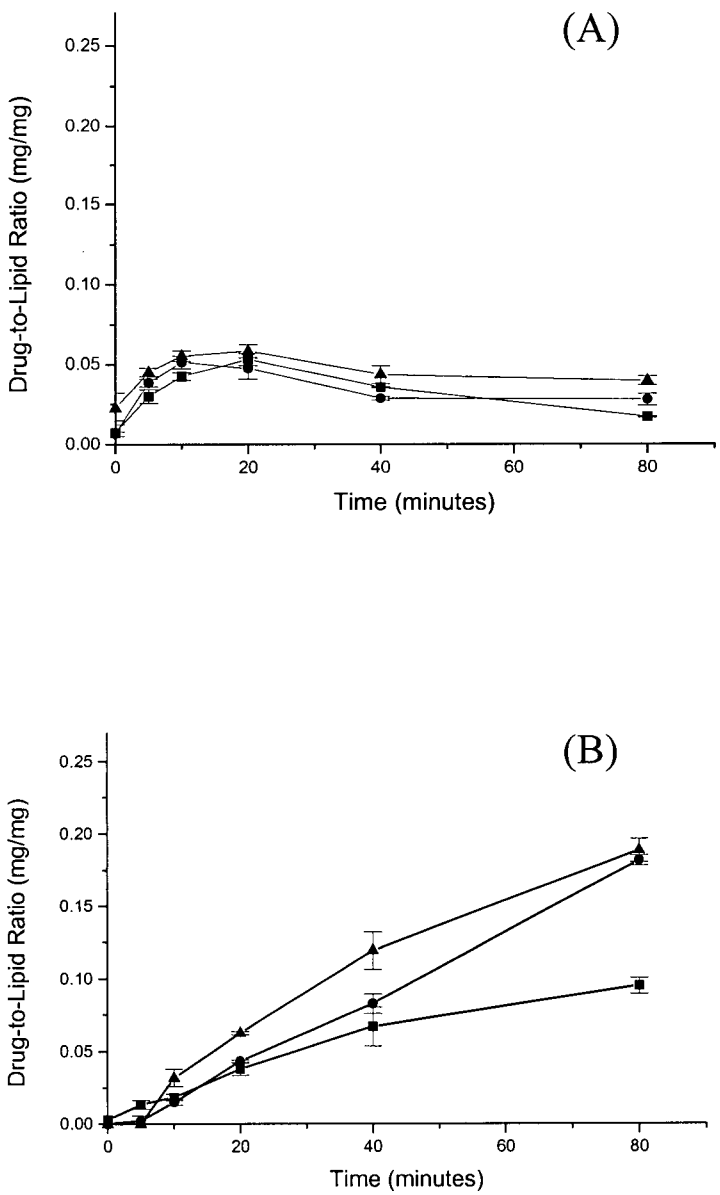
(A)
Drug-to-Lipid Ratio (mg/mg)
0.25
0.20
0.15
0.10
0.05
0.00
0
20
40
60
80
Time (minutes)
(B)
Drug-to-Lipid Ratio (mg/mg)
0.25
0.20
0.15
0.10
0.05
0.00
0
20
40
60
80
Time (minutes)

to liposomes and encapsulated at a 0.05 drug-to-lipid ratio (wt/wt) using the citrate procedure (resulting in > 95% encapsulation efficiency). Doxorubicin was also added to liposomes at either a 0.05 or 0.2 drug-to-lipid ratio (wt/wt) and encapsulated using the $MnSO_4$ procedure (resulting in > 95% encapsulation efficiency as well). Samples were then incubated at either 37°C or 42°C and changes in drug-to-lipid ratio were measured at the indicated time points (Figure 6.2.). All liposome formulations retained drug at 37°C over 60 min. For the formulations prepared using pH gradients (citrate) to encapsulate doxorubicin, > 90% of the encapsulated drug was released within 5 min when incubated at 42°C. Doxorubicin release from liposomes loaded using the manganese complexation procedure, loaded at either 0.05 or 0.2 drug-to-lipid ratios (wt/wt), exhibited comparable drug release attributes at 42°C, with approximately 85% drug release observed within 10 min.

6.2.3. Cryo-Transmission Electron Microscopic Analysis of Drug Loaded LTSL

As shown in Chapter 3 (Figure 3.4.), doxorubicin can form a precipitate within liposomes and the appearance of this precipitate is different in liposomes loaded using citrate (low pH) or the $MnSO_4$ metal complexation encapsulation procedures. Cryo-electron micrographs of LTSL were obtained before and after drug loading to confirm this observation. Figure 6.3. provides representative images of liposomes, prior to drug loading, prepared in either citrate buffer (Figure 6.3.(A)) or $MnSO_4$ (Figure 6.3.(C)) after the exterior buffer was exchanged to HBS (pH 7.5) for citrate containing liposomes or SHE (pH 7.5) for $MnSO_4$ containing liposomes. Regardless of the encapsulated solution, the liposomes appeared polyhedron in shape which is consistent with previous cTEM images of thermosensitive liposomes below the Tc (existing in the gel state) (Ickenstein et al., 2003).

Figure 6.2. In vitro Release of Doxorubicin From DPPC/MSPC/DSPE-PEG (90/10/4 mol ratio) Liposomes Loaded Using Either the Citrate or the $MnSO_4$ Procedure. Drug release was determined for liposomes loaded with doxorubicin

(A): at a 0.05 drug-to-lipid ratio (wt/wt) using the citrate loading procedure or

(B): at a 0.05 drug-to-lipid ratio (wt/wt) using the $MnSO_4$ procedure or

(C): at a 0.2 drug-to-lipid ratio (wt/wt) using the $MnSO_4$ procedure. Samples were either incubated at 37°C (■) or at 42°C (▲). Following the separation of encapsulated and unencapsulated drug on Sephadex G-50 spin columns, doxorubicin was quantitated by the A_{480} of a detergent-solubilized sample and lipid concentrations were quantitated using ^3H-CHE. Data points represent mean drug-to-lipid ratios of at least three replicate experiments and the error bars indicate the standard deviation.

Figure 6.2.

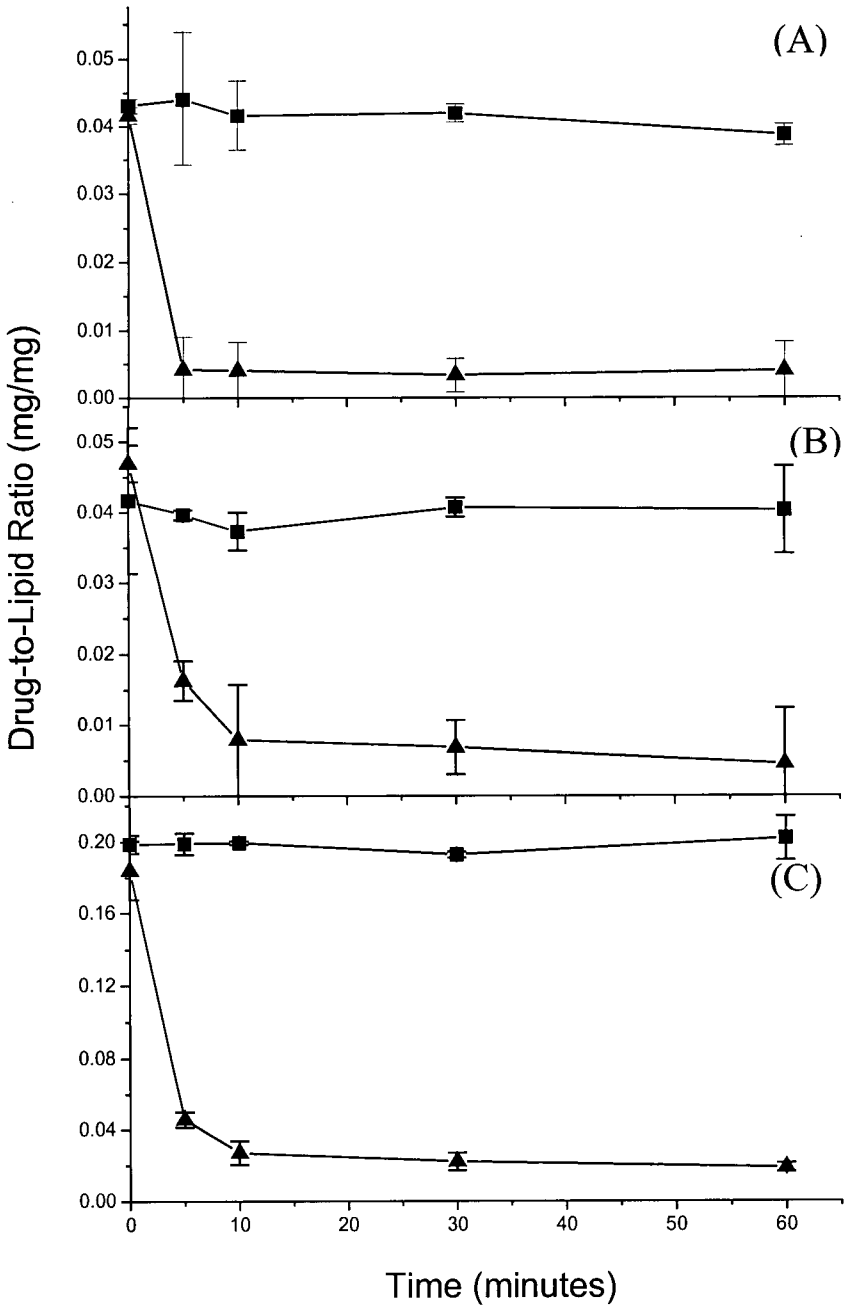
(A)
(B)
(C)
Drug-to-Lipid Ratio (mg/mg)
Time (minutes)
0.05
0.04
0.03
0.02
0.01
0.00
0.20
0.16
0.12
0.08
0.04
0.00
0
10
20
30
40
50
60

Following the accumulation of doxorubicin to a final drug-to-lipid ratio (wt/wt) of 0.05 using the citrate-based procedure (Figure 6.3.(B)), thin linear structures (fibre bundles) were observed within liposomes. Images were also obtained of manganese-doxorubicin containing liposomes loaded with drug at a 0.05 drug-to-lipid ratio (wt/wt) (Figure 6.3.(D)). Following the accumulation of doxorubicin to a final drug-to-lipid ratio of 0.2 (wt/wt) using the $MnSO_4$ procedure (Figure 6.3.(E)), a punctate and diffuse morphology within liposomes was apparent, observations that were consistent with previous studies using cholesterol containing formulations (Chapter 3, Figure 3.4.)(Abraham et al., 2002) and also confirmed that higher or lower intra-liposomal concentrations of doxorubicin did not affect precipitate morphology.

6.2.4. The Encapsulation of Doxorubicin Within Thermosensitive Liposomes Using the $MnSO_4$ Procedure in Conjunction With the A23187 Ionophore

Studies with cholesterol-containing formulations suggest that doxorubicin release from liposomes prepared with the $MnSO_4$ procedure release drug more rapidly *in vivo* when compared to doxorubicin loaded liposomes prepared using pH gradients (Chapter 3, Table 3.2.) (Abraham et al., 2002). These results confirmed earlier studies indicating that protonated doxorubicin within an acidic environment will display decreased drug release rates (Mayer et al., 1990b). Based on these results, it was suggested that it may be advantageous to generate thermosensitive formulations with high drug-to-lipid ratios containing doxorubicin within an acidic interior. Two approaches were considered. Firstly, the A23187 ionophore could be used to generate a pH gradient across the bilayers of the

Figure 6.3. Cryo-Transmission Electron Microscopy Images of DPPC/MSPC/DSPE-PEG (90/10/4 mol ratio) Liposomes Prior to or After Doxorubicin Loading Using Either the Citrate or the $MnSO_4$ Loading Procedures. Liposomes were prepared as described in Chapter 2, section 2.3., 2.4.1. and 2.9.,

(A): in the presence of citrate and

(B) loaded at a 0.05 drug-to-lipid ratio (wt/wt). Liposomes were also

(C) prepared in the presence of $MnSO_4$ and loaded at either a

(D) 0.05 or

(E) 0.2 drug-to-lipid ratio (wt/wt). Drug-loaded samples were incubated at 37°C for 80 minutes to facilitate doxorubicin encapsulation. The bar in panel (A) represents 100 nm. Each individual panel is representative of at least 15 images obtained.

Figure 6.3.

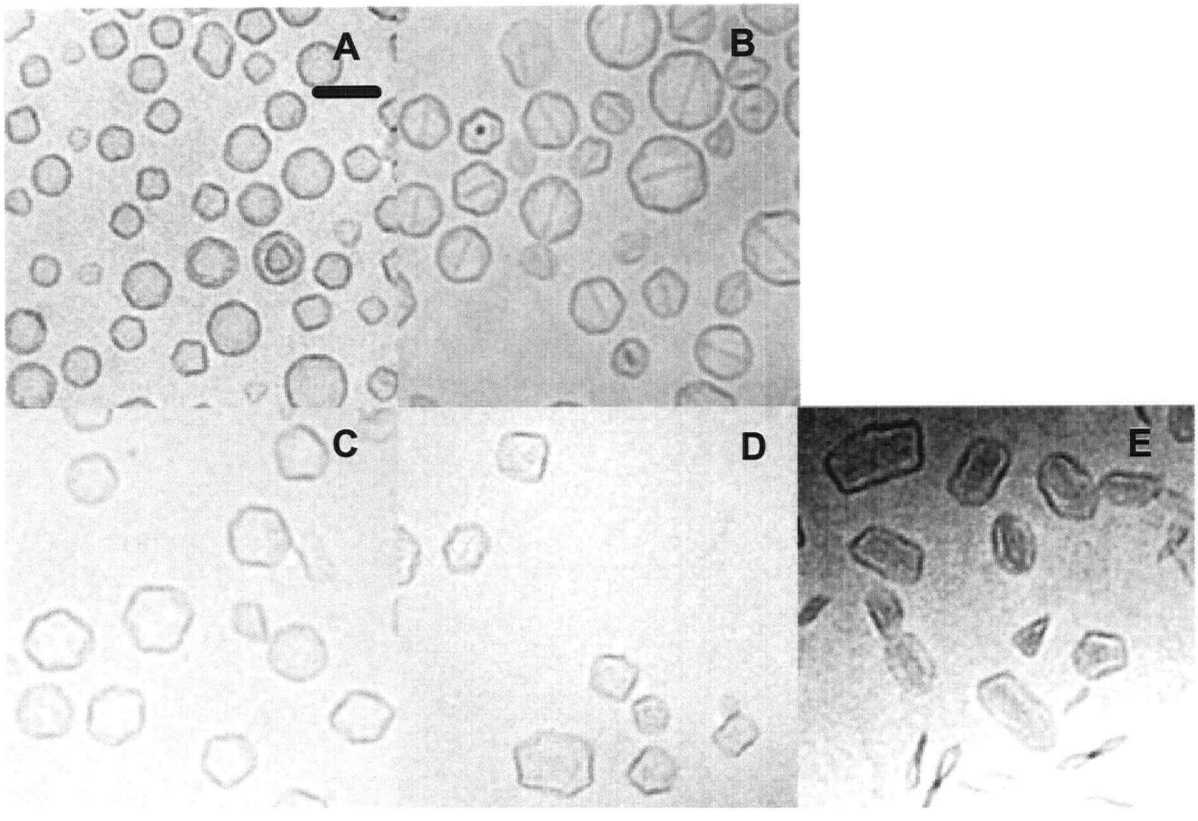

$MnSO_4$ containing liposomes prior to the addition of doxorubicin. Alternatively, following doxorubicin loading within $MnSO_4$-containing liposomes, a pH gradient could be imposed by the addition of A23187 (Chapter 5, section 5.2.1.). Figure 6.4. summarises the results obtained when doxorubicin was encapsulated within $MnSO_4$ containing LTSL using A23187 to maintain the transmembrane pH gradient during drug loading. Doxorubicin was added to $MnSO_4$ containing liposomes (pre-incubated with A23187), to achieve a 0.1, 0.2 or 0.3 drug-to-lipid ratio (wt/wt). An assessment of drug uptake at 37°C over 80 min (Figure 6.4.), indicated that the maximal drug-to-lipid ratio (wt/wt) achievable was 0.05. This result was essentially identical to that observed with citrate (low pH) containing liposomes (Figure 6.1.(A)). A representative cryo-electron micrograph of this formulation loaded with A23187 (Figure 6.4. inset), suggests that the resulting liposomes contain the doxorubicin precipitate. To address the potential of generating a pH gradient using A23187 after doxorubicin loading, LTSL containing $MnSO_4$ and loaded with doxorubicin to achieve a drug-to-lipid ratio of 0.2 (wt/wt) were incubated at 37°C with A23187. These doxorubicin-loaded formulations released approximately 60% of the encapsulated drug over 60 minutes following addition of A23187 (Figure 6.5.). In the absence of A23187, these liposomes would have exhibited no drug loss over the same time course (Figure 6.2.(C)). Interestingly, the drug-to-lipid ratio (wt/wt) measured at 60 min was ~0.08, a value similar to that observed for LTSL loaded with doxorubicin through use of $MnSO_4$ liposomes in conjunction with A23187. Cryo-transmission electron microscopy images of the resulting liposomes suggest the presence of the doxorubicin fibre bundle within these liposomes, even though this precipitate was not observed prior to A23187 addition.

Figure 6.4. Doxorubicin Encapsulation into DPPC/MSPC/DSPE-PEG (90/10/4 molar ratio) Liposomes Using the $MnSO_4$ Plus A23187 Loading Procedure. Liposomes were prepared as described in Chapter 2, section 2.3. and 2.4.1., and were loaded at either a 0.1(■), 0.2 (•) or a 0.3 (▲) drug-to-lipid ratio (wt/wt). A23187 was added and incubated 5 min prior to the addition of drug. Following the separation of encapsulated and unencapsulated drug on Sephadex G-50 spin columns, doxorubicin was quantitated by the A_{480} of a detergent-solubilized sample and lipid concentrations were quantitated using ^{3}H-CHE. Data points represent mean drug-to-lipid ratios of at least three replicate experiments and the error bars indicate the standard deviation.

Inset: cTEM image of doxorubicin loaded DPPC/MSPC/DSPE-PEG (90/10/4 molar ratio) liposomes using the $MnSO_4$ plus A23187 procedure. Liposomes were loaded at a 0.05 drug-to-lipid ratio (wt/wt) using A23187. Samples were incubated at 37°C for 80 minutes to facilitate doxorubicin encapsulation. The bar in the panel represents 100 nm. Each individual panel is representative of at least 15 images obtained.

Figure 6.4.

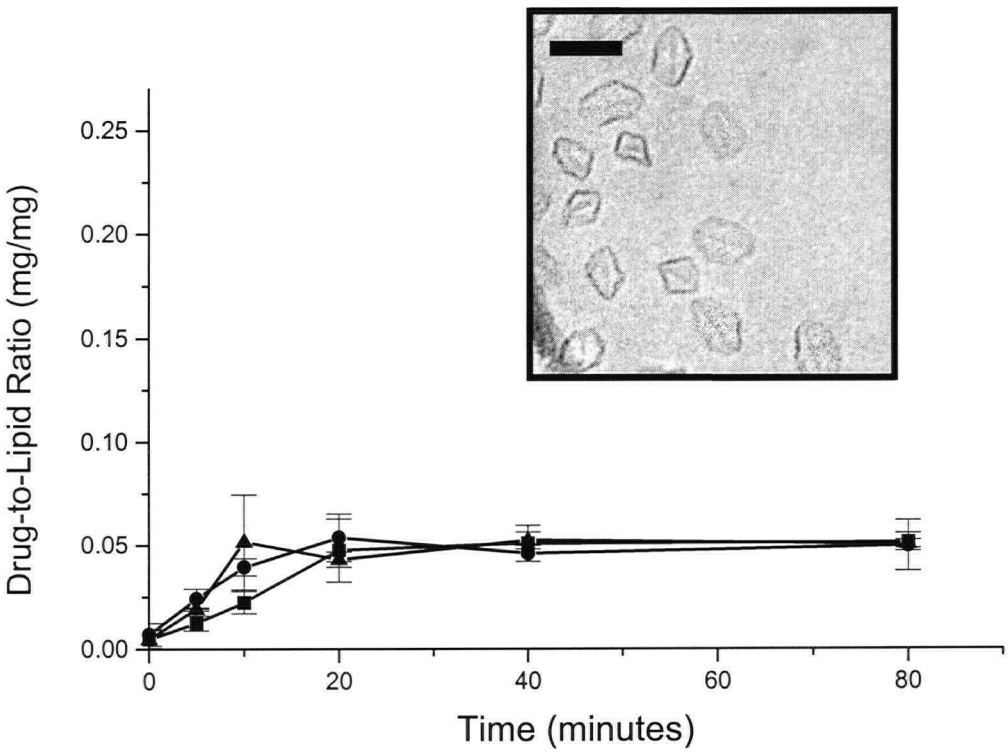
Drug-to-Lipid Ratio (mg/mg)
0.25
0.20
0.15
0.10
0.05
0.00
0
20
40
60
80
Time (minutes)

Figure 6.5. In Vitro Release of Doxorubicin From DPPC/MSPC/DSPE-PEG (90/10/4 molar ratio) Liposomes Loaded Using the $MnSO_4$ Procedure with Addition of the A23187 After Drug Loading. Drug release was determined *in vitro* with liposomes loaded with doxorubicin at a drug-to-lipid ratio of 0.2 (wt/wt). Liposomes were prepared in the presence of $MnSO_4$, with the addition of A23187 to the drug loaded samples (at t = 0) and incubated at 37°C. Following the separation of encapsulated and unencapsulated drug on Sephadex G-50 spin columns, doxorubicin was quantitated by the A_{480} of a detergent-solubilized sample and lipid concentrations were quantitated using ^{3}H-CHE. Data points represent mean drug-to-lipid ratios of at least three replicate experiments and the error bars indicate the standard deviation.

Inset: cTEM image of doxorubicin loaded DPPC/MSPC/DSPE-PEG (90/10/4 molar ratio) liposomes using the $MnSO_4$ procedure with the addition of A23187 after loading. Liposomes were loaded at a 0.05 drug-to-lipid ratio (wt/wt) with incubation at 37°C for 80 minutes to facilitate doxorubicin encapsulation. Samples were cooled and A23187 was added and incubated at 37°C for 30 min. The bar in the panel represents 100 nm. Each individual panel is representative of at least 15 images obtained.

Figure 6.5.

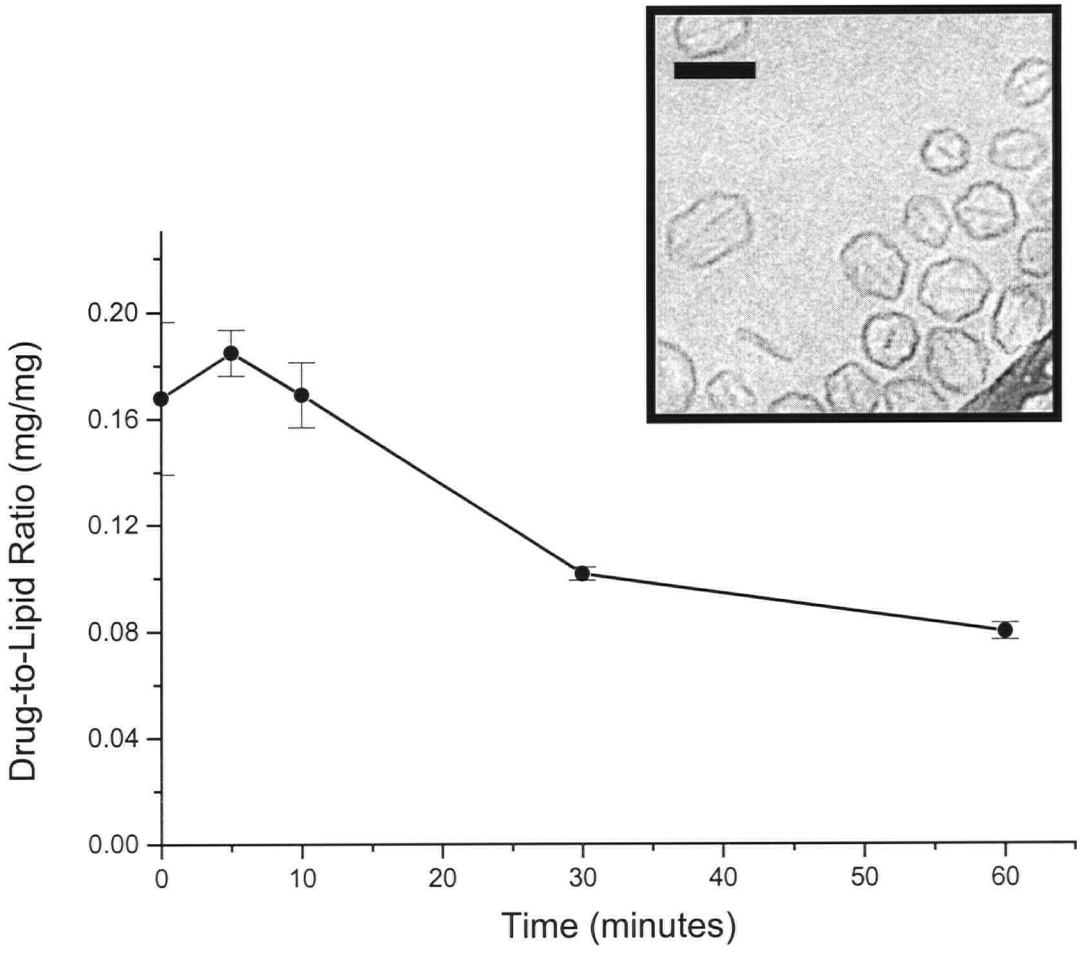
Drug-to-Lipid Ratio (mg/mg)
0.00
0.04
0.08
0.12
0.16
0.20
0
10
20
30
40
50
60
Time (minutes)

6.3. DISCUSSION

Drug carriers for chemotherapy have a seemingly simplistic goal; they must carry the encapsulated cytotoxic agent to the target site, and release their contents within the vicinity of the diseased tissue. Under optimal (ideal) conditions, the carrier must be designed such that on systemic administration, the carrier is stable in the blood compartment, retaining contents and protecting non-target tissues from the encapsulated cytotoxic load. Following localisation of the carrier to the target site however, these liposomes should then efficiently release their contents in a manner that results in a therapeutic advantage over free drug. Liposomes that can be induced to release contents in response to mild heating may provide a method of achieving significantly improved control of drug release from liposomes that have localised in the tumour tissue. Such a formulation has recently been described (Needham et al., 2000). Our goal was to develop a drug loading method that efficiently encapsulated drug while maintaining efficient drug release when incubated at a temperature known to induce liposome destabilisation (in this case 42°C).

Using the $MnSO_4$ encapsulation procedure, doxorubicin could be encapsulated within DPPC/MSPC/DSPE-PEG liposomes at a 0.2 drug-to-lipid ratio (wt/wt) (> 95% encapsulation efficiency), a 4-fold improvement over previously described pH gradient based loading methods. Drug loading using either pH gradient or metal chelation techniques resulted in formulations that released > 85% of their contents within 10 min when incubated at 42°C. The $MnSO_4$-doxorubicin loaded formulations released drug rapidly regardless of whether the drug was loaded to a 0.05 or a 0.2 drug-to-lipid ratio (wt/wt) (Figure 6.2.).

One of the most obvious differences noted in these studies concern the formation of a doxorubicin precipitate in the LTSL. It is interesting to speculate why drug loading is increased in LTSL that do not exhibit this organised precipitate. Within liposomes with an average diameter of 120 nm, the intra-liposomal doxorubicin concentration can be estimated to be 43 mM when the drug-to-lipid ratio is 0.05 (wt/wt), assuming a trapped aqueous volume of 1.2 μl/μmol lipid and negligible membrane partitioning. Using $MnSO_4$ encapsulation techniques, internal doxorubicin concentrations can exceed 170 mM at drug-to-lipid ratios of 0.2 (wt/wt). Clearly different encapsulation efficiencies and drug precipitate morphologies are obtained with the two different encapsulation techniques. With citrate or sulfate containing doxorubicin liposomes composed of phospholipid and cholesterol (55/45) the formation of doxorubicin fibre-bundles has been well characterised (Lasic, 1996; Li et al., 2000; Li et al., 1998). Doxorubicin fibre bundles are believed to form by the stacking of the planar doxorubicin molecules which comprise individual fibres, which in turn are thought to pack in a hexagonal fashion (as described in Chapter 3, section 3.3). What was clearly noted in these previous studies with cholesterol containing liposomes was that at 0.2 drug-to-lipid ratios (wt/wt) doxorubicin fibre bundle formation was associated with dramatic changes in liposome shape. These liposomes (typically with 45 mol% Chol) appear to elongate to accommodate the doxorubicin fibre bundle. Fibre bundle formation can stretch the liposomes and when visualised by cryo-TEM, the resulting drug loaded structures appear to adopt a 'coffee bean'-like image (Abraham et al., 2002; Harrigan et al., 1993; Li et al., 1998). It can be suggested that a potential contributing factor limiting pH gradient loading of doxorubicin within thermosensitive formulations may be due to the inability of the liposome membrane, in the rigid gel state, to accommodate formation of large doxorubicin fibre

bundles. If the fibre bundle can not extend for more than 100 nm (within the 120 nm liposomes) this may limit loading. In contrast, manganese-doxorubicin complexation does not engender fibre bundle formation and hence higher drug-to-lipid ratios are achievable.

We have characterised a thermosensitive liposomal-doxorubicin formulation exhibiting high drug-to-lipid ratios. The resulting formulation exhibited thermosensitive attributes as judged by rapid (in less than 10 min) release of > 85% of the encapsulated drug when incubated at 42°C. It will be important to evaluate this formulation *in vivo* in order to establish if the resulting thermosensitive liposomes displaying high drug-to-lipid ratios exhibit improved stability following i.v. administration. If increased *in vivo* stability can be demonstrated, then the resulting formulation should exhibit improved therapeutic effects compared to doxorubicin-loaded LTSL prepared using pH gradient techniques.

CHAPTER 7

DISCUSSION

Currently, there are several different techniques available to encapsulate anticancer drugs within liposomes. It is well established that the chemistry of the drug and the composition of the lipid carrier contribute, in part, to drug release profiles from liposomes. Empirical approaches have played a large part in determining appropriate active encapsulation techniques to achieve specific formulation goals (Bolotin et al., 1994; Lasic et al., 1995; Madden et al., 1990; Maurer-Spurej et al., 1999; Mayer et al., 1985a). Few studies (Li et al., 2000; Li et al., 1998) however, have examined how various encapsulation procedures may play different roles if any, in contributing to drug encapsulation and ramifications to drug release.

The studies in this thesis focused on furthering the understanding of methods used to encapsulate drugs within liposomes and how these methods can be used to obtain novel formulations exhibiting improved encapsulation efficiencies and release profiles. This was achieved through the analysis of physical and chemical characteristics using cryo-TEM, circular dichroism, absorbance spectrophotometric analysis, drug loading, the *in vitro* and the *in vivo* release attributes of encapsulated anticancer drugs, where drug loading was promoted by use of manganese ion gradients. In an attempt to resolve issues surrounding limitations to current methodologies, a better understanding of the chemical properties of the encapsulated drug itself was also sought.

In Chapter 3, studies characterised interactions between the transition metal manganese and doxorubicin, an interaction that promotes the accumulation of drug inside

liposomes that contain this metal. The resulting drug-loaded liposomes are unique in that the complexed drug is maintained in a form that is distinct from that identified for loading methods relying on maintenance of a pH gradient. Depending on liposome lipid composition, metal complexation loading techniques can alter drug release rates with respect to pH-dependent mechanisms (see Chapter 3, Table 3.2.). In the case of manganese-doxorubicin chelates within DSPC/Chol liposomes that exhibit no pH gradient, increased drug release rates may be due to increased internal concentrations of readily available un-protonated doxorubicin (uncharged doxorubicin crosses the lipid bilayer at a substantially greater rate than the protonated form) (see Figure 7.1.). In the studies preformed here, it is assumed that because manganese as a relatively weaker chelator of doxorubicin in relation to other metals (Bouma et al., 1986), drug metal chelation will play a minor role in contributions to drug release rates.

Metal complexation procedures may also be applicable to other drugs having chemical groups capable of complexing transition metals like manganese. Ligands that are capable of co-ordinating with transition metals include amines, carbonyl groups, ethers, ketones, acyl groups, thiols or other groups capable of donating electrons to the metal ion, thereby forming co-ordination complexes (Basolo and Johnson, 1986). Drugs that have been already shown to bind metals include anthracyclines (Beraldo et al., 1985; Fiallo et al., 1999), camptothecins (Kuwahara et al., 1986; Kuwahara et al., 1985) and anticancer antibiotics such as bleomycin (Dabrowiak et al., 1978; Suzuki et al., 1984). Future studies will need to investigate the possibilities of loading various drugs using different transition metals capable of forming different co-ordination complexes. Because different transition metals will have different affinities with various drugs, there exists the potential of

Figure 7.1. Schematic Representation of Doxorubicin Equilibria Within Liposomes Using Either the Citrate or the Manganese Sulfate Encapsulation Procedure. Doxorubicin loading using citrate:(A) results in the formation of doxorubicin bundle fibres within a buffered acidic environment. The majority of un-precipitated doxorubicin will exist in a protonated form resulting in decreased rates of release from low pH intra-liposomal environments. Doxorubicin loading using manganese sulfate (B) results in the formation of doxorubicin manganese chelates in a diffuse morphology under neutral conditions. The majority of un-precipitated doxorubicin will exist in an un-protonated form resulting in increased rates of release.

Figure 7.1.

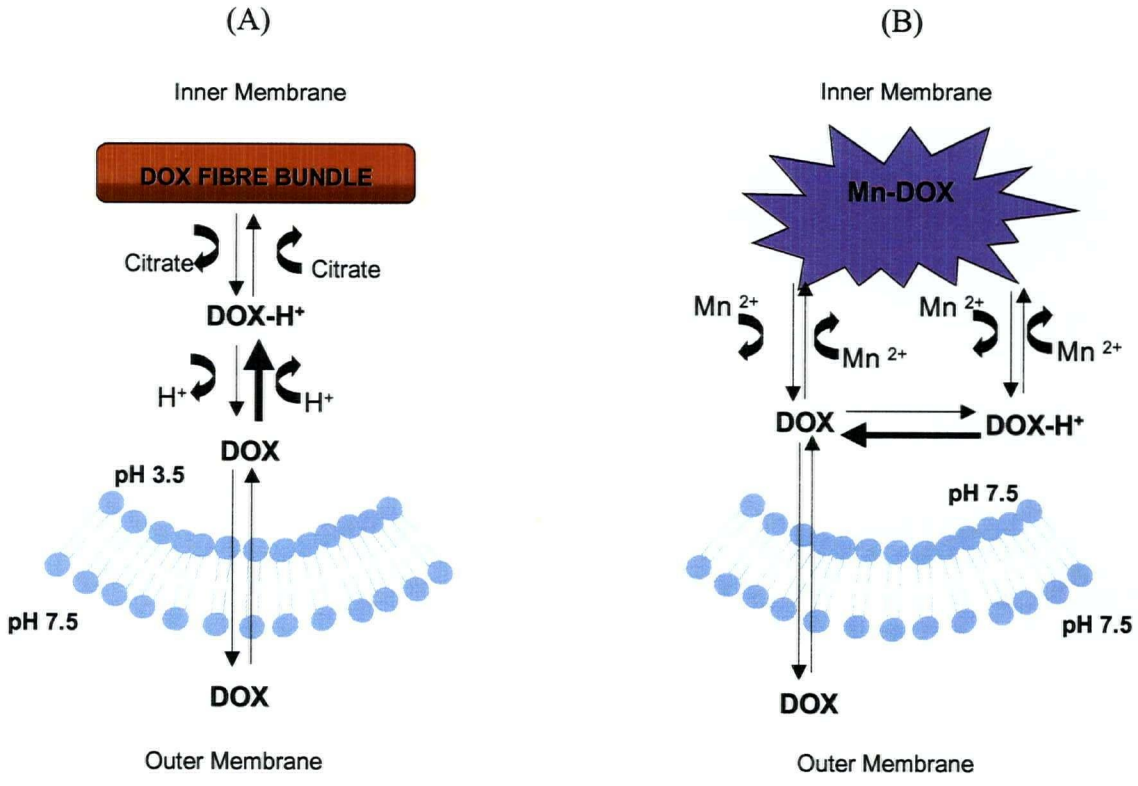
(A)
Inner Membrane
DOX FIBRE BUNDLE
Citrate
Citrate
DOX-H+
H+
H+
DOX
pH 3.5
pH 7.5
DOX
Outer Membrane
(B)
Inner Membrane
Mn-DOX
Mn 2+
Mn 2+
Mn 2+
Mn 2+
DOX
DOX-H+
pH 7.5
pH 7.5
DOX
Outer Membrane

controlling drug release with the complexation of specific metals with relatively high binding affinities to specific drugs. This could result in the ability to design drug carriers that would exhibit specifically designed release parameters ideal to the specific drug of choice. With the creation of different drug co-ordination complexes, not only will encapsulation and release profiles need to be determined with each individual drug co-ordination complex but, any changes in activity of the drug will need to be determined. Potential toxic effects associated with the specific metals selected will also need to be determined.

In Chapter 4, both the ammonium sulfate and the manganese sulfate + A23187 based loading procedures, proved to be superior encapsulation methods with respect to that of non-sulfate containing methods and resulted in stable formulations of topotecan. These liposomes could be prepared at drug-to-lipid ratios of 0.3 (wt/wt) with > 95% encapsulation efficiency. Studies also demonstrated that for the loading methods used, the resulting liposomes exhibited a precipitated structure within the aqueous core. Visually similar, thin linear particles were observed within liposomes regardless of encapsulation procedure used. As with doxorubicin fibre bundles, the presence of sulfate may stabilise the linear topotecan particles without direct participation in precipitate formation itself. Results clearly demonstrate the importance of intra-liposomal chemical composition on both drug encapsulation and drug release profiles and how the selection of an appropriate encapsulation method is critical to obtaining an optimised liposome formulation.

Based on results indicating that selected drugs could be encapsulated using distinct loading mechanisms involving manganese complexation (Chapter 3) and pH gradient loading (Chapter 4), the co-encapsulation of doxorubicin and vincristine using a combination of both procedures was characterised in Chapter 5. An established manganese metal gradient across

liposomes permitted the efficient loading of doxorubicin due to formation of a drug-metal complex. Sufficient levels of un-complexed Mn^{2+} remained to support the establishment of a transmembrane pH gradient following addition of A23187, an ionophore capable of transferring one Mn^{2+} ion out of the liposomes in exchange for two protons. The pH gradient formed supported the efficient loading of vincristine, in a manner that appeared comparable to that obtained for topotecan. Despite the fact that free doxorubicin and free vincristine are administered together in many chemotherapy protocols (Christou et al., 2001; Krol et al., 2001; Northfelt et al., 1998), studies in Chapter 5 indicate that a co-encapsulated formulation of the drugs proved to be antagonistic when the activity was assessed in the MDA 435 LCC6 tumour model. It is anticipated that this co-encapsulation procedure will be applicable to a wide range of drugs that have chemical groups capable of complexing transition metals like manganese (as indicated above) and second agents that can be encapsulated using pH gradients (for example mitoxantrone, camptothecins and vinca alkaloids (Burke and Gao, 1994; Fenske et al., 1998; Lim et al., 1997; Madden et al., 1990)). The doxorubicin and vincristine drug release profiles from individually loaded DSPC/Chol liposomes are not significantly different from the drug release rates observed in the co-encapsulated formulation suggesting that the drugs have likely not precipitated together or interact in a manner that affects their release from the liposomes. Studies completed in Chapter 5 were designed, as an initial step of co-encapsulating multiple agents and further studies will need to evaluate the feasibility of encapsulating more than two agents. Results presented in Chapter 5, section 5.2.4., suggest that for future studies, *in vitro* assays could contribute to evaluate the potential of whether the selected drugs for co-encapsulation interact in an additive or superadditive fashion.

In Chapter 6, a thermosensitive liposomal doxorubicin formulation exhibiting high drug-to-lipid ratios and efficient rates of drug release was assessed. The formulation resulted in efficient drug accumulation using metal chelation techniques in contrast to pH gradient methods. The formulation exhibited rapid drug release when heated to its Tc, consistent with complete loss of the permeability barrier. It will be important to evaluate this formulation *in vivo* in order to establish that, thermosensitive liposomes displaying high drug-to-lipid ratios will retain their contents following i.v. administration and tumour accumulation culminating into substantial controlled drug release once heated. It will be also important to evaluate other drugs encapsulated using this formulation to determine if this manner of drug delivery will result improved drug therapeutic indexes. The question remains as to why metal chelation encapsulation techniques offer an advantage to load doxorubicin within thermosensitive liposome formulations in contrast to pH encapsulation techniques. It is postulated here that perhaps the elongation of the doxorubicin fibre bundle in the thermosensitive liposomes is inhibited due to steric constraints imposed by the rigid liposomes. This testable hypothesis can be addressed in future studies examining doxorubicin fibre bundle formation after drug loading of liposomes with varying diameters to determine if vesicle size limits doxorubicin fibre bundle formation elongation which may in turn affect encapsulation efficiencies.

The $MnSO_4$ encapsulation procedure, as a means of encapsulating drug using metal complexation has great potential as a new active encapsulation technique. This thesis outlines potential benefits of using transition metal chemistry in directly capturing drugs with carriers. In addition to drug encapsulation, studies indicate (Koenig et al., 1988; Unger et al., 1993; Vigilanti et al., 2003) that manganese-containing liposomes can also be utilised as

imaging agents. Drug delivery using liposomes containing drug-metal chelates can therefore be monitored and may lead to an increased understanding of delivery obstacles encountered *in vivo*. The $MnSO_4$ encapsulation procedure has also served as an excellent learning tool in this thesis based on its versatility in conjunction with the A23187, to examine various parameters affecting drug encapsulation and release. Work presented clearly support that encapsulation procedures play an important role in liposome drug formulation. Results from this thesis will hopefully lead to furthering the development of liposomal drug formulations with applications for clinical use.

REFERENCES

Abra, R.M. and Hunt, C.A. (1981) Liposome disposition in vivo. III. Dose and vesicle-size effects. *Biochim Biophys Acta*, 666, 493-503.

Abraham, S.A., Edwards, K., Karlsson, G., MacIntosh, S., Mayer, L.D., McKenzie, C. and Bally, M. (2002) Formation of Transition Metal-Doxorubicin Complexes Inside Liposomes. *Biochim Biophys Acta*, 1565, 41-54.

Abraham S.A., Waterhouse D.N., Mayer L.D., Cullis P.R., Madden T., Bally M.B. (2004) The Liposomal Formulation of Doxorubicin. Methods in Enzymology vol 387

Ahmad, I. and Allen, T.M. (1992) Antibody-mediated specific binding and cytotoxicity of liposome-entrapped doxorubicin to lung cancer cells in vitro. *Cancer Res*, 52, 4817-4820.

Alakhov, V., Klinski, E., Lemieux, P., Pietrzynski, G. and Kabanov, A. (2001) Block copolymeric biotransport carriers as versatile vehicles for drug delivery. *Expert Opin Biol Ther*, 1, 583-602.

Albon, N. and Sturtevant, J.M. (1978) Nature of the gel to liquid crystal transition of synthetic phosphatidylcholines. *Proc Natl Acad Sci U S A*, 75, 2258-2260.

Allen, C., Dos Santos, N., Gallagher, R., Chiu, G.N., Shu, Y., Li, W.M., Johnstone, S.A., Janoff, A.S., Mayer, L.D., Webb, M.S. and Bally, M.B. (2002) Controlling the Physical Behavior and Biological Performance of Liposome Formulations through Use of Surface Grafted Poly(ethylene Glycol). *Bioscience Reports*, 22, 225-250.

Allen, T.M. and Chonn, A. (1987) Large unilamellar liposomes with low uptake into the reticuloendothelial system. *FEBS Lett*, 223, 42-46.

Allen, T.M., Hansen, C. and Lopes de Menezes, D. (1995) Pharamacokinetics of Long Circulating Liposomes. *Advanced Drug Delivery Reviews*, 16, 267-284.

Allen, T.M., Hansen, C., Martin, F., Redemann, C. and Yau-Young, A. (1991) Liposomes containing synthetic lipid derivatives of poly(ethylene glycol) show prolonged circulation half-lives in vivo. *Biochim Biophys Acta*, 1066, 29-36.

Allen, T.M., Hansen, C. and Rutledge, J. (1989) Liposomes with prolonged circulation times: factors affecting uptake by reticuloendothelial and other tissues. *Biochim Biophys Acta*, 981, 27-35.

Almgren, M., Edwards, K. and Karlsson, G. (2000) Cryo transmission electron microscopy of liposomes and related structures. *Colloids and Surfaces*, 174, 3-21.

Anderson, V.C. and Thompson, D.H. (1992) Triggered release of hydrophilic agents from plasmalogen liposomes using visible light or acid. *Biochim Biophys Acta*, 1109, 33-42.

Anyarambhatla, G. and Needham, D. (1999) Enhancement of the Phase Transition Permeability of DPPC Liposomes by Incorporation of MPPC: A New Temperature-Sensitive Liposome for use with Mild Hyperthermia. *Journal of Liposome Research*, 7, 491-506.

Bahadori, H.R., Green, M.R. and Catapano, C.V. (2001) Synergistic interaction between topotecan and microtubule-interfering agents. *Cancer Chemother Pharmacol*, 48, 188-196.

Bally, M., Hope, M., Van Echteld, C. and Cullis, P. (1985) Uptake of Safranine and Other Lipophilic Cations into Vesicles in Response to a Membrane Potential. *Biochim. Biophys. Acta*, 812, 66-76.

Bally, M.B., Mayer, L.D., Loughrey, H., Redelmeier, T., Madden, T.D., Wong, K., Harrigan, P.R., Hope, M.J. and Cullis, P.R. (1988) Dopamine accumulation in large unilamellar vesicle systems induced by transmembrane ion gradients. *Chem Phys Lipids*, 47, 97-107.

Bally, M.B., Nayar, R., Masin, D., Hope, M.J., Cullis, P.R. and Mayer, L.D. (1990) Liposomes with entrapped doxorubicin exhibit extended blood residence times. *Biochim Biophys Acta*, 1023, 133-139.

Bangham, A.D., Standish, M.M. and Watkins, J.C. (1965) Diffusion of univalent ions across the lamellae of swollen phospholipids. *J Mol Biol*, 13, 238-252.

Banks, A.R., Jones, T., Koch, T.H., Friedman, R.D. and Bachur, N.R. (1983) Prevention of adriamycin toxicity. *Cancer Chemother. Pharmacol.*, 11, 91-93.

Barenholz, Y. (2003) Relevancy of Drug Loading to Liposomal Formulation Therapeutic Efficacy. *Journal of Liposome Research*, 13, 1-8.

Barranco, S.C., Gerner, E.W., Burk, K.H. and Humphrey, R.M. (1973) Survival and cell kinetics effects of adriamycin on mammalian cells. *Cancer Res*, 33, 11-16.

Barratt, G. (2003) Colloidal drug carriers: achievements and perspectives. *Cell Mol Life Sci*, 60, 21-37.

Basolo, F. and Johnson, R.C. (1986) *Coordination Chemistry*. Science Reviews.

Batist, G., Barton, J., Chaikin, P., Swenson, C. and Welles, L. (2002) Myocet (liposome-encapsulated doxorubicin citrate): a new approach in breast cancer therapy. *Expert Opin Pharmacother*, 3, 1739-1751.

Batist, G., Ramakrishnan, G., Rao, C.S., Chandrasekharan, A., Gutheil, J., Guthrie, T., Shah, P., Khojasteh, A., Nair, M.K., Hoelzer, K., Tkaczuk, K., Park, Y.C. and Lee, L.W. (2001) Reduced cardiotoxicity and preserved antitumor efficacy of liposome-encapsulated doxorubicin and cyclophosphamide compared with conventional doxorubicin and cyclophosphamide in a randomized, multicenter trial of metastatic breast cancer. *J Clin Oncol*, 19, 1444-1454.

Beraldo, H., Garnier-Suillerot, A., Tosi, L. and Lavelle, F. (1985) Iron(III)-adriamycin and Iron(III)-daunorubicin complexes: physicochemical characteristics, interaction with DNA, and antitumor activity. *Biochemistry*, 24, 284-289.

Betageri, G., Jenkins, S.A. and Parsons, D.L. (1993) *Liposome Drug Delivery Systems*. Technomic Publishing Company Inc.

Blok, M.C., van der Neut-Kok, E.C., van Deenen, L.L. and de Gier, J. (1975) The effect of chain length and lipid phase transitions on the selective permeability properties of liposomes. *Biochim Biophys Acta*, 406, 187-196.

Blum, R.H. and Carter, S.K. (1974) Adriamycin. A new anticancer drug with significant clinical activity. *Ann Intern Med*, 80, 249-259.

Boggs, J.M. (1987) Lipid intermolecular hydrogen bonding: influence on structural organization and membrane function. *Biochim Biophys Acta*, 906, 353-404.

Bolotin, E.M., Cohen, R., Bar, L.K., Emanuel, N., Ninio, S., Lasic, D.D. and Barenholz, Y. (1994) Ammonium Sulfate Gradients For Efficient and Stable Remote Loading of Amphipathic Weak Bases into Liposomes and Ligandoliposomes. *Journal of Liposome Research*, 4, 455-479.

Boman, N.L., Mayer, L.D. and Cullis, P.R. (1993) Optimization of the retention properties of vincristine in liposomal systems. *Biochim Biophys Acta*, 1152, 253-258.

Bouma, J., Beijnen, J.H., Bult, A. and Underberg, W.J. (1986) Anthracycline antitumour agents. A review of physicochemical, analytical and stability properties. *Pharm Weekbl Sci*, 8, 109-133.

Broom, C. (1996) Clinical studies of topotecan. *Ann N Y Acad Sci*, 803, 264-271.

Brown, J.M. and Giaccia, A.J. (1998) The unique physiology of solid tumors: opportunities (and problems) for cancer therapy. *Cancer Res*, 58, 1408-1416.

Burke, T.G. (1996) Chemistry of the camptothecins in the bloodstream. Drug stabilization and optimization of activity. *Ann N Y Acad Sci*, 803, 29-31.

Burke, T.G. and Bom, D. (2000) Camptothecin design and delivery approaches for elevating anti-topoisomerase I activities in vivo. *Ann N Y Acad Sci*, 922, 36-45.

Burke, T.G. and Gao, X. (1994) Stabilization of topotecan in low pH liposomes composed of distearoylphosphatidylcholine. *J Pharm Sci*, 83, 967-969.

Burke, T.G. and Mi, Z. (1994) The structural basis of camptothecin interactions with human serum albumin: impact on drug stability. *J Med Chem*, 37, 40-46.

Burke, T.G., Mishra, A.K., Wani, M.C. and Wall, M.E. (1993) Lipid bilayer partitioning and stability of camptothecin drugs. *Biochemistry*, 32, 5352-5364.

Burns, J.H. (1972) Vincristine Sulfate. *Analytical Profiles of Drug Substances and Excipients*, 1, 463-448.

Byrn, S.R., Pfeiffer, R.R. and Stowell, J.G. (1999) Introduction to the Solid-State Chemistry of Drugs. In *Solid-State Chemistry of Drugs*. Library of Congress Cataloging-in-Publication Data.

Capranico, G., Kohn, K.W. and Pommier, Y. (1990) Local sequence requirements for DNA cleavage by mammalian topoisomerase II in the presence of doxorubicin. *Nucleic Acids Res*, 18, 6611-6619.

Chabner, B.A. (1982) The Role of Drugs in Cancer Treatment. In Chabner, B.A. (ed.), *Pharmacolgic Principles of Cancer Treatment*. W.B. Saunders Company, Bethesda.

Chaires, J.B., Dattagupta, N. and Crothers, D.M. (1982) Self-association of daunomycin. *Biochemistry*, 21, 3927-3932.

Chapman, D. (1975) Fluidity and phase transitions of cell membranes. *Biomembranes*, 7, 1-9.

Chelvi, T.P. and Ralhan, R. (1997) Hyperthermia potentiates antitumor effect of thermosensitive-liposome-encapsulated melphalan and radiation in murine melanoma. *Tumour Biol*, 18, 250-260.

Cheung, B.C., Sun, T.H., Leenhouts, J.M. and Cullis, P.R. (1998) Loading of doxorubicin into liposomes by forming Mn2+-drug complexes. *Biochim Biophys Acta*, 1414, 205-216.

Chou, T.C. and Hayball, M.P. (1996) CalcuSyn. *Windows Software for Dose Effect Analysis*. Biosoft, Cambridge, UK, pp. 1-56.

Chou, T.C. and Talalay, P. (1984) Quantitative analysis of dose-effect relationships: the combined effects of multiple drugs or enzyme inhibitors. *Adv Enzyme Regul*, 22, 27-55.

Christou, L., Hatzimichael, E., Chaidos, A., Tsiara, S. and Bourantas, K.L. (2001) Treatment of plasma cell leukemia with vincristine, liposomal doxorubicin and dexamethasone. *Eur J Haematol*, 67, 51-53.

Cohen, B.E. (1975) The permeability of liposomes to nonelectrolytes. I. Activation energies for permeation. *J Membr Biol*, 20, 205-234.

Connor, J., Yatvin, M.B. and Huang, L. (1984) pH-sensitive liposomes: acid-induced liposome fusion. *Proc Natl Acad Sci U S A*, 81, 1715-1718.

Corvera, E., Mouritsen, O.G., Singer, M.A. and Zuckermann, M.J. (1992) The permeability and the effect of acyl-chain length for phospholipid bilayers containing cholesterol: theory and experiment. *Biochim Biophys Acta*, 1107, 261-270.

Cowens, J.W., Creaven, P.J., Greco, W.R., Brenner, D.E., Tung, Y., Ostro, M., Pilkiewicz, F., Ginsberg, R. and Petrelli, N. (1993) Initial clinical (phase I) trial of TLC D-99 (doxorubicin encapsulated in liposomes). *Cancer Res*, 53, 2796-2802.

Cullis, P.R., Bally, M.B., Madden, T.D., Mayer, L.D. and Hope, M.J. (1991) pH Gradients and Membrane Transport in Liposomal Systems. *TIBTECH*, 9, 268-272.

Cullis, P.R. and Hope, M.J. (1985) Physical Properties and Functional Roles of Lipids in Membranes. In Vance, D.E. and Vance, J.E. (eds.), *Biochemistry of Lipids and Membranes*. Benjamin Cummings, Menlo Park, pp. pp.25-72.

Cullis, P.R., Hope, M.J., Bally, M.B., Madden, T.D., Mayer, L.D. and Fenske, D.B. (1997) Influence of pH gradients on the transbilayer transport of drugs, lipids, peptides and metal ions into large unilamellar vesicles. *Biochim Biophys Acta*, 1331, 187-211.

Cullis, P.R., Hope, M.J., Bally, M.B., Madden, T.D., Mayer, L.D. and Janoff, A.S. (1987) Liposomes as Pharmaceuticals. In Ostro, M.J. (ed.), *Liposomes From Biophysics to Therapeutics*. Marcel Dekker Inc, New York, pp. 39-72.

Cullis, P.R., Mayer, L.D., Bally, M.B., T.D., M. and Hope, M.J. (1989) Generating and Loading of Liposomal Systems For Drug-Delivery Applications. *Advanced Drug Delivery Reviews*, 3, 267-282.

Cunningham, C.M., Kingzette, M., Richards, R.L., Alving, C.R., Lint, T.F. and Gewurz, H. (1979) Activation of human complement by liposomes: a model for membrane activation of the alternative pathway. *J Immunol*, 122, 1237-1242.

Dabrowiak, J.C., Greenaway, F.T. and Grulich, R. (1978) Transition-metal binding site of bleomycin A2. A carbon-13 nuclear magnetic resonance study of the zinc(II) and copper(II) derivatives. *Biochemistry*, 17, 4090-4096.

Damen, J., Regts, J. and Scherphof, G. (1981) Transfer and exchange of phospholipid between small unilamellar liposomes and rat plasma high density lipoproteins. Dependence on cholesterol content and phospholipid composition. *Biochim Biophys Acta*, 665, 538-545.

de Valeriola, D. (1994) Dose optimization of anthracyclines. *Anticancer Res*, 14, 2307-2313.

Deamer, D.W. and Nichols, J.W. (1989) Proton flux mechanisms in model and biological membranes. *J Membr Biol*, 107, 91-103.

Deleers, M. and Malaisse, W.J. (1980) Ionophore-Mediated Calcium Exchange Diffusion in Liposomes. *Biochemical and Biophysical Research Communications*, 95, 650-657.

Desjardins, J.P., Abbott, E.A., Emerson, D.L., Tomkinson, B.E., Leray, J.D., Brown, E.N., Hamilton, M., Dihel, L., Ptaszynski, M., Bendele, R.A. and Richardson, F.C. (2001) Biodistribution of NX211, liposomal lurtotecan, in tumor-bearing mice. *Anticancer Drugs*, 12, 235-245.

Dewhirst, M.W., Tso, C.Y., Oliver, R., Gustafson, C.S., Secomb, T.W. and Gross, J.F. (1989) Morphologic and hemodynamic comparison of tumor and healing normal tissue microvasculature. *Int J Radiat Oncol Biol Phys*, 17, 91-99.

Drummond, D.C., Meyer, O., Hong, K., Kirpotin, D.B. and Papahadjopoulos, D. (1999) Optimizing liposomes for delivery of chemotherapeutic agents to solid tumors. *Pharmacol Rev*, 51, 691-743.

Dunton, C.J. (1997) New options for the treatment of advanced ovarian cancer. *Semin Oncol*, 24, S5-2-S5-11.

Dvorak, H.F., Nagy, J.A., Dvorak, J.T. and Dvorak, A.M. (1988) Identification and characterization of the blood vessels of solid tumors that are leaky to circulating macromolecules. *Am J Pathol*, 133, 95-109.

Embree, L., Gelmon, K.A., Lohr, A., Mayer, L.D., Coldman, A.J., Cullis, P.R., Palaitis, W., Pilkiewicz, F., Hudon, N.J., Heggie, J.R. and et al. (1993) Chromatographic analysis and pharmacokinetics of liposome-encapsulated doxorubicin in non-small-cell lung cancer patients. *J Pharm Sci*, 82, 627-634.

Emerson, D.L. (2000) Liposomal delivery of camptothecins. *PSTT*, 3, 205-209.

Emerson, D.L., Besterman, J.M., Brown, H.R., Evans, M.G., Leitner, P.P., Luzzio, M.J., Shaffer, J.E., Sternbach, D.D., Uehling, D. and Vuong, A. (1995) In vivo antitumor activity of two new seven-substituted water-soluble camptothecin analogues. *Cancer Res*, 55, 603-609.

Enoch, H.G. and Strittmatter, P. (1979) Formation and properties of 1000-A-diameter, single-bilayer phospholipid vesicles. *Proc Natl Acad Sci U S A*, 76, 145-149.

Fassberg, J. and Stella, V.J. (1992) A kinetic and mechanistic study of the hydrolysis of camptothecin and some analogues. *J Pharm Sci*, 81, 676-684.

Fenske, D.B., Wong, K.F., Maurer, E., Maurer, N., Leenhouts, J.M., Boman, N., Amankwa, L. and Cullis, P.R. (1998) Ionophore-mediated uptake of ciprofloxacin and vincristine into large unilamellar vesicles exhibiting transmembrane ion gradients. *Biochim Biophys Acta*, 1414, 188-204.

Ferrans, V.J. (1978) Overview of cardiac pathology in relation to anthracycline cardiotoxicity. *Cancer Treat Rep*, 62, 955-961.

Fiallo, M.M., Garnier-Suillerot, A., Matzanke, B. and Kozlowski, H. (1999) How Fe3+ binds anthracycline antitumour compounds. The myth and the reality of a chemical sphinx. *J Inorg Biochem*, 75, 105-115.

Fiallo, M.M., Tayeb, H., Suarato, A. and Garnier-Suillerot, A. (1998) Circular dichroism studies on anthracycline antitumor compounds. Relationship between the molecular structure and the spectroscopic data. *J Pharm Sci*, 87, 967-975.

Field, S.B. and Bleehen, N.M. (1979) Hyperthermia in the treatment of cancer. *Cancer Treat Rev*, 6, 63-94.

Finley, R.S. (1991) Principles of Cancer Treatment. In Finley, R.S. (ed.), *Concepts in Oncology Therapeutics*. American Society of Hospital Pharmacists, Bethesda.

Fiske, C.H. and Subbarow, Y. (1925) The colorimetric determination of phosporus. *The Journal of Biological Chemistry*, 2, 375-395.

Friedland, M.L. (1992) Combinational Chemotherapy. In M.C., P. (ed.), *The Chemotherapy Source Book*. Williams And Wilkins, Baltimore, Maryland.

Gaber, M.H., Hong, K., Huang, S.K. and Papahadjopoulos, D. (1995) Thermosensitive sterically stabilized liposomes: formulation and in vitro studies on mechanism of doxorubicin release by bovine serum and human plasma. *Pharm Res*, 12, 1407-1416.

Gaber, M.H., Wu, N.Z., Hong, K., Huang, S.K., Dewhirst, M.W. and Papahadjopoulos, D. (1996) Thermosensitive liposomes: extravasation and release of contents in tumor microvascular networks. *Int J Radiat Oncol Biol Phys*, 36, 1177-1187.

Gabizon, A., Goren, D., Cohen, R. and Barenholz, Y. (1998) Development of liposomal anthracyclines: from basics to clinical applications. *J Control Release*, 53, 275-279.

Gabizon, A. and Papahadjopoulos, D. (1988) Liposome formulations with prolonged circulation time in blood and enhanced uptake by tumors. *Proc Natl Acad Sci U S A*, 85, 6949-6953.

Gariepy, J. and Kawamura, K. (2001) Vectorial delivery of macromolecules into cells using peptide-based vehicles. *Trends Biotechnol*, 19, 21-28.

Gelmon, K.A., Tolcher, A., Diab, A.R., Bally, M.B., Embree, L., Hudon, N., Dedhar, C., Ayers, D., Eisen, A., Melosky, B., Burge, C., Logan, P. and Mayer, L.D. (1999) Phase I study of liposomal vincristine. *J Clin Oncol*, 17, 697-705.

Gennaro, A.R. (ed.). (1995) *Vincristine Sulfate*. Mack Publishing Company, Easton.

Gewirtz, D.A. (1999) A critical evaluation of the mechanisms of action proposed for the antitumor effects of the anthracycline antibiotics adriamycin and daunorubicin. *Biochem Pharmacol*, 57, 727-741.

Gianni, L. (2002) The future of targeted therapy: combining novel agents. *Oncology*, 63, 47-56.

Goldfeder, A., Brown, D.M. and Berger, A. (1979) Enhancement of radioresponse of a mouse mammary carcinoma to combined treatments with hyperthermia and radiosensitizer misonidazole. *Cancer Res*, 39, 2966-2970.

Goldie, J.H. (2001) Drug resistance in cancer: a perspective. *Cancer Metastasis Rev*, 20, 63-68.

Greco, F.A. and Hainsworth, J.D. (1995) Etoposide phosphate or etoposide with cisplatin in the treatment of small cell lung cancer: randomized phase II trial. *Lung Cancer*, 12 Suppl 3, S85-95.

Greenaway, F.T. and Dadrowiak, J.C. (1982) The Binding of Copper Ions to Daunomycin and Adriamycin. *Journal of Inorganic Biochemistry*, 16, 91-107.

Gregoriadis, G. and Davis, C. (1979) Stability of liposomes in vivo and in vitro is promoted by their cholesterol content and the presence of blood cells. *Biochem Biophys Res Commun*, 89, 1287-1293.

Grochow, L.B., Rowinsky, E.K., Johnson, R., Ludeman, S., Kaufmann, S.H., McCabe, F.L., Smith, B.R., Hurowitz, L., DeLisa, A., Donehower, R.C. and et al. (1992) Pharmacokinetics and pharmacodynamics of topotecan in patients with advanced cancer. *Drug Metab Dispos*, 20, 706-713.

Gruner, S.M. (1987) Materials Properties of Liposomal Bilayers. In J.Ostro, M. (ed.), *Liposomes From Biophysics to Therapeutics*. Marcel Dekker Inc, New York, pp. 1-38.

Gruner, S.M., Lenk, R.P., Janoff, A.S. and Ostro, M.J. (1985) Novel multilayered lipid vesicles: comparison of physical characteristics of multilamellar liposomes and stable plurilamellar vesicles. *Biochemistry*, 24, 2833-2842.

Grunt, T.W., Lametschwandtner, A. and Staindl, O. (1985) The vascular pattern of basal cell tumors: light microscopy and scanning electron microscopic study on vascular corrosion casts. *Microvasc Res*, 29, 371-386.

Guo, L.S., Hamilton, R.L., Goerke, J., Weinstein, J.N. and Havel, R.J. (1980) Interaction of unilamellar liposomes with serum lipoproteins and apolipoproteins. *J Lipid Res*, 21, 993-1003.

Guo, X., MacKay, J.A. and Szoka, F.C., Jr. (2003) Mechanism of pH-Triggered Collapse of Phosphatidylethanolamine Liposomes Stabilized by an Ortho Ester Polyethyleneglycol Lipid. *Biophys J*, 84, 1784-1795.

Haleblian, J.K. (1975) Characterization of habits and crystalline modification of solids and their pharmaceutical applications. *J Pharm Sci*, 64, 1269-1288.

Haran, G., Cohen, R., Bar, L.K. and Barenholz, Y. (1993) Transmembrane ammonium sulfate gradients in liposomes produce efficient and stable entrapment of amphipathic weak bases. *Biochim Biophys Acta*, 1151, 201-215.

Harrigan, P.R., Hope, M.J., Redelmeier, T.E. and Cullis, P.R. (1992) Determination of transmembrane pH gradients and membrane potentials in liposomes. *Biophys J*, 63, 1336-1345.

Harrigan, P.R., Wong, K.F., Redelmeier, T.E., Wheeler, J.J. and Cullis, P.R. (1993) Accumulation of doxorubicin and other lipophilic amines into large unilamellar vesicles in response to transmembrane pH gradients. *Biochim Biophys Acta*, 1149, 329-338.

Hatefi, A. and Amsden, B. (2002) Camptothecin delivery methods. *Pharmaceutical Research*, 19, 1389-1399.

Haxby, J.A., Kinsky, C.B. and Kinsky, S.C. (1968) Immune response of a liposomal model membrane. *Proc Natl Acad Sci U S A*, 61, 300-307.

Hertzberg, R.P., Caranfa, M.J. and Hecht, S.M. (1989) On the mechanism of topoisomerase I inhibition by camptothecin: evidence for binding to an enzyme-DNA complex. *Biochemistry*, 11, 4629-4638.

Herzog, T.J. (2002) Update on the role of topotecan in the treatment of recurrent ovarian cancer. *Oncologist*, 7 Suppl 5, 3-10.

Hill, B.T. and Whelan, R.D. (1980) Comparative effects of vincristine and vindesine on cell cycle kinetics in vitro. *Cancer Treat Rev*, 7 Suppl 1, 5-15.

Hill, B.T. and Whelan, R.D. (1981) Comparative cell killing and kinetic effects of vincristine or vindesine in mammalian cell lines. *J Natl Cancer Inst*, 67, 437-443.

Hill, R.P. and Tannock, I.F. (1998) Introduction to Cancer Biology. In Tannock, I.F. and Hill, R.P. (eds.), *The Basic Science of Oncology*. McGraw-Hill, New York.

Hobbs, S.K., Monsky, W.L., Yuan, F., Roberts, W.G., Griffith, L., Torchilin, V.P. and Jain, R.K. (1998) Regulation of transport pathways in tumor vessels: role of tumor type and microenvironment. *Proc Natl Acad Sci U S A*, 95, 4607-4612.

Hope, M.J., Bally, M., Mayer, L.D., Janoff, A.S. and Cullis, P.R. (1986) Generation of Multilamellar and Unilamellar Phospholipid Vesicles. *Chemistry and Physics of Lipids*, 40, 89-107.

Hope, M.J., Bally, M.B., Webb, G. and Cullis, P.R. (1985) Production of Large Unilamellar Vesicles by a Rapid Extrusion Procedure. Characterization of Size, Distribution, Trapped Volume And Ability to Maintain a Membrane Potential. *Biochim Biophys Acta*, 812, 55-65.

Hortobagyi, G.N. (1997) Anthracyclines in the treatment of cancer. An overview. *Drugs*, 54, 1-7.

Houslay, M.D. and Stanley, K.K. (1982) *Dynamics of Biological Membranes*. Wiley, New York.

Hsiang, Y.H., Hertzberg, R., Hecht, S. and Liu, L.F. (1985) Camptothecin induces protein-linked DNA breaks via mammalian DNA topoisomerase I. *J Biol Chem*, 260, 14873-14878.

Hsiang, Y.H. and Liu, L.F. (1988) Identification of mammalian DNA topoisomerase I as an intracellular target of the anticancer drug camptothecin. *Cancer Res*, 48, 1722-1726.

Hsiang, Y.H., Liu, L.F., Wall, M.E., Wani, M.C., Nicholas, A.W., Manikumar, G., Kirschenbaum, S., Silber, R. and Potmesil, M. (1989) DNA topoisomerase I-mediated DNA cleavage and cytotoxicity of camptothecin analogues. *Cancer Res*, 49, 4385-4389.

Huang, C., Li, S., Wang, Z.Q. and Lin, H.N. (1993) Dependence of the bilayer phase transition temperatures on the structural parameters of phosphatidylcholines. *Lipids*, 28, 365-370.

Hunter, J.A., Shahrokh, Z., Forte, T.M. and Nichols, A.V. (1982) Aggregation of low density lipoproteins with unilamellar phosphatidylcholine vesicles. *Biochem Biophys Res Commun*, 105, 828-834.

Hussein, M.A., Wood, L., Hsi, E., Srkalovic, G., Karam, M., Elson, P. and Bukowski, R.M. (2002) A Phase II trial of pegylated liposomal doxorubicin, vincristine, and reduced-dose dexamethasone combination therapy in newly diagnosed multiple myeloma patients. *Cancer*, 95, 2160-2168.

Ickenstein, L.M. (2003) Triggered Drug Release From Thermosensitive Liposomes. *Pharmacy*. University of British Columbia, Vancouver, p. 300.

Ickenstein, L.M., Arfvidsson, M.C., Needham, D., Mayer, L.D. and Edwards, K. (2003) Disc formation in cholesterol-free liposomes during phase transition. *Biochim Biophys Acta*, 1614, 135-138.

Iga, K., Hamaguchi, N., Igari, Y., Ogawa, Y., Gotoh, K., Ootsu, K., Toguchi, H. and Shimamoto, T. (1991) Enhanced antitumor activity in mice after administration of thermosensitive liposome encapsulating cisplatin with hyperthermia. *J Pharmacol Exp Ther*, 257, 1203-1207.

Israelachvili, J.N., Marcelja, S. and Horn, R.G. (1980) Physical principles of membrane organization. *Q Rev Biophys*, 13, 121-200.

Jain, R.K. (1987) Transport of molecules across tumor vasculature. *Cancer Metastasis Rev*, 6, 559-593.

Jain, R.K. (1991) Therapeutic implications of tumor physiology. *Curr Opin Oncol*, 3, 1105-1108.

Jaxel, C., Kohn, K.W., Wani, M.C., Wall, M.E. and Pommier, Y. (1989) Structure-activity study of the actions of camptothecin derivatives on mammalian topoisomerase I: evidence for a specific receptor site and a relation to antitumor activity. *Cancer Res*, 49, 1465-1469.

Johnstone, S.A., Masin, D., Mayer, L. and Bally, M.B. (2001) Surface-associated serum proteins inhibit the uptake of phosphatidylserine and poly(ethylene glycol) liposomes by mouse macrophages. *Biochim Biophys Acta*, 1513, 25-37.

Kamps, J.A. and Scherphof, G.L. (1998) Receptor versus non-receptor mediated clearance of liposomes. *Adv Drug Deliv Rev*, 32, 81-97.

Kaplan, M.H. and Volanakis, J.E. (1974) Interaction of C-reactive protein complexes with the complement system. I. Consumption of human complement associated with the reaction of C-reactive protein with pneumococcal C-polysaccharide and with the choline phosphatides, lecithin and sphingomyelin. *J Immunol*, 112, 2135-2147.

Kaufman, D. and Chabner, B.A. (1996) Clinical Strategies for Cancer Treatment. In Chabner, B.A. and Longo, D.L. (eds.), *Cancer Chemotherapy and Biotherapy*. Lippincott-Raven, Philadelphia.

Kehrer, D.F., Bos, A.M., Verweij, J., Groen, H.J., Loos, W.J., Sparreboom, A., de Jonge, M.J., Hamilton, M., Cameron, T. and de Vries, E.G. (2002a) Phase I and pharmacologic study of liposomal lurtotecan, NX 211: urinary excretion predicts hematologic toxicity. *J Clin Oncol*, 20, 1222-1231.

Kehrer, D.K.S., Bos, A.M., Verweij, J., Groen, H.J., Loos, W.J., Sparreboom, A., deJonge, M.J.A., Hamilton, M., Cameron, T. and de Vries, E.G.E. (2002b) Phase I and pharmacologic study of liposomal lurtotecan, NX 211: urinary excretion predicts hematologic toxicity. *Journal of Clinical Oncology*, 20, 1222-1231.

Kim, S.H. and Kim, J.H. (1972) Lethal effect of adriamycin on the division cycle of HeLa cells. *Cancer Res*, 32, 323-325.

Kingsbury, W.D., Boehm, J.C., Jakas, D.R., Holden, K.G., Hecht, S.M., Gallagher, G., Caranfa, M.J., McCabe, F.L., Faucette, L.F., Johnson, R.K. and et al. (1991) Synthesis of water-soluble (aminoalkyl)camptothecin analogues: inhibition of topoisomerase I and antitumor activity. *J Med Chem*, 34, 98-107.

Kinsky, S.C. (1972) Antibody-complement interaction with lipid model membranes. *Biochim Biophys Acta*, 265, 1-23.

Klapisz, E., Masliah, J., Bereziat, G., Wolf, C. and Koumanov, K.S. (2000) Sphingolipids and cholesterol modulate membrane susceptibility to cytosolic phospholipase A(2). *J Lipid Res*, 41, 1680-1688.

Koenig, S.H., Brown, R.D., 3rd, Kurland, R. and Ohki, S. (1988) Relaxivity and binding of Mn2+ ions in solutions of phosphatidylserine vesicles. *Magn Reson Med*, 7, 133-142.

Kong, G., Anyarambhatla, G., Petros, W.P., Braun, R.D., Colvin, O.M., Needham, D. and Dewhirst, M.W. (2000) Efficacy of liposomes and hyperthermia in a human tumor xenograft model: importance of triggered drug release. *Cancer Res*, 60, 6950-6957.

Krogh, C.M.E. (ed.). (1994) *Adriamycin*. Canadian Pharmaceutical Association, Ottawa.

Krol, A.D., Berenschot, H.W., Doekharan, D., Henzen-Logmans, S., van der Holt, B. and van 't Veer, M.B. (2001) Cyclophosphamide, doxorubicin, vincristine and prednisone chemotherapy and radiotherapy for stage I intermediate or high grade non-Hodgkin's lymphomas: results of a strategy that adapts radiotherapy dose to the response after chemotherapy. *Radiother Oncol*, 58, 251-255.

Kuwahara, J., Suzuki, T., Funakoshi, K. and Sugiura, Y. (1986) Photosensitive DNA cleavage and phage inactivation by copper(II)-camptothecin. *Biochemistry*, 25, 1216-1221.

Kuwahara, J., Suzuki, T. and Sugiura, Y. (1985) Studies on antitumor drugs targeting DNA: photosensitive DNA cleavage of copper-camptothecin. *Nucleic Acids Symp Ser*, 201-204.

Larsen, A.K., Gilbert, C., Chyzak, G., Plisov, S.Y., Naguibneva, I., Lavergne, O., Lesueur-Ginot, L. and Bigg, D.C.H. (2001) Unusual potency of BN 80915, a novel fluorinated

E-ring modified camptothecin toward human colon carcinoma cells. *Cancer Research*, 61, 2961-2967.

Lasic, D.D. (1996) Doxorubicin in sterically stabilized liposomes. *Nature*, 380, 561-562.

Lasic, D.D., Ceh, B., Stuart, M.C., Guo, L., Frederik, P.M. and Barenholz, Y. (1995) Transmembrane gradient driven phase transitions within vesicles: lessons for drug delivery. *Biochim Biophys Acta*, 1239, 145-156.

Lasic, D.D., Frederik, P.M., Stuart, M.C., Barenholz, Y. and McIntosh, T.J. (1992) Gelation of liposome interior. A novel method for drug encapsulation. *FEBS Lett*, 312, 255-258.

Lee, R.J., Wang, S., Turk, M.J. and Low, P.S. (1998) The effects of pH and intraliposomal buffer strength on the rate of liposome content release and intracellular drug delivery. *Biosci Rep*, 18, 69-78.

Leonessa, F., Green, D., Licht, T., Wright, A., Wingate-Legette, K., Lippman, J., Gottesman, M.M. and Clarke, R. (1996) MDA435/LCC6 and MDA435/LCC6MDR1: ascites models of human breast cancer. *Br J Cancer*, 73, 154-161.

Leonetti, J.P., Machy, P., Degols, G., Lebleu, B. and Leserman, L. (1990) Antibody-targeted liposomes containing oligodeoxyribonucleotides complementary to viral RNA selectively inhibit viral replication. *Proc Natl Acad Sci U S A*, 87, 2448-2451.

Leserman, L.D., Barbet, J., Kourilsky, F. and Weinstein, J.N. (1980) Targeting to cells of fluorescent liposomes covalently coupled with monoclonal antibody or protein A. *Nature*, 288, 602-604.

Li, X., Cabral-Lilly, D., Janoff, A.S. and Perkins, W.R. (2000) Complexation of Internalized Doxorubicin into Fiber Bundles Affects Its Release Rate From Liposomes. *Journal of Liposome Research*, 10, 15-27.

Li, X., Hirsh, D.J., Cabral-Lilly, D., Zirkel, A., Gruner, S.M., Janoff, A.S. and Perkins, W.R. (1998) Doxorubicin physical state in solution and inside liposomes loaded via a pH gradient. *Biochim Biophys Acta*, 1415, 23-40.

Lim, H.J., Masin, D., Madden, T.D. and Bally, M.B. (1997) Influence of drug release characteristics on the therapeutic activity of liposomal mitoxantrone. *Journal Of Pharmacology And Experimental Therapeutics*, 281, 566-573.

Liu, J.J., Hong, R.L., Cheng, W.F., Hong, K., Chang, F.H. and Tseng, Y.L. (2002a) Simple and efficient liposomal encapsulation of topotecan by ammonium sulfate gradient: stability, pharmacokinetic and therapeutic evaluation. *Anticancer Drugs*, 13, 709-717.

Liu, X., Lynn, B.C., Zhang, J., Song, L., Bom, D., Du, W., Curran, D.P. and Burke, T.G. (2002b) A versatile prodrug approach for liposomal core-loading of water-insoluble camptothecin anticancer drugs. *J Am Chem Soc*, 124, 7650-7651.

Lopez-Berestein, G. (1987) Liposomes as carriers of antimicrobial agents. *Antimicrob Agents Chemother*, 31, 675-678.

Lynam, E., Landfair, D.J. and Wiles, M.E. (1999) Camptothecin Analogue Efficacy In Vitro: Effect of Liposomal Encapsulation of GI147211C (NX211). *Drug Delivery*, 6, 51-62.

Madden, T.D. (1997) Model membrane systems. In Bittar, E.E. and Bittar, N. (eds.), *Principles of Medical Biology*. JAI Press Inc., Greenwich, Vol. 7A.

Madden, T.D., Harrigan, P.R., Tai, L.C., Bally, M.B., Mayer, L.D., Redelmeier, T.E., Loughrey, H.C., Tilcock, C.P., Reinish, L.W. and Cullis, P.R. (1990) The accumulation of drugs within large unilamellar vesicles exhibiting a proton gradient: a survey. *Chem Phys Lipids*, 53, 37-46.

Malecki, E.A. (2001) Manganese toxicity is associated with mitochondrial dysfunction and DNA fragmentation in rat primary striatal neurons. *Brain Res Bull*, 55, 225-228.

Margolis, L.B., Victorov, A.V. and Bergelson, L.D. (1982) Lipid-cell interactions. A novel mechanism of transfer of liposome-entrapped substances into cells. *Biochim Biophys Acta*, 720, 259-265.

Maruyama, K., Unezaki, S., Takahashi, N. and Iwatsuru, M. (1993) Enhanced delivery of doxorubicin to tumor by long-circulating thermosensitive liposomes and local hyperthermia. *Biochim Biophys Acta*, 1149, 209-216.

Maurer-Spurej, E., Wong, K.F., Maurer, N., Fenske, D.B. and Cullis, P.R. (1999) Factors influencing uptake and retention of amino-containing drugs in large unilamellar vesicles exhibiting transmembrane pH gradients. *Biochim Biophys Acta*, 1416, 1-10.

Mayer, L.D. (1998) Future developments in the selectivity of anticancer agents: drug delivery and molecular target strategies. *Cancer Metastasis Rev*, 17, 211-218.

Mayer, L.D., Bally, M.B. and Cullis, P.R. (1986a) Uptake of adriamycin into large unilamellar vesicles in response to a pH gradient. *Biochim Biophys Acta*, 857, 123-126.

Mayer, L.D., Bally, M.B., Hope, M.J. and Cullis, P.R. (1985a) Uptake of antineoplastic agents into large unilamellar vesicles in response to a membrane potential. *Biochim Biophys Acta*, 816, 294-302.

Mayer, L.D., Bally, M.B., Hope, M.J. and Cullis, P.R. (1986b) Techniques for encapsulating bioactive agents into liposomes. *Chem Phys Lipids*, 40, 333-345.

Mayer, L.D., Bally, M.B., Loughrey, H., Masin, D. and Cullis, P.R. (1990a) Liposomal vincristine preparations which exhibit decreased drug toxicity and increased activity against murine L1210 and P388 tumors. *Cancer Res*, 50, 575-579.

Mayer, L.D., Cullis, P.R. and Bally, M.B. (1994) The Use of Transmembrane pH Gradient-Driven Drug Encapsulation in the Pharmacodynamic Evaluation of Liposomal Doxorubicin. *Journal of Liposome Research*, 4, 529-553.

Mayer, L.D., Hope, M.J., Cullis, P.R. and Janoff, A.S. (1985b) Solute distributions and trapping efficiencies observed in freeze- thawed multilamellar vesicles. *Biochim Biophys Acta*, 817, 193-196.

Mayer, L.D., Madden, T.D., Bally, M.B. and Cullis, P.R. (1984) pH Gradient-Mediated Drug Entrapment in Liposomes. In Gregoriadis, G. (ed.), *Liposome Technology*. CRC Press, Boca Raton, Vol. 2, pp. 27-44.

Mayer, L.D., Nayar, R., Thies, R.L., Boman, N.L., Cullis, P.R. and Bally, M.B. (1993) Identification of vesicle properties that enhance the antitumour activity of liposomal vincristine against murine L1210 leukemia. *Cancer Chemother Pharmacol*, 33, 17-24.

Mayer, L.D., Tai, L.C., Bally, M.B., Mitilenes, G.N., Ginsberg, R.S. and Cullis, P.R. (1990b) Characterization of liposomal systems containing doxorubicin entrapped in response to pH gradients. *Biochim Biophys Acta*, 1025, 143-151.

Mayer, L.D., Tai, L.C., Ko, D.S., Masin, D., Ginsberg, R.S., Cullis, P.R. and Bally, M.B. (1989) Influence of vesicle size, lipid composition, and drug-to-lipid ratio on the biological activity of liposomal doxorubicin in mice. *Cancer Res*, 49, 5922-5930.

Menozzi, M., Valentini, L., Vannini, E. and Arcamone, F. (1984) Self-association of doxorubicin and related compounds in aqueous solution. *J Pharm Sci*, 73, 766-770.

Merlin, J.L. (1991a) Encapsulation of doxorubicin in thermosensitive small unilamellar vesicle liposomes. *Eur J Cancer*, 27, 1026-1030.

Merlin, J.L. (1991b) In vitro evaluation of the association of thermosensitive liposome-encapsulated doxorubicin with hyperthermia. *Eur J Cancer*, 27, 1031-1034.

Merlin, J.L., Marchal, S., Ramacci, C., Notter, D. and Vigneron, C. (1993) Antiproliferative activity of thermosensitive liposome-encapsulated doxorubicin combined with 43 degrees C hyperthermia in sensitive and multidrug-resistant MCF-7 cells. *Eur J Cancer*, 29A, 2264-2268.

Moghimi, S.M. and Patel, H.M. (1988) Tissue specific opsonins for phagocytic cells and their different affinity for cholesterol-rich liposomes. *FEBS Lett*, 233, 143-147.

Moribe, K. and Maruyama, K. (2002) Pharmaceutical design of the liposomal antimicrobial agents for infectious disease. *Curr Pharm Des*, 8, 441-454.

Muhtadi, F.J. and Afify, A. (1993) Vincristine Sulfate. *Analytical Profiles of Drug Substances and Excipients*, 22, 517-549.

Mukherjee, A.B., Orloff, S., Butler, J.D., Triche, T., Lalley, P. and Schulman, J.D. (1978) Entrapment of metaphase chromosomes into phospholipid vesicles (lipochromosomes): carrier potential in gene transfer. *Proc Natl Acad Sci U S A*, 75, 1361-1365.

Needham, D., Anyarambhatla, G., Kong, G. and Dewhirst, M.W. (2000) A new temperature-sensitive liposome for use with mild hyperthermia: characterization and testing in a human tumor xenograft model. *Cancer Res*, 60, 1197-1201.

Needham, D. and Dewhirst, M.W. (2001) The development and testing of a new temperature-sensitive drug delivery system for the treatment of solid tumors. *Adv Drug Deliv Rev*, 53, 285-305.

Needham, D., McIntosh, T.J. and Evans, E. (1988) Thermomechanical and transition properties of dimyristoylphosphatidylcholine/cholesterol bilayers. *Biochemistry*, 27, 4668-4673.

Needham, D. and Nunn, R.S. (1990) Elastic deformation and failure of lipid bilayer membranes containing cholesterol. *Biophys J*, 58, 997-1009.

New, R.R.C. (1990) Introduction. In New, R.R.C. (ed.), *Liposomes a practical approach*. Oxford University Press, Oxford.

Newell, M., Milliken, S., Goldstein, D., Lewis, C., Boyle, M., Dolan, G., Ryan, S. and Cooper, D.A. (1998) A phase II study of liposomal doxorubicin in the treatment of HIV- related Kaposi's sarcoma. *Aust N Z J Med*, 28, 777-783.

Nichols, J.W. and Deamer, D.W. (1976) Catecholamine uptake and concentration by liposomes maintaining pH gradients. *Biochim Biophys Acta*, 455, 269-271.

Niesman, M.R., Bacic, G.G., Wright, S.M., Swartz, H.J. and Magin, R.L. (1990) Liposome encapsulated MnCl2 as a liver specific contrast agent for magnetic resonance imaging. *Invest Radiol*, 25, 545-551.

Northfelt, D.W., Dezube, B.J., Thommes, J.A., Miller, B.J., Fischl, M.A., Friedman-Kien, A., Kaplan, L.D., Du Mond, C., Mamelok, R.D. and Henry, D.H. (1998) Pegylated-liposomal doxorubicin versus doxorubicin, bleomycin, and vincristine in the treatment of AIDS-related Kaposi's sarcoma: results of a randomized phase III clinical trial. *J Clin Oncol*, 16, 2445-2451.

Oku, N. and Namba, Y. (1994) Long-circulating liposomes. *Crit Rev Ther Drug Carrier Syst*, 11, 231-270.

Olson, F., Hunt, C.A., Szoka, F.C., Vail, W.J. and Papahadjopoulos, D. (1979) Preparation of liposomes of defined size distribution by extrusion through polycarbonate membranes. *Biochim Biophys Acta*, 557, 9-23.

O'Niel, M.J. (ed.). (2001a) *Citrate*. Merck and Company Inc, Whitehouse Station.

O'Niel, M.J. (ed.). (2001b) *Doxorubicin*. Merck and Company Inc., Whitehouse Station.

O'Niel, M.J. (ed.). (2001c) *Topotecan*. Merck and Company Inc., Whitehouse Station.

O'Niel, M.J. (ed.). (2001d) *Vincristine*. Merck and Company Inc., Whitehouse Station.

Owellen, R.J., Hartke, C.A., Dickerson, R.M. and Hains, F.O. (1976) Inhibition of tubulin-microtubule polymerization by drugs of the Vinca alkaloid class. *Cancer Res*, 36, 1499-1502.

Owellen, R.J., Owens, A.H., Jr. and Donigian, D.W. (1972) The binding of vincristine, vinblastine and colchicine to tubulin. *Biochem Biophys Res Commun*, 47, 685-691.

Papahadjopoulos, D., Jacobson, K., Nir, S. and Isac, T. (1973) Phase transitions in phospholipid vesicles. Fluorescence polarization and permeability measurements concerning the effect of temperature and cholesterol. *Biochim Biophys Acta*, 311, 330-348.

Pastorino, F., Stuart, D., Ponzoni, M. and Allen, T.M. (2001) Targeted delivery of antisense oligonucleotides in cancer. *J Control Release*, 74, 69-75.

Patel, H.M., Tuzel, N.S. and Ryman, B.E. (1983) Inhibitory effect of cholesterol on the uptake of liposomes by liver and spleen. *Biochim Biophys Acta*, 761, 142-151.

Perkins, W.R. and Cafiso, D.S. (1987) Characterization of H+/OH- currents in phospholipid vesicles. *J Bioenerg Biomembr*, 19, 443-455.

Pizzolato, J.F. and Saltz, L.B. (2003) The camptothecins. *The Lancet*, 361, 2235-2242.

Platel, D., Bonoron-Adele, S., Dix, R.K. and Robert, J. (1999) Preclinical evaluation of the cardiac toxicity of HMR-1826, a novel prodrug of doxorubicin. *Br J Cancer*, 81, 24-27.

Pool, G.L., French, M.E., Edwards, R.A., Huang, L. and Lumb, R.H. (1982) Use of radiolabeled hexadecyl cholesteryl ether as a liposome marker. *Lipids*, 17, 448-452.

Poznansky, M.J. and Lange, Y. (1978) Transbilayer movement of cholesterol in phospholipid vesicles under equilibrium and non-equilibrium conditions. *Biochim Biophys Acta*, 506, 256-264.

Rahman, A., Dusre, L., Forst, D., Thierry, A., Roh, J.K., Greenspan, A. and Treat, J. (1990) Membrane alterations by liposomes to enhance clinical efficacy of cytotoxic drugs. *Prog Clin Biol Res*, 343, 281-304.

Rahman, A., Kessler, A., More, N., Sikic, B., Rowden, G., Woolley, P. and Schein, P.S. (1980) Liposomal protection of adriamycin-induced cardiotoxicity in mice. *Cancer Res*, 40, 1532-1537.

Redelmeier, T.E., Mayer, L.D., Wong, K.F., Bally, M.B. and Cullis, P.R. (1989) Proton flux in large unilamellar vesicles in response to membrane potentials and pH gradients. *Biophys J*, 56, 385-393.

Reynolds, J.E.F. (ed.). (1989a) *Doxorubicin Hydrochloride*. The Pharamaceutical Press, London.

Reynolds, J.E.F. (ed.). (1989b) *Vincristine Sulfate*. The Pharmaceutical Press, London.

Richards, R.L., Gewurz, H., Osmand, A.P. and Alving, C.R. (1977) Interactions of C-reactive protein and complement with liposomes. *Proc Natl Acad Sci U S A*, 74, 5672-5676.

Rihova, B. (2002) Immunomodulating activities of soluble synthetic polymer-bound drugs. *Adv Drug Deliv Rev*, 54, 653-674.

Roth, J.A., Horbinski, C., Higgins, D., Lein, P. and Garrick, M.D. (2002) Mechanisms of manganese-induced rat pheochromocytoma (PC12) cell death and cell differentiation. *Neurotoxicology*, 23, 147-157.

Sadzuka, Y., Hirotsu, S. and Hirota, S. (1998) Effect of liposomalization on the antitumor activity, side-effects and tissue distribution of CPT-11. *Cancer Lett*, 127, 99-106.

Sambrano, G.R. and Steinberg, D. (1995) Recognition of oxidatively damaged and apoptotic cells by an oxidized low density lipoprotein receptor on mouse peritoneal macrophages: role of membrane phosphatidylserine. *Proc Natl Acad Sci U S A*, 92, 1396-1400.

Sarris, A.H., Hagemeister, F., Romaguera, J., Rodriguez, M.A., McLaughlin, P., Tsimberidou, A.M., Medeiros, L.J., Samuels, B., Pate, O., Oholendt, M., Kantarjian, H., Burge, C. and Cabanillas, F. (2000) Liposomal vincristine in relapsed non-Hodgkin's lymphomas: early results of an ongoing phase II trial. *Ann Oncol*, 11, 69-72.

Saxon, D., Mayer, L. and Bally, M. (1999) Liposomal anticancer drugs as agents to be used in combination with other anticancer agents: studies on a liposomal formulation with two encapsulated drugs. *Journal of Liposome Research*, 9, 507-522.

Scherphof, G., Damen, J. and Hoekstra, D. (1981) Interactions of liposomes with plasma proteins and components of the immune system. In Knight, V. (ed.), *Liposomes: From Physical Structure to Therapeutic Applications*. Elsevier/North-Holland Biomedical Press.

Schmitt-Sody, M., Strieth, S., Krasnici, S., Sauer, B., Schulze, B., Teifel, M., Michaelis, U., Naujoks, K. and Delian, M. (2003) Neovascular Targeting Therapy: Paclitaxel Encapsulated in Cationic Liposomes Improves Antitumoral Efficacy. *Clinical Cancer Research*, 9, 2335-2341.

Seelig, J. and Waespe-Sarcevic, N. (1978) Molecular order in cis and trans unsaturated phospholipid bilayers. *Biochemistry*, 17, 3310-3315.

Semple, S.C., Chonn, A. and Cullis, P.R. (1996) Influence of cholesterol on the association of plasma proteins with liposomes. *Biochemistry*, 35, 2521-2525.

Senior, J. and Gregoriadis, G. (1982) Stability of small unilamellar liposomes in serum and clearance from the circulation: the effect of the phospholipid and cholesterol components. *Life Sci*, 30, 2123-2136.

Shabbits, J.A. and Mayer, L.D. (2003) Intracellular delivery of ceramide lipids via liposomes enhances apoptosis in vitro. *Biochim Biophys Acta*, 1612, 98-106.

Sharpe, M., Easthope, S.E., Keating, G.M. and Lamb, H.M. (2002) Polyethylene glycol-liposomal doxorubicin: a review of its use in the management of solid and haematological malignancies and AIDS-related Kaposi's sarcoma. *Drugs*, 62, 2089-2126.

Shum, P., Kim, J.M. and Thompson, D.H. (2001) Phototriggering of liposomal drug delivery systems. *Adv Drug Deliv Rev*, 53, 273-284.

Sieber, S.M., Mead, J.A. and Adamson, R.H. (1976) Pharmacology of antitumor agents from higher plants. *Cancer Treat Rep*, 60, 1127-1139.

Sikic, B.I., Ehsan, M.N. and Harker, W.G. (1985) Dissociation of antitumor potency from anthracycline cardiotoxicity in a doxorubicin analogue. *Science*, 228, 1544-1546.

Simpkins, H., Pearlman, L.F. and Thompson, L.M. (1984) Effects of adriamycin on supercoiled DNA and calf thymus nucleosomes studied with fluorescent probes. *Cancer Res*, 44, 613-618.

Streltsov, S.A., Grokhovsky, S.L., Kudelina, I.A., Oleinikov, V.A. and Zhuze, A.L. (2001) The Behavior of the DNA Topoisomerase I Inhibitor Topotecan in Aqueous Solution. *J. Biomol. Struct. Dynam.*, 18, 913-914.

Stryer, L. (1989) Introduction to Biological Membranes. In Stryer, L. (ed.), *Biochemistry*. W.H. Freeman and Company, New York.

Subczynski, W.K., Wisniewska, A., Yin, J.J., Hyde, J.S. and Kusumi, A. (1994) Hydrophobic barriers of lipid bilayer membranes formed by reduction of water penetration by alkyl chain unsaturation and cholesterol. *Biochemistry*, 33, 7670-7681.

Subramanian, D. and Muller, M.T. (1995) Liposomal encapsulation increases the activity of the topoisomerase I inhibitor topotecan. *Oncol Res*, 7, 461-469.

Suzuki, T., Kuwahara, J. and Sugiura, Y. (1984) DNA cleavages of bleomycin-transition metal complexes induced by reductant, hydrogen peroxide, and ultraviolet light: characteristics and biological implication. *Nucleic Acids Symp Ser*, 161-164.

Svoboda, G.H. (1961) Alkaloids of Vinca rosea (Catharanthus roseus). Extraction and Characterization of Leurosidine and Leurocristine. *Lloydia*, 24, 173-178.

Swenson, C.E., Bolcsak, L.E., Batist, G., Guthrie, T.H., Jr., Tkaczuk, K.H., Boxenbaum, H., Welles, L., Chow, S.C., Bhamra, R. and Chaikin, P. (2003) Pharmacokinetics of doxorubicin administered i.v. as Myocet (TLC D-99; liposome-encapsulated doxorubicin citrate) compared with conventional doxorubicin when given in combination with cyclophosphamide in patients with metastatic breast cancer. *Anticancer Drugs*, 14, 239-246.

Szebeni, J., Hauser, H., Eskelson, C.D., Watson, R.R. and Winterhalter, K.H. (1988) Interaction of hemoglobin derivatives with liposomes. Membrane cholesterol protects against the changes of hemoglobin. *Biochemistry*, 27, 6425-6434.

Szoka, F., Jr. and Papahadjopoulos, D. (1978) Procedure for preparation of liposomes with large internal aqueous space and high capture by reverse-phase evaporation. *Proc Natl Acad Sci U S A*, 75, 4194-4198.

Szoka, F., Jr. and Papahadjopoulos, D. (1980) Comparative properties and methods of preparation of lipid vesicles (liposomes). *Annu Rev Biophys Bioeng*, 9, 467-508.

Szoka, F., Olson, F., Heath, T., Vail, W., Mayhew, E. and Papahadjopoulos, D. (1980) Preparation of unilamellar liposomes of intermediate size (0.1-0.2 mumol) by a combination of reverse phase evaporation and extrusion through polycarbonate membranes. *Biochim Biophys Acta*, 601, 559-571.

Takimoto, C.H., Wright, J. and Arbuck, S.G. (1998) Clinical applications of the camptothecins. *Biochimica et Biophysica Acta*, 1400, 107-119.

Tanford, C. (1991) *The Hydrophobic Effect: Formation of Micelles and Biological Membranes*. Krieger Publishing Company, Malabar.

Tardi, P., Choice, E., Masin, D., Redelmeier, T., Bally, M. and Madden, T.D. (2000) Liposomal encapsulation of topotecan enhances anticancer efficacy in murine and human xenograft models. *Cancer Res*, 60, 3389-3393.

Tejada-Berges, T., Granai, C.O., Gordinier, M. and Gajewski, W. (2002) Caelyx/Doxil for the treatment of metastatic ovarian and breast cancer. *Expert Rev Anticancer Ther*, 2, 143-150.

Tong, W.Q., Clarke, J., Franklin, M.L., Jozwiakowski, J.P., Lemmo, J.B., Sisco, J.M. and Whight, S.R. (1996) Identification and characterization of the sulfate precipitate in GI147211C IV formulation. *PDA J Pharm Sci Technol*, 50, 326-329.

Triton, T.R. and Yee, G. (1982) The anticancer agent adriamycin can be actively cytotoxic without entering cells. *Science*, 217, 248-250.

Tsavaris, N., Kosmas, C., Vadiaka, M., Giannouli, S., Siakantaris, M.P., Vassilakopoulos, T. and Pangalis, G.A. (2002) Pegylated liposomal doxorubicin in the CHOP regimen for older patients with aggressive (stages III/IV) non-Hodgkin's lymphoma. *Anticancer Res*, 22, 1845-1848.

Ulukan, H. and Swaan, P.W. (2002) Camptothecins: a review of their chemotherapeutic potential. *Drugs*, 62, 2039-2057.

Unger, E., Fritz, T., Shen, D.K. and Wu, G. (1993) Manganese-based liposomes. Comparative approaches. *Invest Radiol*, 28, 933-938.

Unger, E.C., McCreery, T.P., Sweitzer, R.H., Caldwell, V.E. and Wu, Y. (1998) Acoustically active lipospheres containing paclitaxel: a new therapeutic ultrasound contrast agent. *Invest Radiol*, 33, 886-892.

Vaage, J., Donovan, D., Mayhew, E., Uster, P. and Woodle, M. (1993) Therapy of mouse mammary carcinomas with vincristine and doxorubicin encapsulated in sterically stabilized liposomes. *Int J Cancer*, 54, 959-964.

Valero, V., Buzdar, A.U., Theriault, R.L., Azarnia, N., Fonseca, G.A., Willey, J., Ewer, M., Walters, R.S., Mackay, B., Podoloff, D., Booser, D., Lee, L.W. and Hortobagyi, G.N. (1999) Phase II trial of liposome-encapsulated doxorubicin, cyclophosphamide, and fluorouracil as first-line therapy in patients with metastatic breast cancer. *J Clin Oncol*, 17, 1425-1434.

Vance, D.E. (2002) *Biochemistry of Lipids, Lipoproteins and Membranes*. Elsevier, Boston.

Vigilanti, B., Abraham, S.A., Michelich, C.R., Yarmolenko, P.S., MacFall, J., Bally, M.B. and Dewhirst, M. (2003) In vivo Monitoring of Real Time Tissue Pharmacokinetics of Liposome/Drug using MRI: Illustration of Targeted Delivery. *Magnetic Resonance in Medicine*, In press.

Volanakis, J.E. and Kaplan, M.H. (1971) Specificity of C-reactive protein for choline phosphate residues of pneumococcal C-polysaccharide. *Proc Soc Exp Biol Med*, 136, 612-614.

Volanakis, J.E. and Wirtz, K.W. (1979) Interaction of C-reactive protein with artificial phosphatidylcholine bilayers. *Nature*, 281, 155-157.

Von Hoff, D.D., Rozencweig, M. and Piccart, M. (1982) The cardiotoxicity of anticancer agents. *Semin Oncol*, 9, 23-33.

Wall, M.E. (1998) Camptothecin and taxol: discovery to clinic. *Med Res Rev*, 18, 299-314.

Wall, M.E., Wani, M.C., Nicholas, A.W., Manikumar, G., Tele, C., Moore, L., Truesdale, A., Leitner, P. and Besterman, J.M. (1993) Plant antitumor agents. 30. Synthesis and structure activity of novel camptothecin analogs. *J Med Chem*, 36, 2689-2700.

Wang, E., Taylor, R.W. and Pfeiffer, D.R. (1998) Mechanism and Specificity of Lanthanide Series Cation Transport by Ionophores A23187, 4-BrA23187 and Ionomycin. *Biophysical Journal*, 75, 1244-1254.

Warren, B.A. (1979) The Vascular Morphology of Tumors. In Peterson, H. (ed.), *Tuomor Blood Circulation: Angiogenisis, Vascular Morphology and Blood Flow of Experimental and Human Tumors*. CRC Press Inc, Boca Raton.

Weinstein, J.N., Magin, R.L., Yatvin, M.B. and Zaharko, D.S. (1979) Liposomes and local hyperthermia: selective delivery of methotrexate to heated tumors. *Science*, 204, 188-191.

Weiss, R.B., Sarosy, G., Clagett-Carr, K., Russo, M. and Leyland-Jones, B. (1986) Anthracycline analogs: the past, present, and future. *Cancer Chemother Pharmacol*, 18, 185-197.

Williams, K.J., Phillips, M.C. and Rodrigueza, W.V. (1998) Structural and metabolic consequences of liposome-lipoprotein interactions. *Adv Drug Deliv Rev*, 32, 31-43.

Winer, E.P. and Burstein, H.J. (2001) New combinations with Herceptin in metastatic breast cancer. *Oncology*, 61, 50-57.

Wolfe, S.L. (1993) *Molecular and Cellular Biology*. Wadsworth Publishing Company.

Woodle, M.C. and Lasic, D.D. (1992) Sterically stabilized liposomes. *Biochim Biophys Acta*, 1113, 171-199.

Woodle, M.C. and Papahadjopoulos, D. (1989) Liposome preparation and size characterization. *Methods Enzymol*, 171, 193-217.

Wust, P., Hildebrandt, B., Sreenivasa, G., Rau, B., Gellermann, J., Riess, H., Felix, R. and Schlag, P.M. (2002) Hyperthermia in combined treatment of cancer. *Lancet Oncol*, 3, 487-497.

Yatvin, M.B., Weinstein, J.N., Dennis, W.H. and Blumenthal, R. (1978) Design of liposomes for enhanced local release of drugs by hyperthermia. *Science*, 202, 1290-1293.